MOLECULAR AND FUNCTIONAL DETERMINANTS OF SYNAPTIC VESICLE RECYCLING IN CNS SYNAPSES

APPROVED BY SUPERVISORY COMMITTEE

Ege T. Kavalali, Ph.D.

Joseph P. Albanesi, Ph.D.

Kimberly M. Huber, Ph.D.

Thomas C. Südhof, M.D.

To my family

for their endless support of my every endeavor

MOLECULAR AND FUNCTIONAL DETERMINANTS OF SYNAPTIC VESICLE RECYCLING IN CNS SYNAPSES

by

TUHIN VIRMANI

DISSERTATION

Presented to the Faculty of the Graduate School of Biomedical Sciences

The University of Texas Southwestern Medical Center at Dallas

In Partial Fulfillment of the Requirements

For the Degree of

DOCTOR OF PHILOSOPHY

The University of Texas Southwestern Medical Center at Dallas

Dallas, Texas

April, 2005

ACKNOWLEDGMENTS

I would like to thank a number of people, without whom this work would not have been possible. First and foremost, I would like to thank my mentor Ege Kavalali. There are few words that could describe how much he has contributed not only to my work, but also to my growth and development as a scientist. His unwavering enthusiasm, constant motivation and uplifting spirit, were always a beacon through the good times and more importantly the bad. The way he treated me as a peer from my first day in the lab to our diverse conversations on all sorts of topics (even sometimes on science) helped make life in the lab both stimulating and more importantly enjoyable, and for this I cannot thank him enough. I hope many more students are able to benefit from his knowledge and mentorship.

I would also like to thank various members of the Kavalali Lab for their help and support over the years. Yildirim, for teaching me the ins and outs of patch clamp recording, Marina for training me in the finer points of real-time fluorescent imaging and Feri for helping me with all the molecular biology techniques I required. I would also like to thank Deniz, Mert, Catherine, Sanket and ChiHye for many helpful discussions over the years.

A lot of this work was performed with extensive collaborations. Specifically, the spontaneous recycling story was performed in collaboration with Yildirim Sara. Ferenc Deák also provided both experimental and technical assistance with the synaptobrevin and HRP experiments in the spontaneous recycling story. I also collaborated extensively with Deniz Atasoy to study the activity dependent regulation of vesicle recycling. Weiping Han and Thomas Südhof provided us with the synaptotagmin constructs, and I would especially like to thank Tom for taking the time out of his extremely busy schedule to re-write the syt7 paper, ensuring that we were ultimately able to publish that work. I would like to thank Anton Maximov for providing me with the synaptotagmin 7 mouse lines as well as genotyping them. Xinran Liu provided extensive technical expertise, providing us with electronmicrographs in almost all my projects, without which none of the stories would have been complete. I would also like to thank Sandy Hofmann and Praveena Gupta for their extensive help and expertise in the PPT1 project. Praveena provided me with the mouse pups and also performed the tunel assays and immunocytochemistry experiments described. Joseph Albanesi and Pawel Wlodarski generously provided us with the dynamin constructs and the rab5 constructs were provided by Philip Stahl (Washington University) and Thomas Südhof. I would also like to thank Terri Gemelli and Lisa Monteggia for re-engineering the rab5 constructs, and Melissa Mahgoub for her technical expertise. I would like to thank Misty Deming for taking the time to critically read this manuscript.

I would also like to thank the members of my committee, Joseph Albanesi, Kimberly Huber and Thomas C. Südhof for their many useful discussions. I would like to thank the MST and Neuroscience Programs for their support, Kasey, Robin and Stephanie for all their help, and especially Rod Ulane, without whom I would not be at UT Southwestern.

Of course, last but in no way the least, I would like to thank my family and friends. I would especially like to thank my mom, dad, Nipun and Misty, for their love and support, particularly during all the testing times. Without their constant encouragement I would not have been able to achieve any of this.

MOLECULAR AND FUNCTIONAL DETERMINANTS OF SYNAPTIC VESICLE RECYCLING IN CNS SYNAPSES

Publication No. _____

Tuhin Virmani, Ph.D.

The University of Texas Southwestern Medical Center at Dallas, 2005

Supervising Professor: Ege Taner Kavalali, Ph.D.

Chemical neurotransmission is the basis for information processing in the brain, and presynaptic terminals respond to a large range of stimulation patterns including baseline rhythms of activity that coordinate neuronal ensembles, to short bursts of activity that encode information. They also release neurotransmitter spontaneously in the absence of any activity. The question then is how can a single subcellular compartment with approximately 100 synaptic vesicles coordinate these complex functions? We used a multifaceted approach to address this question. We first studied the role of synaptotagmin 7 (syt7), a highly alternatively spliced synaptic plasma membrane protein, whose short splice forms inhibit clathrin-mediated endocytosis. We found that in hippocampal synapses, the splice variants formed a bi-directional molecular switch targeting vesicles to kinetically distinct recycling pathways. Additionally, syt7 knockout synapses had less fast endocytosis, while calcium

binding site mutant synapses showed increased vesicle endocytosis. We further investigated the slower recycling pathways by exploring rab5 function. A dominant negative rab5 mutation did not alter synaptic function, but constitutively active rab5 or the inhibition of vesicle budding from endosomes by the PI3-kinase inhibitor wortmannin, decreased vesicle pool size and release kinetics. This suggests that central synapses are tuned towards faster modes of recycling. The model of spontaneous neurotransmitter release from this same evoked recycling pool places additional constraints on this system. We explored this hypothesis by directly visualizing presynaptic recycling of spontaneous vesicles using FM dyes, syt1 antibodies and HRP uptake. We found that there are actually two sets of vesicle pools, one for evoked release, and one for spontaneous release that have minimal interaction with one another. Can presynaptic function be a substrate for diseases of the CNS? To test this important question, we studied a mouse model for infantile Batten disease. We found that underlying synaptic deficits in vesicle pool size and mini frequency could produce the neurological phenotypes exhibited by patients well before the onset of neurodegeneration. Taken together, these results show that synaptic vesicle recycling is a very plastic entity and that synapses have the intrinsic ability to modulate their vesicle trafficking pathways in response to the varying demands placed on them.

TABLE OF CONTENTS

PUBLICATIONS

Virmani, T. and Kavalali, E.T. (2005) Synaptic Vesicle Recycling As A Substrate For Neural Plasticity. In Stanton, P.K., Bramham, C., and Scharfman, H.E. (Eds.), *Synaptic Plasticity and Transsynaptic Signaling*. Springer Science + Business Media. (in press)

Virmani, T., Gupta, P., Liu, X., Kavalali, E. T., Hofmann, S.L. (2005) Progressively reduced synaptic vesicle pool size in cultured neurons derived from neuronal ceroid lipofuscinosis-1 knockout mice. *Neurobiol Dis.* Apr 22 [epub. ahead of print]

Luikart, B., Nef, S., Virmani, T., Lu, Y., Kavalali, E. T., Parada. L. F. (2005) TrkB Has a Cell Autonomous Role in the Establishment of Hippocampal Schaffer Collateral Synapses. *J. Neurosci.* **25**, 3774-86

Sara, Y.*, Virmani, T.*, Deák F., Liu, X., Kavalali, E. T. (2005) An isolated pool of vesicles recycles at rest and drives spontaneous neurotransmission. *Neuron* **45**, 563-73.

Virmani, T., Han, W., Liu, X., Sudhof, T. C., and Kavalali, E. T. (2003). Synaptotagmin 7 splice variants differentially regulate synaptic vesicle recycling. *Embo J* **22**, 5347-57.

*equal contribution

FIGURES

ABBREVIATIONS

4α-PMA	4-α- phorbol 12-myristate 13-acetate
AP	action potential
AP-5	2-amino-5-phosphonopentanoic acid
AZ	active zone
Ca^{2+}	calcium ions
CFP	cyan fluorescent protein
CNS	central nervous system
CNQX	6-cyano-7-nitroquinoxaline-2,3-dione
div	days in vitro
EM	electronmicrographs
ECFP	enhanced cyan fluorescent protein
EGFP	enhanced green fluorescent protein
EPSC	excitatory postsynaptic currents
GED	GTPase effector domain
GFP	green fluorescent protein
GTPase	Guanine triphosphate transferase
het	heterozygous mice
homo	homozygous mice
Hz	hertz
INCL	infantile neuronal ceroid lipofsucinoses
ki	knockin
ko	knockout
K^+	potassium ions
mEPSC	miniature excitatory postsynaptic currents
min	minutes
minis	spontaneous miniature release events

mM	millimolar
mut	homozygous mutant mice
NMJ	neuromuscular junction
NCL	neuronal ceroid lipofuscinoses
pA	pico amperes
PH	pleckstrin homology
PI3K	phosphatidyl inositol-3-kinase
PMA	phorbol 12-myristate 13-acetate
PPT1	palmitoyl protein thioesterase
PRD	proline-rich domain
PSD	post-synaptic density
RP	reserve pool
RRP	readily releasable pool
s	seconds
SEM	standard error of the mean
SH3	Src homology 3 domain
SVs	synaptic vesicles
syn	synaptophysin
syt1	synaptotagmin 1
syt7	synaptotagmin 7
syt7A	synaptotagmin 7 long form
syt7B	synaptotagmin 7 short form
syt7B*	synaptotagmin 7 mutated short form
syt12	synaptotagmin 12
TTX	tetrodotoxin
wt	wild-type

CHAPTER 1: General Introduction

The human brain consists of millions of cells called neurons. The principal site of contact and communication between neurons is the synaptic junction. There are two major types of synapses, chemical synapses and electrical synapses. Electrical synapses are the less frequent of the two types and bi-directionally couple two neuronal cells via gap junctions between their membranes. Chemical synapses are more numerous but are also more complex in their organization. Communication at the chemical synapse is primarily uni-directional, however instances of molecules acting as retrograde messengers have been described.

Ultrastructure of The Chemical Synapse

Chemical synapses are composed of two functionally and structurally distinct compartments, a presynaptic terminal and a postsynaptic specialization. The presynaptic active zone is precisely aligned with the postsynaptic neurotransmitter receptors and the post-synaptic density (PSD). Presynaptic terminals release chemical neurotransmitter in response to an incoming action potential into the synaptic cleft. The neurotransmitter molecules diffuse across the cleft and bind to receptors on the postsynaptic density. Activation of these receptors results in the influx of ions into the postsynaptic cell that depolarizes the membrane and invokes several signaling cascades. This multi step process of information transfer at the synapse provides abundant substrates for the regulation of this system.

In the presynaptic nerve terminal neurotransmitter substances are packaged into synaptic vesicles, organelles with a diameter of 35 to 40 nm. Typical nerve endings in the central nervous system (CNS) contain up to 100-200 synaptic vesicles. Synaptic vesicles recycle locally within the terminal, independent of the cell body or other membrane compartments in the secretory pathway. In the simplest case, vesicles in a CNS terminal can be divided into two pools (Figure 1.1).

The first pool of vesicles is generally referred to as the immediately releasable pool or the readily releasable pool (RRP). This pool contains a relatively small fraction (5-10%) of the total vesicles present in the synapse. Functionally, the RRP vesicles are defined as the pool of vesicles that can be released by rapid uncaging of intrasynaptic Ca^{2+}

(Schneggenburger et al., 1999), a 10-millisecond Ca^{2+}-current pulse (Wu and Borst, 1999), a brief high-frequency train of action potentials (Murthy and Stevens, 1999) or by hypertonic stimulation (Rosenmund and Stevens, 1996). Structurally, the RRP vesicles are generally defined as the vesicles located in close proximity to the active zone, generally referred to as "docked" vesicles. However, it has been shown that not all morphologically docked vesicles are necessarily release competent at any given time (Schikorski and Stevens, 2001) and a "priming" step in addition to the morphological docking is required to make vesicles fully release competent (Jahn et al., 2003). Recent evidence suggests that docking and priming reactions can occur quickly, within 300 ms (Zenisek et al., 2000).

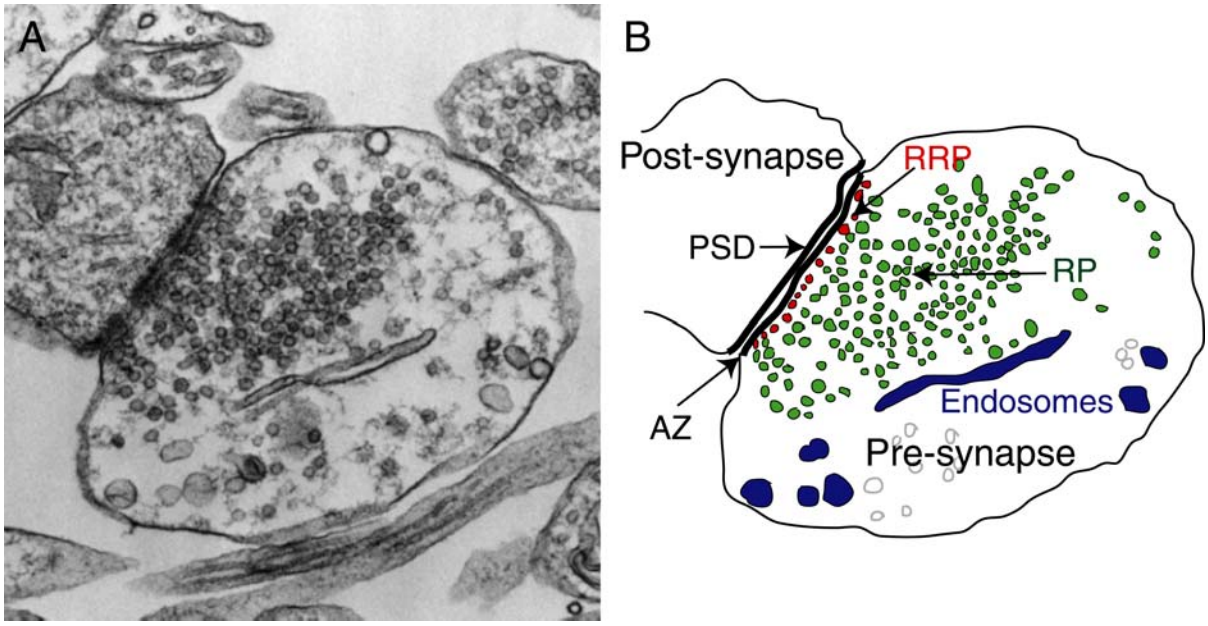

Figure 1.1. Structure of a chemical synapse. **(A)** Electronmicrograph of a typical hippocampal synapse with well-defined presynaptic and postsynaptic terminals. **(B)** Line figure of synapse shown in (A) showing the location of key elements of synaptic structure. PSD – postsynaptic density, AZ – active zone, RRP – readily releasable pool, RP – reserve pool.

In contrast to this prevailing view on the architecture of the RRP, a recent study in the frog neuromuscular junction showed that there may not be a one to one correspondence between the morphologically docked vesicle pool and the functionally competent readily releasable pool (Rizzoli and Betz, 2004). Using serial EM sections of photoconverted FM

dyes, the authors of the study showed that some vesicles that are a distance away from the active zone might have a priority to release over vesicles that appear to be morphologically docked.

A secondary pool of vesicles, the reserve pool (RP), is spatially distant from the active zone. The primary function of this pool of vesicles is to replenish the readily releasable pool of vesicles after they exocytose. Since the probability of vesicle release is a function of the number of vesicles present in the RRP and the single vesicle release probability, the rate and pathways by which vesicles in the RRP are replenished is a crucial determinant of presynaptic efficacy. The initial release of vesicles from the RRP and subsequent replenishment and release from the reserve pool results in biphasic release kinetics, with a fast release phase corresponding to release from the RRP and a slower release phase due to the mobilization and release of vesicles from the reserve pool. Recent evidence indicates that intrasynaptic Ca^{2+} can facilitate the rate of replenishment of RRP vesicles from the RP (Dittman and Regehr, 1998; Stevens and Wesseling, 1998; Wang and Kaczmarek, 1998).

In addition to these two functionally distinct pools, several lines of evidence support the presence of a non-recycling pool of vesicles in the synapse. The function of this "resting" (or "dormant") pool remains to be determined (Harata et al., 2001; Südhof, 2000). It is also possible that this pool may be a graveyard of vesicles that have lost essential components required to keep them actively recycling. This idea is supported by evidence in chromaffin cells where as vesicles age, they migrate towards the central regions of the cells (Duncan et al., 2003).

Parallel Pathways For Vesicle Recycling In CNS Synapses

Presynaptic terminals are exceptionally dynamic vesicle trafficking machines. Most forms of short-term synaptic plasticity (milliseconds to minutes) as well as some forms of long-term plasticity arise from persistent alterations in the dynamics of vesicle trafficking in presynaptic terminals. What makes presynaptic forms of plasticity particularly interesting is that they not only increase or decrease the amplitude of synaptic responses, but also cause

frequency-dependent changes in chemical neurotransmission. In this manner, plasticity can alter the information coding in neural circuits beyond simple scaling of synaptic responses.

Over the past few years, several studies have demonstrated that neurotransmission is not sustained by mobilization of vesicles from a large reservoir but by constant recycling of a handful of vesicles. After exocytosis, vesicles must endocytose, refill neurotransmitter, and become release competent again. Therefore, the rate and the pathway of vesicle trafficking can critically determine synaptic efficiency during activity. However, very little is known about the processes that regulate vesicle trafficking in the synapse beyond vesicle fusion. However, what is becoming clear is that with vesicle exocytosis occurring in milliseconds, and most estimates of the time constant for vesicle recycling being on the order of tens of seconds (Betz and Bewick, 1993; Liu and Tsien, 1995; Ryan and Smith, 1995), central synapses, with their limited pool size, should be rapidly depleted of release competent vesicles. This is definitely not the case and a consensus is emerging that there may be numerous embedded pathways that allow vesicles to become re-available for release with different time frames. Since some brain regions experience activity on the order of hundreds of hertz, this would allow central synapses the flexibility to maintain their releasable vesicle pool.

Clathrin-dependent Pathway

Amongst the vesicle recycling pathways, perhaps the best studied is the so-called "classical" or "clathrin-dependent" model for vesicle recycling (Figure 1.2A). In this pathway, during exocytosis, complete collapse of the vesicle membrane occurs at the active zone. Subsequently, vesicles bud off the membrane at sites peripheral to the active zone in a classical clathrin/dynamin dependent manner. A v-type ATPase then lowers the pH in these vesicles and subsequently the vesicles are refilled with neurotransmitter, two steps that are thought to be extremely rapid. Clathrin coats are removed from the vesicles following which the uncoated vesicles repopulate the reserve or resting pool of vesicles. The uncoating reaction is thought to be extremely rapid as free-coated vesicles are rarely observed under EM. The rate-limiting step in this pathway of vesicle recycling is thought to be the formation of the clathrin coats.

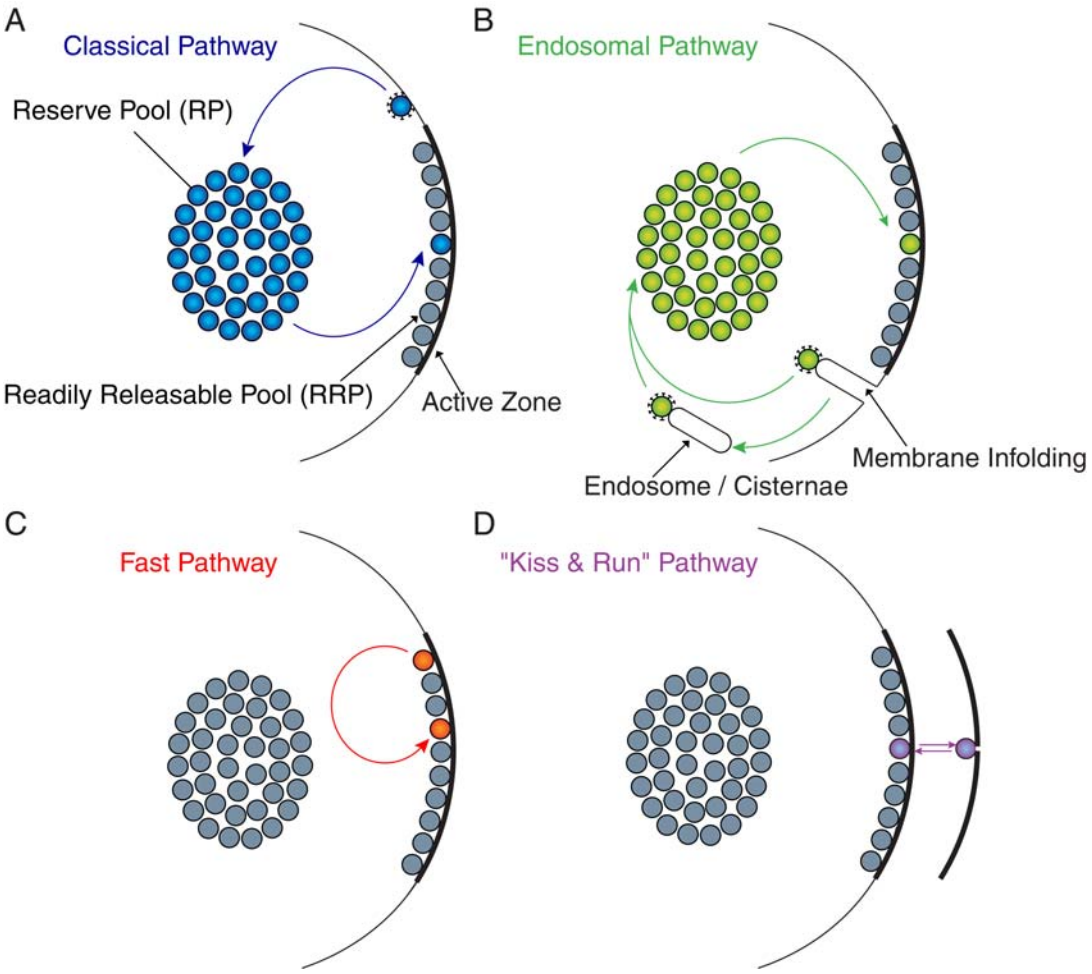

Figure 1.2. Models of synaptic vesicle recycling. **(A)** Classical clathrin-dependent vesicle endocytosis and recycling. Endocytosing vesicles recycle through the reserve pool. **(B)** Endosomal recycling. Vesicles endocytose via clathrin mediated endocytosis and undergo an additional step of fusion and budding of endosomal intermediates before repopulating the reserve pool. Additionally vesicles may bud of invaginating membranous cisternae and recycle to the reserve pool. **(C)** Fast vesicle recycling. Vesicles locally recycle in the readily releasable pool. **(D)** Kiss and Run recycling. A special case of fast recycling where vesicles may maintain their position at the active zone and release neurotransmitter via transient opening of a fusion pore.

Endosomal Pathway

Endocytosis of clathrin-coated vesicles has also been shown to occur from membrane infoldings or endosomal cisternae, primarily at the neuromuscular junction synapse (Figure

1.2B) (Koenig and Ikeda, 1996; Richards et al., 2000; Takei et al., 1996). This process is slower than the direct budding of clathrin coated vesicles off the plasma membrane and has been estimated to occur on the order of many minutes. Whether or not this pathway is present in central synapses is yet to be determined. The fact that most vesicles have the endosomal marker, rab5, on their surface suggests that such a pathway exists in all synapses. However under normal conditions, most hippocampal and cortical synapses lack endosomal structures under EM. It is possible however that this pathway exists and may serve more to replenish the protein content in the vesicle membrane, rather than actively partake in the recycling pathway during stimulation.

Fast Pathway or "Kiss and Run" Recycling

Recent studies provide evidence for an additional fast pathway of vesicle recycling that prevents vesicle depletion and maintains synaptic responses in the face of repetitive stimulation (Aravanis et al., 2003; Delgado et al., 2000; Gandhi and Stevens, 2003; Pyle et al., 2000; Sara et al., 2002; Südhof, 2000). The mechanisms underlying this pathway are the least well understood, but are thought to involve local vesicle recycling of the RRP of vesicles (Figure 1.2C). This process may or may not involve a pathway commonly referred to as "kiss and run" (Figure 1.2D) in which the fusion pore opens transiently without complete collapse of the vesicle (Ceccarelli et al., 1973; Henkel and Almers, 1996; Valtorta et al., 2001). In central synapses, the presence of a fast mode of vesicle recycling is supported by reports studying the effects of hypertonic challenge and strong electrical stimulation ((Kavalali et al., 1999a; Klingauf et al., 1998; Pyle et al., 2000; Stevens and Williams, 2000) but also see (Sankaranarayanan and Ryan, 2000; Sankaranarayanan and Ryan, 2001)). In the next few chapters, we will explore potential molecular regulators of this pathway.

Spontaneous Vesicle Recycling Pathway

The current model of synaptic vesicle fusion assumes that the same vesicles that can release neurotransmitter in response to a single action potential also have a very low probability of spontaneous fusion. The calcium influx into the terminal during an action potential increases this probability of release several fold (Katz, 1969). However this hypothesis has never been directly tested even though spontaneous neurotransmitter release

serves multiple functions including the proper wiring of neurons in the brain during early development as well as the maintenance of these synaptic connections well into adulthood. However recent evidence from genetic studies in mice challenges this hypothesis. In mice lacking synaptotagmin 1 or complexins, proteins critical for evoked synchronous neurotransmitter release, the spontaneous fusion rate was unchanged (Geppert et al., 1994; Reim et al., 2001). Similarly, loss of the active zone scaffolding protein RIM1α impairs vesicle priming, thus impairing hypertonic sucrose-induced and Ca^{2+}-evoked transmission, but does not significantly alter spontaneous fusion rate (Calakos et al., 2004). In contrast, the spontaneous fusion rate is significantly reduced after deletion of synaptobrevin2/VAMP2 or completely abolished after genetic deletion of munc-18 or munc-13 isoforms (Schoch et al., 2001; Varoqueaux et al., 2002; Verhage et al., 2000). The selective role of proteins such as synaptotagmin 1, complexins and RIM1α in evoked neurotransmitter release in contrast to the substantial role of synaptobrevin, munc-18 or munc-13 in both forms of vesicle trafficking is consistent with the premise that the two forms of release may originate from distinct recycling pathways. This idea will be further explored in chapter 5.

Studies On Molecular Determinants Of Synaptic Vesicle Recycling

Given the importance of synaptic vesicle endocytosis and recycling, a number of molecular players have been studied, the arrangement of some of which are shown in figure 1.3. Most of these relate to the classical clathrin-mediated endocytosis pathway from which vesicles are thought to recycle into the reserve pool. Whether these proteins also function in other pathways of vesicle endocytosis still needs to be resolved. Very little is known about the molecules that regulate faster modes of endocytosis or the targeting of endocytosing vesicles to the kinetically distinct recycling pathways. In this section, a brief overview of some of the most studied molecules in clathrin-mediated endocytosis will be provided (for more detailed reviews see (De Camilli et al., 2001)).

Clathrin

The central molecule in the complex of proteins involved in classical endocytosis is the namesake molecule clathrin. The formation of the clathrin coat involves a number of different levels of assembly. At the base of this structure clathrin is composed of a heavy

chain and a light chain. While the heavy chain forms the major structural component of the coat, the light chain may modulate its assembly and disassembly (Schmid et al., 1984). The clathrin triskelia are composed of three clathrin dimers that in turn assemble together to form the honeycomb shaped clathrin coat (Heuser, 1980). This complex organization has led to significant debate on the energetic requirements for the formation of such a complex coat. It was initially proposed that the clathrin lattice assembled in a hexagonal array flat on the surface of the plasma membrane. Following this it was believed that certain adaptor proteins would reconfigure the lattice to include pentagon shaped arrays allowing for the formation of curvature, similar to the classic buckyball (Heuser, 1980). However the molecular rearrangements and energetic requirements for such a transformation would be quite large, so an alternative view was proposed whereby the curvature of the coat was already defined and only a transition from a low curvature to a high curvature state would be required (Musacchio et al., 1999). However the developmental mechanism of such a preordained curvature, or the molecules that would be involved in establishing such a state are yet to be determined. Therefore the question of the actual mechanism by which clathrin coats facilitate curvature formation is still a matter of debate.

AP-2

Clathrin alone cannot accomplish vesicle endocytosis, and there are a number of adaptor proteins described that allow it to facilitate this complex function. The heterotetrameric protein AP-2 appears to be a central player, linking clathrin to key components of the endocytic pathway. AP-2 binds to phospholipids, and mutant forms of the α-subunit of AP-2 (α-adaptin) defective in phosphoinositide binding are no longer recruited to coated pits, and inhibit endogenous AP-2 function (Gaidarov and Keen, 1999). Additionally, AP-2 binds the C2B domain of synaptotagmins (Li et al., 1995a; Zhang et al., 1994), potentially providing a link for exo-endo coupling of synaptic vesicles. AP-2 subunits also contain binding sites for certain endocytic motifs found on proteins that undergo receptor-mediated endocytosis (Heilker et al., 1999). This could provide a mechanism for recruitment of synaptic vesicle proteins to the clathrin bud. Finally, AP-2 binds to a number

of accessory proteins such as AP-180, amphiphysin, Eps15, epsin and auxilin, which also play significant roles in clathrin-mediated endocytosis.

AP-180

The other major clathrin adaptor protein is AP-180. This protein, like AP-2, binds phosphoinositides and clathrin and promotes clathrin coat formation. The production of clathrin coats in the presence of AP-180 leads to a more homogenous distribution in the size of the clathrin cage (Ye and Lafer, 1995). This has lead to the suggestion that the primary function of this molecule may be to regulate synaptic vesicle size.

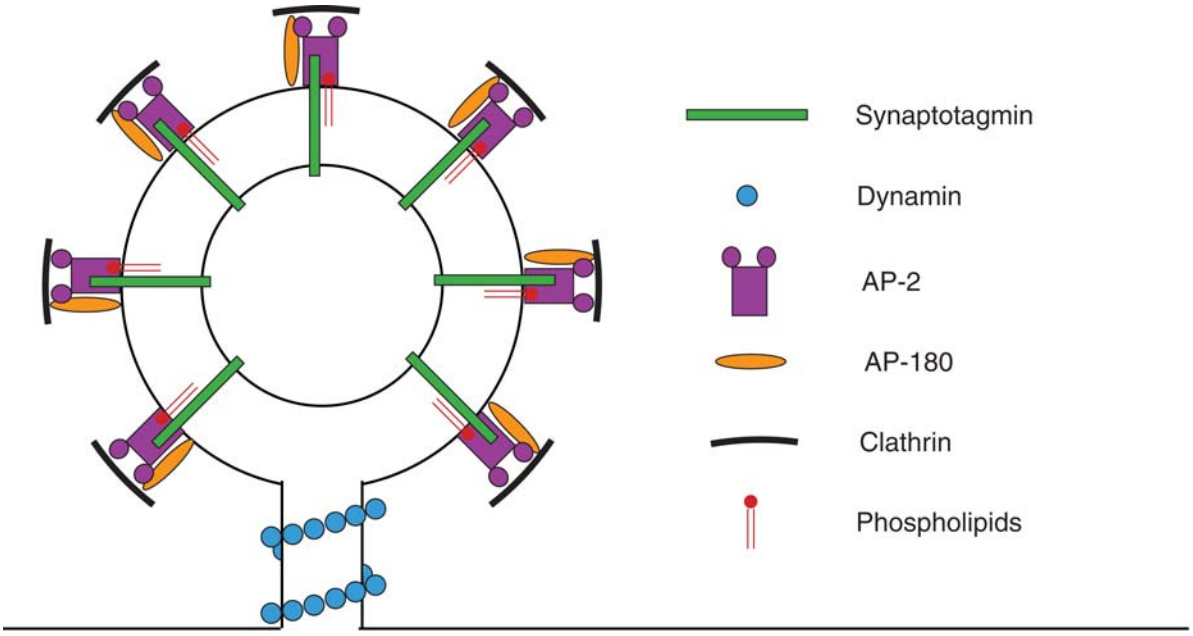

Figure 1.3. Proteins involved in clathrin mediated endocytosis. Diagram of an endocytosing vesicle showing the putative location of proteins thought to be involved in clathrin mediated endocytosis.

Dynamin

Dynamin was one of the first endocytic proteins identified when the *drosophila shibire* mutation was identified as the locus for the dynamin gene. It has three known isoforms, with dynamin 1 being the most highly expressed in the brain. Dynamin is

comprised of an N-terminal GTPase domain, a pleckstrin homology (PH) domain, a GTPase effector domain (GED) and a proline-rich domain (PRD) at the C-terminus. Mutations in the GTPase domain (ex. *shibire*) and the PH domain (which interacts with phosphoinositides) (Achiriloaie et al., 1999; Barylko et al., 2001), result in a dominant negative inhibition of clathrin mediated endocytosis. Additionally, recent evidence suggests that the GED domain is essential for the self-assembly and proper functioning of the protein (Song et al., 2004). The PRD domain contains SH3 binding sites and interacts with a host of proteins including amphiphysin (David et al., 1996; Grabs et al., 1997) and endophilin (Ringstad et al., 1999). Dynamin functions by oligomerizing in a coiled structure around the neck of invaginating clathrin coated pits, and pinching them off the plasma membrane. The mechanism by which this pinching off is accomplished is still a matter of considerable debate. One major view regards dynamin as a mechanochemical enzyme that directly pinches vesicles off the membrane (Stowell et al., 1999; Takei et al., 1999), while the opposing view has dynamin acting as a classical GTPase, recruiting other proteins to perform the actual fission reaction (Sever et al., 1999).

Several studies using the *drosophila* temperature sensitive dynamin mutant *shibire* have provided strong support for a relationship between vesicle recycling and synaptic release during sustained stimulation. Using this system, Koenig and Ikeda showed that vesicle recycling can occur through two pathways, one at the active zone of the *Drosophila* neuromuscular junction, the other in its vicinity (Koenig and Ikeda, 1996; Koenig and Ikeda, 1999). The active zone and non-active zone pathways were shown to populate different pools of vesicles at different time scales, with the active zone pathway repopulating the RRP within 1 minute of moving from the non-permissive (no dynamin function) to the permissive temperature (dynamin is functional), while reserve pool replenishment from the slower pathway occurred on the order of 25 minutes. Recent experiments in *Drosophila* neuromuscular junction compared the rate of synaptic depression between wild type and *shibire* flies. In this study synapses from *shibire* flies at non-permissive temperatures rapidly depressed without a plateau phase in response to high frequency stimulation. The kinetic difference between this rate of depression and the normal rate of depression when

endocytosis is intact revealed a recycling rate of one to two vesicles per second per active zone (Delgado et al., 2000), a rate considerably faster than previous estimates at the NMJ and in line with estimations from hippocampal synapses (Sara et al., 2002).

Endophilin

Endophilin 1 is the most abundant endophilin family member in the brain. It has an N-terminal lysophosphatidic acyl transferase domain, a short variable connecting domain and a C-terminal SH3 binding domain. The former domain catalyzes the incorporation of arachadonic acid into lysophosphatidic acid resulting in the formation of phosphatidic acid which could allow the molecule to play a role in the regulation of vesicle curvature (Schmidt et al., 1999). The SH3 domain binds synaptojanin preferentially, but can also interact with dynamin (Ringstad et al., 1997).

Recent results in *C. elegans* suggest that the interaction of this molecule with synaptojanin may be the prominent function of this molecule, since mutations in either or both of these molecules show similar phenotypes (Schuske et al., 2003). In all combinations of mutants studied, there was a profound decrease in mini frequency without a significant change in amplitude. There was also a decrease in the amplitude of the first evoked response with an increase in the rate of synaptic depression. A similar study on the null mutant of the *Drosophila* homolog of endophilin (Verstreken et al., 2002) also showed that in spite of an increase in fast synaptic depression, neurotransmission was still maintained under prolonged stimulation. This would indicate that vesicle recycling was still maintained at these synapses in contrast to *shibire* mutant flies where complete depletion of the recycling pool was observed. This finding suggests that a clathrin independent endocytic mechanism can sustain neurotransmission. The size of the total recycling pool was also decreased at these neuromuscular junction synapses, a common theme seen in all studies inhibiting clathrin-mediated endocytosis.

Amphiphysin

Amphiphysin is another putative clathrin adaptor protein that can link a number of prominent members of this cascade. Its N-terminal region has a lipid bilayer binding site (Takei et al., 1999) in addition to its importance in the protein's dimerization (Slepnev et al.,

1998). The central region of the molecule has both AP-2 and clathrin binding consensus sequences (McMahon et al., 1997; Slepnev et al., 1998), and the C-terminal region has SH3 domains and avidly binds dynamin and synaptojanin (David et al., 1996; de Heuvel et al., 1997). In mice deficient in this molecule, a form of vesicle recycling was still intact although the total size of the recycling pool and the kinetics of FM dye release decreased due to disruption of clathrin-mediated endocytosis (Di Paolo et al., 2002).

Synaptojanin

Synaptojanin 1, the major isoform in brain tissue, is a poly-phosphoinositide phosphatase (Cremona et al., 1999). It also contains C-terminal SH3 domain binding sites that most specifically interacts with endophilin and amphiphysin (de Heuvel et al., 1997; Ringstad et al., 1997). Mice lacking the synaptojanin 1 gene had decreased survival and several neurological deficits. These mice also had defects following prolonged stimulation in which the amplitude of the slow phase of synaptic depression was increased in both hippocampal slice preparations and inhibitory cortical neurons in culture (Cremona et al., 1999; Luthi et al., 2001). This data suggest that vesicles were unable to repopulate the reserve pool. As there is still neurotransmission occurring at these synapses, albeit at a lower steady state amplitude, this is consistent with a mode of recycling occurring which may not require the normal functioning of synaptojanin.

Synaptotagmins

A critical hallmark of the synaptic vesicle cycle is the tight coupling of exo- and endocytosis, a fact well illustrated by defective vesicle endocytosis in mice lacking the major exocytotic protein synaptobrevin 2 (Deák et al., 2004). Recent studies have extensively focused on synaptotagmins as potential mediators of this coupling. Synaptotagmins are characterized by an N-terminal transmembrane domain, a central linker and two C-terminal C2 domains (Marqueze et al., 2000; Südhof, 2000). These proteins have been extensively studied as Ca^{2+} sensors for vesicle exocytosis, primarily through the characterization of synaptotagmin 1 (Fernandez-Chacon et al., 2001; Geppert et al., 1994). While synaptotagmin 1 and 2 are located on the synaptic vesicle, synaptotagmins 3, 6 and 7 are present on the synaptic plasma membrane (Butz et al., 1999; Sugita et al., 2001). The C2 domain of

synaptotagmin has a high affinity binding site for AP-2 and possibly stonin, two proteins believed to be important in clathrin-mediated endocytosis (Li et al., 1995a; Martina et al., 2001; Zhang et al., 1994). In a recent study, rapid light induced inactivation of synaptotagmin 1 in the *Drosophila* neuromuscular junction impaired delayed endocytosis supporting the biochemical results discussed above (Poskanzer et al., 2003). Additionally it has been shown that in mice lacking synaptotagmin 1, endocytosis and recycling rates are decreased (Nicholson-Tomishima and Ryan, 2004). Among the plasma membrane synaptotagmins, synaptotagmin 7 is of particular interest since the truncated splice variant of synaptotagmin 7 (syt7B), produced due to a conserved stop codon in the second exon of the alternatively spliced region (Sugita et al., 2001), inhibits receptor mediated endocytosis in a number of non-neuronal cell lines (von Poser et al., 2000). These splice variants could potentially regulate the trafficking of vesicles to fast and slow recycling pathways as shown in the following chapter (Virmani et al., 2003).

Taken together genetic interventions that disrupt the endocytic proteins dynamin and clathrin argue for a strong relationship between vesicle recycling and synaptic output during sustained activity. Furthermore these studies suggest that a clathrin-independent pathway may operate in parallel and sustain neurotransmission and vesicle recycling. However several questions remain unanswered. Although a consensus is emerging on the presence of a "kiss and run" like mechanism that can retrieve vesicles "fast" and preserve their molecular identity, nothing is known of the molecular basis of this pathway. Are clathrin and its accessory proteins involved in this fast recycling pathway? Is there a dynamin independent mode of vesicle recycling? What factors contribute to a vesicles decision to endocytose and recycle to these kinetically distinct recycling pathways? Does the endosomal recycling pathway exist in central synapses? Where do spontaneously releasing vesicles fit into the scheme of synaptic vesicle pools? Are neurological disease states manifestations of presynaptic vesicle dysfunction? These and other questions will begin to be addressed in the proceeding chapters.

CHAPTER 2: Synaptotagmin 7 Splice Variants Differentially Regulate Synaptic Vesicle Recycling

Background

In the classical model of synaptic vesicle recycling, vesicles fuse with the plasma membrane at the active zone, release their neurotransmitter and completely collapse onto the membrane (Cremona and De Camilli, 1997; Heuser and Reese, 1973; Südhof, 1995). This process occurs on the time scale of milliseconds. Subsequently clathrin, through its adaptor proteins, is recruited to regions on or near the active zone and coats vesicles that bud off the plasma membrane with the help of the GTPase dynamin. Endocytosis of clathrin coated vesicles may also occur from membrane infoldings or endosomal cisternae that form near the active zone (Koenig and Ikeda, 1996; Richards et al., 2000; Takei et al., 1996). After endocytosis, vesicles rapidly re-acidify and refill with neurotransmitter. The entire process for exocytosed vesicles to be re-available for release is thought to occur within 40 and 90 seconds (Betz and Bewick, 1993; Liu and Tsien, 1995; Ryan and Smith, 1995). Recent studies provide evidence of an additional fast pathway of vesicle recycling that prevents vesicle depletion and maintains synaptic responses in the face of intense stimulation (Delgado et al., 2000; Pyle et al., 2000; Sara et al., 2002; Südhof, 2000). This process may involve a pathway referred to as "kiss and run" in which the fusion pore opens transiently without complete collapse of the vesicle (Ceccarelli et al., 1973; Henkel and Almers, 1996; Valtorta et al., 2001). In central synapses this hypothesis is supported by reports studying the affects of hypertonic challenge and sustained electrical stimulation (Kavalali et al., 1999b; Klingauf et al., 1998; Pyle et al., 2000; Sankaranarayanan and Ryan, 2001; Stevens and Tsujimoto, 1995). However, molecular mechanisms that regulate the targeting of vesicles to these slow or fast recycling pathways are not known.

Synaptotagmins are a family of proteins that have been implicated in synaptic vesicle exocytosis, as best characterized for synaptotagmin 1 (Geppert et al., 1994), as well as endocytosis (Nicholson-Tomishima and Ryan, 2004; Poskanzer et al., 2003). Synaptotagmins have an N-terminal transmembrane domain, a central linker, and two C-terminal C_2 domains

(Marqueze et al., 2000; Südhof, 2002) that in most synaptotagmins bind Ca^{2+}. Synaptotagmin 7 is of particular interest because of its extensive alternative splicing. One of the synaptotagmin 7 splice variants includes a conserved exon with an in-frame stop codon, resulting in a short synaptotagmin 7 variant lacking C_2-domains (Figure 2.1A) (Sugita et al., 2001). The C_2B-domains of synaptotagmins contain a high-affinity binding site for AP-2 and possibly stonin which are involved in clathrin-mediated endocytosis (Haucke and De Camilli, 1999; Haucke et al., 2000; Jarousse and Kelly, 2001; Li et al., 1995a; Martina et al., 2001; Zhang et al., 1994), suggesting a role for synaptotagmins in endocytosis in addition to exocytosis. This hypothesis is attractive because it would provide a molecular mechanism to account for the efficient coupling of exo- and endocytosis during neurotransmitter release. Consistent with this hypothesis, vesicles are depleted in C. elegans lacking synaptotagmin 1 (Jorgensen et al., 1995), and truncated synaptotagmins similar to the normally occurring short synaptotagmin 7 splice variant are potent inhibitors of clathrin-mediated endocytosis in transfected non-neuronal cells (von Poser et al., 2000). The presence of short synaptotagmin 7 splice variants in neurons (Sugita et al., 2001) raised the possibility that alternative splicing of synaptotagmin 7 may regulate synaptic vesicle recycling. In this study, we employed optical and electrophysiological recordings from transfected cultured neurons and electronmicroscopy to explore this possibility. Our results demonstrate that the short synaptotagmin 7 variant lacking C_2-domains accelerates endocytic recycling of synaptic vesicles, whereas a regular variant containing C_2-domains decelerates recycling. These data suggest that two splice variants of a synaptic protein exert opposite actions in regulating vesicle recycling.

Materials and methods

Cell culture

Dissociated hippocampal cultures were prepared from 1-2 day-old Sprague-Dawley rats as described (Kavalali et al., 1999b), and transfected after 6 div using a calcium phosphate transfection protocol with pCMV5-vectors containing CFP fusion proteins of full-length synaptotagmin 7 (syt7A), truncated synaptotagmin 7 (syt7B) or truncated synaptotagmin 7 with C to A mutations at residues 38 and 41 in the transmembrane region of the protein (syt7B*) (Figure 2.1). The constructs were made from cDNA clones as described (Sugita et al., 2001). Cells were imaged at day 10-11 in vitro 4-5 days after transfections.

Fluorescence Imaging

Synaptic boutons were loaded with either FM2-10 (400 μM) or FM1-43 (4 μM) (Molecular Probes, Eugene, OR) using either electric field stimulation in the presence of 4 mM K^+, 2 mM Ca^{2+} solution, or 90 s incubation in hyperkalemic solution 47 mM K^+/2 mM Ca^{2+}. Modified Tyrode solution containing (in mM) 150 NaCl, 4 KCl, 2 $MgCl_2$, 10 Glucose, 10 HEPES, and 2 $CaCl_2$ (pH 7.4, ~310 mOsm) was used in all experiments. Hypertonic solution was prepared by addition of 500 mM sucrose to the modified Tyrode solution. The 90 mM K^+ solutions contained equimolar substitution of KCl for NaCl. Field stimulation was applied through parallel platinum electrodes immersed into the perfusion chamber delivering 25 mA - 1 ms pulses. All staining protocols were performed with 10 μM CNQX and 50 μM AP-5 to prevent recurrent activity. Images were taken after 10-min washes in dye-free solution in nominal Ca^{2+} to minimize spontaneous dye loss. Destaining of hippocampal terminals with hypertonic/high-potassium challenge was achieved by direct perfusion of solutions onto the field of interest by gravity (2 ml/min). Images were obtained by a cooled-intensified digital CCD camera (Roper Scientific, Trenton, NJ) during illumination (1Hz-60 ms) at 480 ± 20 nm (505 DCLP, 535 ± 25 BP) via an optical switch (Sutter Instruments, Novato, CA). Images were acquired and analyzed using Axon Imaging Workbench Software (Axon Instruments, Union City, CA).

Electrophysiology

Whole-cell recordings from pyramidal cells were acquired with an Axopatch 200B amplifier and Clampex 8.0 software (Axon Instruments, Union City, CA). Recordings were filtered at 2 kHz and sampled at 200 μs. Pipette internal solution included (in mM): 115 Cs-$MeSO_3$, 10 CsCl, 5 NaCl, 10 HEPES, 0.6 EGTA, 20 TEACl, 4 Mg^{2+}-ATP, 0.3 Na_2GTP, 10 QX-314 (pH 7.35, 300 mOsm).

Electron microscopy

Transfected cells were stimulated with 90 mM K^+ solution or control buffer for 90 s, fixed in 1% glutaraldehyde, 2% paraformaldehyde in PBS (pH 7.4), and examined by immuno-electronmicroscopy using a rabbit antibody to GFP essentially as described (Sugita et al., 2001).

Immunostaining

For immunocytochemistry, neurons were fixed with 4% formaldehyde/PBS and were permeabilized in 0.4% saponin. Primary antibodies used in this study were anti-synaptophysin monoclonal (1:1000) [to identify presynaptic terminals], anti-GFP polyclonal (1:1000) [to identify transfected proteins]. Secondary antibodies were Alexa 488-conjugated goat anti-rabbit and Alexa 568-conjugated goat anti-mouse (Molecular Probes). Fluorescence micrographs were taken using a Leica TCS SP2 Laser Scanning Spectral Confocal Microscope.

Miscellaneous

All error bars denote standard error of the mean (SEM); all n values correspond to individual coverslips unless mentioned otherwise; all statistical assessments were performed with the 2-tailed t-test.

Results

Monitoring synaptic vesicle exo- and endocytosis in transfected neurons

To establish an approach that allows measurements of synaptic vesicle exo- and endocytosis in synapses from transfected neurons, we employed plasmids encoding two splice variants of synaptotagmin 7 that were fused to ECFP (Enhanced Cyan Fluorescent Protein; Figure 2.1A). We used one regular splice variant of synaptotagmin 7 that includes two C_2-domains (referred to as Syt7A), and a second short splice variant that lacks C_2-domains (referred to as Syt7B). In addition, we employed a mutant of the short variant in which two cysteine residues in the transmembrane region were substituted by alanine residues (referred to as Syt7B*). We examined the localization of the ECFP-synaptotagmin 7 fusion proteins in transfected rat hippocampal neurons by fluorescence microscopy, and used staining with FM1-43 to identify presynaptic terminals that contain actively recycling vesicles (Figures 2.1B-D). The expressed ECFP-synaptotagmins were present throughout the axons, but enriched in nerve terminals coincident with FM1-43 staining, suggesting that synaptic terminals containing transfected ECFP-synaptotagmin 7 can be readily identified by FM staining and ECFP fluorescence. Transfected ECFP-Synaptotagmin 1 protein (Syt1) also showed similar localization (Fig 2.1E). Immunocytochemistry performed using antibodies against ECFP and the presynaptic marker synaptophysin, also showed significant localization of the transfected constructs to presynaptic terminals (Figure 2.2).

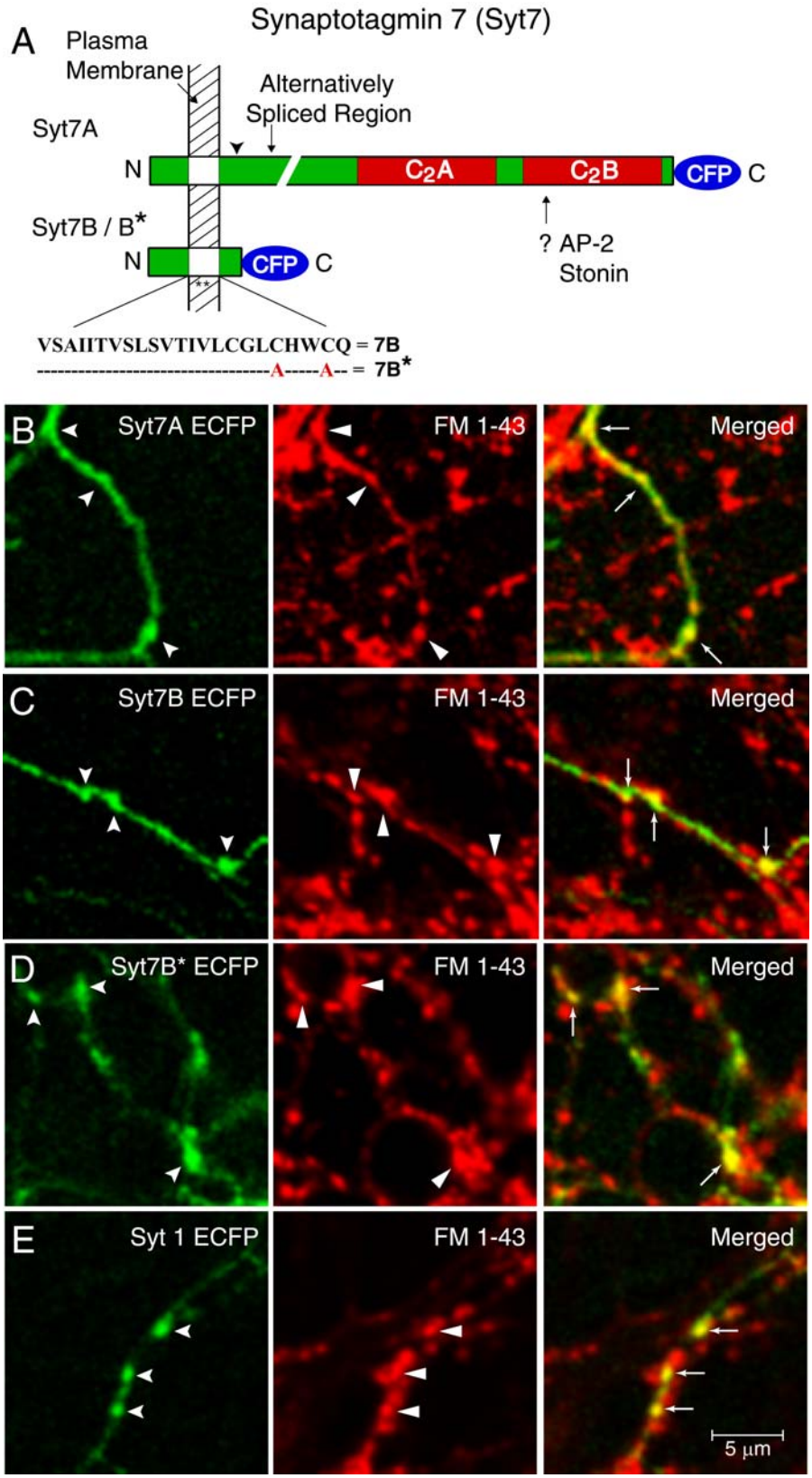
A
Synaptotagmin 7 (Syt7)
Plasma Membrane
Alternatively Spliced Region
Syt7A
N
C2A
C2B
CFP
C
Syt7B / B*
N
CFP
C
? AP-2 Stonin
VSAIITVSLSVTIVLCGLCHWCQ = 7B
----------A-----A-- = 7B*
B
Syt7A ECFP
FM 1-43
Merged
C
Syt7B ECFP
FM 1-43
Merged
D
Syt7B* ECFP
FM 1-43
Merged
E
Syt 1 ECFP
FM 1-43
Merged
5 µm

Figure 2.1. Expression of synaptotagmin 7 splice variants in transfected neurons. **(A)** Structure of synaptotagmin 7 splice variants (Sugita et al., 2001). All variants share a short N-terminal extracellular sequence and a single transmembrane region but differ in the cytoplasmic sequences where regular synaptotagmin 7 variants contain a variable linker and two C-terminal C_2-domains, whereas short synaptotagmin 7 variants contain a conserved exon with an in-frame stop codon right after the transmembrane region. The current study employs a regular synaptotagmin 7 variant with a small linker (Syt7A), a short variant with no additional exons (Syt7B), and a mutant short variant in which two cysteine residues in the transmembrane region (see indicated sequence) were substituted for alanine residues to abolish dimerization (Syt7B*; ref. 30). All proteins were fused to enhanced cyan fluorescence protein (CFP). **(B-E)** Fluorescence images of transfected hippocampal neurons expressing regular (Syt7A; B), the short synaptotagmin 7 (Syt7B; C), the mutated short synaptotagmin 7 (Syt7B*; D) or synaptotagmin 1 (Syt 1; E). Neurons were stained with FM1-43 under stimulation to visualize active presynaptic nerve terminals; merged images of ECFP and FM1-43 fluorescence signals are shown on the right to visualize the presence of transfected synaptotagmin 7 variants in nerve terminals.

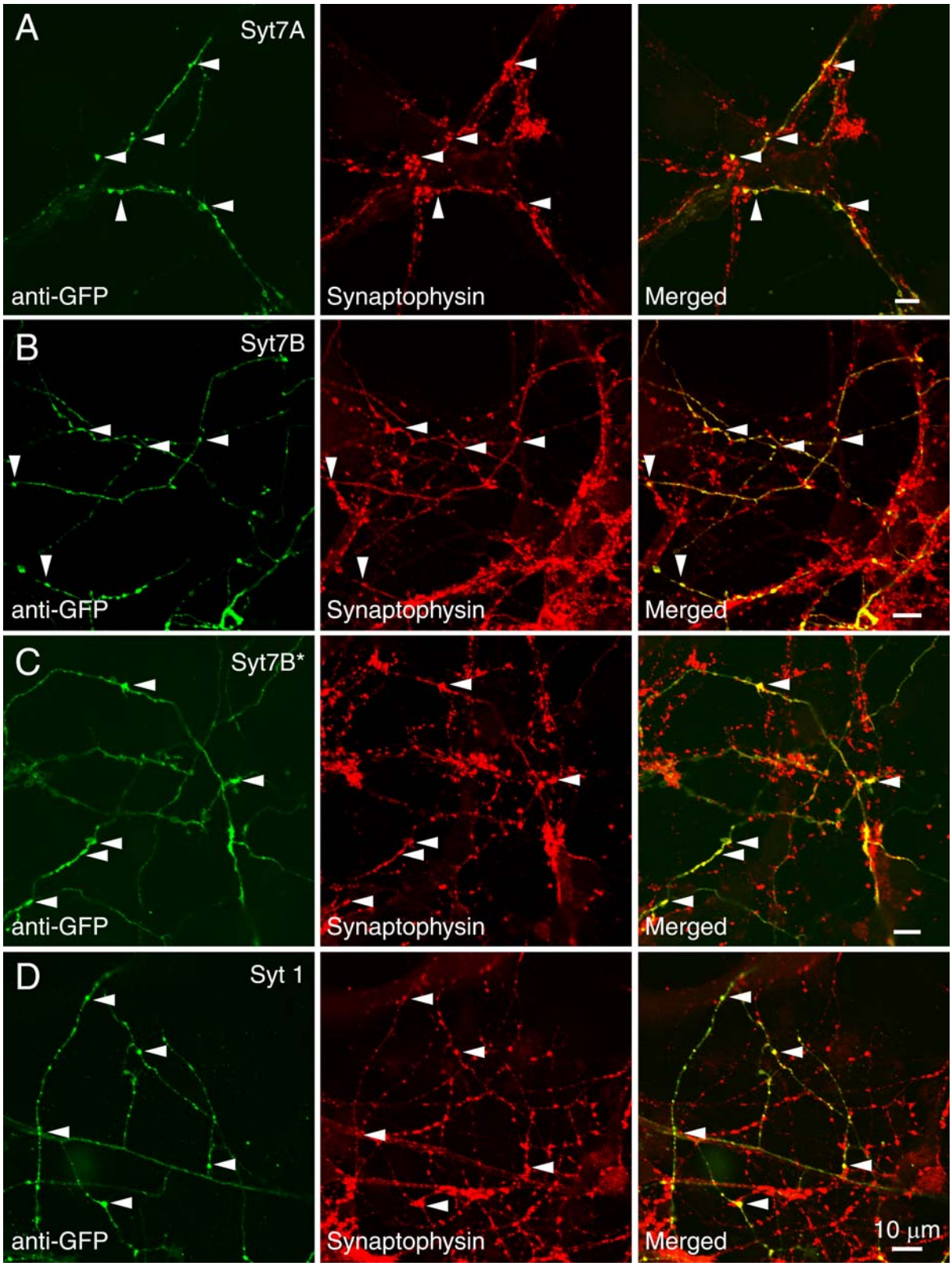
A
Syt7A
anti-GFP
Synaptophysin
Merged
B
Syt7B
anti-GFP
Synaptophysin
Merged
C
Syt7B*
anti-GFP
Synaptophysin
Merged
D
Syt 1
anti-GFP
Synaptophysin
Merged
10 µm

Figure 2.2. Immunocytochemistry. **(A-D)** Transfected cultures were stained with an antibody that recognizes the ECFP fusion proteins, in addition to synaptophysin, a marker for presynaptic terminals. We see similar staining patterns for GFP in Syt7A (A), Syt7B (B), Syt7B* (C) and Syt 1 (D) cultures (left column). There is some diffuse axonal staining; however the transfected proteins are concentrated in punctate regions that co-localize with synaptophysin (middle and right columns) indicating that they are present in presynaptic puncta.

The short synaptotagmin 7 splice variant accelerates synaptic vesicle endocytosis

To test whether synaptotagmin 7 participates in regulating synaptic vesicle endocytosis, we examined the size of the synaptic vesicle pools that are labeled with FM1-43 in synapses containing transfected synaptotagmin 7 variants (Figure 2.3A). We first induced exo- and endocytosis of synaptic vesicles by a brief, intense stimulus (field stimulation at 30 Hz for 2 s) that selectively induces exocytosis of the readily-releasable vesicle pool (Mozhayeva et al., 2002; Pyle et al., 2000). Stimulations were carried out in the presence of FM1-43 which was washed out immediately afterwards, and the size of the recycling vesicle pool was measured by fluorescence imaging as the amount of FM1-43 destaining triggered by four applications of 90 mM K^+ (ΔF_1). Thereafter we stained the same synapses again with FM1-43, but employed a longer stimulus (10 Hz for 2 min) that mobilizes the total pool of recycling vesicles. After the stimulation and subsequent washes, the amount of FM1-43 taken up during the longer stimulus was also imaged as FM destaining caused by K^+ applications (ΔF_2). The second FM1-43 measurements were performed to control for differences between presynaptic terminals in the pools of recycling vesicles and the efficiency of dye labeling. In these experiments, 50-150 nerve terminals were monitored simultaneously on each cover slip, and the data were plotted as cumulative distributions of nerve terminal fluorescence intensities (Figures 2.3B and 2.3C). The medians of such distributions reflect the average size, and their slopes reflect the heterogeneity of vesicle pools in the terminals.

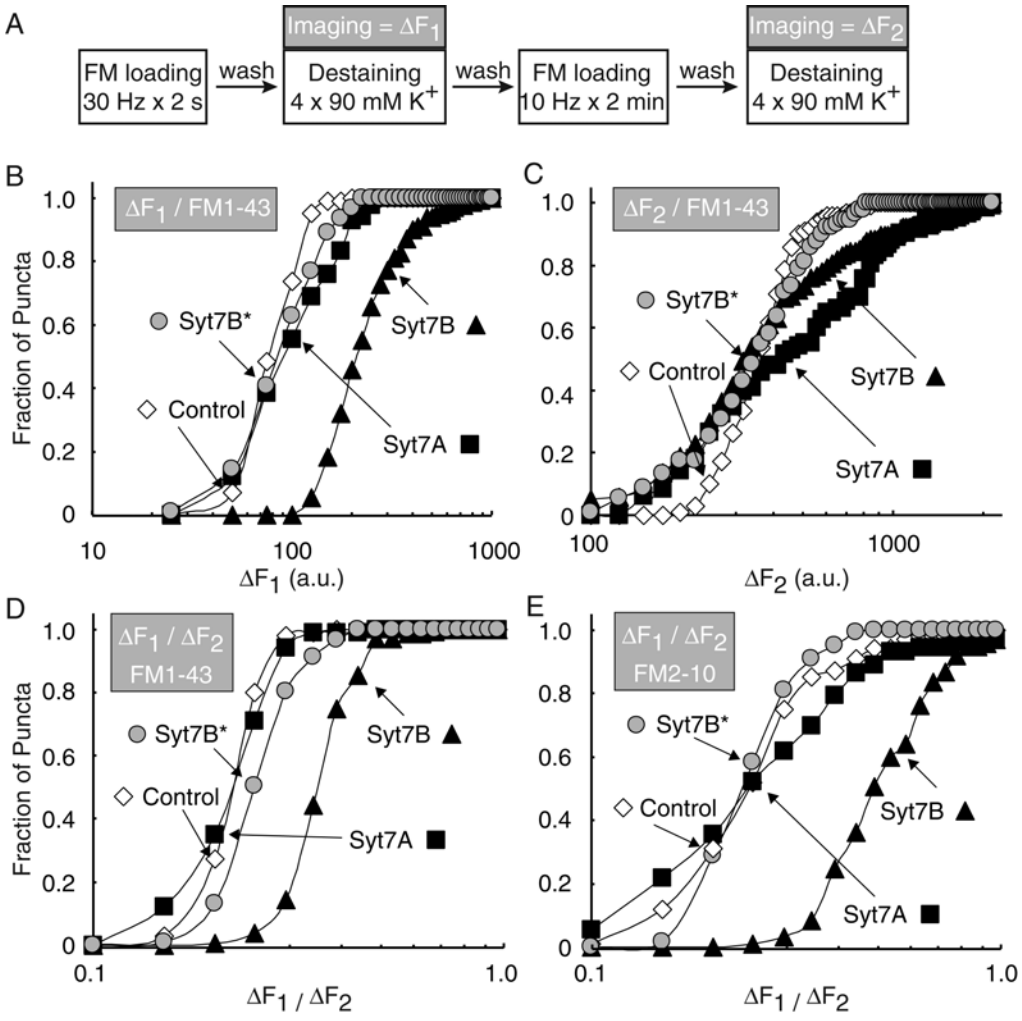

Figure 2.3. Effect of short and regular synaptotagmin 7 variants on FM dye uptake during stimulation of exocytosis. **(A)** Experimental design. Neurons were exposed to FM1-43 or FM2-10 during brief electrical stimulation (30 Hz for 2 s), washed for 10 min, and the loss of FM dye from nerve terminals was imaged during repeated stimulations with 90 mM K^+/2 mM Ca^{2+} solution to quantify the amount of FM dye that was taken up by actively recycling vesicles during the initial 2 s stimulation (ΔF_1). After a 5 min wash, the same synapses were reloaded with FM1-43 or FM2-10 during prolonged electrical stimulation (10 Hz for 2 min), washed for 10 min, and again imaged during repeated stimulations with 90 mM K^+/2 mM Ca^{2+} (ΔF_2). **(B and C)** Cumulative histograms of the distributions of ΔF_1 and ΔF_2, respectively, in control terminals and in nerve terminals expressing either regular synaptotagmin 7 (Syt7A) or wild type and mutant short synaptotagmin 7 variants (Syt7B and Syt7B*, respectively). Data shown are from a representative experiment obtained with FM1-43. **(D and E)** Cumulative histograms of $\Delta F_1/\Delta F_2$ ratios from representative experiments obtained with FM1-43 and FM2-10, respectively.

We found that the size and heterogeneity of vesicle pools labeled during the brief initial stimulus (Figure 2.3B) or the longer second stimulus (Figure 2.3C) were very similar for control terminals and terminals expressing the regular synaptotagmin 7 variant (Syt7A). However, expression of the short synaptotagmin 7 splice variant (Syt7B) caused a 2-3 fold increase in the size of the pool labeled by the brief, intense stimulus (Figure 2.3B), whereas it had no significant effect on the size of the pool labeled by the longer second stimulus (Figure 2.3C), as more clearly revealed in plots of the $\Delta F_1/\Delta F_2$ ratio (Figure 2.3D). A similar effect was observed when FM1-43 was replaced with another dye, FM2-10, which has faster departitioning properties (Figure 2.3E). The effect by the short synaptotagmin 7 variant was abolished when two cysteine residues in the transmembrane region were mutated to alanine residues (Figure 2.3D,E). In addition to increasing the $\Delta F_1/\Delta F_2$ ratio, the short synaptotagmin 7 variant also decreased the slope of the population curve approximately 3-fold, suggesting that it made the synapses more heterogeneous.

A potential problem of FM staining and destaining experiments is interexperimental variability due, at least in part, to differences between cultures. This variability may be aggravated in transfected neurons because of the nature of the transfections. The actions of the short synaptotagmin 7 variant identified in the present experiments, however, were highly reproducible. The average median $\Delta F_1/\Delta F_2$ ratio for synapses expressing the short synaptotagmin 7 splice variant was 3-fold higher (0.68 ± 0.13; $p<0.01$) than that of control synapses (0.23 ± 0.02) or synapses expressing the long synaptotagmin 7 splice variant (0.21 ± 0.03; $p<0.01$; data are means ± SEMs, n= 5-9 for all comparisons, statistical significance was measured with the two-tailed t-test). The specificity of the changes induced by the short synaptotagmin 7 variant was confirmed by the finding that nerve terminals containing the mutant short synaptotagmin 7 variant Syt7B* had a two-fold lower mean $\Delta F_1/\Delta F_2$ ratio (0.34 ± 0.07; $p<0.05$; n=4) than synapses containing the wild type short synaptotagmin 7 variant. Thus a substitution of only two amino acids in the short synaptotagmin 7 variant (Figure 2.1A) largely abolished its activity. The decrease in average slope induced by the short synaptotagmin 7 transfection was also highly significant statistically (Control = 7.8 ± 0.8; Syt7A = 6.2 ± 1.6; Syt7B = 2.7 ± 0.7; $p<0.002$ for control and Syt7A vs. Syt7B). Although

the number of FM2-10 experiments was too low to allow a statistical analysis, we observed the same difference among transfected synaptotagmin 7 variants as in the FM1-43 experiments, suggesting that the selective effect we observed with the short synaptotagmin 7 splice variant is not a dye-specific phenomenon.

The short synaptotagmin 7 variant accelerates endocytosis

The data of Figure 2.3 demonstrate that expression of the short but not a regular synaptotagmin 7 variant induced a major change in the size of the vesicle pool labeled when exocytosis of the readily releasable pool is stimulated. At the same time, the short synaptotagmin 7 variant does not alter the size of the total recycling pool of vesicles. At least two hypotheses could explain the observed effect: 1. The short synaptotagmin 7 variant could increase the number of vesicles that undergo exocytosis and subsequent endocytosis during the 30 Hz x 2 s stimulation. Such an increase may involve an enhanced size of the readily releasable pool or an accelerated rate with which vesicles are recruited into the readily releasable pool during stimulation. 2. Endocytosis of vesicles after exocytosis may be accelerated in synapses overexpressing the short synaptotagmin 7 variant. According to this hypothesis, not all vesicles immediately undergo endocytosis after exocytosis, and an enhanced number of vesicles are labeled during the 30 Hz × 2 s stimulation because the short synaptotagmin 7 variant decreases the delay between exo- and endocytosis.

To distinguish between these hypotheses, we first examined the relative size of the readily releasable pool in synapses that express short and long synaptotagmin 7 variants, and the rate with which this pool is emptied upon stimulation. We labeled the total recycling pool of synaptic vesicles with FM2-10 by extensive stimulation (10 Hz for 2 min), washed out the accessible dye, and destained the synapses during imaging with the same 30 Hz × 2 s stimulus used to load synapses in the previous protocol (see Figure 2.3A) to measure the readily-releasable pool. Afterwards, we destained the synapses with four applications of 90 mM K^+ to measure the entire recycling pool of vesicles (Figure 2.4A). We observed no significant difference between control synapses and synapses expressing the short or long synaptotagmin 7 variants in the relative size of the readily-releasable pool (Figure 2.4B) or the rate with which the pool was destained (also see Figure 2.8). The same results were

obtained when we used hypertonic sucrose to measure the readily releasable pool size (Rosenmund and Stevens, 1996) (data not shown).

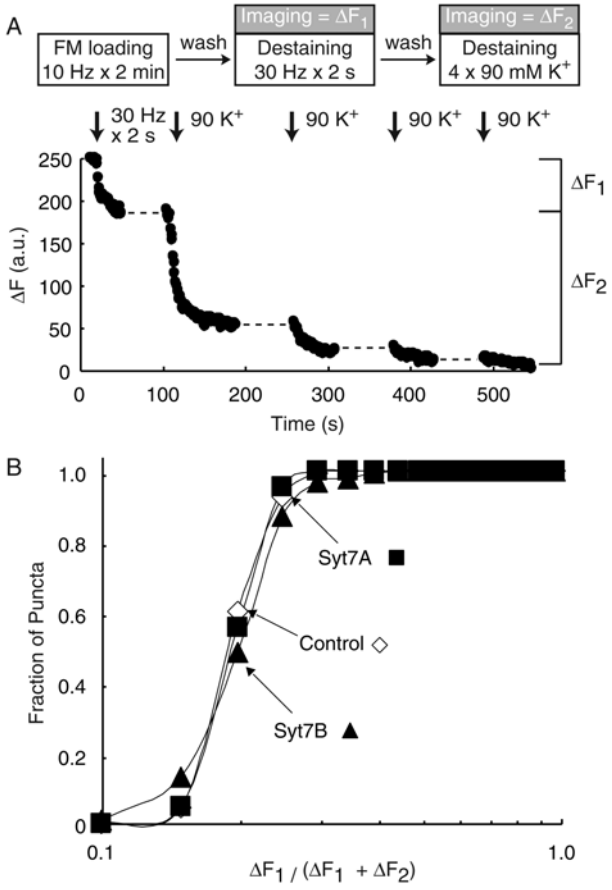

Figure 2.4. Expression of synaptotagmin 7 variants does not alter the size of the readily releasable pool. **(A)** Experimental design and sample traces. Nerve terminals were stained with FM2-10 during electrical stimulation at 10 Hz for 2 min, washed for 10 min, and FM destaining was imaged while exocytosis of vesicles in the readily releasable pool was induced by 60 stimuli (30 Hz for 2 s; ΔF_1). Afterwards the terminals were washed, and exocytosis of the total pool of recycling vesicles was induced by four applications of 90 mM K^+/2 mM Ca^{2+} (ΔF_2). **(B)** Cumulative distribution of the ratio of the readily releasable pool, measured as ΔF_1, to the total pool size measured as $\Delta F_1 + \Delta F_2$ in control synapses and synapses expressing either short or regular synaptotagmin 7 variants. Data shown are from a representative experiment obtained with FM2-10.

We next tested whether expression of the short synaptotagmin 7 variant increases the rate of endocytosis. The "acceleration hypothesis" as described above implies that vesicle endocytosis is usually incomplete when FM1-43 is washed out after the brief 30 Hz x 2 s stimulus. Thus we examined whether delaying the washout of FM1-43 after stimulation alters the size of the labeled vesicle pools in control synapses and synapses expressing short or long synaptotagmin 7 variants (Figure 2.5A). Indeed, a 3 min delay of the wash after the 30 Hz x 2 s stimulation increased the size of the labeled vesicle pool in control synapses and in synapses expressing regular synaptotagmin 7 (Syt7A), but had no effect on terminals containing the short synaptotagmin 7 variant (Figure 2.5B,C). As a result, the pool sizes after labeling with a 3 min delay are indistinguishable between control synapses and synapses expressing the short synaptotagmin 7 variant. In contrast, without the delay an almost threefold difference is observed (Figure 2.5C), suggesting that expression of the short synaptotagmin 7 variant accelerates the speed of endocytosis.

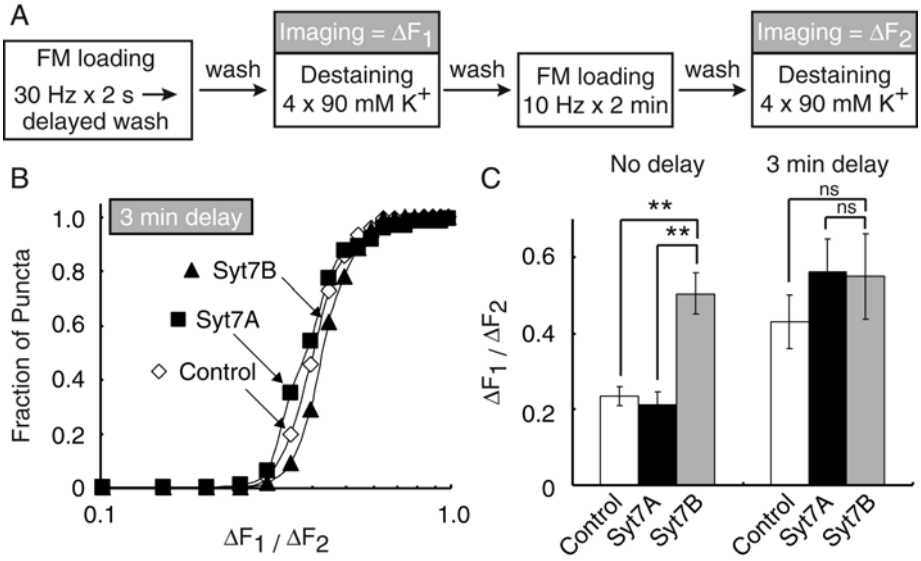

Figure 2.5. Expression of the short synaptotagmin 7 variant accelerates endocytosis. **(A)** Experimental design. Nerve terminals were stained and destained as described for Figure 2, except that after the initial electrical stimulation at 10 Hz for 2 min, the washout of the FM dye was delayed for 3 min. **(B)** Cumulative distribution of the $\Delta F_1/\Delta F_2$ ratios observed in nerve terminals measured with a 3 min delay of the wash. (**C)** Bar graphs of the average median $\Delta F_1/\Delta F_2$ ratios measured without a delay in the wash, or with the 3 min delay (error bars = ± SEMs; n = 3-4 coverslips from 2-3 independently transfected cultures; statistical significance was calculated with Student's t-test; ** $p<0.01$).

Facilitation of fast vesicle recycling by the short synaptotagmin 7 variant

In hippocampal synapses, rapidly endocytosed vesicles are thought to go through fast recycling and become re-available for exocytosis within seconds (Pyle et al., 2000; Sara et al., 2002). To quantify the re-availability of vesicles after initial dye uptake, we developed a pulse chase type of experiment for FM dye by modifying the protocol shown in Figure 2.3A with the addition of a second 30 Hz × 2 s stimulation. The initial stimulation is applied in the presence of dye, leading to dye uptake and the second stimulation is applied after rapid dye washout to check for availability of dye-loaded vesicles for a subsequent round of exocytosis (Figure 2.6A). Here, due to the residual dye on cells during the dye washout period, it is not feasible to image dye destaining induced by the second 30 Hz × 2 s stimulation for the short time intervals ($\Delta t \leq 30$ s) between the two stimulations. Therefore, to determine the extent of dye release by the second 30 Hz × 2 s pulse, we quantified the amount of dye remaining in the synapses after complete destaining with 90 mM K^+, applied 10 minutes following the second 30 Hz × 2 s stimulation. In addition, to facilitate dye washout and to increase the accuracy of the measurements, we used FM2-10, a dye with a faster membrane departitioning rate than FM1-43 (Klingauf et al., 1998; Ryan et al., 1996).

In non-transfected control synapses, application of a brief 30 Hz × 2 s stimulation leads to dye uptake with a distribution around 30% of the total pool (gray bars Figure 2.6B). 30 seconds later, application of a second 30 Hz × 2 s stimulation shifted this distribution towards 20% of the total pool (due to dye loss from the recycled vesicles) without a significant change in its shape (open bars). This shift suggests that control synapses have a uniform rate of recycling, and they recycled more than 10% of the total pool within the 30 seconds time interval. In the case of synapses expressing the short splice variant syt7B, the distribution of dye uptake during the 30 Hz × 2 s stimulation was much broader than that of controls (gray bars, Figure 2.6C). After a second stimulation, this distribution shifted leftward, and also sharpened around 20% of the total pool (open bars, Figure 2.6C). The substantial change in the shape of this distribution tells us that faster endocytosing synapses, comprising the long tail of the distribution, also exhibit faster vesicle recycling. Thus in these synapses, as a consequence of faster recycling, more vesicles become re-available for release

during the 30s interstimulus interval, substantially lowering their ratio of 30 Hz × 2 s to 10 Hz × 2 min loading. In contrast, synapses expressing the full-length form of synaptotagmin (syt7A) showed no significant shift in this distribution after a second stimulus train (Figure 2.6D). This result suggests that contrary to control and syt7B overexpressing synapses; overexpression of syt7B prevents vesicles from becoming re-available for release within 30 s.

To determine whether the action of the truncated splice variant requires dimerization, we performed the same analysis with synapses overexpressing syt7B with cysteine mutations (syt7B*). In these synapses the distribution of dye uptake during 30 Hz × 2 s stimulation was slightly broader than that of controls and peaked around 35% of the total pool (Figure 2.6E). However, this distribution was sharper than the distribution obtained with the non-mutated truncated isoform. After a second stimulus at 30s, as in controls, the distribution shifted leftward without any significant change in its shape. This lends additional support to the hypothesis that the truncated isoform promotes fast recycling since the dimerization deficient mutated form of the same protein no longer shows the same extent of vesicle re-availability during the second 30 Hz × 2 s stimulation.

To examine the time course of vesicle recycling in these synapses we performed the same experiments depicted in Figure 2.6A, with 5 and 15 second time intervals between the two 30 Hz × 2 s stimulations in addition to the 30 s time point described above. We plotted the median fluorescence loss induced by the second 30 Hz × 2 s, a measure of the fraction of vesicles that were re-available for release, with respect to the time delay from the initial dye loading stimulation (Figure 2.6F). This analysis revealed that by 30 s there was a two-fold increase in the fraction of vesicles that became re-available for release in syt7B overexpressing synapses compared to controls (Figure 2.6F). In contrast, in syt7A expressing synapses none of the vesicles loaded by the brief stimulation train were re-available within the first 30 s. Additionally, the mutated form of syt7B (syt7B*) matched the control rate of recycling by 30 s indicating that facilitation of fast endocytosis and rapid recycling by syt7B required dimerization of the molecule. These results suggest that the two splice variants of synaptotagmin 7 may function as critical regulators of the rate of vesicle recycling.

According to these observations, increased levels of syt7B augments the rate of vesicle recycling whereas the full-length syt7A slows down vesicle recycling.

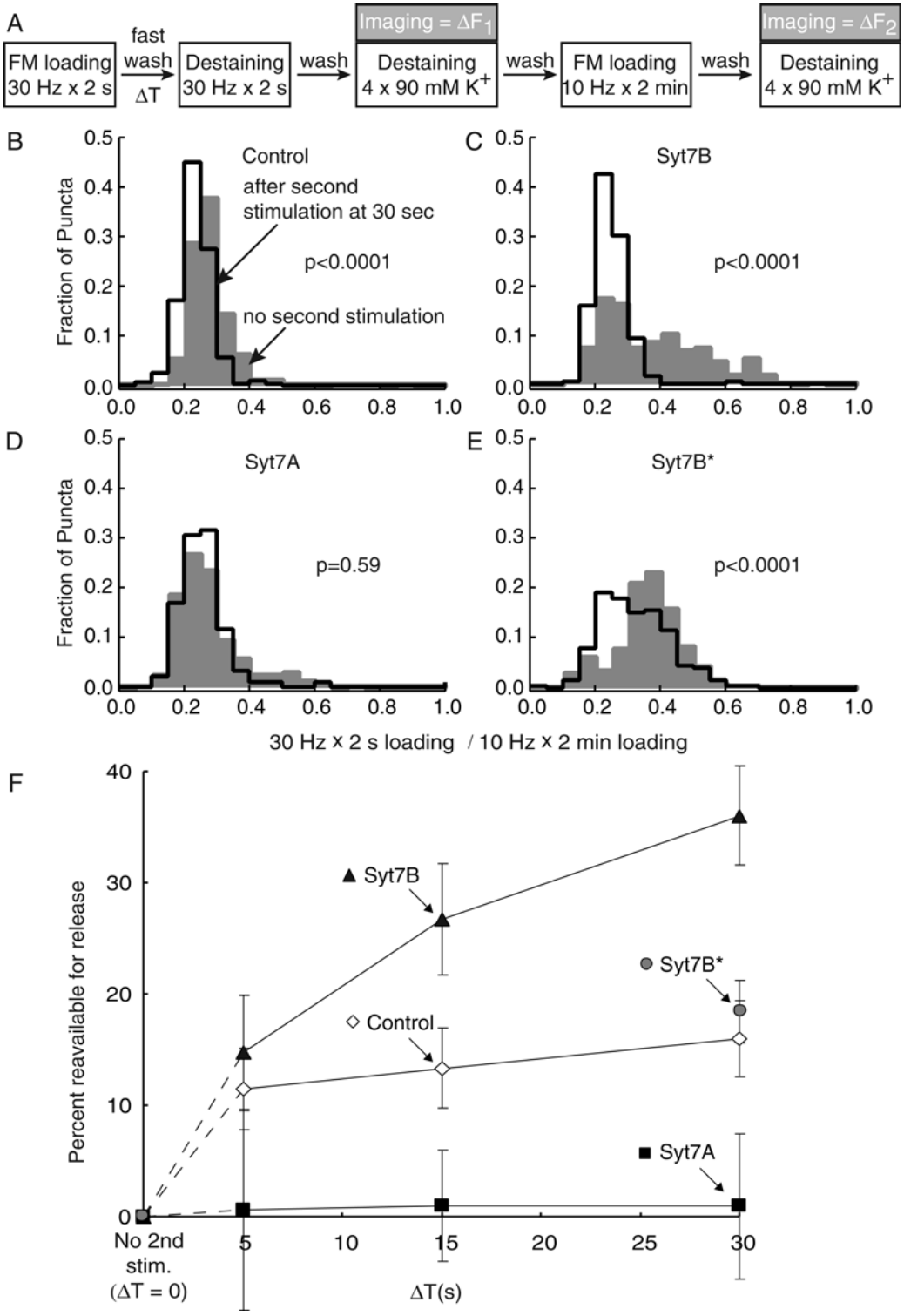

Figure 2.6. Synapses overexpressing syt7B exhibit faster recycling kinetics, whereas syt7A inhibits fast recycling. **(A)** Synapses were stained with FM2-10 with 30 Hz action potential stimulation for 2 s. Immediately after stimulation, FM2-10 was washed out by perfusion of dye-free solution at 10 ml/min. At different time intervals (Δt), after the end of the first stimulation, synapses were stimulated again with a 30 Hz train of action potentials for 2 s to destain vesicles that had become re-available for release during the time interval Δt. After the second stimulation, synapses were washed for 10 min and then imaged after exhaustive stimulation by multiple applications of 90 mM K^+/2 mM Ca^{2+}. Finally, after a brief washout period the same synapses were loaded with FM2-10, but this time by maximal stimulation (10 Hz for 2 min), and destained with 90 mM K^+/2 mM Ca^{2+} to determine the total recycling pool size (10 Hz × 2 s loading), which was then used to normalize the signal obtained in the first imaging (30 Hz × 2 s loading / 10 Hz × 2 min loading). **(B-E)** The distribution of the ratio of 30 Hz × 2 s to 10 Hz × 2 min loadings are plotted for synapses before or after a second stimulation applied at t = 30 s. Following a second 30 Hz × 2 s stimulation, synapses overexpressing syt7B (C) show a dramatic redistribution of ratios, suggesting extensive fast recycling. In contrast, control synapses (B) and synapses expressing the mutated form of syt7B (sytB*****, E) show a small shift in the distribution indicating a uniform rate of vesicle recycling. Syt7A synapses show no redistribution of ratios after the second stimulation, suggesting inhibition of fast recycling in these synapses (D). Statistical significances of the shifts in these distributions were calculated using the Kolmogorov-Smirnov (KS) test. **(F)** To determine the time-dependent change in vesicle re-availability in transfected and nontransfected synapses, we plotted the fractional dye loss induced by the second 30 Hz × 2 s stimulation versus Δt. These values were calculated using the normalized difference between the medians of the distributions at t = 5, 15, and 30 s time points with respect to the t = 0 (no second stimulation) time point (fractional dye loss at Δt = t is given by (Berglund et al., 2002) / [30 Hz × 2 s / 10 Hz × 2 min loading (Δt = 0)]). Note that syt7B-overexpressing synapses manifest a faster recycling compared to control whereas syt7A-expressing synapses show no recycling up to 30 s after the loading stimulus. The errors were propagated by standard error propagation methods (if z = x/y, and δx , δy are the errors in x and y, the fractional error in z is $\delta z/z = ((\delta x/x)^2 + (\delta y/y)^2)^{1/2})$), which due to the small numbers resulted in large error values. However, even with large propagation errors, the results were still significant. For each symbol, the number of synapses ranges between 100 to 350, from 4 to 6 coverslips each.

The long but not short synaptotagmin 7 variant alters FM labeling in response to K^+-stimulation

The data of Figs. 2.3-2.6 showed that the short synaptotagmin 7 variant likely accelerates vesicle endocytosis and recycling, while the regular synaptotagmin 7 variant

decreases the rate of recycling without any effect on fast endocytosis. This bi-directional effect supports the specificity of the observations made for the short synaptotagmin 7 variant, but does not rule out a role for the regular variant on endocytosis since all of the assays used preferentially detect changes in fast vesicle endocytosis, and would have missed any change in slower endocytic pathways. To test whether a role of the regular synaptotagmin 7 variant in endocytosis could be detected under stronger stimulation conditions that make it easier to uncover decreases in the rate of endocytosis, we examined the size of synaptic vesicles pools that are loaded with FM1-43 or FM2-10 during K^+-depolarization which causes maximal exo- and endocytosis (Ryan et al., 1993). We determined the median fluorescence value (ΔF) of control synapses and synapses expressing the short and regular synaptotagmin 7 variants as described above (Figure 2.3), and normalized all data for those of control synapses (Figure 2.7A).

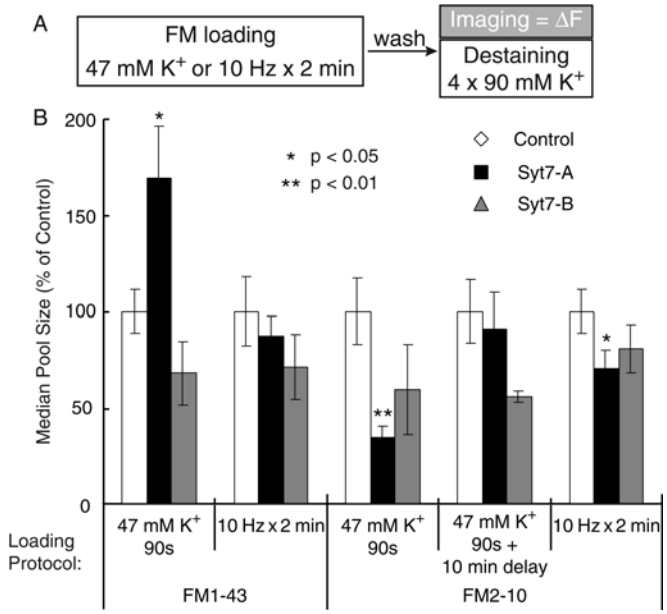

Figure 2.7. Size of synaptic vesicle pools stained by FM1-43 and FM2-10 during K^+-depolarization. **(A)** Experimental design. Nerve terminals were stained with FM1-43 or FM2-10 by K^+ depolarization (47 mM K^+/2 mM Ca^{2+} for 90 s) or 10 Hz x 2 min field stimulation, washed for 10 min, and FM destaining was imaged during repeated K^+ depolarizations to quantify the amount of FM dye taken up in the initial stimulation. **(B)** Bar graphs of the average median ΔF values of transfected synapses normalized to non-transfected control synapses under the different loading protocols (n=4-15 coverslips from 2-8 independently transfected cultures; * $p<0.05$; ** $p<0.005$ student's t-test).

Expression of the regular synaptotagmin 7 variant increased the size of the vesicle pool stained by FM1-43 during K^+-depolarization almost two-fold (Syt7A = 169 ± 27% of control; $p<0.05$; n = 11-15), but decreased the pool stained by FM2-10 more than two-fold (Syt7A = 35 ± 5% of control; $p<0.005$; n=7-9) (Figure 2.7B). The short synaptotagmin 7 variant had no significant effect, demonstrating that the changes caused by the regular synaptotagmin 7 variant are not a transfection artifact. Overexpression of synaptotagmin 1, which is very similar in structure to regular synaptotagmin 7, did not show this differential dye uptake (see Figure 2.9B), lending additional support to the specificity of the synaptotagmin 7 effect. The differential effect of the regular synaptotagmin 7 variant on the vesicle pool sizes stained by FM1-43 and FM2-10 suggests that under the conditions of the experiments, the two dyes label at least partly non-overlapping pools. At the neuromuscular junction, FM1-43 becomes trapped during extensive stimulation before endocytosis is completed, while FM2-10 with a faster rate of departitioning is washed out; as a result, the FM1-43 labeled pool is larger and includes vesicles recycling via cisternae that are not detected by FM2-10 (Richards et al., 2000). If this mechanism applied to central synapses, the regular synaptotagmin 7 variant must have shifted synaptic vesicle recycling dramatically from a faster into a slower recycling pathway. This transition must occur without changing the overall amount of exocytosis since FM1-43 labeling increases, whereas FM2-10 labeling decreases. The magnitude of the changes suggests that this shift involves the majority of vesicles undergoing exocytosis during the K^+ stimulation.

To test this hypothesis, we examined whether leaving FM2-10 in the solution longer may enable the slowly recycling pool to take up more FM2-10, comparable to the delay experiments described in Figure 2.5. After loading FM2-10 into terminals during K^+-depolarization, we incubated synapses for an additional 10 min in FM2-10 in normal extracellular buffer before washing out the dye. The delayed removal of FM2-10 dramatically increased the apparent pool size labeled in synapses expressing the regular synaptotagmin 7 variant, but not in control synapses or synapses expressing the short synaptotagmin 7 variant (Figure 2.7B). This effect was found to be specific to high K^+ loadings as we did not see any significant increase in FM1-43 uptake in syt7A

overexpressing synapses during 10 Hz x 2 min stimulation while there was even a slight but significant decrease in FM2-10 uptake during the same loading protocol (Figure 2.7B).

The rate of synaptic vesicle exocytosis is unaltered under prolonged stimulation

Since the data in Figure 2.7 appears to show that central synapses do not normally recycle vesicles via slower endosomal recycling pathways, the question arose whether the increased recycling pool size in Syt7A expressing synapses altered the rate of exocytosis under prolonged stimulation. In order to test this possibility, we compared the kinetics of exocytosis between transfected and control synapses. After maximally labeling the total recycling pool with either FM1-43 or FM2-10 using 47 mM K^+/2 mM Ca^{2+} stimulation for 90 s, we stimulated the synapses at 10 Hz or 30 Hz for 90 s to monitor the kinetics of destaining (Figure 2.8A). The kinetics of destaining for FM2-10 loaded synapses overexpressing either syt7A or syt7B were not significantly different compared with control synapses during 10 Hz or 30 Hz stimulation (Figure 2.8C,E). However, in Syt7A expressing synapses loaded with FM1-43 the destaining in response to action potentials at 30 Hz stimulation diverged from control and sytB expressing synapses (Figure 2.8D), while the rate of dye loss at 10 Hz was the same for all three conditions (Figure 2.8C). We were able to fit all three 30 Hz traces with two exponential curves while keeping the same rate constants for the fast and slow phases and altering only their relative amplitudes. This result is consistent with the observation that the mean FM1-43 fluorescence trapped by synapses overexpressing SytA after high K^+ induced staining was larger compared to non-transfected controls and syt7B expressing synapses (Figure 2.7B). This observation also suggests that neither syt7A nor syt7B overexpression alters the kinetics of exocytosis and vesicle mobilization in this preparation.

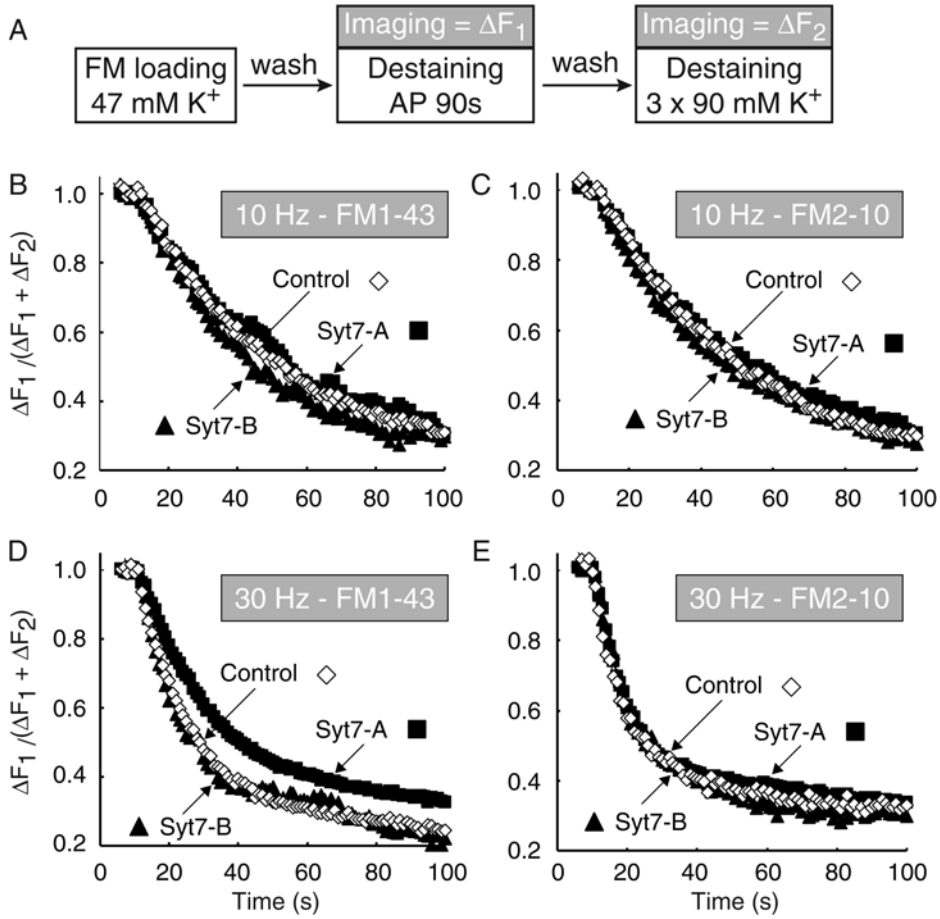

Figure 2.8. Kinetics of exocytosis unaffected by expression of either synaptotagmin 7 variant. **(A)** Experimental design. Synapses were stained with either FM1-43 or FM2-10 for 90s in the presence of 47 mM K^+. After a 10 min wash the synapses were then imaged during 90s of either 10Hz or 30Hz stimulation followed by maximal destaining using three rounds of 90 mM K^+. **(B-C)** No change in exocytosis during 10Hz stimulation after either FM1-43 loading (B) or FM2-10 loading (C). **(D)** Overexpression of syt7A shows an apparent significant decrease in the rate of release in response to 30Hz stimulation ($p<0.03$ compared to control at steady state). However all three conditions could be fit with two exponential curves, with the same rates (τ_{fast} = 16, τ_{slow} = 380) but different amplitudes of the two components (ratio of $A_{fas}t/A_{slow}$ for control = 2.1 ± 0.1, syt7A = 1.1 ± 0.1, and syt7B = 1.9± 0.2; $p<0.02$ between control and Syt7A), suggesting that the higher plateau was due to lesser availability of vesicles loaded by the endosomal to mobilization by 30Hz stimulation. **(E)** No change in exocytosis during 30Hz stimulation after FM2-10 loading. (n=4-5 coverslips from 2-3 independently transfected cultures for each condition).

Synaptotagmin 1 overexpression does not replicate the phenotype of the long form of synaptotagmin 7

The great similarity in the structure of the long synaptotagmin 7 splice variants and synaptotagmin 1 raised the possibility that the overexpression of Syt7A may be acting through a synaptotagmin 1 pathway. Recent studies have shown that very minor modifications to these proteins can change their targeting from the vesicle to the plasma membrane or vice versa (Han et al., 2004; Kang et al., 2004). To test this possibility we over expressed syt1 in our cultures and tested two main syt7A phenotypes described in Figures 2.7 and 2.8. We observed that in syt1 expressing synapses there was no increase in either FM1-43 or FM2-10 loading by $47K^+$ (Figure 2.9A, B) nor was their any divergence in the destaining kinetics of FM1-43 in response to 30 Hz stimulation. These data further confirm the specificity of the Syt7A expression phenotype as well as establish that the high levels of

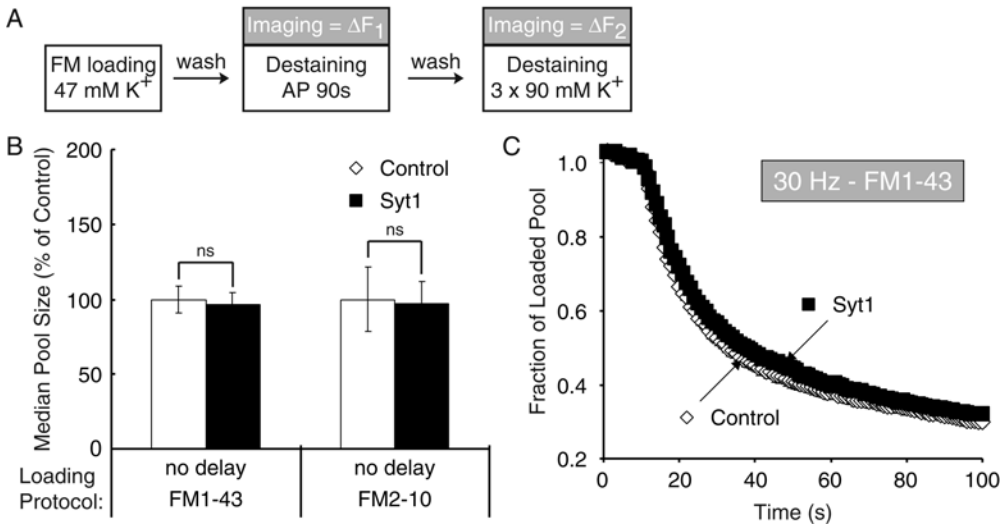

Figure 2.9. Synaptotagmin 1 overexpression does not alter vesicle pool size or exocytosis kinetics. **(A)** Experimental design. Synapses were loaded with FM1-43 or FM2-10 during $47K^+$ application for 90s. Following a 10min washout, synapses were imaged during 30Hz destaining for 90s followed by maximal destaining using 3 rounds of 90 mM K^+. **(B)** No change in loaded pool size in synaptotagmin 1 expressing synapses (syt1) compared to controls either with FM1-43 or FM2-10. **(C)** No change in FM1-43 destaining kinetics in response to 30Hz field action potentials (n=5 coverslips from 2 independently transfected cultures each).

overexpression cannot result in anomalous functioning of the proteins. It should however be noted, that it was recently observed that this synaptotagmin 1 ECFP fusion protein was unable to rescue normal synaptotagmin function in knock out mice (Han et al., 2005).

Increased large vesicular structures in electronmicrographs of stimulated synapses expressing the long form of synaptotagmin 7

Among the strongest evidence for two distinct synaptic vesicle recycling pathways are morphological studies in neuromuscular junctions showing that vesicles undergo endocytosis either at the active zone or in the area surrounding the active zone (Koenig and Ikeda, 1996). To determine whether overexpression of synaptotagmin 7 variants have a stimulation-dependent effect on the structure of nerve terminals that could correspond to the large changes in FM staining observed in the experiments described in Figure 1.7, we examined transfected neurons – unstimulated or immediately after exposure to 90 mM K^+ – by electron microscopy. Synapses overexpressing the synaptotagmin 7 variants were identified by immunogold labeling with an antibody to the CFP-moiety attached to the transfected synaptotagmin 7 (Figure 2.10). In these electron micrographs, we potentiated the immunogold signal by silver-enhancement; as a result, the immunoreactive material only reports on the general area but not the precise location of the antigen. Nevertheless, consistent with earlier immunoelectron microscopy of endogenous synaptotagmin 7 in brain (Sugita et al., 2001), ECFP-synaptotagmin 7 immunoreactivity was primarily detected close to the plasma membrane or over interior membranes in nerve terminals, whereas the vesicle cluster remained unlabeled (Figure 2.10).

We then studied the structures of the labeled nerve terminals. We observed no major alterations in unstimulated terminals expressing or lacking synaptotagmin 7 variants. In stimulated nerve terminals, however, overexpression of the regular but not the short synaptotagmin 7 variant induced massive changes: synaptic vesicles were depleted, and large membranous structures – either representing endosomes or plasma membrane cisternae – appeared (Figure 2.10). Quantification from two independent experiments confirmed that the short synaptotagmin 7 variant showed only a minor but significant decrease in synaptic vesicle density, whereas the regular synaptotagmin 7 variant caused a 3-4 fold decrease in the

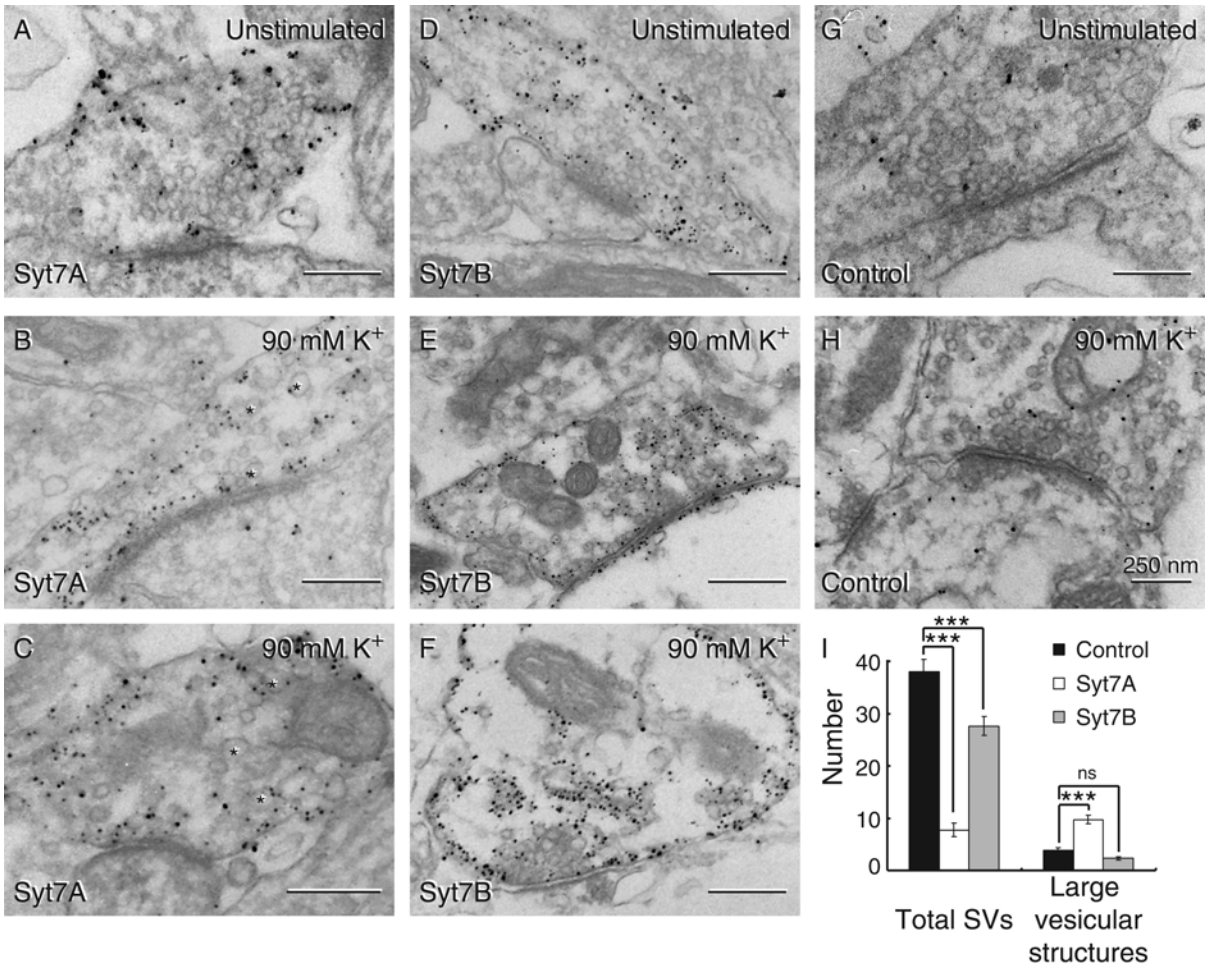

Figure 2.10. Effect of synaptotagmin 7 overexpression on synaptic ultrastructure. **(A – H)** Representative immuno-electron micrographs of synapses from transfected neurons examined without stimulation or after stimulation by K^+ depolarization (90 mM K^+/ 2 mM Ca^{2+} for 90 s). Neurons were labeled with antibodies to GFP, and signals were amplified by silver enhancement to identify nerve terminals expressing CFP-tagged synaptotagmin 7 variants. Note that boutons containing regular synaptotagmin 7 (Syt7A) display a depletion of synaptic vesicles and an increase in large vesicular structures (asterisks, diameter >90 nm). **(I)** Quantification of the number of vesicles and large vesicular structures from electron micrographs. We observed a marked decrease in vesicles (~40 nm) in synapses overexpressing the regular syt7A (n = 26 synapses) compared with nontransfected controls (n = 32 synapses) and syt7B-overexpressing synapses (n = 26 synapses) (***p<0.001). In addition, there was an increase in large vesicular structures in syt7A-expressing synapses compared with control and syt7B-transfected synapses (***p<0.001).

density of synaptic vesicles, and a 2-3 fold increase in the density of large non-vesicular

membranes in the terminals (Figure 2.10). These findings, consistent with the FM loading results described in Figure 2.7 and 2.8, indicate that only the regular form of synaptotagmin 7 induces a shift in synaptic vesicle recycling towards a delayed pathway.

Overexpression of the regular synaptotagmin 7 variant enhances synaptic depression during repetitive stimulation

Are the changes observed upon synaptotagmin 7 overexpression physiologically significant? Viewed together, our data suggest that the two synaptotagmin 7 splice variants examined here, the short variant lacking C_2-domains and the regular variant containing C_2-domains, direct synaptic vesicle recycling into opposite directions: the short variant accelerates recycling, whereas the regular variants promotes a slower, possibly endosomal recycling pathway. However, at least in the case of the regular synaptotagmin 7 variant, we only obtained evidence for a regulatory effect in recycling upon stimulation of exocytosis by strong, non-physiological K^+-depolarizations. More direct would be to measure synaptic transmission, which is difficult to do in transfected neurons. To achieve this, we optimized the transfection procedure to obtain transfection of at least 10-15 % of neurons in our cultures, and then performed recordings during repetitive 10 Hz electrical field stimulation from neurons in regions with a high density of transfected synapses.

When challenged with 10 Hz stimulation, synapses expressing the regular synaptotagmin 7 variant exhibited a significantly faster rate of synaptic depression (τ_{fast} = syt7A; 25.2 ± 6.4, ECFP; 82.9 ± 21.5, syt1; 106.3 ± 24.8 syt7B; 83.6 ± 22.1; $p<0.03$ for ECFP, syt 1 and syt7B vs. Syt7A; n=11-12) and a lower steady-state plateau than synapses expressing either ECFP or syt 1 as transfection controls (syt7A; 0.12 ± 0.02, ECFP; 0.24 ± 0.04, syt 1; 0.21 ± 0.04; $p<0.03$) (Figure 2.11A, B). In contrast, neurons from cultures transfected with the short synaptotagmin 7 variant displayed a slightly elevated level of sustained release (0.27 ± 0.04). The starting amplitudes of synaptic responses, as measured in multiple independent experiments, were also similar for all the different conditions studied (Syt7A: -1214 ± 162 pA; Syt7B: -1345 ± 230 pA; ECFP: -1092 ± 174 pA; Syt 1: -1158 ± 171 pA; n = 11-12), but significantly lower than those of untransfected cultures (control: -1677 ± 226 nA), presumably because the transfection procedure decreases the number of

functional synapses in cultures. The similar size of synaptic responses after expression of the short or regular synaptotagmin 7 variant indicates that these variants do not cause differential

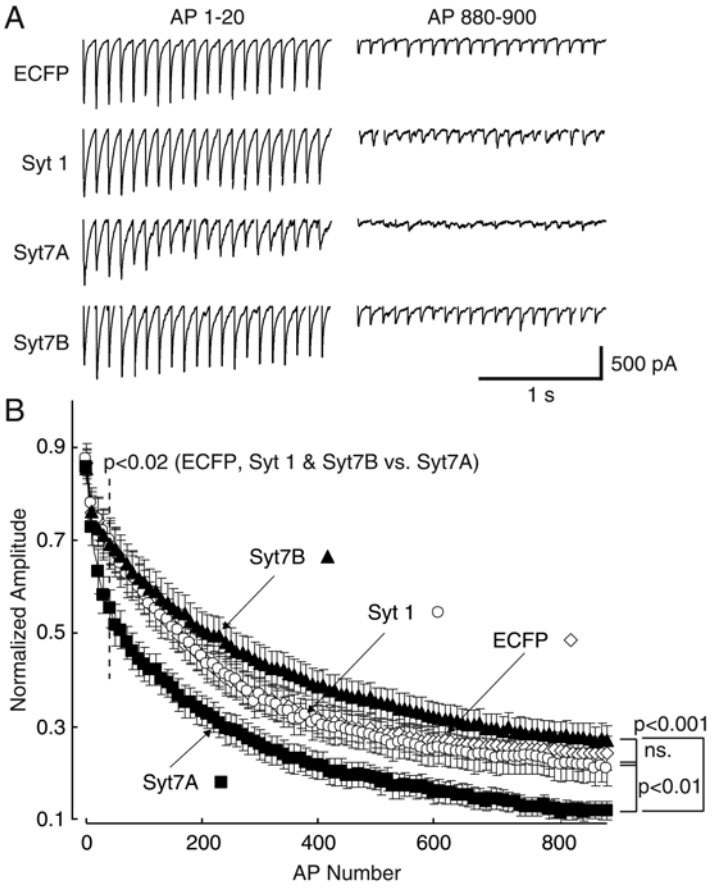

Figure 2.11. Effect of synaptotagmin 7 overexpression on synaptic responses recorded electrophysiologically. **(A)** Representative whole-cell recordings in neurons from cultures transfected at high efficiency with regular synaptotagmin 7 (Syt7A), short synaptotagmin 7 (Syt7B) and two control proteins, synaptotagmin 1 (syt 1) and ECFP alone. Recordings were made during 10 Hz stimulation from high-density cultures with each signal resulting from multiple synapses per neuron; only the first and last 20 responses during a total of 900 stimuli are shown. **(B)** Average normalized response amplitudes from nontransfected cells stimulated at 10 Hz by field electrodes. Each point represents the average of 10 consecutive responses. Syt7B overexpression results in a higher steady-state plateau of response amplitudes. In contrast, syt7A overexpression results in faster depression of the initial responses ($p<0.02$; $n=12$) as well as a lower response amplitude at steady state compared with both controls ($p<0.03$; $n=11$-12) and Syt7B ($p<0.001$; $n=11$) overexpression.

effects on the number of synapses or synaptic vesicle release probability. Thus the distinct effects of the two synaptotagmin 7 variants on the rate of use-dependent depression during the 10 Hz stimulation (Figure 2.11) must be related to the endocytosis and recycling of synaptic vesicles.

Synaptic recovery after depression is enhanced by overexpression of the short synaptotagmin 7 variant

We previously showed that synaptic vesicle recycling was bi-directionally regulated, with the short synaptotagmin variant (syt7B) enhancing the re-availability of FM dye for release while the long form (syt7A) decreased re-availability (Figure 2.6). However electrophysiologically we only observed a statistically significant increase in the depression of the response amplitude in syt7A expressing synapses. While it is likely that this is due to the limitations of the transfection efficiency, thereby providing us with a heterogeneous population of synapses onto the cells being recorded from, we wanted to try and unmask a physiological effect of the short form overexpression. To do this we studied the recovery of response amplitudes after prolonged synaptic depression. This experimental paradigm should provide us with electrophysiological insight similar to the dye recycling experiment where the terminals were allowed to recover for a certain time (Δt) before receiving the second destaining tetanus. We first subjected our cultures to 900 APs at either 10 Hz or 30 Hz through field electrodes and then recorded the recovery of their responses after 1 second during a train of 120 AP delivered at 1 Hz (Figure 2.12A). What we observed was that recovery from depression was significantly faster in syt7B expressing synapses both after 10 Hz depression (Figure 2.12B) and 30 Hz stimulation (figure 2.12C) while recovery by syt7A expressing synapses was not significantly different from controls. This data further supports the bi-directionality of synaptotagmin 7 splice variants on endocytosis and synaptic vesicle recycling.

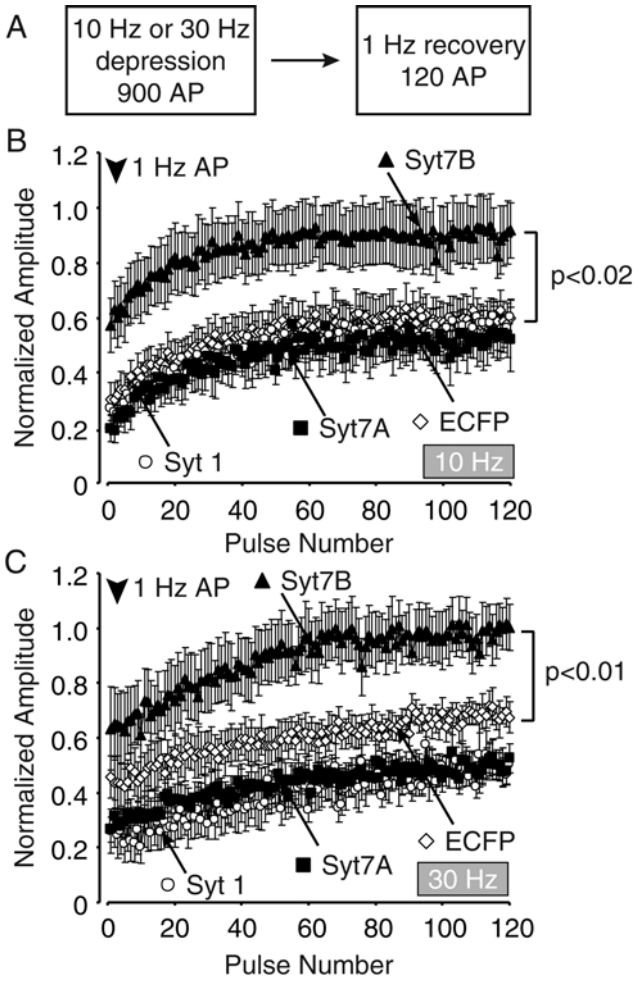

Figure 2.12. Expression of short synaptotagmin 7 variant results in faster synaptic recovery from depression. **(A)** Experimental protocol. Cells were stimulated for 900 AP by either 10Hz or 30Hz field stimulation, and following a 1s gap recovery from depression was recorded in response to 120 APs at 1 Hz. **(B-C)** Non-transfected cells surrounded by a high portion of syt7B overexpressing synapses showed significantly faster recovery from both 10Hz (B) and 30Hz (C) depression compared to cells surrounded by ECFP or Syt1 expressing synapses ($p<0.02$ at 120AP). There was no change in recovery for cells in a Syt7A expressing synapse background. (n = 4-9 cells each)

Synaptotagmin 7 splice forms may have differential expression in different brain regions

It is possible that the levels of synaptotagmin 7 splice variants could set the steady-state tone for synaptic vesicle recycling in different brain regions. We tested this by using

antibodies against the alternatively spliced domain of synaptotagmin 7 we performed a western blot analysis on brain tissue homogenates from different brain regions (Figure 2.13). Preliminary evidence suggests that the levels of the short form may be highly regulated (syt7B). We only saw significant bands migrating at the appropriate size in spinal cord and brain stem, with a faint band present in cerebellum. However, this analysis needs to be repeated with the expression of purified short form as a control to show that this antibody binds these splices variants. The longest forms of synaptotagmin (syt7L, figure 2.13), which when expressed in our system showed localization primarily to the cell body and proximal dendrites, appear to have lower levels in these same regions. Thus it is possible that this may be an artifact of the processing of these samples, therefore repetition of this experiment would be necessary for conclusively say that these splice forms show differential expression. It is also possible that this protein is under more tight regulation in regions such as the cortex or hippocampus, which is why we do not observe any short form as the levels may be kept low until required. However the preliminary results are promising and further exploration is warranted.

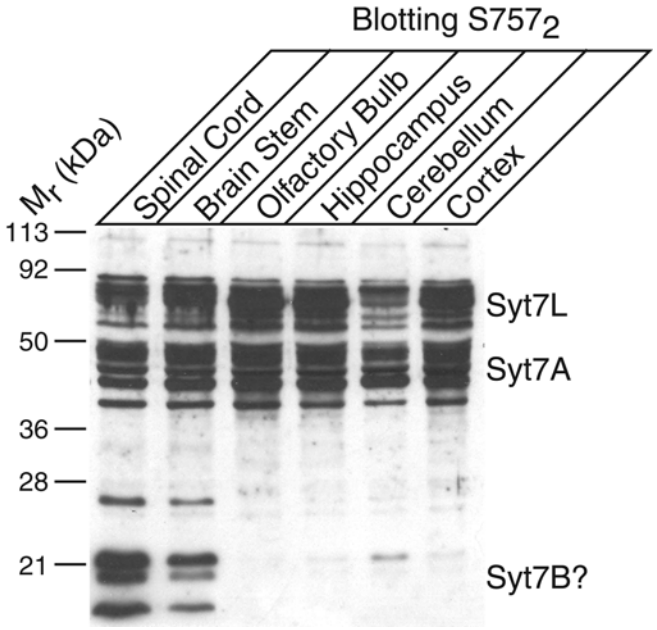

Figure 2.13. Western blot of synaptotagmin 7 splice variants. Preliminary western blot analysis shows that these splice variants may be differentially regulated in different regions of the brain, allowing for establishment of different steady state levels of vesicle recycling.

Discussion

Nerve terminals contain at least two different pools of synaptic vesicles, a readily-releasable pool and a reluctant or reserve pool (Neher, 1998). When a nerve terminal is stimulated, readily releasable vesicles undergo exocytosis first, while reserve vesicles are recruited for exocytosis when the readily releasable pool has been exhausted. After exocytosis, the two pools appear to be re-filled via at least two recycling pathways: a fast pathway that preferentially refills the readily-releasable pool, and a slower pathway that preferentially directs vesicles into the reserve pool (Li and Murthy, 2001; Richards et al., 2000). In spite of extensive physiological characterization, the molecular mechanisms involved in the release and recycling of vesicle pools remain unclear. In the present study, we show that two splice variants of synaptotagmin 7 differentially affect synaptic vesicle recycling. Our results build on previous studies demonstrating that in non-neuronal cells, truncated synaptotagmin 7 inhibits clathrin-mediated endocytosis (von Poser et al., 2000), and that in neuronal cells, a splice variant of synaptotagmin 7 encoding a truncated form is normally expressed (Sugita et al., 2001). Our data are consistent with a simplistic model (Figure 2.13) whereby a "checkpoint" after exocytosis controls the recycling pathway of a vesicle, and the checkpoint is manned by alternatively spliced variants of synaptotagmin 7.

In these experiments, we have made two principal observations: (i) The short synaptotagmin 7 variant accelerates endocytosis and recycling of synaptic vesicles, (ii) in contrast, the regular C_2-domain containing synaptotagmin 7 variant directs synaptic vesicles into a slower recycling pathway. The first conclusion is based on the following evidence: (i) The short synaptotagmin 7 variant increased FM labeling of recycling vesicles during brief, intense stimuli (Figure 2.3). (ii) The increase in FM labeling under these conditions was abolished when the FM dye was not washed out immediately after the stimulation (Figure 2.5). (iii) The short splice variant increased the rate of FM dye re-availability as measured by a pulse chase dye experiment (Figure 2.6). (iv) The short variant increased the rate of recovery from synaptic depression (Figure 2.12). (v) The short synaptotagmin 7 variant had no significant effect on other parameters, including the structure of nerve terminals as

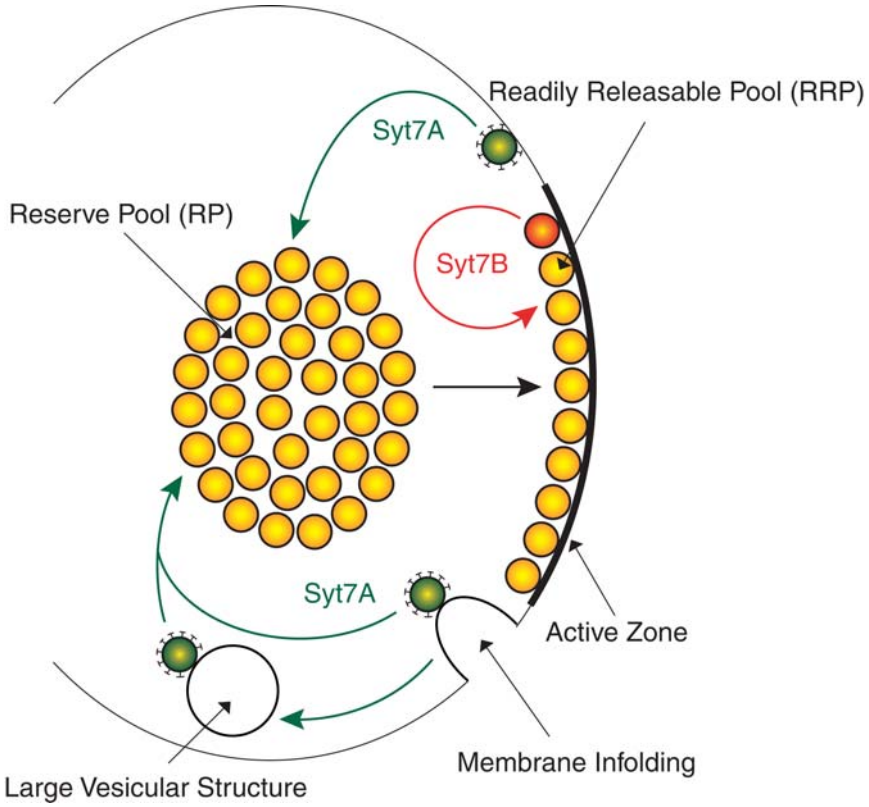

Figure 2.14. Model of syt7 function. The short splice variant of synaptotagmin 7 (syt7B) lacking the two C2 domains directs vesicles towards a fast local recycling pathway. The regular splice variant, syt7A, targets vesicles towards slower trafficking pathways. These slower pathways include classical clathrin mediated retrieval of individual vesicles from the plasma membrane or from intermediate membranous structures.

visualized by electron microscopy (Figure 2.10), the rate of exocytosis (Figure 2.8), the relative size of the readily releasable pool (Figure 2.4), or the amount of release that was stimulated by a single action potential (Figure 2.11). Conversely, the second conclusion - that the regular synaptotagmin 7 variant redirects recycling vesicles into a slow recycling pathway is based on the following evidence: (i) Overexpression of the regular synaptotagmin 7 variant caused a large shift in pool sizes of vesicles labeled with FM1-43 and FM2-10 when terminals were stimulated maximally by K^+-depolarization (Figure 2.7). No such shift was observed for less extensive labeling conditions, e.g. application of 1200 action potentials at 10 Hz for 2 min (Figure 2.3 and 2.7). (ii) Stimulation of nerve terminals containing overexpressed regular synaptotagmin 7 variant caused depletion of synaptic vesicles and

generation of large endosomal structures (Figure 2.10). (iii) The regular variant slowed recycling in a pulse chase type experiment (Figure 2.6). (iv) The regular synaptotagmin 7 variant did not alter the amount of initial release as measured electrophysiologically, but induced faster synaptic depression during 10 Hz stimulation consistent with delayed recycling (Figure 2.11). (v) In all other parameters measured, i.e. size of the readily releasable pool (Figure 2.4), kinetics of release (Figure 2.8), and amount of FM labeled vesicles under submaximal stimulation conditions (Figure 2.3 and 2.7), nerve terminals containing transfected regular synaptotagmin 7 variant were undistinguishable from controls. This indicates that synaptotagmin 7 did not alter the structure of resting nerve terminals, which is consistent with the electron micrographs of resting nerve terminals containing overexpressed synaptotagmin 7 (Figure 2.10).

Regulation of synaptic vesicle recycling by alternative splicing of synaptotagmin 7, as illustrated in the model of Figure 2.14, may participate in shaping synaptic transmission during high-frequency trains of action potentials, as is commonly observed in central neurons (Brumberg et al., 2000; Connors and Amitai, 1997). A strength of our findings lies in the fact that the two splice variants of synaptotagmin 7 tested exerted distinct effects in every assay used. The two variants thus control for each other, and exclude transfection/overexpression artifacts. In particular, the observed changes are not an effect created by ECFP overexpression since all proteins contained the same ECFP moieties in spite of having distinct actions. The findings that the action of the shorter splice variant can be abolished by point mutations in the transmembrane region which interfere with palmitoylation, and that synaptotagmin 1 does not mimic the regular length splice variant further argues against a simple overexpression artifact. However, we cannot exclude the possibility that the overexpressed proteins, in their opposing effects, do not mimic the actions of the endogenous proteins. To attempt to resolve this question, knockout mice and subsequent knockins will be analyzed in the next chapter.

What is the mechanism by which the two synaptotagmin 7 variants direct vesicles into distinct recycling pathways? Mutation of two cysteine residues in the transmembrane region (Figure 2.1A) abolishes the effect of the short variant (see Figure 2). These cysteines

were shown to be palmitoylated and to mediate synaptotagmin 7 dimerization (von Poser et al., 2000), suggesting that synaptotagmin 7 dimerization may be essential for its action. The C_2-domains of synaptotagmin 7 bind to all negatively charged phospholipids (Li et al., 1995a; Shin et al., 2002), preferentially those with multiple negative charges such as phosphatidylinositol bisphosphate, which has been shown to function in endocytosis (Cremona et al., 1999; Ford et al., 2001). The C_2B-domain binds with high affinity to the endocytic adaptor protein AP-2 (Li et al., 1995a), and may also interact with stonins as shown for synaptotagmin 1 (Martina et al., 2001; Walther et al., 2001), although this has not yet been tested. Viewed together, these findings are consistent with the hypothesis that interactions of the synaptotagmin 7 C_2-domains with molecules involved in endocytosis (PIP2, AP-2, and possibly stonin) promote clathrin-coated endocytosis only when the C_2-domains are attached to a dimer of synaptotagmin 7 variants in which both protein molecules contain C_2-domains. This hypothesis is supported by previous studies demonstrating that a truncated synaptotagmin 7 variant which is similar to the normally expressed short splice variant, when overexpressed in fibroblasts, inhibits the recruitment of clathrin coats to the plasma membrane (von Poser et al., 2000). This hypothesis would explain the differential effects of short and regular synaptotagmin 7 variants on endocytic recycling of synaptic vesicles: overexpression of the short synaptotagmin 7 variant would titrate out endogenous full-length synaptotagmin 7, and thereby downregulate clathrin-dependent endocytosis, whereas overexpression of the regular synaptotagmin 7 variant would dilute out endogenous short synaptotagmin 7 variant and thereby promote clathrin coated endocytosis. A balance between splice variants is attractive as a regulatory mechanism because it allows fine-tuning, a hypothesis that will require further testing in the future.

CHAPTER 3: Synaptotagmin 7 Mutant Mice Show Subtle Defects In Synaptic Vesicle Endocytosis And Recycling

Background

The process of synaptic vesicle exocytosis is highly regulated (Südhof, 2004). Of the known molecules involved in synaptic vesicle exocytosis, the most studied, and arguably the most important molecules are the SNARE proteins and the synaptotagmin family of proteins. The SNARE proteins involved in synaptic vesicle recycling consist of the vesicular SNARE synaptobrevin 2 (VAMP2), and the plasma membrane SNAREs syntaxin1A and SNAP25. These molecules form core complexes via their SNARE motifs in what is believed to be a zippering action, thereby allowing fusion of the vesicle membrane to the active zone plasma membrane (Jahn et al., 2003). The synaptotagmins on the other hand, are thought to function as the calcium sensors that trigger the process of vesicle fusion through their interaction with SNARE proteins.

The synaptotagmin family of proteins are characterized by an N-terminal transmembrane domain, a central linker, and two C-terminal C_2 domains (Marqueze et al., 2000; Südhof, 2002) that bind Ca^{2+} in most synaptotagmins. There are at least 15 putative members of this family, synaptotagmin 1 and 2 are the most abundantly expressed, followed by synaptotagmin 3 and 7. There are three main characteristics that distinguish the various members of the family, (i) the length of the central linker, (ii) the calcium binding affinities of the C2 domains, and (iii) the location of the protein (on synaptic vesicles or on the plasma membrane). While synaptotagmin 1 and 2 are located on the plasma membrane and their C_2 domains have low affinity binding for calcium ($EC_{50} \approx$ 10-40 μM Ca^{2+}), synaptotagmins 3 and 7 are located on the plasma membrane and show high affinity binding for calcium ($EC_{50} \approx$ 1-2 μM Ca^{2+})(Sugita et al., 2002). These differing properties have lead to the suggestion that these molecules form a hierarchy of calcium sensors for regulated exocytosis. While the role of synaptotagmin 1 in this process is well established, the roles of other synaptotagmin family members in exocytosis are just beginning to be elucidated (Fukuda et al., 2004; Iezzi et al., 2004; Jaiswal et al., 2004; Zhang et al., 2004).

The efficient coupling of exo- and endocytosis has also lead to the proposal that the molecules that function in exocytosis also may play a subsequent role in endocytosis. Recent results suggest that this proposal may indeed have some validity. Evidence from synaptobrevin null mice shows a significant slowing down of synaptic vesicle endocytosis (Deák et al., 2004). Additionally, results from synaptotagmin 1 knock out lines in drosophila (Poskanzer et al., 2003) and mice (Nicholson-Tomishima and Ryan, 2004) also suggest a role for synaptotagmin 1 in vesicle endocytosis and recycling subsequent to the calcium dependent exocytosis step. We also showed in the previous chapter, albeit in an overexpression paradigm, that the splice variants of synaptotagmin 7 can act as a molecular switch to determine whether endocytosing vesicles recycle via slow or fast recycling pathways (Virmani et al., 2003). The C_2B-domains of synaptotagmins contain a high-affinity binding site for AP-2 and possibly stonin which are involved in clathrin-mediated endocytosis (Haucke and De Camilli, 1999; Haucke et al., 2000; Jarousse and Kelly, 2001; Li et al., 1995a; Martina et al., 2001; Zhang et al., 1994), and truncated synaptotagmins similar to the normally occurring short synaptotagmin 7 splice variant are potent inhibitors of clathrin-mediated endocytosis in transfected non-neuronal cells (von Poser et al., 2000). These findings lend additional credence to the role of these molecules in both endocytosis and exocytosis.

In the present study, we studied genetically engineered lines of synaptotagmin 7, both a classical knock out mouse and a calcium binding site mutant knock in mouse to follow up on prior studies and explore the dual role of synaptotagmin 7 in exocytosis and endocytosis. To this end we employed both optical and electrophysiological recordings from cortical cultures derived from these mouse lines. Our results demonstrate that the synaptotagmin 7 null has a selective minor deficit in fast endocytosis, with normal synchronous fast exocytosis. On the other hand, the calcium binding site mutant mouse line displays faster synaptic vesicle endocytosis as well as defects in short-term synaptic plasticity. However, even in the knock in line, the synchronous release in response to single action potentials is unaffected suggesting that synaptotagmin 7 does not function in conjunction with synaptotagmin 1 for synchronous release in central synapses.

Materials and Methods

Knock out and knock in mice

The synaptotagmin 7 knock out and knock in mice were prepared using normal procedures by the Südhof laboratory (unpublished data).

Cell culture

Dissociated cortical cultures were prepared from 1-2 day-old littermate mouse pups cultured individually, as described (Kavalali et al., 1999b). Experiments were performed at 14-21 days in vitro when cells in culture have fully matured (Mozhayeva et al., 2002).

Fluorescence Imaging

Synaptic boutons were loaded with either FM1-43 (16 μM) (Molecular Probes, Eugene, OR) using either electric field stimulation in the presence of 4 mM K^+, 2 mM Ca^{2+} solution, or 90 s incubation in hyperkalemic solution 47 mM K^+/2 mM Ca^{2+}. Modified Tyrode solution containing (in mM) 150 NaCl, 4 KCl, 2 $MgCl_2$, 10 Glucose, 10 HEPES, and 2 $CaCl_2$ (pH 7.4, ~310 mOsm) was used in all experiments. Hypertonic solution was prepared by addition of 500 mM sucrose to the modified Tyrode solution. The 90 mM K^+ solutions contained equimolar substitution of KCl for NaCl. Field stimulation was applied through parallel platinum electrodes immersed into the perfusion chamber delivering 25 mA - 1 ms pulses. All staining protocols were performed with 10 μM CNQX and 50 μM AP-5 to prevent recurrent activity. Images were taken after 10-min washes in dye-free solution in nominal Ca^{2+} to minimize spontaneous dye loss. Destaining of hippocampal terminals with hypertonic/high-potassium challenge was achieved by direct perfusion of solutions onto the field of interest by gravity (2 ml/min). Images were obtained by a cooled-intensified digital CCD camera (Roper Scientific, Trenton, NJ) during illumination (1Hz-60 ms) at 480 ± 20 nm (505 DCLP, 535 ± 25 BP) via an optical switch (Sutter Instruments, Novato, CA). Images were acquired and analyzed using Axon Imaging Workbench Software (Axon Instruments, Union City, CA).

Electrophysiology

Whole-cell recordings from pyramidal cells were acquired with an Axopatch 200B amplifier and Clampex 8.0 software (Axon Instruments, Union City, CA). Recordings were filtered at 2 kHz and sampled at 200 μs. Pipette internal solution included (in mM): 115 Cs-$MeSO_3$, 10 CsCl, 5 NaCl, 10 HEPES, 0.6 EGTA, 20 TEACl, 4 Mg^{2+}-ATP, 0.3 Na_2GTP, 10 QX-314 (pH 7.35, 300 mOsm).

Miscellaneous

All error bars denote standard error of the mean (SEM); all N values correspond to individual coverslips unless mentioned otherwise; all statistical assessments were performed with the 2-tailed t-test. All experiments and analyses were performed blind to the genotype of the cultures.

Results

Generation of synaptotagmin 7 knock out and knock in mouse lines

In order to establish whether synaptotagmin 7 was essential for the normal functioning of synapses, two different mouse lines were established in the Südhof lab. The strategy is shown in Figure 3.1A (Maximov and Südhof, 2005b). A neo cassette flanked by loxP sites was inserted between exons 12 and 13 of the gene. The six calcium-binding sites, three in the C2A domain (D225, D227 and D233) and three in the C2B (D303, D357 and D359) were mutated to alanines (D->A) (Figure 3.1A). Homologous recombination allowed insertion of the vector into the genome. The mouse line with the neo cassette inserted effectively resulted in a synaptotagmin 7 knockout mouse (syt7 ko, Figure 3.1B). By removing the neo cassette using cre recombinase, a calcium binding site mutant knock-in mouse was obtained (syt7 C2AB, Figure 3.1B). Western blots from brains of these mice showed complete absence of protein in the syt7 ko mouse, but incomplete recovery of expression in the syt7 C2AB mouse (Figure 3.1B). Quantitative immunoblotting using I_{125} again showed minimal levels of synaptotagmin 7 protein in the syt7 ko line compared to wild-type (wt) littermate controls, showing that this mouse could be effectively used as a synaptotagmin 7 knock-out. However, after excision of the neo cassette, there was only about 30% recovery of the regular synaptotagmin 7 splice variants expression (syt7A constructs used in Chapter 2) and about 20-25% recovery of the longer splice variants (Figure 3.1C). This complicates the interpretation of this mouse line.

Both the homozygous mouse lines were born healthy and lived a normal life span, suggesting that the presence of this protein was not essential for synapse survival. They also showed normal weight gain over their lifespan (Maximov and Südhof, 2005b). In order to further study the effects of loss of protein, heterozygous mice were bred, and cortical cultures were made from the brains of 1-2 day old postnatal littermate control and knock out mice pups. The genotype of the mice was determined prior to culturing by a second investigator, but was withheld from my knowledge till after all experiments had been performed and analyzed. Experiments were performed after the cultures were allowed to mature for 14-21 days in-vitro.

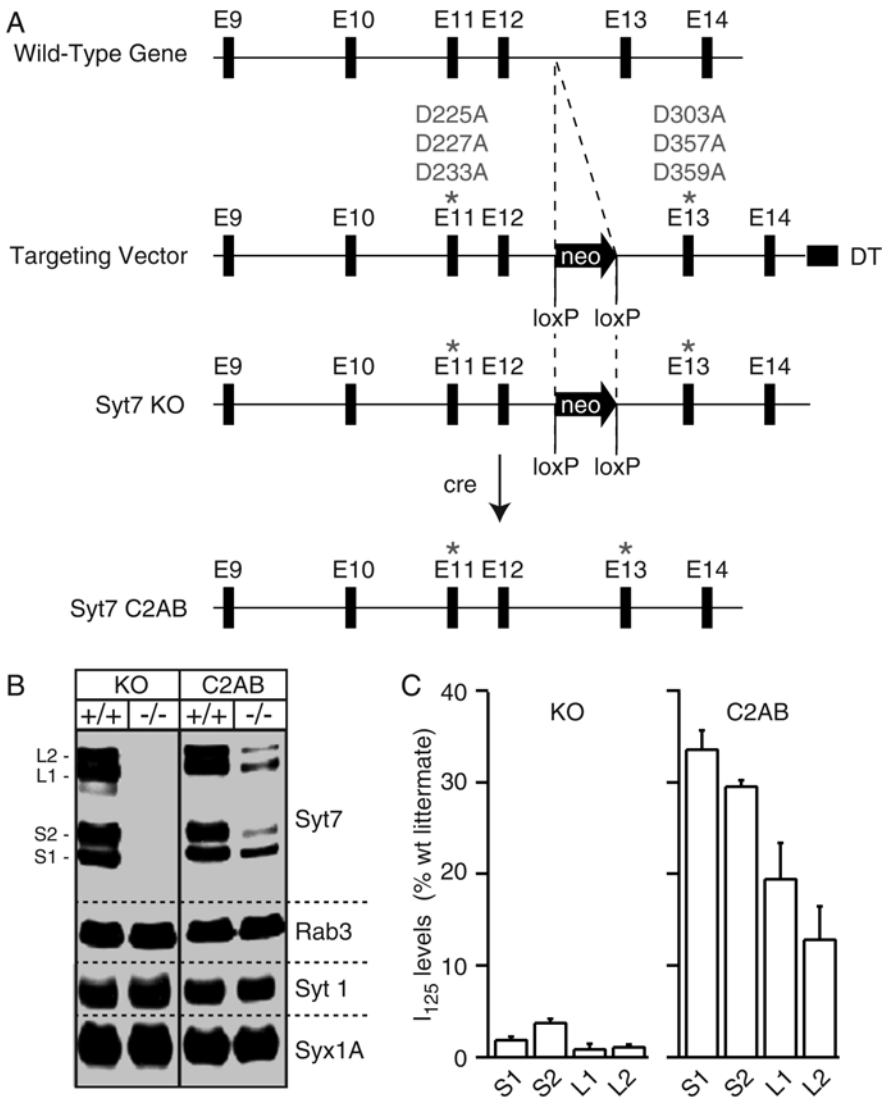

Figure 3.1. Generation of synaptotagmin 7 mouse lines. **(A)** Strategy for generation of synaptotagmin 7 knock out mice (syt7 ko) and synaptotagmin 7 calcium binding site mutant knock in mice (Syt7 C2AB). **(B)** Western blot showing absence of protein in syt 7 ko line, and incomplete recovery of expression in syt7 C2AB line. **(C)** Quantitative immunoblotting analysis using I_{125} labeling. There are very low levels of protein in syt7 ko, but less than 40% recovery of expression in the syt7 C2AB knock-in mouse.

Synaptotagmin 7 null mice show normal synchronous evoked responses and short-term synaptic plasticity

Synaptotagmin 1 (syt1) has been previously shown to be the major calcium sensor for evoked synchronous release (Geppert et al., 1994) and as a result it has been postulated that the other synaptotagmins may either complement this role of syt1 or play a role in regulating asynchronous release (Südhof, 2002; Sugita et al., 2002). To test whether there was normal synchronous release in the absence of synaptotagmin 7, we performed whole cell patch clamp recordings on pyramidal cells in the cortical cultures and evoked responses using extracellular field electrodes. Stimulating the cells at 10Hz, we saw normal synchronous release in syt7 null mice as well as littermate wt controls (Figure 3.2A inset). The amplitude of the response to a single action potential was similar in both conditions (Figure 3.2B). We next measured synaptic depression in response to prolonged repetitive stimulation. Stimulating the cells at 10Hz for 900 AP we did not see any difference in the depression of the normalized response amplitude between syt7 null cells and wt littermate controls (Figure 3.2A). Recording the recovery of the synaptic response after the prolonged depression using a train of 120AP delivered at 1 Hz, again there was no significant difference between wt and ko cells (Figure 3.2A).

We next assessed whether there was any alteration in short-term plasticity in the synapses of syt7 null cells. To do this we delivered a pair of stimuli and varied the interpulse interval from 33-1000 ms corresponding to 1 Hz to 30 Hz stimulation frequencies. Plotting the ratio of the second response to the first response in each pair we do not see any significant change in paired pulse ratio at any interpulse interval, nor is the slope of the plot altered, suggesting that the release probability is not altered by the loss of synaptotagmin 7.

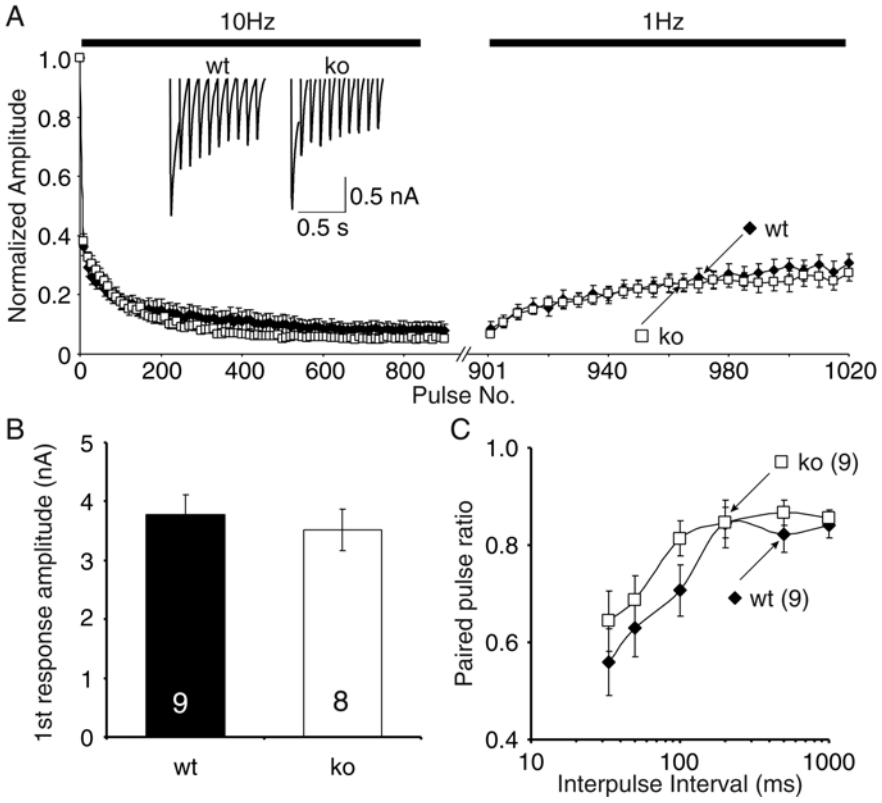

Figure 3.2. Normal synchronous release and short-term plasticity in cortical cultures from syt7 knockout mice. **(A)** Normalized average response amplitudes of 900 AP delivered at 10 Hz shows no significant change in the rate of synaptic depression (N = 8-9 cells each). Sample traces are shown in inset. Recovery from depression monitored by applying a 1 Hz train of APs to cells previously exposed to a 90 s train of 10 Hz APs, showed no change in the rate of recovery from depression (N = 8-9). **(B)** The absolute amplitude of the response to the first AP is unchanged (p = 0.61). **(C)** Paired pulse depression, measured as the ratio of the second response to the first response at different interpulse intervals was unaffected by knocking out syt7 (N = 8-9 cells each, p values range from 0.12-0.98).

Normal spontaneous and sucrose responses in synaptotagmin 7 null mice

In order to determine whether there was any more general deficiency in synapses in the null mice, spontaneous miniature postsynaptic currents (minis) were recorded from pyramidal cells in the cortical cultures in 2 mM extracellular Ca^{2+} and 1μM tetrodotoxin (TTX), sample traces of which are shown in Figure 3.3A. There was no significant difference in either mini frequency (Figure 3.3B) or amplitude (Figure 3.3C) in cells from

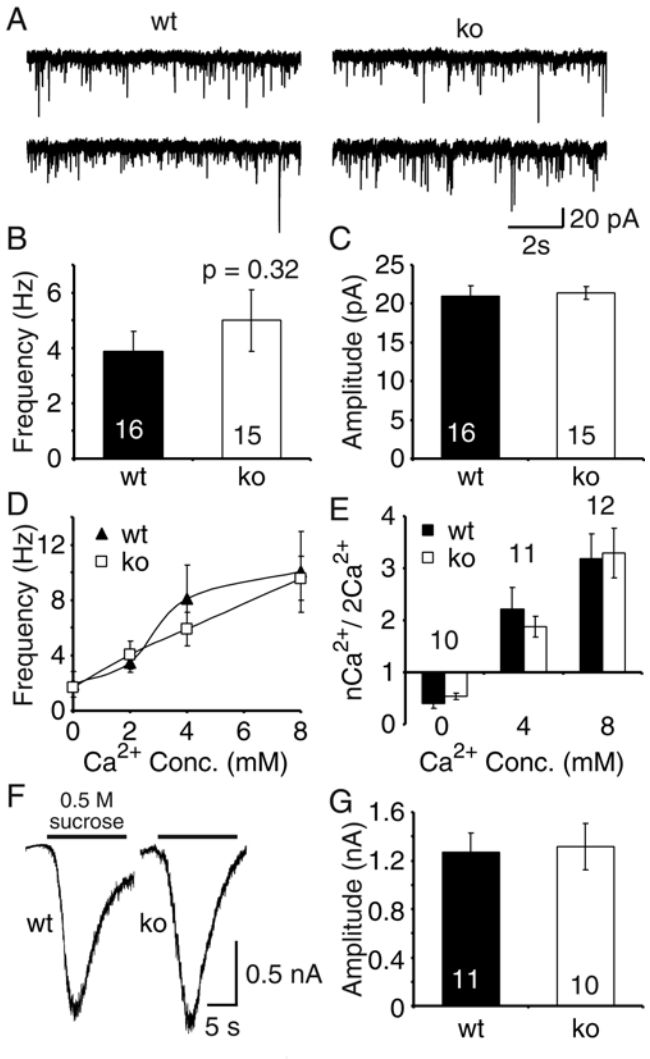

Figure 3.3. Mini frequency and calcium dependence as well as sucrose responses are unaffected by syt7 loss. **(A)** Sample traces recorded in 2 mM Ca^{2+}. **(B-C)** Mini frequency (B) and amplitude (C) are unchanged in syt7 ko cells (N = 15-16 cells each). **(D-E)** Calcium dependence of mini frequency is not altered measured either as absolute frequency (D) or measured as the ratio with respect to the mini frequency in 2mM Ca^{2+} (E) (N = 10-12 each, p values range between 0.17-0.82). **(F)** Sample traces of sucrose responses. **(G)** Quantification of peak sucrose current shows no difference between ko and wt littermate cells (N = 10-11 cells each, p = 0.86).

syt7 ko mice compared to littermate wt controls. Since synaptotagmin 7, like synaptotagmin 1 has numerous calcium-binding sites and binds lipids in a calcium dependent manner (Sugita and Südhof, 2000), the possibility still existed that syt7 may play a role in the

calcium dependence of minis. To test this possibility, we varied the extracellular calcium concentration from 0 - 8 mM. In cells recorded from wt cultures, there was almost a 6 fold increase in mini frequency going from 0-8 mM Ca^{2+} when looking at absolute frequency (Figure 3.3D). A similar range was observed in syt7 null cells. Normalizing to the mini frequency at 2 mM Ca^{2+} also showed no difference in the calcium dependence of minis between the two culture conditions (Figure 3.3E). This suggests that synaptotagmin 7 does not play a role in the regulation of minis. When we measured the response of cells to application of a 0.5 M sucrose solution, which has been previously shown to release the readily releasable pool (RRP) of synaptic vesicles in a calcium independent manner, we again saw no difference between wt and ko cells in the amplitude of sucrose responses (Figure 3.3F, G)

Taken together the normal mini and sucrose responses of cells in syt7 ko cultures suggests that normal synaptic development has taken place in these cultures and that synapse density and RRP pool size are unaffected by the absence of synaptotagmin 7.

Synaptic vesicle pool size, readily releasable pool and exocytosis rates are normal in synaptotagmin 7 null mice

We have shown that overexpression of the regular splice variant of synaptotagmin 7 in hippocampal cultures leads to an increase in the total pool of vesicles that can be stained by FM1-43 (Figure 2.7). In order to determine whether the complete loss of the protein alters the recycling vesicle pool size, we loaded synapse with FM1-43 using either 1200 AP delivered at 10 Hz or using 47 mM K+ for 90s. After a 10-minute washout period synapses were imaged during destaining by 10Hz stimulation for 90s followed by maximal destaining using 3 rounds of 90mM K^+. We observed that neither of these loading paradigms unmasked any significant change in vesicle pool size in the synaptotagmin 7 null mice (Figure 3.4A). The rate of destaining kinetics in response to 10Hz stimulation was also unaffected (Figure 3.4B).

While there was no change in the amplitude of the sucrose response, we wanted to check for changes in the readily releasable pool (RRP) of vesicles using imaging techniques as well. To this end, we loaded synapses using 10 Hz stimulation for 2 min, and following

dye washout, challenged the synapse with a tetanus of 60AP delivered at 30Hz. This stimulus has been shown by us and other labs to selectively release vesicles from the RRP. When we plotted the ratio of this drop in fluorescence to the total amount of dye trapped in the synapses (determined by imaging during 4 rounds of 90mM K^+ application after the tetanus), we found no significant change in the ratio of the RRP to total pool, suggesting that there was no physiological redistribution of vesicles in the cortical synapses of syt7 null mice.

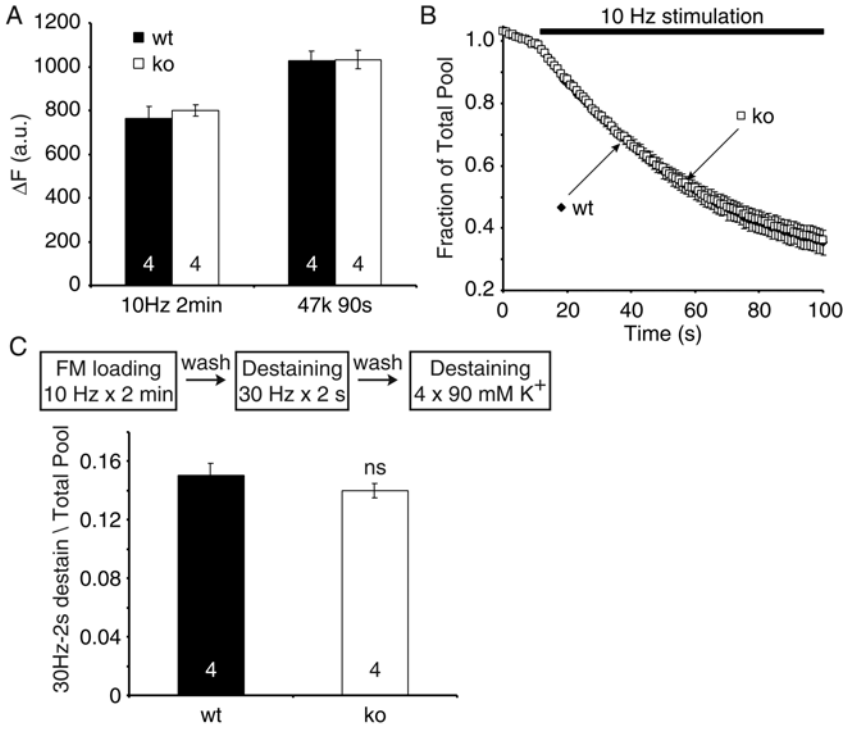

Figure 3.4. Pool size, exocytosis rates and RRP size are unaltered in syt7 ko mice. **(A)** Pool size as measured by FM1-43 dye uptake during 10 Hz field stimulation for 2 minutes or 47 mM K^+ for 90 s was similar in syt7 ko and littermate wt cortical synapses (N= 4 coverslips each). **(B)** The rate of FM1-43 dye exocytosis under 10 Hz field stimulation after maximal 47mM K^+ loading was not affected by loss of syt7 (N= 4 coverslips each). **(C)** Plot of the ratio of 30Hz-2s destaining to the total pool loaded by 10Hz-2min stimulation in the presence of FM1-43 shows no change in RRP in syt7 ko mice compared to littermate controls (N= 4 coverslips each).

Decrease in endocytosis rate in cortical synapses of synaptotagmin 7 null mice

In previous work we found that overexpression of a short splice variant of synaptotagmin 7 lead to an increased rate of vesicle endocytosis and recycling, while overexpression of regular variants decreased the rate of vesicle recycling without altering the rate of endocytosis. To determine whether the absence of synaptotagmin 7 would have an effect on the kinetics of endocytosis, we loaded synapses with a brief tetanus of 60AP at 30Hz and then rapidly washed out the extracellular dye in order to measure the amount of endocytosis that occurred during that brief 2s time period that dye was present in the bath (Figure 3.5A). After a 10-minute washout period we imaged the synapses during exhaustive stimulation with 90 mM K^+ to calculate the dye trapped during the 2 s of endocytosis. We observed that synapses from syt7 ko mice showed a small but significant decrease in dye uptake during the 2s loading compared to littermate control synapses (Figure 3.5B, C). It should again be stressed at this time that all experiments and subsequent analyses were performed blind to the genotype of the cultures.

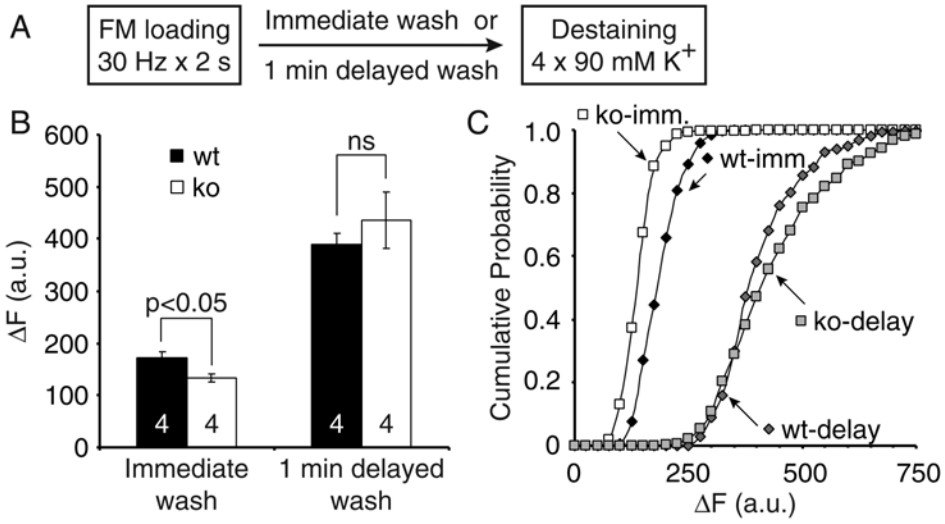

Figure 3.5. The rate of endocytosis in syt7 ko synapses is decreased. **(A)** Experimental protocol. Synapses were loaded with FM1-43 using a brief train of 60 AP delivered at 30 Hz followed by either immediate or 1 min delayed rapid dye washout. After a 10 min wash period synapses were imaged during maximal destaining using 4 rounds of 90 mM K^+. **(B)** Bar graph showing that syt7 synapses show a slight but significant decrease in dye uptake during the 30Hz-2s stimulation, which is lost upon delayed washout of the dye by 1 min. (N = 4 coverslips each, $p<0.05$ with immediate dye washout) **(C)** Cumulative histogram showing the distribution of all synapses imaged (N = 400-450 synapses each).

We previously showed that there was no change in the size of the total vesicle pool, the rate at which vesicles exocytose, or the proportion of vesicles that can be released by the 30Hz 60AP tetanus in syt7 null synapses (Figure 3.4). Taken together this suggests that the decreased dye uptake was due to a decrease in the rate of endocytosis. If the number of vesicles exocytosed in 2 s is similar between the two conditions, then delaying the washout of FM dye should allow the slower endocytosing vesicles to take up dye. Indeed when we delayed the washout of dye by just 1 min the difference in dye loading was lost (Figure 3.5B, C), lending additional credence to the slow down in endocytosis in these synapses.

Synaptotagmin 7 C2AB domain mutant mice

The minor phenotype observed in the synaptotagmin 7 null mice, coupled with the dramatic phenotypes observed on overexpression of the synaptotagmin 7 splice variants in a similar culture system suggests that it is not simply the presence or absence of the protein that is important, but quite possibly the functional levels of the splice variants of the protein. Therefore we proceeded to analyze the calcium binding site mutant mouse described above (Syt7 C2AB, Figure 3.1). This mouse has all forms of synaptotagmin (Figure 3.1B), but the sites at which calcium binds to the C2 domains have been mutated to prevent calcium binding (Figure 3.1A). One caveat to this analysis, as mentioned earlier, is that only 20-30% of the normal protein levels of the different splice variants were recovered on excision of the neo cassette. In another line, where only the C2B mutations remain, full recovery of protein was observed (Maximov and Südhof, 2005a); suggesting that mutation of all six sites may be destabilizing the protein. It is however necessary to keep this fact in mind when analyzing the phenotype of this mouse as it adds an extra level of complexity to the analysis. Also since there is not a good antibody available to the shorter synaptotagmin variants, it is not possible to tell whether these proteins are up or down regulated in this mouse, which is detrimental to the analysis of this mouse model. However the expression levels of other synaptic proteins was normal (Figure 3.1B)

Keeping these caveats in mind, we proceeded to analyze basic synaptic function in cortical cultures made from P1-P2 mouse pups, homozygous, heterozygous, and wt for these mutations. Again all experiments and subsequent analyses were performed blind to the

genotype of the mice, which was determined by a second investigator prior to culturing so as to increase the efficiency of obtaining all three genotypes in a single culture session. Cortical cultures were also used once again to allow for the production of a number of culture plates from a single pup.

Faster synaptic depression and slower recovery in synaptotagmin 7 C2AB mutant mice

Although we did not see any change in synaptic depression and recovery in the synaptotagmin 7 null mice, we have previously observed bi-directional modulation of depression by overexpression of long and short synaptotagmin 7 splice variants (Figure 2.11). To determine if the binding of calcium to the regular and long forms of synaptotagmin was involved in this process we checked the response of wild type synapses (wt), and synapses heterozygous (het) and homozygous (mut) for the mutation to depression in response to prolonged 10Hz stimulation. Surprisingly, we found that although there was no significant change in the amplitude of the first response (Figure 3.6A and B (inset)), when we plotted the averaged normalized amplitude over the 900 AP train, the heterozygous and homozygous cells showed faster synaptic depression compared to littermate wt controls (Figure 3.6B). This was most significant between pulse numbers 50-400 for wt and mut cells (Figure 3.6C).

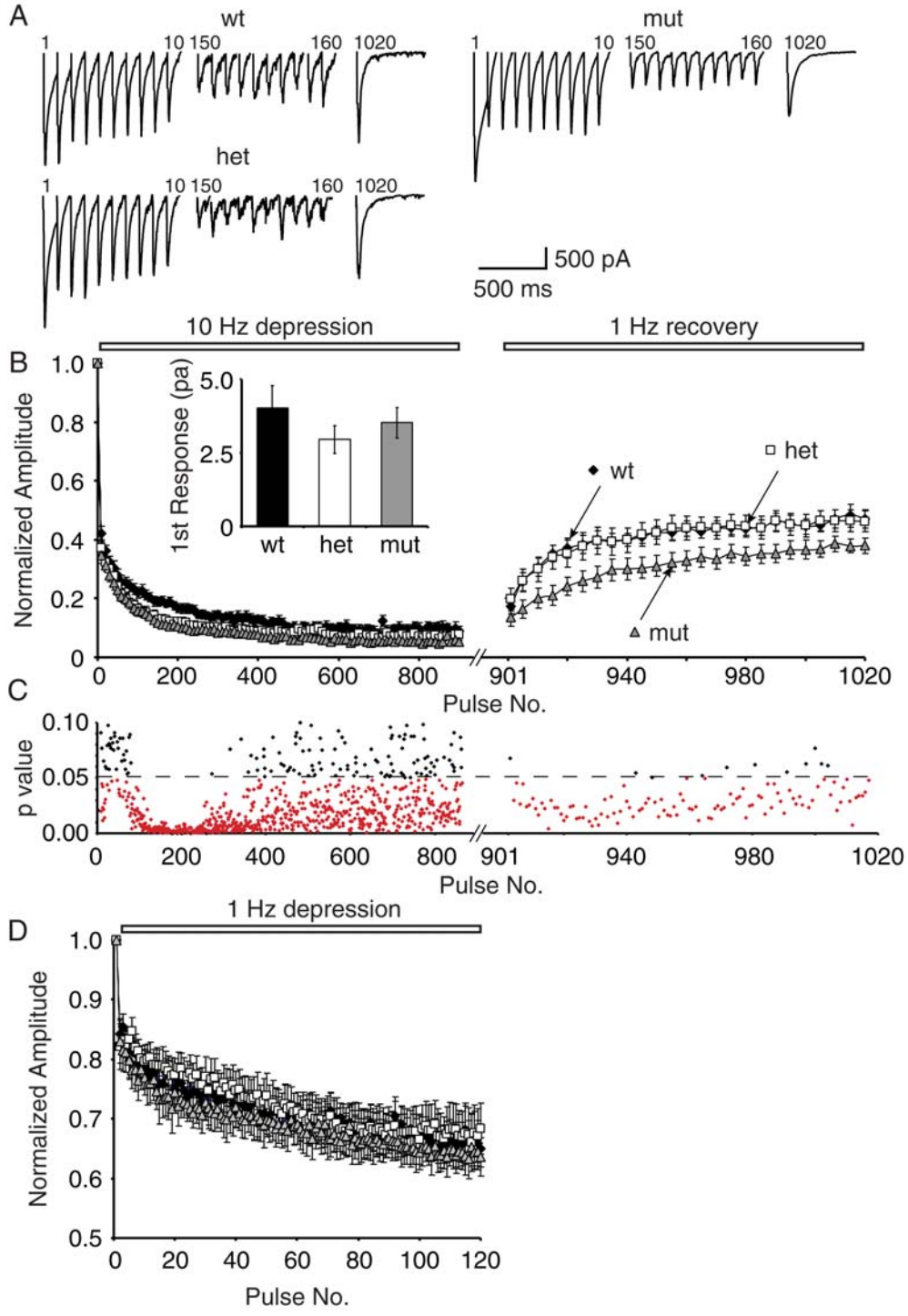
A
wt
mut
het
1
10
150
160
1020
500 pA
500 ms
10 Hz depression
1 Hz recovery
B
Normalized Amplitude
1st Response (pa)
wt
het
mut
Pulse No.
C
p value
Pulse No.
1 Hz depression
D
Normalized Amplitude
Pulse No.

Figure 3.6. Faster depression and slower recovery in homozygous mutant cells from syt7 C2AB mouse cortical cultures. **(A)** Sample traces of responses 1-10, 150-160 to a 900 AP train at 10Hz delivered using filed electrodes to measure synaptic depression. This was followed 1 s later by a train of 120 APs at 1 Hz to measure recovery, of which the last response is shown (AP #1020 of the total train). **(B-C)** Plot showing averaged normalized response amplitudes (B) and the significance between syt7 Ca^{2+} mutant cells (mut) and wild type (wt) littermate controls at each response (C). There is faster depression in heterozygote (het) and mut cells compared to wt, which is highly significant between wt and mut cells between responses 50-400 (N = 15-16 cells each, average p = 0.01). Recovery from depression is significantly slower in mutant cells compared to wt (average p = 0.05). The inset in B shows no significant change in the first response amplitude. (N = 15-16 cells for each line, with all recordings and analyses being performed blind to the genotype of the cultures). **(D)** Plot showing average normalized response amplitudes to depression at 1 Hz stimulation frequency. There was no difference between wt, het or mut cells (N = 9 cells each).

If in these mice the shorter forms of synaptotagmin 7 were the dominant splice forms, or the longer forms with mutated C2 domains functioned as dominant negatives, then as is the case with syt7 short form overexpression we might expect to see slower rates of synaptic depression. However we actually observed faster synaptic depression more analogous to the overexpression of the regular form of synaptotagmin 7 (Figure 2.11). At first glance, this seems somewhat contradictory to our previous results. However, a number of issues prevent us from drawing this rather simple conclusion. Firstly and perhaps most importantly, the protein expression of the C2 domain containing splice variants in these mice is at most 30% that of normal levels (Figure 3.1B, C). This could have a major bearing on the phenotypes that we observe. Secondly, only the calcium binding sites in the C2 domains have been mutated. The protein could still signal through its various other interaction partners, albeit in a calcium independent manner. This would make it difficult to compare the two vastly different conditions. Thirdly, the lack of a good antibody to the shorter splice variants does not allow us to determine whether or not the endogenous ratio of the splice variants is altered by the mutations. As it is possible that relative levels are still the same, and the overexpression data from chapter 2 suggests that it is the relative levels of the various forms that is functionally relevant, this data is even harder to interpret. Nevertheless, we can still

conclude that mutating the calcium binding sites is dominantly inhibiting some process that regulates the rate of synaptic depression.

We then proceeded to study how the synaptic responses recover after depression in response to a 1 Hz train of 120 APs. What we observed was that in homozygous mutant cells (mut) the synaptic responses recovered more slowly than either the wt or heterozygote control cells. This suggests a number of things. The faster depression and subsequent slower recovery in homozygous mutant cells suggests that there is a defect in synaptic vesicle recycling and vesicles take a longer time to recycle when the C2 calcium binding sites of the protein are mutated. In addition, the fact that the heterozygote shows faster depression, but normal recovery suggests that during extensive stimulation, the loss of one copy of the protein at the low expression levels is unable to compensate and allow normal vesicle recycling, however during the less intense stimulation during synaptic recovery, only when both copies are mutated, do we continue to see a slow down in vesicle recovery. An alternative explanation could also be that the requirements of vesicle recycling during synaptic depression and synaptic recovery may be different and therefore require different levels of functional protein.

To further explore this idea of the dichotomy between the requirements for vesicle recycling during different levels of synaptic activity, we monitored synaptic depression in response to the less intense 1 Hz stimulation. In this instance we did not observe any significant difference in depression kinetics between mutant synapses and either wt or heterozygous controls (Figure 3.6D). This suggests that the calcium dependent functions of synaptotagmin 7 may be required at higher stimulation frequencies when the workload of the synapse is higher.

Normal spontaneous event frequency and amplitude in synaptotagmin 7 C2AB mutant mice

To ascertain whether there was any other physiological synaptic deficit in the mutant mice, we recorded spontaneous postsynaptic potentials (minis) from cortical cultures in the presence of tetrodotoxin (TTX), sample traces of which are shown in Figure 3.7A. While there was an increase in mini frequency in heterozygous cultured cells, there was no

significant difference between wt and mut cells (Figure 3.7B). There was also no significant difference in mini amplitudes between any of these conditions (Figure 3.7C). This suggests that there is normal synapse density and normal postsynaptic responsiveness and receptor density in cultures made from the mutant mice.

Since these mice have mutations in the calcium binding sites of the C2 domains, we also wanted to ascertain if syt7 may play a role in the calcium dependence of mini frequency (Figure 3.3). Thus we recorded minis in the presence of 0, 2, 4 and 8 mM extracellular calcium. Again, no difference in mini frequency was observed under these conditions between mutant, heterozygote or wt cortical cultures (Figure 3.7D).

Decreased sucrose responsiveness in synaptotagmin 7 C2AB mutant mice

However, when we recorded the response of homozygous mutant cells (mut) to 0.5 M sucrose application, which releases the readily releasable pool of vesicles in a calcium independent manner, we observed a small but significant decrease in the amplitude of the sucrose current compared to controls (wt) and heterozygous (het) cells (Figure 3.7E, F). Since synapse density appears to be normal, and mini frequency and amplitude are unaffected, this suggests that there may be a decrease in the RRP of these synapses.

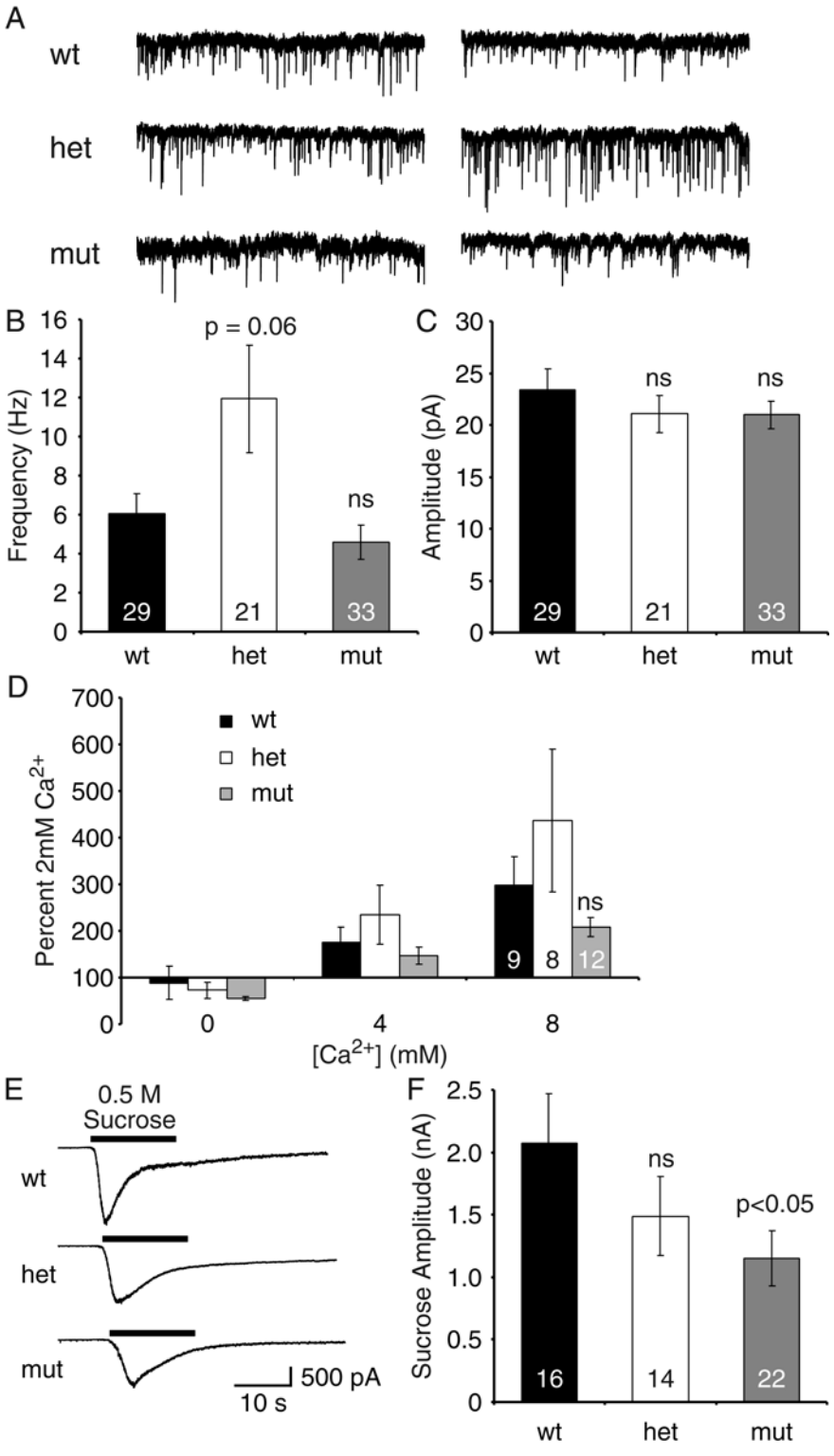
A
wt
het
mut
B
Frequency (Hz)
p = 0.06
ns
29
21
33
wt
het
mut
C
Amplitude (pA)
ns
ns
29
21
33
wt
het
mut
D
Percent 2mM Ca2+
wt
het
mut
ns
9
8
12
0
4
8
[Ca2+] (mM)
E
0.5 M
Sucrose
wt
het
mut
500 pA
10 s
F
Sucrose Amplitude (nA)
ns
p<0.05
16
14
22
wt
het
mut

Figure 3.7. Decrease in amplitude of sucrose responses in syt7 Ca^{2+} mutant mice. **(A)** Sample traces of spontaneous miniature postsynaptic potentials recordings (minis). **(B)** No significant difference in mini amplitudes between wt and mutant cultures ($p = 0.28$, N =29-33 cells each). The frequency of minis in het cultures is significantly larger than mut ($p = 0.02$, N = 21 cells). **(C)** No difference in mini amplitude between cultures. **(D)** No significant difference in the Ca^{2+} dependence of mini frequency between the different littermate cultures (N = 8-14 cells each, p ranges from 0.18-0.70). **(E)** Sample traces of sucrose responses. **(F)** There is a significant decrease in the amplitude of sucrose responses in syt7 mutant mice compared to littermate wt controls ($p<0.05$) There is no difference between heterozygous and control responses ($p=0.62$) (N=14-22 cells for each line).

Exocytosis rates and readily releasable pool size measured using FM dyes are normal in synaptotagmin 7 C2AB mutant mice

In order to determine whether the C2AB mutations have any effect on synaptic vesicle exocytosis, we switched to more presynaptic measures. We loaded synapses in culture with FM1-43 using 1200 AP delivered at 10 Hz, and after a 10-minute washout period imaged synapses during destaining by 10 Hz stimulation for 90s followed by maximal destaining using 3 rounds of 90mM K^+. We observed that the rate of destaining kinetics in response to 10Hz stimulation was unaltered (Figure 3.8A) in the mutant cultures compared to littermate het or wt cultures.

We did observe a small change in the amplitude of the sucrose response in mutant cells measured electrophysiologically, so we wanted to check for changes in the readily releasable pool (RRP) of vesicles using imaging techniques as well. To this end, we loaded synapses using 10 Hz stimulation for 2 min, and following dye washout, challenged the synapse to 30 Hz 2 s stimulation to release vesicles from the RRP (Figure 3.8B). When we plotted the ratio of this drop in fluorescence to the total amount of dye trapped in the synapses (determined by imaging during 4 rounds of 90 mM K^+ application after the tetanus), we found no significant change in the ratio of the RRP to total pool (Figure 3.8C), suggesting that there was no physiological redistribution of vesicles in the cortical synapses of syt7 C2AB mutant mice. This is somewhat surprising, given that there was a decrease in the sucrose releasable pool, however it is still not entirely clear what exactly the mechanism

of sucrose release is and whether it is indeed identical to the pool that can be released by action potentials.

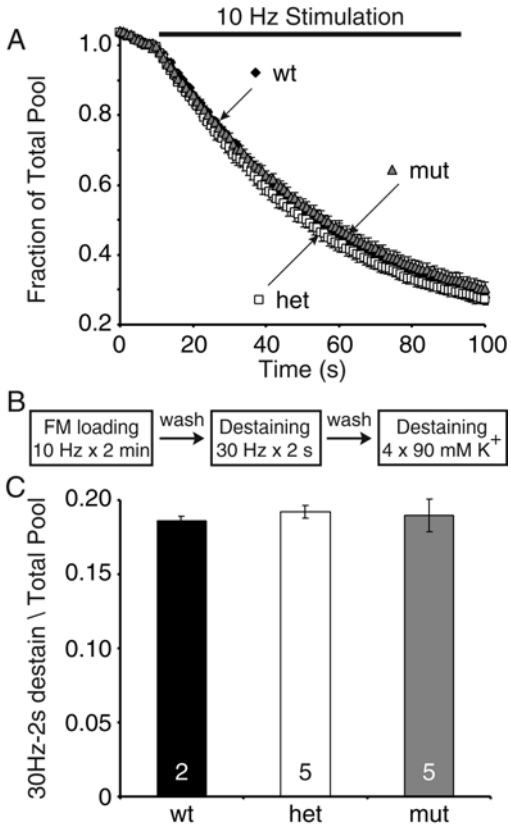

Figure 3.8. No changes in FM dye exocytosis rate or RRP size in syt7 C2AB mice. **(A)** No change in kinetics of dye exocytosis in response to 10Hz stimulation. **(B)** Experimental Protocol. Dye was loaded using a 10Hz-2min stimulus in the presence of FM1-43. After dye washout, a brief 30Hz-2s pulse was delivered and the change in fluorescence monitored, followed by multiple rounds of 90 mM K^+ to release all trapped dye. **(C)** The ratio of the brief release to the total dye trapped during 10Hz stimulation showed no significant difference (N = 2-5 coverslips each).

Increase in endocytosis rate in cortical synapses of synaptotagmin C2AB mutant mice

In previous work we found that overexpression of a short splice variant of synaptotagmin 7 leads to an increased rate of vesicle endocytosis and recycling. To determine whether the C2AB mutations in synaptotagmin 7 would alter the kinetics of endocytosis we performed the identical experiment to that shown in Figure 2.3. We first

loaded synapses with a brief tetanus of 60 AP at 30 Hz and then rapidly washed out the extracellular dye. Following a 10 minute washout period we imaged the synapses during exhaustive stimulation with 90 mM K^+ in order to measure the amount of endocytosis that occurred during that brief 2s time period that dye was present in the bath (Figure 3.9A). Then after a brief wash period we preformed a second round of dye loading using the more extensive stimulation of 1200 APs delivered at 10 Hz to quantify the total vesicle pools in the same synapse. What we observed was that synapses from homozygous syt7 C2AB mice (mut) showed a significant increase in dye uptake during the 2s loading compared to littermate control synapses plotted either as the average of the medians of each experiment (Figure 3.9B; $p<0.05$ between wt and mutant synapses, N = 5 coverslips each) or as a cumulative distribution of all synapses imaged (Figure 3.9C). It should again be stressed at this time that all experiments and subsequent analyses were performed blind to the genotype of the cultures.

The total recycling pool measured in the same synapses in the second round of FM dye loading and destaining was unchanged between mutant and wt or het littermate controls either plotting the average median of each individual experiment (Figure 3.9D) or the cumulative distribution of all synapses imaged (Figure 3.9E). When we determined the ratio of the brief to prolonged loading for each individual synapse and then plotted either the average median of these values for each experiment (Figure 3.9F) or the cumulative distribution (Figure 3.9G) we saw a larger ratio in the mut cultures, which confirms that there is increased dye uptake during the brief stimulation and it is not due to a larger vesicle pool size in those synapses. Taken together with the fact that the rate at which vesicles exocytose, and the proportion of vesicles that can be released by a 30 Hz 60 AP tetanus is unaltered in mut cultures (Figure 3.8), the increased dye uptake is most likely due to an increased rate of endocytosis. These findings are reminiscent of the increased endocytosis rate observed due to overexpression of the short synaptotagmin 7 splice variants in hippocampal cultures (Figure 2.3).

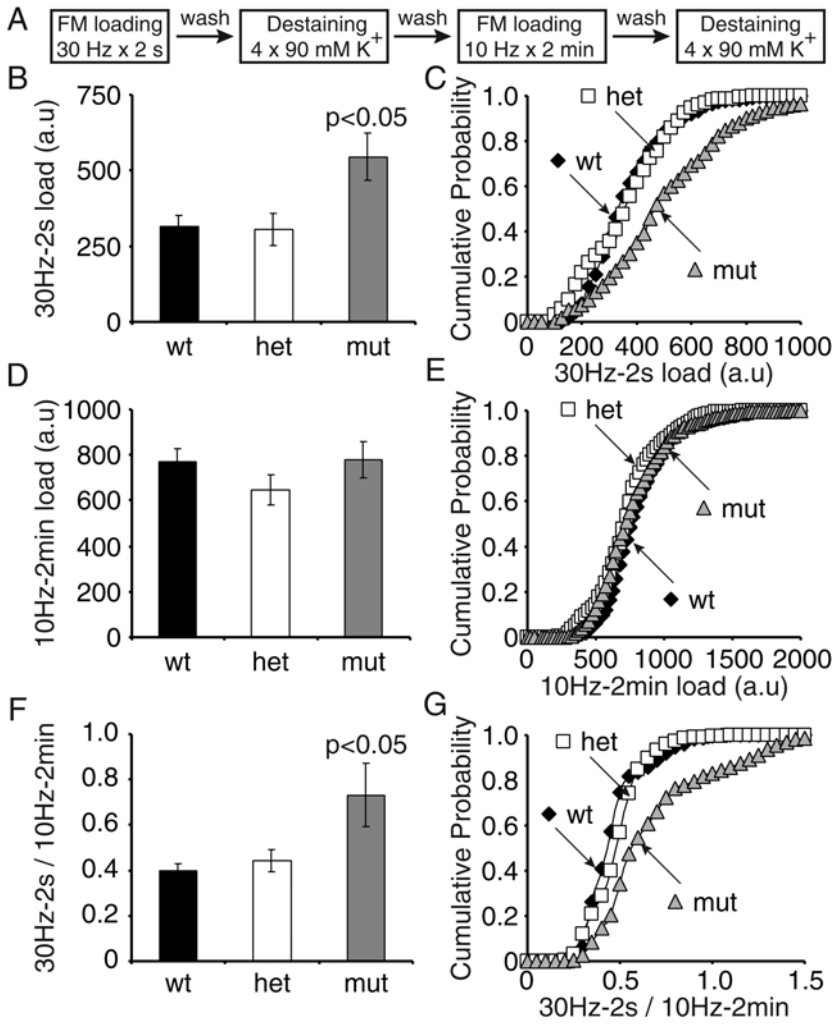

Figure 3.9. Increased endocytosis rate in syt7 C2AB mutant cortical cultures. **(A)** Experimental Protocol. **(B)** Increased dye uptake and release in mutant cultures compared to wild type and het (N =5, $p<0.05$ between wt and mut). **(C)** Plotting a cumulative distribution of all synapses analyzed shows a significant rightward shift in ΔF values for mutant synapses. **(D)** No difference in total pool size as measured by 10Hz x 2min loading. **(E)** Cumulative distribution of all synapses imaged shows no change in pool size distribution. **(F)** Ratio of brief to prolonged loading also shows an increase in dye uptake in brief loading (N=5, $p<0.05$ between wt and mut). **(G)** Cumulative distribution shows a significant shift in the ratio of short to prolonged loadings for all synapses imaged.

Discussion

In order to follow up on our earlier work that suggested a role for synaptotagmin 7 splice variants in the modulation of synaptic vesicle recycling (chapter 2), we analyzed two lines of synaptotagmin deficient mice. One line effectively knocked out the expression of the synaptotagmin 7 protein (syt7 ko) while the other line had mutations in key residues of all six calcium-binding sites of the C2 domains of the protein (syt7 C2AB). The key finding from the analysis of the knock out line was a decreased rate of endocytosis. The evidence for this is: (i) Decreased dye uptake during brief dye application and stimulation (60AP, 2s) in syt7 ko cultures compared to littermate wt controls (Figure 3.5). (ii) Equal due loading by 30 Hz 2 s after a 1 min delayed dye washout. (iii) No significant change in any other presynaptic parameter studied such as RRP pool size as measured by FM release (Figure 3.4C), total pool size (Figure 3.4A) or the rate of exocytosis (Figure 3.4B).

The synchronicity of stimulated responses was unaffected by the loss of synaptotagmin 7 (Figure 3.2A,inset). No other electrophysiologically measured parameters were altered such as depression and recovery kinetics (Figure 3.2A, B), paired-pulse depression (Figure 3.2C), minis and their calcium dependence (Figure 3.3A-E), or electrophysiological recordings of sucrose response amplitudes (Figure 3.3F, G). These findings rule out the possibility that the role of synaptotagmin 7 is as a supplementary fast synchronous release sensor to synaptotagmin 1. However, this data does not shed any light on the question of whether synaptotagmin 7 is the sensor for slow asynchronous synaptic vesicle release. This question is currently under investigation by others.

The analysis of the synaptotagmin 7 knock in line produced more dramatic results, however hard they may be to interpret due to the incomplete recovery of protein levels. The salient findings were an increased rate of fast vesicle endocytosis in homozygous mutant cortical cultures, alterations in short-term plasticity, and decreased sucrose responsiveness. The evidence for these findings is as follows: (i) There was an increased FM dye uptake during brief 30 Hz stimulation for 2 s in homozygous mutant (mut) synapses (Figure 3.9B, F), without any change in the total pool size (Figure 3.9D), exocytosis rate (Figure 3.8A), or the fraction of vesicles in the RRP measured by FM dye release during a 30 Hz 2 s

stimulation (Figure 3.8C). (ii) Faster synaptic depression in response to 10 Hz stimulation without any change in the initial response amplitudes (Figure 3.6A) for both het and mutant cells compared to wt controls. (iii) Slower recovery at 1 Hz sampling frequency after 10 Hz 900 AP depression in mut cells compared to littermate controls. (iv) No change in the rate of synaptic depression in response to 1 Hz stimulation. (v) Decreased amplitude of sucrose current in mut cells compared to littermate wt controls, measured electrophysiologically (Figure 3.7D, E).

While the findings from the C2AB mutant line suggest that these synapses have deficits in synaptic vesicle endocytosis and recycling, the results are hard to interpret and somewhat counterintuitive. On the one hand there is an increase in synaptic vesicle endocytosis. On the other hand, a faster rate of depression and slower recovery are suggestive of slower endocytosis and recycling (Virmani et al., 2003). However, evidence that there are fundamental differences in the physiological properties of hippocampal and neocortical synapses may help somewhat in resolving this discrepancy (Virmani et al., 2005). Briefly, while it appears that structurally hippocampal and neocortical synapses are very similar, their baseline levels of activity, synaptic vesicle recycling and functional vesicle pool sizes are very different. While hippocampal synapses show slow synaptic depression and fast recovery, neocortical synapses show faster depression and slower recovery. However at baseline, it is the cortical synapses that actually show faster rates of vesicle recycling. We have also observed that synaptotagmin 7 splice variants may have different baseline levels in different brain regions (Figure 2.13). If we apply this concept to the faster depression we see in the C2AB mutant mice, then the faster depression could also be interpreted in terms of faster recycling, and this fits better with the faster endocytosis rates observed using FM dyes. Unfortunately due to breeding issues, it was not possible to obtain the required cultures to test vesicle recycling directly using FM dyes.

The findings from the overexpression and mouse studies coupled with the direct evidence from differential recycling properties of hippocampal and neocortical synapses suggest that functional requirements for different proteins may vary dependent on regional localization. This concept is not entirely new. There are a number of different synapse types

that have fairly specialized functions. While it is very easy to identify the structure/function differences between neuromuscular junction terminals and central synapses, it is possible that there are different functional requirements of synapses in different regions, and the structural consequences occur not on the gross morphological level, but more on the level of protein composition.

One of the concerns about these findings is that the changes observed are fairly small changes. They are not like the complete loss of synchronous release in the synaptotagmin 1 knock out mouse (Geppert et al., 1994), or the loss of activity dependent release in the synaptobrevin 2 knock out mouse (Schoch et al., 2001). However, one point to be made is that the severity of the synaptotagmin 1 and synaptobrevin phenotypes resulted in the death of these mice, whereas both of the mouse lines we have studied breed normally and live normal life spans. This in itself suggests that no gross phenotype in synaptic function should be expected from either of these mice lines. This does not mean that the analysis is any less informative. Recent studies in cortical cultures from synaptotagmin 1 knock out mice show that the changes in endocytosis and recycling in these mice as measured using FM dyes is only on the order of 20-30% (Nicholson-Tomishima and Ryan, 2004). In amphiphysin knockout mice, one of the major interaction partners with dynamin, thought to be required for pinching vesicles of the membrane, only minor changes in vesicle exocytosis and about a 10-20% decrease in vesicle recycling rate were observed (Di Paolo et al., 2002). We see a 2 fold increase in dye uptake in 2 s, which is quite a dramatic change in relation to these other findings. This suggests that such a fundamental process as endocytosis, which occurs from receptor mediated endocytosis to simple pinocytosis, is highly developed and probably a highly regulated process on a number of levels, and the loss of a single protein can be compensated to allow the continued functioning of this important process.

Our findings using both transfection studies (Chapter 2) and mouse models (Chapter 3) in two different brain region culture systems of mice and rats, strongly suggest that synaptotagmin 7 plays a role in modulating synaptic vesicle endocytosis and recycling in these regions. Whether it is the baseline levels of the splice variants that are different, or their modulation in response to activity that differs, still remains to be determined. Ideally a

system whereby one could control the levels of the different splice variants within physiological range, and monitor the changes in these fundamental synaptic processes in relation to changes in relative levels of the splice variants would be the only way to determine the exact role of synaptotagmin 7 in vesicle recycling. However at this point such a system is not within our means, but these results are a good starting point for understanding the complex function of this protein.

CHAPTER 4: The Role Of Key Molecules In Regulating Different Stages Of The Synaptic Vesicle Cycle

Introduction

The cycle of the synaptic vesicle can be broken down into three major steps: exocytosis, endocytosis and vesicle recycling. While the process of exocytosis has been widely studied and a number of regulatory molecules for this process are well known, the role various other molecules play in synaptic vesicle endocytosis and recycling in central nervous system synapses is not very well established. In this chapter we describe results on a number of different molecules thought to play roles at different points in the synaptic vesicle cycle (Figure 4.1). A brief rationale for our choice of molecules to study is described below. Further elaboration on the relevant background for each protein is provided in each individual section.

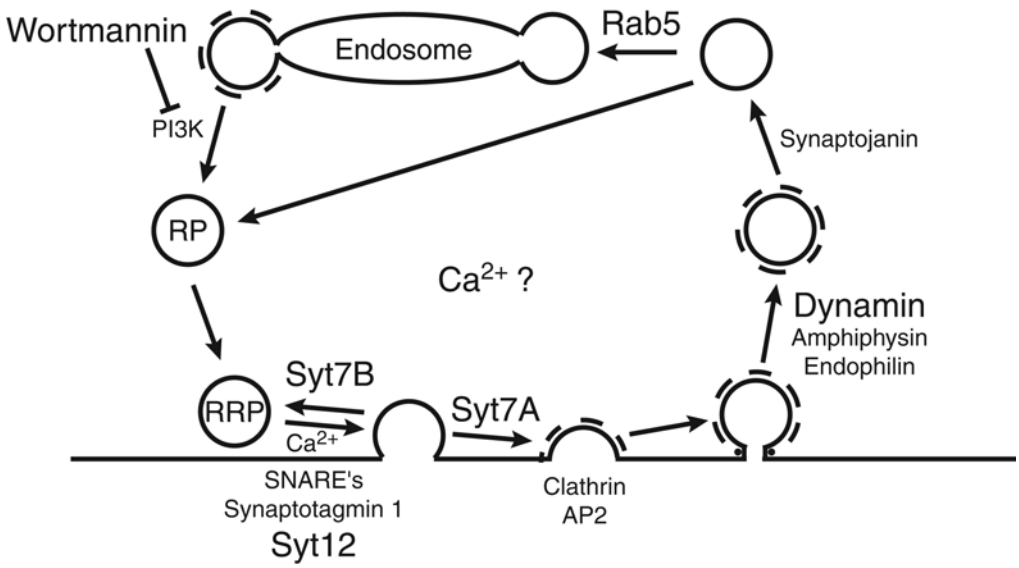

Figure 4.1. Proteins analyzed in relation to the synaptic vesicle cycle. Diagram of the synaptic vesicle cycle with proteins that will be studied shown in bold.

After synaptic vesicle exocytosis, the first important point of regulation is at vesicle endocytosis. Vesicles can either endocytose via a fast pathway, of which very little is known, or a slow clathrin dependent pathway (Aravanis et al., 2003; Gandhi and Stevens, 2003). We have shown that synaptotagmin 7 may play a role in this decision (Virmani et al., 2003), and it has also been shown that synaptotagmin 1 may play a role (Nicholson-Tomishima and Ryan, 2004; Poskanzer et al., 2003). Synaptotagmin 12 is another member of this rapidly growing family of proteins that has been shown to interact in a dominant negative manner with synaptotagmin 1 (Maximov and Südhof, 2005a). In this chapter, we will explore whether this putative interaction with synaptotagmin 1 has any physiological consequences on the rate of synaptic vesicle endocytosis.

Dynamin is another molecule whose role in the fission of endocytosing clathrin-coated vesicles from the plasma membrane is well accepted. However whether dynamin plays a similar role in fast recycling or "kiss and run" endocytosis is a matter of considerable debate. We tried to address this issue by expressing wild type and dominant negative dynamin constructs in hippocampal cultures and studying their effect on the kinetics of synaptic vesicle endocytosis. Our principle aim was to discover whether there was any synaptic vesicle endocytosis when dominant negative dynamin was expressed.

After endocytosis, vesicles either rapidly recycle locally in the readily releasable pool or recycle via slower pathways through the reserve pool. In neuromuscular junction synapses, where the size of the vesicle pool is large and therefore does not impose kinetic restrictions, vesicles have also been shown to recycle through endosomal intermediates (Richards et al., 2000). In central synapses, where vesicle recycling appears tuned toward faster pathways to optimize the limited vesicle pool size, the exact role of the slow endosomal pathways is unclear. Rab5 is a synaptic vesicle protein that is thought to function in fusing vesicles with endosomes. Therefore, in order to explore the role of endosomal recycling in central synapses, we used dominant negative and constitutively active forms of rab5 and studied their effect on the kinetics of vesicle recycling. Using another approach to address the same question, we treated hippocampal cultures with the phosphatidyl inositol-3

(PI3) kinase inhibitor wortmannin, which has been shown to inhibit also been shown to inhibit early endosome formation in cell lines (Li et al., 1995b).

In the process of regulated exocytosis, calcium plays the very important role of triggering the actual fusion event. Without calcium as a signaling molecule there would be no evoked neurotransmitter release. This begs the question as to what role calcium may play in endocytosis and recycling. A plethora of molecules bind calcium to varying degrees and with different affinities. It is quite possible that the varying concentrations of calcium in the synapse could trigger different events in exocytosis and endocytosis with differing temporal spans. To begin to address this question we studied the effect of varying calcium concentration on endocytosis and recycling.

Materials and Methods

Cell culture

Dissociated hippocampal cultures were prepared from 1-2 day-old Sprague-Dawley rats as described (Kavalali et al., 1999b). In transfection experiments, cells were transfected after 6 div using a calcium phosphate transfection protocol with vectors containing our genes of interest under the pCMV5-promoter. The dynamin constructs were generous gifts of Dr. Joseph Albanesi (UT Southwestern Medical Center). The rab5 wild-type construct used in figures 4-6 and 4-7 was gifted by Dr. Thomas Südhof (UT Southwestern Medical Center) while the rab5 constructs used in figures 4-5 and 4-8 were gifted by Dr. Philip Stahl (Washington University). Removal of the EGFP moiety on these constructs was performed with the help of Lisa Monteggia's laboratory (UT Southwestern Medical Center) using standard molecular cloning techniques. Cells were imaged at day 10-11 in vitro 4-5 days after transfections.

Fluorescence Imaging

Synaptic boutons were loaded with either FM2-10 (400 μM) or FM1-43 (4 μM) (Molecular Probes, Eugene, OR) using either electric field stimulation in the presence of 4 mM K^+, 2 mM Ca^{2+} solution, or 90 s incubation in hyperkalemic solution 47 mM K^+/2 mM Ca^{2+}. Modified Tyrode solution containing (in mM) 150 NaCl, 4 KCl, 2 $MgCl_2$, 10 Glucose, 10 HEPES, and 2 $CaCl_2$ (pH 7.4, ~310 mOsm) was used in all experiments. Hypertonic solution was prepared by addition of 500 mM sucrose to the modified Tyrode solution. The 90 mM K^+ solutions contained equimolar substitution of KCl for NaCl. Field stimulation was applied through parallel platinum electrodes immersed into the perfusion chamber delivering 25 mA - 1 ms pulses. All staining protocols were performed with 10 μM CNQX and 50 μM AP-5 to prevent recurrent activity. Images were taken after 10-min washes in dye-free solution in nominal Ca^{2+} to minimize spontaneous dye loss. Destaining of hippocampal terminals with hypertonic/high-potassium challenge was achieved by direct perfusion of solutions onto the field of interest by gravity (2 ml/min). Images were obtained by a cooled-intensified digital CCD camera (Roper Scientific, Trenton, NJ) during illumination (1Hz-60 ms) at 480 ± 20 nm (505 DCLP, 535 ± 25 BP) via an optical switch (Sutter Instruments,

Novato, CA). Images were acquired and analyzed using Axon Imaging Workbench Software (Axon Instruments, Union City, CA). Sample pictures were taken on a Lieca TCS Confocal Microscope.

Miscellaneous

All error bars denote standard error of the mean (SEM); all n values correspond to individual coverslips unless mentioned otherwise; all statistical assessments were performed with the 2-tailed t-test.

Synaptotagmin 12

The role of synaptotagmin 1 (syt1) as the major calcium sensor for synaptic vesicle exocytosis is by now well established. This molecule, as well as other members of the synaptotagmin family of molecules dimerize via cysteine residues in their transmembrane domain to form functional homodimers. It has recently been shown in vitro that synaptotagmin 12 (syt12) can heterodimerize with synaptotagmin 1 molecules and thereby act in a dominant negative manner to compete with synaptotagmin 1 function (Maximov and Südhof, 2005a). To determine if this heterodimerization could play a role in the endogenous regulation of synaptic vesicle endocytosis, we expressed syt1 and syt12 GFP fusion proteins in viral vectors and infected hippocampal primary neuronal cultures at day 7 in-vitro, and studied the effect of this overexpression one week later.

We loaded synapses from these cultures with FM5-95 using electrical field stimulation at 10 Hz for 30 s (300 AP). Dye was then either immediately washed out with a fast perfusion rate of 10 ml/min (immediate washout) or allowed to remain in the chamber for an additional minute (delayed washout). After a 15 minute wash period, we imaged the synapses while destaining maximally using 4 rounds of 90 mM K^+ / 2 Ca^{2+} application to determine the amount of dye trapped during the loading paradigm (Figure 4.2A). We found that in the case of immediate washout, ~66% of synapses overexpressing syt1 loaded greater than 500 a.u. of fluorescence, however only ~49% of synapses overexpressing syt12 loaded greater than this amount (Figure 4.2B). With the delayed wash, this effect was more dramatic, with approximately 85% of syt1 control synapses having ΔF values greater than 500 a.u. while only 52% of syt12 overexpressing synapses had ΔF values that high (Figure 4.2B). Plotting the same data as the average of the medians of each experiment normalized to the value for syt1 control loading we see the same deficits in dye uptake in syt12 expressing synapses (Figure 4.2C).

These data suggest that overexpression of synaptotagmin 12 in cultures results in a deficit in slow endocytosis. This conclusion is based on the decrease in dye uptake during stimulation in syt12 expressing synapses compared to syt1 controls, with minimal uptake during the 1 minute that dye remained in the bath before washout. This suggests that the

competition of syt12 to heterodimerize with syt1 could regulate whether a vesicle were to endocytose via a slow or fast pathway. It would be interesting in the future to study whether these vesicles recycle via slow or fast recycling pathways.

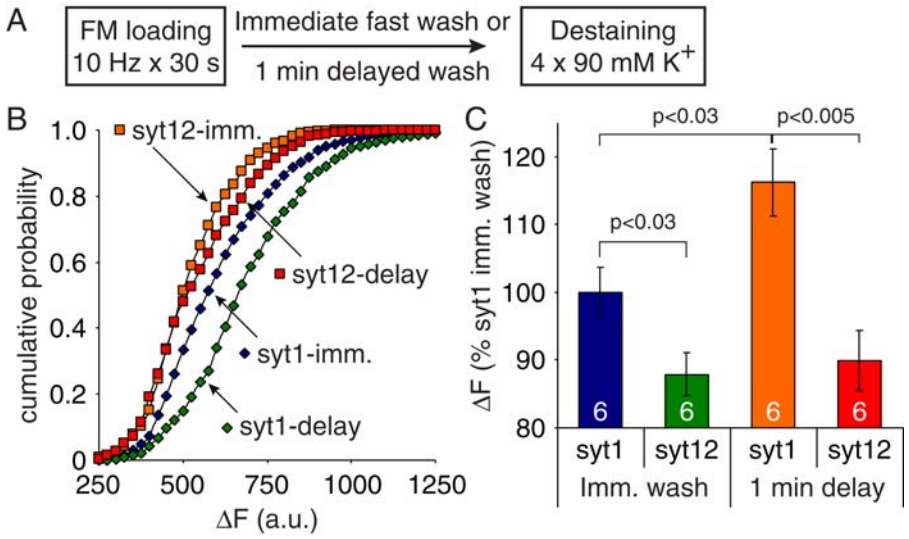

Figure 4.2. Syt 12 overexpression decreases slow endocytosis. **(A)** Protocol. Synapses were loaded with 10 Hz field stimulation for 1 min (600 AP), following which dye was either immediately washed out using a fast perfusion of 10 ml / min or the dye washout was delayed by 1 min. Following a 10 minute washout period, the dye trapped in the synapses was measured by imaging during four rounds of 90 mM K^+ application. **(B)** Cumulative histograms of all synapses imaged shows a leftward shift in synapses overexpressing syt12 compared to control synapses overexpressing syt1. When washout was delayed, the cumulative distribution of ΔF for syt1 shifted to the right, indicating increased dye uptake via slow endocytic pathways, while dye uptake by syt12 overexpressing synapses did not show significant increase. **(C)** Plotting the average ΔF from the median values of individual experiments we see that syt12 overexpressing synapses load only about 88 ± 3% of syt1 control synapses with immediate dye wash ($p<0.03$, N = 6 coverslips each). With delayed wash, syt1 synapses now load 23 ± 4% more than syt12 synapses ($p<0.003$, N =6 coverslips each). This corresponds to a 16 ± 5% increased dye uptake with delay in syt1 expressing synapses with minimal increase in dye uptake in syt12 overexpressing synapses (2 ± 5%).

Dynamin

Background

In the 1970's the temperature sensitive *shibire* mutation was isolated in *Drosophila* (*shi*^{ts}) (Grigliatti et al., 1973; Poodry et al., 1973). When these flies are shifted from the permissive temperature of 19° to the restrictive temperature of 29°C they rapidly become paralyzed, but fully recover on return to the permissive temperature. The flies display normal exocytosis at 29°C, but endocytosis is severely impaired and numerous deeply invaginated pits with electron dense collars around their bases are found present in the plasma membrane (Koenig and Ikeda, 1989). It was later discovered that these flies had a mutation in the cytosolic protein dynamin (Chen et al., 1991; van der Bliek and Meyerowitz, 1991). In mammals dynamin is the collective name given to three alternatively spliced genes, all of which are thought to play an important role in the fission of clathrin coated vesicles from membranes. Dynamin 1 is a 100kDa protein found to be the most highly expressed isoform in neurons. Whether dynamin acts as a mechanochemical enzyme to directly pinch vesicles off the membrane (Stowell et al., 1999; Takei et al., 1999), or if it acts as a GTPase recruiting other proteins to perform the actual fission reaction (Sever et al., 1999) is still a matter of debate.

Having observed that inhibition of clathrin mediated endocytosis and recycling actually accelerates the rate of fast endocytosis and recycling, we wanted to utilize dynamin as an additional tool to study vesicle recycling. This would also allow us to shed light on the question as to whether dynamin is required for kiss and run recycling or whether it functions primarily through classical clathrin dependent recycling pathways.

Results

Dynamin mutations signal apoptotic cell death in cultured hippocampal neurons

In order to study the role of dynamin in synaptic vesicle recycling, we used three different dynamin ECFP fusion constructs under the pCMV5 promoter. A wild-type dynamin 1 construct and two mutant constructs, a K44A mutation and a G273D mutation, both in the GTPase domain of dynamin (Figure 4.3A). Both of these mutations correspond

to the dominant negative *shibire* mutation in *drosophila*, with the K44A mutation always on, and the G273D mutation being temperature sensitive. These constructs were introduced into primary hippocampal neuronal cultures at day 6 in-vitro (div) using calcium phosphate transfection protocols and experiments were performed at 10-11 div.

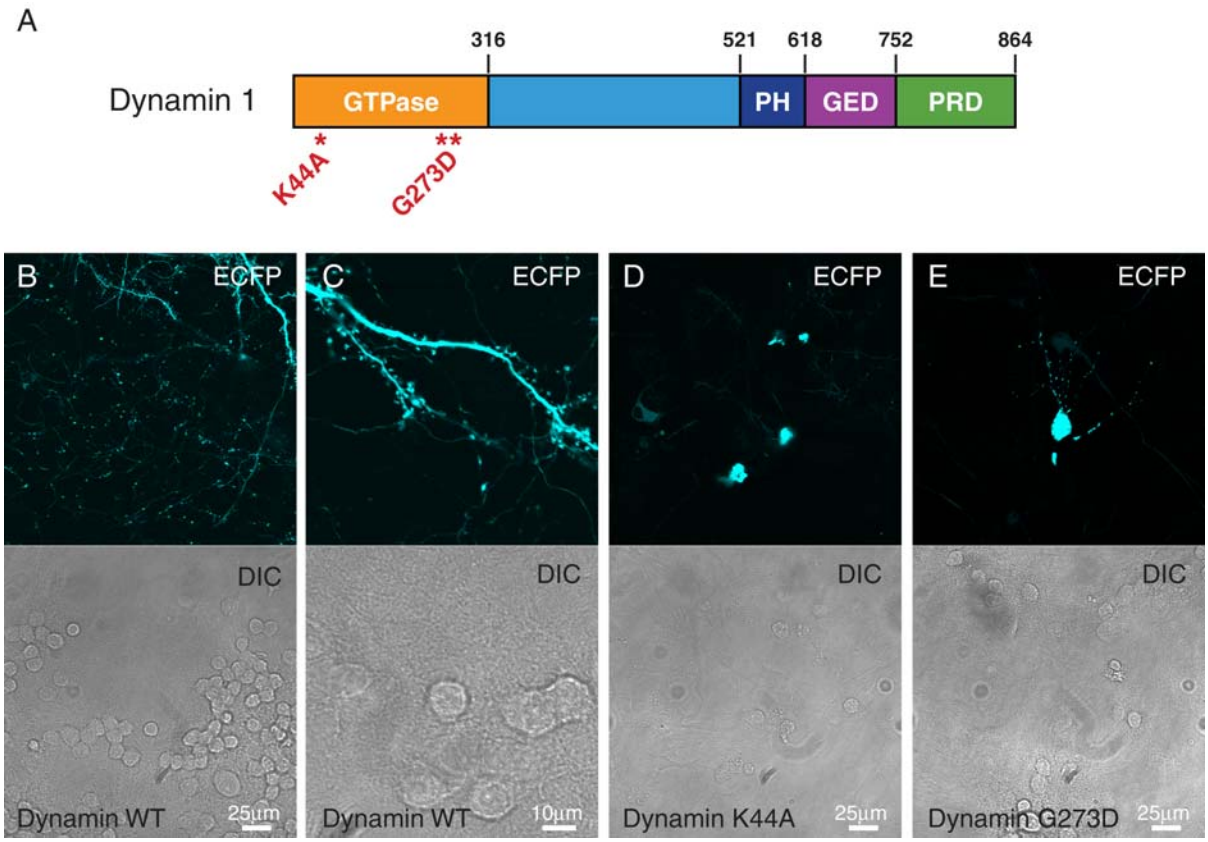

Figure 4.3. Expression of dynamin constructs in hippocampal neurons. **(A)** Domain structure of dynamin. Dynamin has an N-terminal GTPase domain, a PH (pleckstrin-homology domain), a GED (GTPase effector domain) and a C-terminal PRD (proline/arginine-rich domain). Two dominant negative dynamin mutants (K44A and G273D) were tested that have mutations in the GTPase domain. These correspond to the *shibire* mutation in *drosophila*, with the K44A mutations always on, and G273D mutation rendering the protein sensitive to temperature. **(B-C)** ECFP fusion proteins of dynamin wild-type protein show localization to presynaptic terminals (B; upper panel) as well as postsynaptic dendrites and spines (C; upper panel). The lower panel shows DIC images of the same region as the fluorescence image. **(D-E)** Overexpression of the Dynamin K44A (D) or G273D (E) mutant constructs in hippocampal neurons results in apoptotic cell death shown by the pycnotic fluorescent cell bodies.

We found that wild-type dynamin was nicely expressed in both presynaptic terminals (Figure 4.3B) and dendrites and spines (Figure 4.3C) that were easily distinguishable from one another allowing us to use the ECFP tag as a marker for presynaptic terminals expressing the dynamin construct. These ECFP fluorescent presynaptic terminals were selected in subsequent experiments and their FM dye loading and unloading characteristics monitored compared to untransfected control synapses. When we overexpressed the mutant dynamin constructs however we found that the fluorescent cells were unhealthy. A large proportion of pycnotic cells were observed with transfection of both these mutant constructs (Figure 4.3D,E). While there were instances where we could select punctate regions that looked fluorescent (Figure 4.3E), it was not possible to determine whether the synaptic deficits we observed were due to the overexpression of the mutant protein or due to the general sickness of cells undergoing programmed cell death. Therefore we deemed this method unsuitable for studying the structure function relationship of dynamin 1, and these results are not included here. However we did study whether the overexpression of wild-type dynamin had an effect in this system and those experiments are described in the subsequent sections.

Overexpression of wild-type dynamin does not alter the rate of fast endocytosis

In order to test whether the concentration of endogenous dynamin was a limiting determinant in synaptic vesicle endocytosis and recycling, we selected transfected synapses showing ECFP fluorescence and monitored their FM properties. First we tested to see if the rate of endocytosis was affected, using a brief stimulus of 60 AP delivered at 30 Hz we loaded synapses with FM1-43 dye. After washout of extracellular dye for 10 minutes we applied multiple rounds of 90 mM K^+ solution to maximally destain the synapses and measure the dye trapped during the 2 s of dye application. This provides us with a measure of synaptic vesicle endocytosis. After a brief wash period, we performed a second round of loading on the same synapses using a more prolonged stimulation of 10 Hz for 2 min (Figure 4.4A).

We found that dye uptake during either of the two stimulus protocols was unaffected by overexpression of dynamin 1 whether plotted as averages of the median values of individual experiments (Figure 4.4B, D) or cumulative histograms of all synapses measured

(Figure 4.4C, E). In addition, the ratio of brief to prolonged loading was also not affected by overexpression of dynamin 1 (Figure 4.4F, G). This indicates that endogenous dynamin 1 levels do not limit the rate of synaptic vesicle endocytosis.

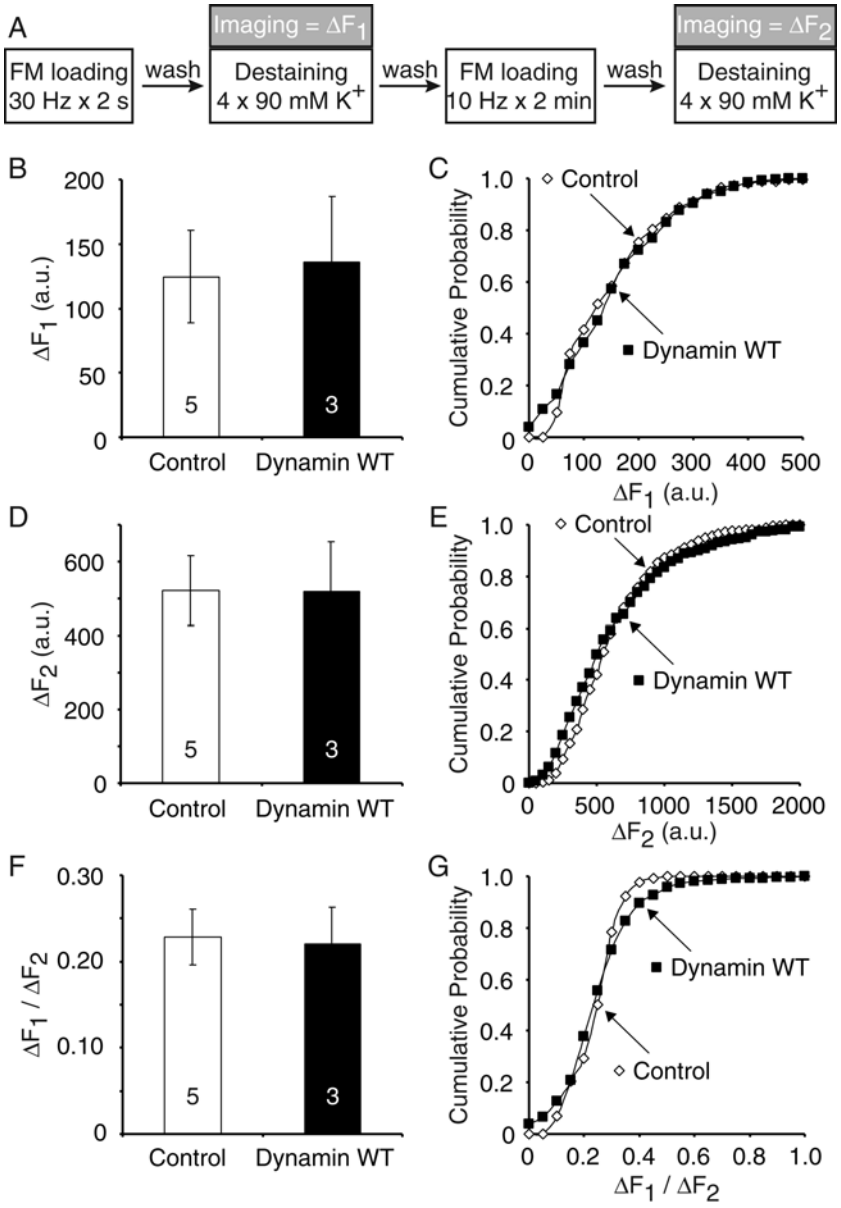

Figure 4.4. Dynamin wt overexpression does not alter the rate of fast endocytosis **(A)** Experimental design. Neurons were exposed to FM1-43 during brief electrical stimulation (30 Hz for 2 s), washed for 10 min, and the loss of FM dye from nerve terminals was imaged during repeated stimulations with 90 mM K^+/2 mM Ca^{2+} solution to quantify the amount of FM dye that was taken up by actively recycling vesicles during the initial 2 s stimulation (ΔF_1). After a 5 min wash, the same synapses were reloaded with FM1-43 during prolonged electrical stimulation (10 Hz for 2 min), washed for 10 min, and again imaged during repeated stimulations with 90 mM K^+/2 mM Ca^{2+} (ΔF_2). **(B)** No change in dye uptake during brief stimulation and release in synapses overexpressing dynamin wt protein compared to controls (N = 5 and 3 for control and dynamin wt expressing synapses respectively). **(C)** Plotting the cumulative distribution of all synapses analyzed shows no shift in ΔF values. **(D)** No difference in total pool size as measured by 10Hz x 2min loading. **(E)** Cumulative distribution of all synapses imaged shows no change in pool size distribution. **(F)** Ratio of brief to prolonged loading shows no change in dye uptake in brief loading **(G)** Cumulative distribution shows no shift in the ratio of short to prolonged loadings for all synapses imaged.

Overexpression of wild-type dynamin alters the kinetics of slow FM dye release

We next tested whether the rate of FM dye exocytosis was altered by dynamin 1 overexpression. We loaded synapses with FM1-43 using a 1200 AP stimulus delivered at 10 Hz, then following a 10 minute washout period we imaged the synapses during a 30 Hz AP train for 90s followed by 3 rounds of 90 mM K^+ to maximally destain the synapses. We found that the synapses overexpressing wild-type dynamin appeared to a have a slightly higher steady state plateau (Figure 4.5A). When we fitted these destaining curves with two exponential fits, we found that while the fast time constant, and the ratio of the amplitudes of the fast and slow components were the same, the rate of the slow component was significantly slower in synapses overexpressing dynamin 1 (Figure 4.5B; $p<0.02$, N = 6 coverslips each). We examined this further by plotting the cumulative distribution of the slow time constants for all synapses imaged. We found that while ~75% of control synapses had slow time constant values less than 250 s, only ~30% of dynamin overexpressing synapses had slow time constants lesser than 250 s. This indicates that under extensive stimulation less dye loaded vesicles are being mobilized and released. Since dynamin is acting at the vesicle budding step of endocytosis this finding suggests that the rate at which vesicles endocytose,

recycle and become re-available for release was faster with dynamin 1 overexpression. However, our data does not allow us to rule out the alternative possibility that the decreased rate of dye release may be due to a decreased rate of vesicle mobilization from the reserve pool.

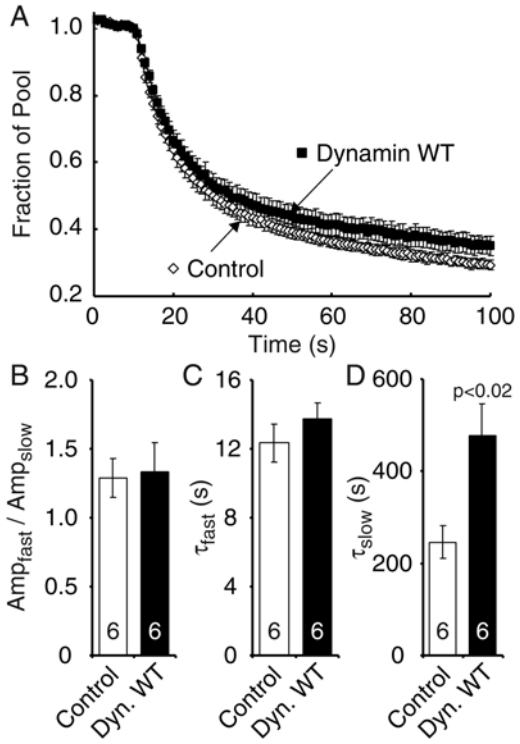

Figure 4.5. Decreased slow time constant of exocytosis in dynamin wt expressing synapses. **(A)** Synapses were loaded by 10Hz-2min stimulation in the presence of FM1-43, washed and then imaged while stimulating first with action potentials at 30Hz followed by multiple $90K^+$ depolarization's to determine the total recycling pool. A slightly elevated plateau was observed in synapses overexpressing dynamin wt protein. **(B-D)** Fitting the destaining curves from individual experiments with two exponentials we see that while there is no change in the ratio of the amplitude of the fast and slow components of destaining (B), or the time constant of the fast component (C), the slow component of destaining (D) is significantly slower in dynamin overexpressing synapses ($p<0.02$, N = 6 coverslips each).

Discussion

Our results show that when the dominant negative GTPase mutant dynamin 1 proteins were overexpressed in hippocampal neurons, these proteins signaled the apoptotic cell death

pathway. Others have previously described this observation. More significantly however, we found that in the case of prolonged stimulation overexpressing dynamin 1 in synapses resulted in a decreases rate of dye destaining during stimulation at 30 Hz. This result could either be due to an increased rate of reuse of blank vesicles under the extensive stimulation, or a slower rate of mobilization of dye filled vesicles from the reserve pool. Given that dynamin functions in the retrieval of vesicles from the plasma membrane, the increased rate of reuse may be the more likely interpretation. However, our data does not allow us to precisely distinguish between these two hypotheses.

Rab 5 and Wortmannin

Background

From the data we have obtained with synaptotagmin 7 it appears that endocytosis and recycling are two distinct events, and that fast endocytosis can occur even when the primary mode of recycling is slow. In classical models of vesicle recycling, clathrin coated vesicles can either directly recycle into the reserve pool of vesicles, or fuse with early endosomes from where they proceed to bud off and repopulate the reserve pool. In order to explore these slower recycling modes, we chose to study rab5 and the phosphatidyl inositol-3 (PI3) kinase inhibitor wortmannin. Rab5 has been shown to be present on synaptic vesicles (de Hoop et al., 1994), and along with a host of other proteins, including two PI[3]-kinases (Christoforidis et al., 1999), targets recycling vesicles to fuse with early endosomes (Bucci et al., 1992). This protein has been recently shown to play a significant role in slow vesicle recycling at the drosophila neuromuscular junction (Wucherpfennig et al., 2003). It has been previously documented that in this preparation, very slow modes of recycling exist, occurring on the order of 30 minutes and longer, where vesicles bud off at sites distinct from the active zone (Koenig and Ikeda, 1999). However, the time course for recycling in central synapses is much faster (Pyle et al., 2000; Sara et al., 2002), and so a role for Rab 5 in this system is still a question that needs to be addressed. Recent results showing single vesicle dynamics at the active zone (Aravanis et al., 2003; Gandhi and Stevens, 2003), have further strengthened the idea that presynaptic terminals at neuromuscular junctions and central synapses may differ fundamentally in the proportion of vesicles that recycle through the kinetically distinct recycling pathways due to their different structures and function.

Wortmannin on the other hand is a PI3 kinase inhibitor that in non-neuronal cell lines, has been shown to inhibit the endosomal fusion produced by constitutively active forms of rab5 (Li et al., 1995b). This effect is seen at nanomolar concentrations and is very specific. This suggests that wortmannin should function similar to dominant negative rab5 and can be used as an additional model to inhibit early endosome formation. Recent results from frog neuromuscular junctions however suggest that wortmannin may have additional targets in central synapses (Richards et al., 2004). These authors showed a decrease in FM dye loading

into synapses and a deficiency in vesicle reformation from endosomes. This suggests that in central synapses, PI3-kinases may play more of a role in budding of vesicles from late endosomes. The same authors also showed that latrunculin A, which disrupts actin filaments, showed similar effects as wortmannin, suggesting that PI3-kinases may play a role in actin dynamics as well.

To determine whether endosomal intermediates play a role in vesicle recycling in central synapses we expressed dominant negative and constitutively active forms of rab5 (Barbieri et al., 1998; Mukhopadhyay et al., 1997; Roberts et al., 1999; Roberts et al., 2000) in hippocampal neuronal cultures. We found that wild type or dominant negative expression does not alter vesicle pool size or the kinetics of dye release, while the constitutively active form decreased pool size and release rate. We observed similar effects to constitutively active form expression when we treated cultures with wortmannin. These results suggest that the endosomal pathway may not play a prominent role in vesicle recycling in central synapses under normal physiological conditions.

Results

Localization of Rab5 expression constructs

In order to study the role of the endosomal pathway in synaptic vesicle recycling in central synapses, we used wild-type rab5 and rab5 mutant constructs. The rab5 mutant constructs employed were a dominant negative construct (S34N) and a constitutively active construct (Q79L). These constructs were introduced into day 6 hippocampal primary cultures using calcium phosphate transfection protocols. Experiments were performed at day 10-11 in vitro (div). The wild type EGFP fusion protein shows both diffuse dendritic localization as well as punctate regions of fluorescence likely corresponding to presynaptic terminals (Figure 4.6A). The dominant negative S34N construct shows similar localization (Figure 4.6B). However the fluorescence pattern produced by the overexpressed constitutively active protein (Q79L) is more interesting. Here we found fluorescence localized to the surface of large membranous vacuolar structures present both in the neuronal cell bodies as well as along the dendrites (Figure 4.6C, D). These are most likely endosomal structures, greatly increased due to the overexpression of this construct.

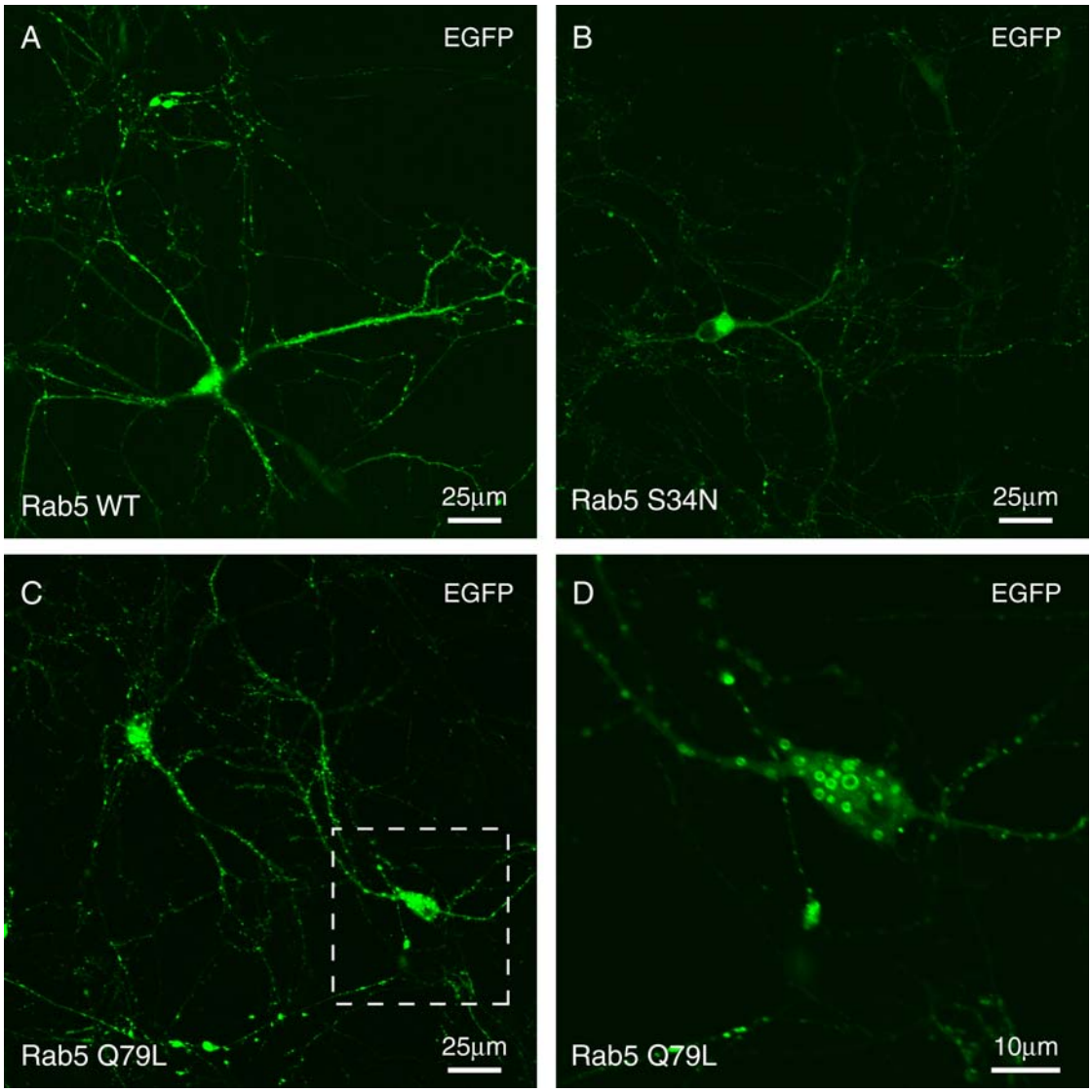

Figure 4.6. Expression of rab5 constructs in hippocampal neurons. **(A)** Wild-type rab5 EGFP fusion protein shows localization to both presynaptic terminals and post synaptic dendrites and spines. **(B)** The dominant negative rab5 S34N EGFP construct also shows localization to both dendrites and presynaptic boutons. **(C)** The constitutively active Q79L construct shows localization to large membranous structures in the cell body and traveling down dendritic processes, as well as punctate structures that may be presynaptic terminals. **(D)** Magnified view of the dashed box in (C) showing the membranous structures labeled with rab5 more clearly. Due to localization both pre- and postsynaptically, subsequent experiments were performed with the EGFP moiety removed from the constructs, and either synaptobrevin-ECFP or synaptotagmin 1-ECFP was co-transfected and used as a marker for presynaptic terminals expressing the rab5 proteins.

While the images suggest that our constructs are being targeted to the correct place, it makes selection and analysis of presynaptic terminals using EGFP fluorescence difficult. Therefore we removed the GFP tag from these constructs and in subsequent experiments co-transfected synaptobrevin 2 or synaptotagmin 1 ECFP fusion constructs along with the rab5 constructs and used these to select presynaptic terminals expressing our rab5 constructs.

Rab5 wild-type protein overexpression does not alter the rate of fast vesicle endocytosis

We first used our standard double loading endocytosis protocol, pairing a brief (30Hz x 2s) and a prolonged (10Hz x 2min) loading, to measure both rapid endocytosis (brief load) and total pool size (prolonged load) in the same synapses (Figure 4.7A). We did not observe any significant change in the dye uptake plotted as cumulative histograms of individual experiments, for the 60 AP loading (Figure 4.7B), the total pool size (Figure 4.7C) or the ratio of the brief to prolonged loading for each individual synapse (Figure 4.7D). Plotting the average of the median ratios from each experiment we also do not observe any significant change with overexpression of rab5 (Figure 4.7D). This suggests that this protein either does not play a role in the endocytosis decision in central synapses, or the endogenous levels of rab5 are adequate at this step in the pathway.

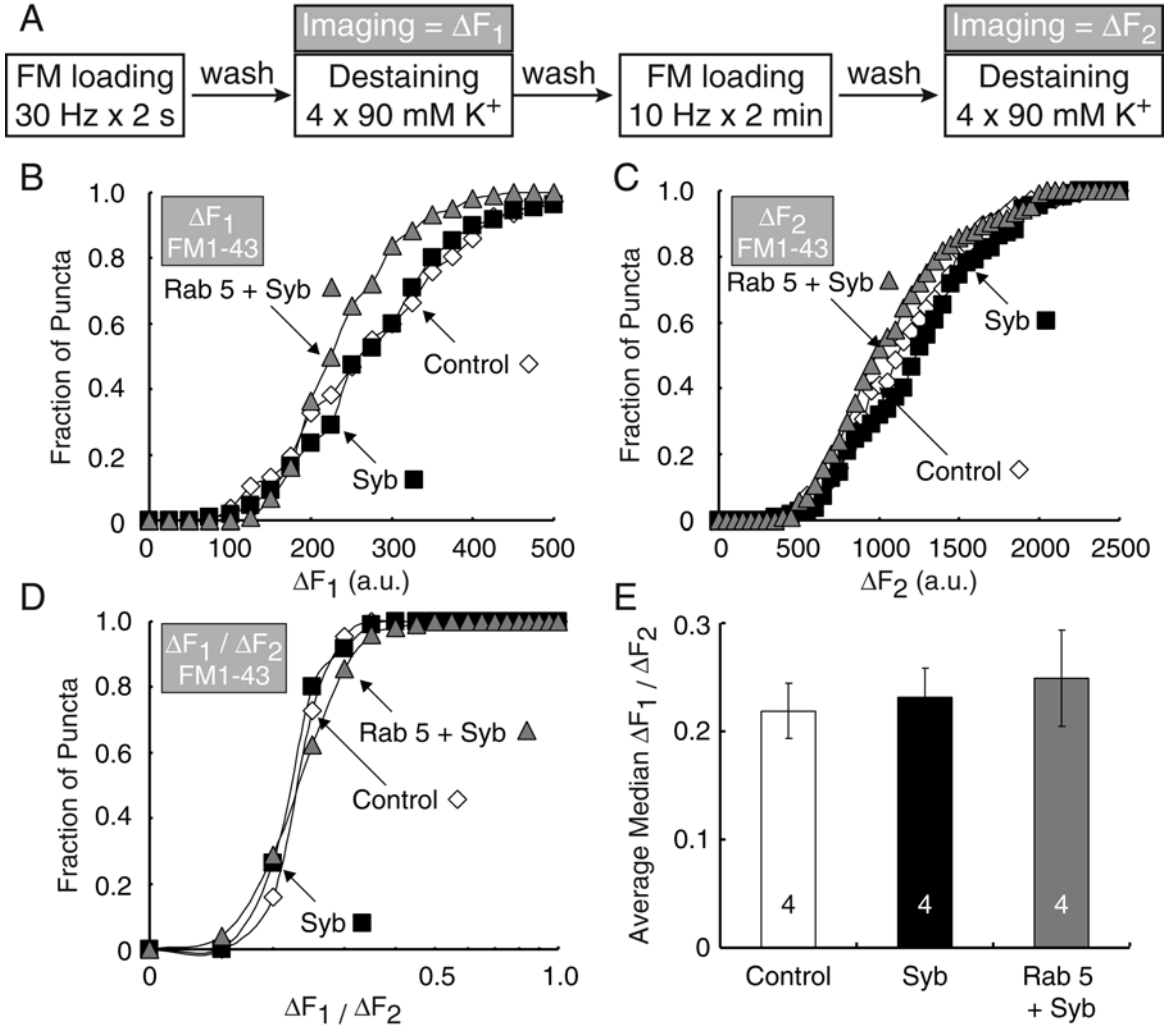

Figure 4.7. Normal fast endocytosis in synapses overexpressing rab5. **(A)** Experimental protocol. Synapses were loaded with brief stimulation (60AP at 30Hz) and after washout, destained to determine the dye trapped by fast endocytosis during the 2s of dye application. Following a brief rest period a second round of loading with more prolonged stimulation (10Hz for 2 min) was performed to quantify the total recycling vesicle pool in the same synapses. **(B-D)** Sample cumulative distributions of experiments showing no change in dye uptake during the short loading (B), prolonged loading (C), and no difference in the ratio of the brief to prolonged loading (D) for each individual synapse in the experiment. **(D)** Average median value showing no change in the rate of fast endocytosis with Rab5 overexpression suggesting that either the protein is not rate limiting in the endocytosis process, or that rab5 function is in the recycling pathway after endocytosis (N = 4 coverslips each).

Rab5 wild-type overexpression does not alter the size of the readily releasable pool, the total recycling pool or the rate of exocytosis

In order to determine whether the endogenous levels of rab5 protein were limiting any other step in the synaptic vesicle cycle, we measured the readily releasable vesicle pool size, the rate of exocytosis and the total recycling pool size in these synapses. To this end, we loaded the total recycling pool of synapses with 1200 APs delivered at 10 Hz. After a 10 minute wash period we stimulated the cells at 30 Hz, either with a brief 2 s pulse to selectively release vesicles in the readily releasable pool, or with a prolonged tetanus of 90 s to measure the rate of exocytosis. Following the action potential trains, we maximally destained the synapses by applying multiple rounds of 90 mM K^+ (Figure 4.8A).

Plotting a cumulative histogram of the ratio of the dye released during the brief 60 AP pulse, to the total dye labeled pool, we found no change in these distributions for individual experiments (Figure 4.8B). Plotting the average of the median of these distributions for a number of experiments we again see no significant change in the ratio of the brief destain to the total pool (Figure 4.8C). As the 30 Hz 60 AP stimulus selectively releases vesicles from the RRP, this suggests that rab5 overexpression does not change the size of the RRP.

When we monitored destaining for 90 s, we found that the average of traces of a number of different experiments align suggesting that rab5 overexpression does not alter the rate of exocytosis (Figure 4.8D). Therefore by increasing the levels of rab5 we cannot force more vesicles to recycle through slow endosomal pathways. Plotting the average median fluorescence trapped in synapses during the 1200 AP loading similarly shows no change in the total recycling pool size with rab5 overexpression (Figure 4.8E).

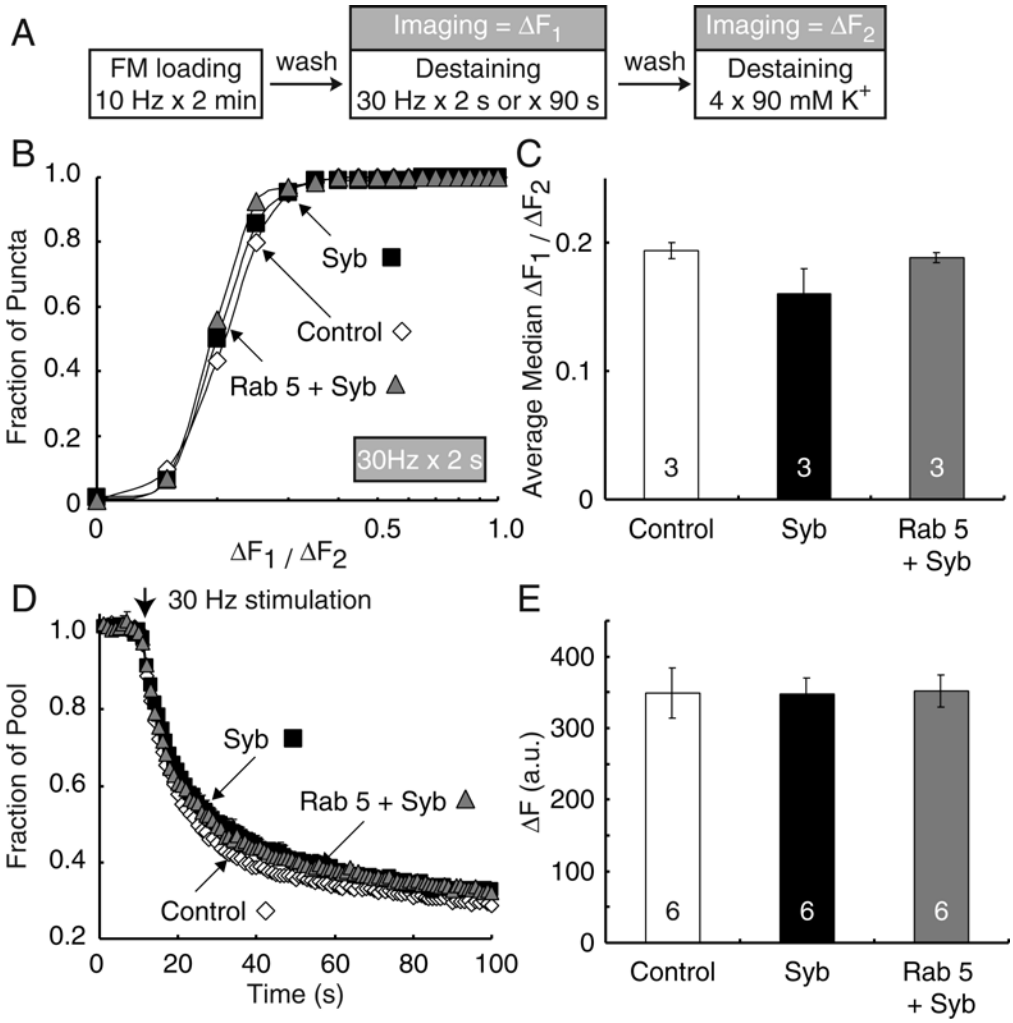

Figure 4.8. No change in the readily releasable pool, total pool or kinetics of exocytosis with rab5 overexpression **(A)** Experimental protocol. Synapses were loaded with 10Hz-2 min stimulation in the presence of FM2-10, washed, and then first stimulated with 30 Hz for either 2 s (to determine RRP size) or 90 s (to determine exocytosis rate) and then subsequently stimulated with multiple rounds of $90K^+$ to determine the total recycling pool. **(B)** Sample histograms from individual experiments showing no difference in RRP size. **(C)** Plotting the average of the medians of 3 experiments we see no significant difference in the ratio of $\Delta F_1/\Delta F_2$. This suggests that overexpression of rab5 does not alter the RRP size or the release probability of synapses. **(D)** No change in release kinetics at 30 Hz (N = 3 coverslips each). **(E)** Plotting the total 10Hz x 2min loadable pool size from these experiments we see no significant change with rab 5 overexpression (N = 6 coverslips each).

Expression of constitutively active rab5 decreases the actively recycling pool size

We next tested the effect of overexpression of the dominant negative and constitutively active rab5 forms on the kinetics of vesicle endocytosis and the size of the recycling pool of vesicles. We loaded synapses with FM1-43 using a maximal stimulation of 47 mM K^+ for 90s. Following a 10 minute dye washout period, we imaged the synapses during 30 Hz stimulation for 90 s followed by maximal destaining using multiple rounds of 90 mM K^+ (Figure 4.9A). We found that while the expression of rab5 wt or S34N mutant constructs did not affect FM dye release kinetics (Figure 4.9B, C), synapses expressing the the constitutively active (Q79L) construct had slower destaining kinetics (Figure 4.9C). However this decrease in kinetics was not statistically significant.

Plotting the average of the median fluorescence values trapped in the synapses during our loading protocol, we found that while the wt rab5 expression and the mutant rab5 S34N expression did not alter the total recycling pool size, expression of the mutant Q79L dramatically decreased the pool size available for loading (Figure 4.9D). This decrease in pool size was statistically significant ($p<0.03$ between syt1 control and rab5 Q79L, N = 3 and 2 respectively). This suggests that vesicles are being trapped in fused endosomal stages, and there is less membrane available for forming the pool of recycling vesicles. This idea is supported by the images of the EGFP labeled fusion protein being localized to a large number of membranous structures distributed throughout the cells.

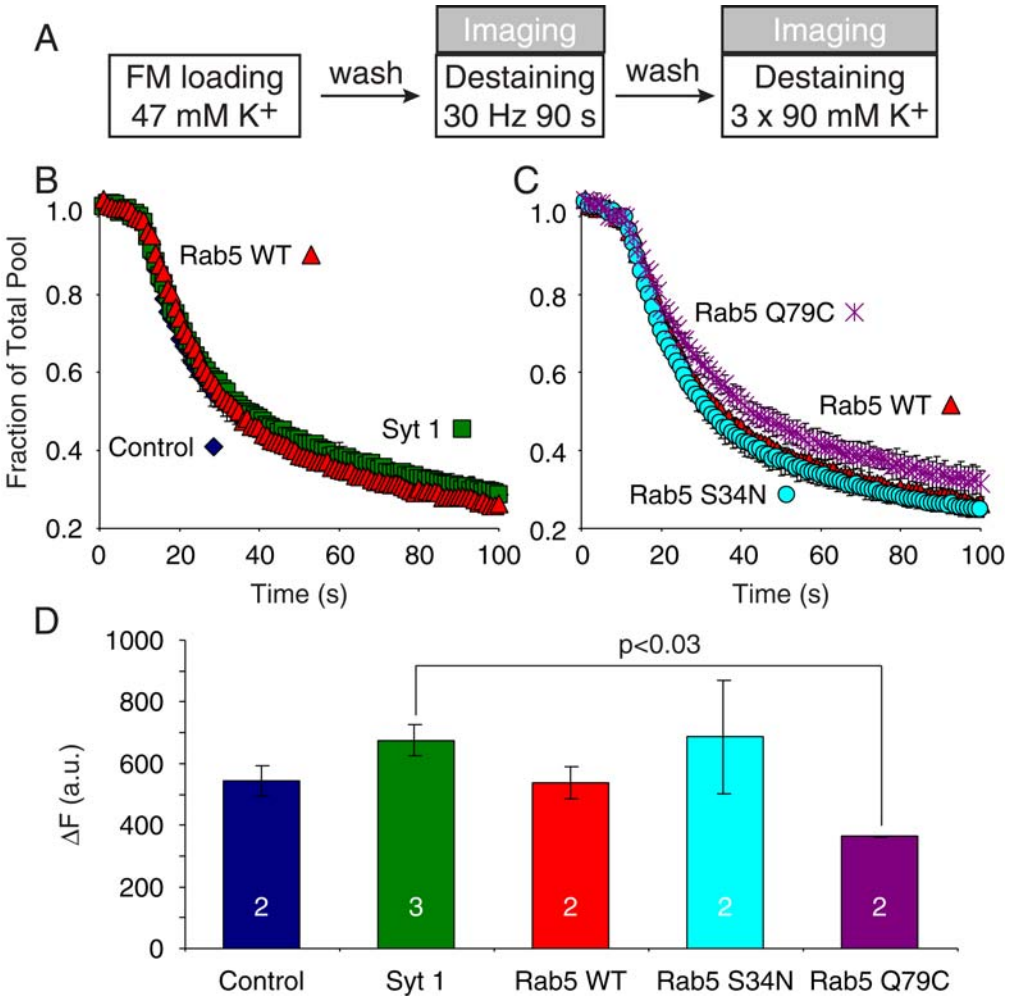

Figure 4.9. Overexpression of the constitutively active rab5 dramatically reduces the recycling pool size. **(A)** Experimental protocol. Synapses were loaded with 47 mM K^+ solution for 90 s, washed for 10 minutes and then destained while imaging, first with a 90 s train of APs at 30 Hz and then with 3 rounds of 90 mM K^+ to maximally destain the synapses. **(B-C)** In this set of experiments, no significant difference in destaining kinetics between non-transfected control synapses and synapses overexpressing the marker syt1 alone or with wt rab5 or dominant negative rab5 S34N were observed. Synapses expressing the constitutively active construct (rab5 Q79L) appear to plateau at a higher level, but due to the low number of experiments significance cannot be determined (N = 2-3 coverslips each). **(D)** The total recycling pool as measured by 10Hz-2min loading is significantly less in synapses overexpressing the constitutively active construct ($p<0.03$ between syt1 and rab5 Q79L, N = 3 and 2 coverslips respectively).

Wortmannin decreases the synaptic vesicle pool size, and decreases the rate of FM dye release

We also tested the effects of the PI3-kinase inhibitor wortmannin on synaptic vesicle exocytosis and recycling pool size. We pretreated hippocampal cultures with 1, 5 or 10 μM wortmannin, or DMSO vehicle control for 1 hour at 37ºC in the incubator. Following treatment, synapses were loaded with FM1-43 dye for 90 s using a 47 mM K^+ / 2mM Ca^{2+} solution to obtain maximal loading. Following dye washout for 10 minutes, the synapses were destained using a 90 s train at 30 Hz followed by multiple rounds of 90 mM K^+ solution to maximally destain the synapses (Figure 4.10A). When we plotted the average of the median fluorescence values of a number of experiments, normalized to the DMSO vehicle controls, we found that there was a dose dependent decrease in the total recycling pool size in wortmannin treated cultures (Figure 4.10B). When we pre-treated cultures for 10 minutes in 10 μM wortmannin, only approximately 25% of the DMSO control pool size was able to take up FM dye. This is in the same direction as the effect observed with overexpression of the Rab5 constitutively active form (Figure 4.10D).

Plotting the destaining kinetics in response to 30 Hz stimulation, we also observed a dose dependent change. Increasing concentrations of wortmannin resulted in the destaining curve to plateau at higher fluorescence values (Figure 4.10C). We were able to fit the destaining traces with two exponential curves, a fast curve with time constant τ_{fast}, and a slow curve with time constant τ_{slow} and plot the average ratio of the amplitudes of these two components (Figure 5.10D) as well as the average time constants (Figure 4.10E, F) for all experiments performed. The result of this analysis showed that while the two time constants of decay were similar for DMSO vehicle controls and wortmannin application at all concentrations (Figure 4.10E, F), there was a dose dependent decrease in the proportion of the fast exponential curve compared to the slow curve (plotted as a decreased ratio of fast to slow amplitude, Figure 4.10D).

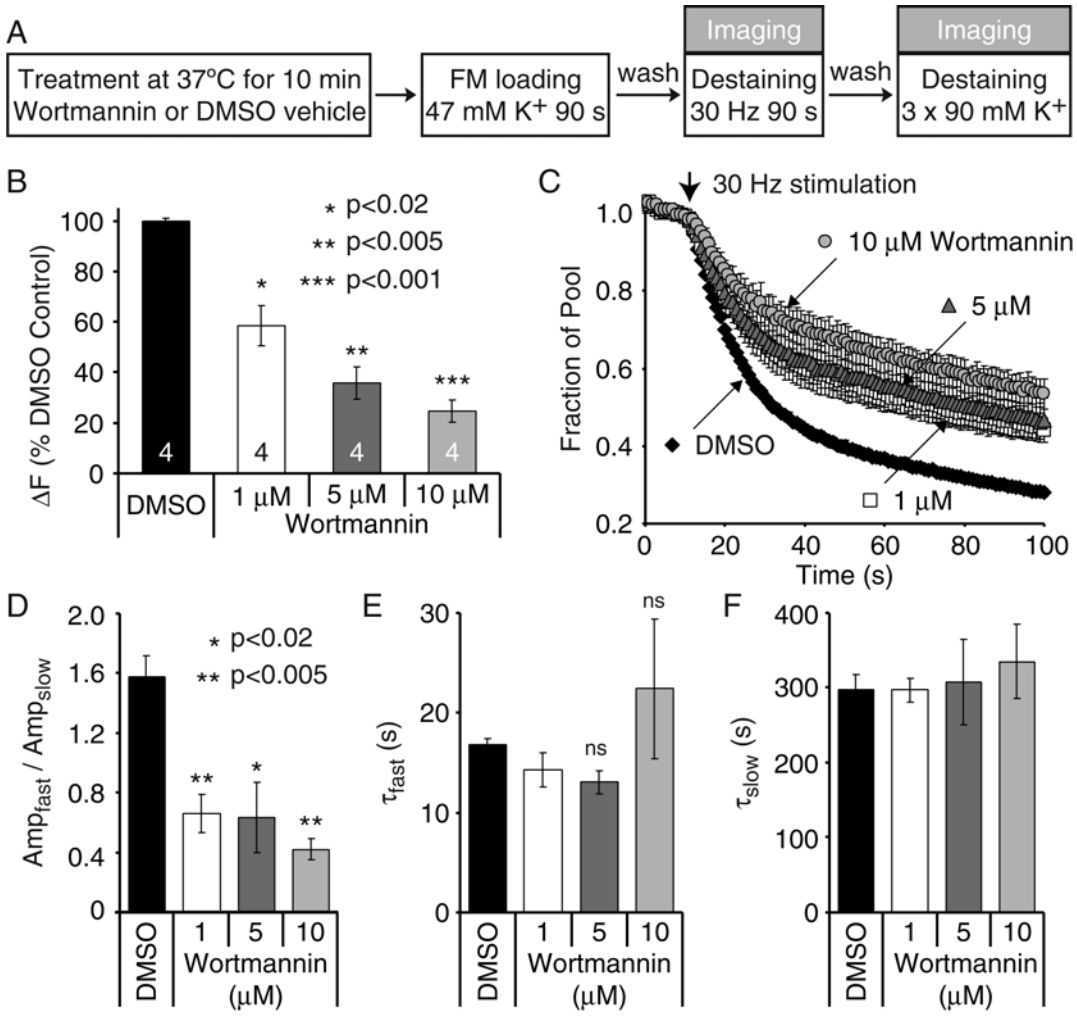

Figure 4.10. Wortmannin treatment decreases synaptic vesicle pool size and the kinetics of dye release. **(A)** Experimental protocol. Cultures were treated with varying concentrations of the PI3-kinase inhibitor wortmannin for 1 hour at 37ºC or DMSO vehicle control. After treatment synapses were loaded with FM1-43 dye using 90 s of 47 mM K^+ solution. Following 10 minutes of dye washout, synapses were imaged during a 30 Hz train of APs for 90 s, followed by multiple rounds of 90 mM K^+ to maximally destain the synapses. **(B)** Plotting the ΔF normalized to the DMSO control we see that increasing wortmannin concentration results in a progressive decrease in the size of recycling vesicle pool. **(C)** Plotting the rate of dye destaining during 30 Hz stimulation, we see that increasing concentrations of wortmannin result in successively higher plateau levels of dye destaining (N = 4 coverslips each). **(D-F)** We fit the dye destaining curves using 2 exponential fits and we have plotted the ratio of the amplitudes of the two components (D) and the time constant of the fast (E) and slow (F) components. While the time constants are unchanged, the ratio of the fast to the slow component decreases with increasing wortmannin concentration.

Discussion

To address whether synaptic vesicles actively recycle through endosomal intermediates, we expressed rab5 constructs in primary hippocampal cell culture. Fluorescent images of EGFP tagged fusion proteins show localization of wild type rab5 protein to both presynaptic and postsynaptic terminals. While dominant negative rab5 had a similar localization, the constitutively active form was localized to a large number of membranous structures; presumably formed by vesicles stuck in late endosomal stages. Physiologically, the expression of wild type rab5 did not alter recycling pool size, exocytosis kinetics, endocytosis rates or the size of the readily releasable pool. Expression of the dominant negative form also did not alter release kinetics or recycling vesicle pool size. However, overexpression of a constitutively active form slightly elevated the steady state level of dye release during 30 Hz stimulation and significantly lowered the size of the recycling vesicle pool. We observed a similar change in synapses treated with the PI3-kinase inhibitor wortmannin for 1 hour. The wortmannin effect was dose dependent with increasing doses resulting in a smaller recycling pool size and a decreased ratio of fast to slow components of dye release during 30 Hz stimulation.

These results are contrary to recent results in *drosophila* NMJ synapses where both pool size and depression kinetics were decreased in dominant negative rab5 knock in flies, while rab5 overexpression resulted in increased efficacy of release (Wucherpfennig et al., 2003). We do not observe either of these phenotypes. However our wortmannin results are very consistent with recent results from Betz and colleagues who showed that in frog neuromuscular junctions there is a dose dependant decrease in synaptic vesicle pool size with increasing concentrations of wortmannin (Richards et al., 2004). The only difference between these two studies was that while we observed a 40% decrease in FM1-43 dye uptake with application of 1 μM wortmannin, Richards et al. showed a 75% decrease in pool size with the same concentration of wortmannin. In both studies, wortmannin application was performed for the same duration of time.

Taken together with the NMJ results, our results suggest that vesicle recycling through endosomes may have different functions in different synapses. In the neuromuscular junction synapse vesicle recycling through endosomal intermediates appears to play a dominant role in the normal recycling of vesicles as disruption of vesicle fusion to endosomes (Wucherpfennig et al., 2003) or vesicle budding from endosomes (Richards et al., 2004), showed decreases in vesicle pool size. In hippocampal synapses however, disrupting rab5 function with dominant negative constructs did not result in a significant phenotype, suggesting that normal vesicle recycling in these synapses does not require an endosomal intermediate. Only the overexpression of a constitutively active form, which resulted in an increased number of large membranous structures, showed that rab5 could traffic vesicles through endosomes. Similar results were obtained by preventing the budding of vesicles from endosomes by wortmannin. These two findings suggest that vesicles can recycle through endosomes, but that vesicle trafficking through endosomes may be more of a house keeping function in central synapses, rather than an actively regulated pathway during intense stimulation. Further elaboration on the mechanism of such a role for rab5 will require a more detailed analysis.

Ca^{2+} dependence of vesicle recycling

Our previous results have suggested that the splice variants of synaptotagmin 7 regulate the targeting of vesicles to kinetically distinct recycling pathways in hippocampal cell cultures. If this finding holds true, then Ca^{2+} would be an ideal molecule to link the exocytic and endocytic pathways. Synaptotagmin 7 has C_2 domains like all other synaptotagmin family members, and synaptotagmin 1 and synaptotagmin 7 are known to have differential affinity for Ca^{2+} (Südhof, 2002). Thus differential levels of calcium during and immediately after exocytosis could link these two pathways by means of the two synaptotagmins, one on the vesicle and one on the plasma membrane. In low Ca^{2+} conditions or after exhaustive stimulation with depletion of intracellular Ca^{2+} stores, the short form lacking C_2 domains would still be able to maintain synaptic transmission by fast recycling of the RRP. Therefore we tested whether extracellular Ca^{2+} concentration played a role in the rate of vesicle endocytosis and recycling.

In order to determine the effect of Ca^{2+} concentration on vesicle recycling in synapses, we loaded synapses with FM2-10 for 2 s using 30 Hz field stimulation (60 AP) in 0.5, 2 or 8 mM extracellular calcium in the presence of AP-5 and CNQX to prevent recurrent activity (Figure 4.10A). Following stimulation, we rapidly washed out extracellular dye with a dye free solution containing 2 mM Ca^{2+}, CNQX and AP-5. In a subset of coverslips we challenged dye loaded synapses to a second 30 Hz 2 s pulse 30s after the end of loading to release any dye loaded vesicles that had recycled during that time. After a 10 minute washout in calcium free solution, we determined the amount of dye trapped in the synapses using multiple rounds of 30 Hz stimulation in the presence of 2 mM Ca^{2+}, CNQX and AP-5 to release all the dye. A second round of 30 Hz 2 s loading was then performed on the same synapses, in the same calcium concentration as the first loading. This allowed us to directly normalize the amount of dye that was released by the second stimulus in dye free solution in the first round, for each individual synapse.

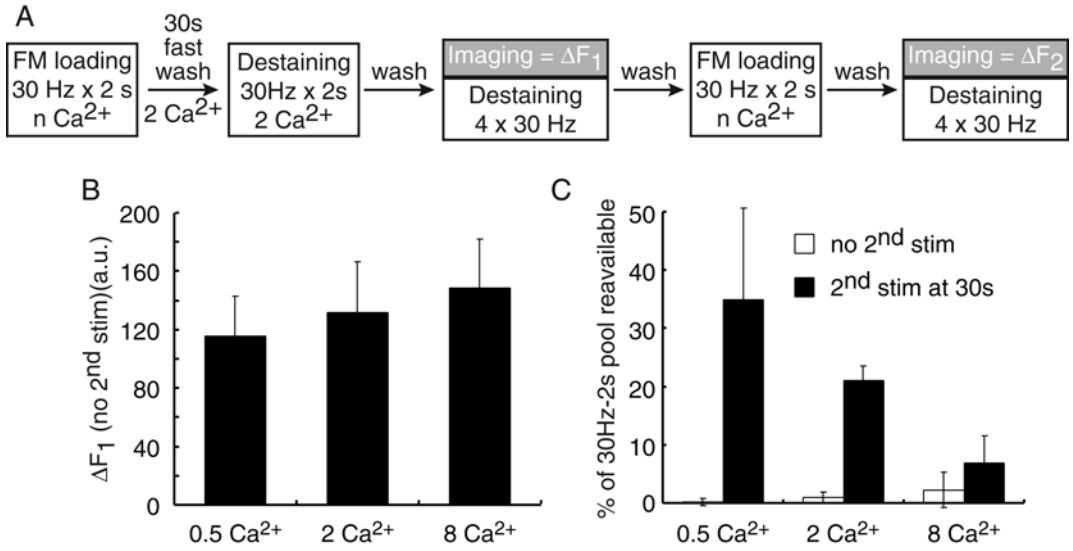

Figure 4.11. Calcium dependence of vesicle recycling. **(A)** Experimental protocol. In order to more directly measure vesicle recycling in synapses, the previous recycling protocol pairing brief and intense stimulations was modified. In this protocol, we subject the synapses to 2 rounds of loading and destaining with 30Hz-2s stimulation. We also subject half the coverslips to a second stimulation 30s after the first dye loading. This allows us to determine the amount of dye released during the second 30Hz-2s pulse in the absence of dye for each synapse as we relabel these same synapses again and determine the total pool labeled by 30Hz-2s stimulation. **(B)** Plotting the average median ΔF for the 30Hz-2s loading in the absence of the 2nd dye free stimulation, we see no significant difference in labeled pool size, although the trend seems to be towards greater loading at higher Ca^{2+} concentration, which is consistent with observations made by other labs under more intense stimulation paradigms (N = 2-3 coverslips each). **(C)** Plotting the percentage of the labeled pool re-available for release within 30 s of the loading stimulation, we see that there is an inverse relation to the Ca^{2+} concentration (N = 2-3 coverslips each).

We first plotted the average median fluorescence trapped in synapses during the initial 30Hz-2s stimulus at the different calcium concentrations (Figure 4.11B). We found that while there was no significant change in the dye uptake with the different calcium concentrations, there was a trend towards more dye uptake in the presence of higher calcium concentrations. This is not surprising, as it is known that the rate of vesicle exocytosis is calcium dependent. This is why we normalized all our subsequent experiments to a second round of loading in the same concentration of calcium. We then plotted the ratio of first to

second loading at the different calcium concentrations with or without the second destaining pulse 30s after the first round of dye loading. We found that there was an inverse relation between calcium concentration and the percent of recycled vesicles with maximal recycling in 0.5 mM calcium. However, due to the low numbers of experiments, these were not significant with a simple t-test analysis.

This result is a little surprising, although consistent with our synaptotagmin data if one were to assume that in the absence of calcium more short synaptotagmin (syt7B) is targeting recycling towards a faster pathway, while in higher concentration, the full-length synaptotagmin (syt7A) dominates and directs vesicles towards a slower recycling pathway. Additionally, evidence from capacitance measurements in the calyx of held synapses similarly suggest that increased rates of stimulation, i.e. higher residual calcium levels, result in slower rates of endocytosis and reuse (Sun et al., 2002). However, this data is still very preliminary, as only 2-3 data points have been obtained for each condition.

CHAPTER 5: Properties Of Spontaneous Vesicle Recycling

Background

All synapses manifest spontaneous neurotransmitter release in the absence of presynaptic action potentials (Katz, 1969). Over the last five decades several studies have examined this form of vesicle fusion to elucidate the mechanisms of neurotransmitter release. In most cases these low probability release events correspond to a single quantum of neurotransmitter that presumably originates from fusion of a single synaptic vesicle (Frerking et al., 1997). Beyond providing great insight to the mechanisms of synaptic transmission and formulation of the quantal hypothesis of synaptic transmission (Del Castillo and Katz, 1954; Katz, 1969), these spontaneous release events may be required for signaling leading to maturation and stability of synaptic networks (McKinney et al., 1999; Verhage et al., 2000), inhibition of local dendritic protein synthesis (Sutton et al., 2004) or may even drive action potential firing in cells with high input resistance (Carter and Regehr, 2002). In contrast to the highly regulated and precisely timed nature of evoked neurotransmitter release, spontaneous synaptic vesicle fusion can only be loosely regulated by extracellular calcium, fluctuations in intracellular calcium and neuromodulators (Angleson and Betz, 2001; Dittman and Regehr, 1996; Llano et al., 2000). This dichotomy led to a debate on the mechanism and location of spontaneous fusion (Colmeus et al., 1982; Deitcher et al., 1998; Van der Kloot, 1996). Recent studies have shown that spontaneous fusion is coupled to endocytosis (Murthy and Stevens, 1999; Ryan et al., 1997; Sun et al., 2002) suggesting the presence of a recycling pathway that operates at rest. These spontaneous release events are generally assumed to be due to low probability fusion of docked synaptic vesicles that are already primed for release (Murthy and Stevens, 1999). However this premise has never been directly tested. To elucidate the mechanisms that lead to spontaneous synaptic vesicle fusion we employed electrophysiological and optical imaging techniques that allowed us to track the synaptic vesicles' history of use. Using these approaches we found that distinct vesicle pools with limited cross talk sustain spontaneous versus activity-dependent synaptic vesicle recycling.

Materials and Methods

Cell culture

Dissociated hippocampal cultures were prepared from 2-3 days old Sprague-Dawley rat pups using previously described methods (Kavalali et al., 1999a). Experiments were performed after 15-25 days in-vitro corresponding to a time period when synapses reach full maturity in culture (Mozhayeva et al., 2002).

For the analysis of synaptobrevin deficient synapses, mice that are heterozygous mutant for synaptobrevin-2 (gift of Dr. T.C. Südhof) were set up for timed-pregnancy. Hippocampal neurons from embryonic day 18 littermate mice were dissociated and cultured using previously described protocols (Schoch et al., 2001). These cultures were used after 15-25 days in vitro.

Immunocytochemistry

The cells were loaded with AM1-44 (Biotium Inc., Hayward, CA) in the presence of 1μM tetrodotoxin (TTX, Calbiochem, La Jolla, CA) for 15 min followed by 10-15 minutes of dye free washout. Polyclonal syt1 lumenal domain antibody (1:100, gift of Dr. T.C. Südhof) was either loaded in the presence of TTX for 15 min or in a 47 mM K^+ solution for 90s. Following washout of the primary for 15 minutes, secondary antibody (Alexa 594 (1:500), Molecular Probes, Eugene, OR) was either loaded spontaneously to live cells in the presence of TTX for 15 min, or after 30 minutes of fixation with 4% paraformaldehyde in PBS containing 4 mM EGTA. In cases when permeabilization was performed, cells were first fixed and then incubated in 1X PBS containing 2% goat serum and 0.4% saponin (Sigma, St Louis, MO) for 1 hour before addition of the secondary antibodies (1:500). The coverslips were then mounted onto frosted uncharged slides. Images were obtained with a Leica TCS confocal microscope and the data was analyzed with the Leica confocal software.

Fluorescence imaging

Modified Tyrode solution used in all experiments contained (mM) 150 NaCl, 4 KCl, 2 $MgCl_2$, 10 Glucose, 10 HEPES and 2 $CaCl_2$ (pH 7.4, ~310 mOsm). High K^+ solutions contained equimolar substitution of KCl (90 mM) for NaCl. Synaptic boutons were loaded with FM2-10 (400 μM, Molecular Probes, Eugene, OR) or AM1-44 (16 μM, Biotium Inc,

Hayward, CA) under conditions outlined in the text. 90s incubation in 47 mM K^+ solution (Tyrode solution with equimolar substitution of KCl (47mM for NaCl)) gives maximal labeling of the recycling vesicle pool in a given synapse (Harata et al., 2001). Spontaneous loadings were performed in modified Tyrode solution containing 1μM TTX to inhibit action potentials induced by network activity inherent in the culture. Phorbol ester treatments were performed at a final concentration of 1μM phorbol 12-myristate 13-acetate (PMA) or 4-α-phorbol 12-myristate 13-acetate (4α-PMA) (Sigma, St. Louis, MO). Stock solutions of PMA and 4α-PMA were prepared in DMSO at a concentration of 1 mM and used at a 1:1000 dilution. At this concentration of DMSO no significant changes in the properties of synaptic transmission were observed (data not shown). Images were taken after 10 min washes in dye-free solution with nominal Ca^{2+} to minimize spontaneous dye loss. Destaining of hippocampal terminals with high-potassium challenge was achieved by direct perfusion of solutions onto the field of interest by gravity (2 ml/min). In a typical experiment, high potassium challenge was applied at least three times (for 90s each separated by 60s intervals) to release all the dye trapped in presynaptic terminals. All staining and destaining protocols were performed in the presence of 10 μM CNQX and 50 μM AP-5 to prevent recurrent activity. Field stimulation was applied through parallel platinum electrodes immersed into the perfusion chamber delivering 30mA, 1ms pulses. In all experiments we selected isolated boutons (~ 1 μm^2) for analysis and avoided apparent synaptic clusters. We did not observe a significant difference in background fluorescence levels between synapses loaded during brief periods of activity, or prolonged periods of spontaneous vesicle release (275 ± 20 a.u. for spontaneously loaded synapses and 336 ± 50 a.u. for activity dependent loaded synapses, $p=0.29$). We did not observe any noticeable focus drift in the majority of experiments. Those experiments where focus drift occurred were easily identifiable by a coordinated jump in the destaining curves of all synapses and were discarded. Images were obtained by a cooled-intensified digital CCD camera (Roper Scientific, Trenton, NJ) during illumination (1 Hz-40 ms) at 480±20 nm (505 DCLP, 535±25 BP) via an optical switch (Sutter Instruments, Novato, CA). Images were acquired and analyzed using Axon Imaging Workbench Software (Axon Instruments, Union City, CA). All statistical analyses were performed using Student's

two-tailed t-test using the number of coverslips as N unless stated otherwise. Experimental results are represented as mean ± S.E.M.

Electron microscopy

Cells were either treated with 90 mM K^+ and HRP (10mg/ml, Sigma) containing Tyrode solution for 120s or 4 mM K^+ Tyrode solution containing HRP and TTX for 15 minutes. Coverslips were quickly rinsed and fixed for 30 min with 2% glutaraldehyde in 0.1 M sodium phosphate buffer, pH 7.4 at 37 °C. For 3,3'-diaminobenzidine (DAB) reaction, coverslips were incubated in Tris-Cl buffer (100mM, pH=7.4) containing DAB (0.1%) and H_2O_2 (0.02%) for 15 min. They were then rinsed twice in buffer and incubated in 1% OsO_4 for 30 min at room temperature. After rinsing with distilled water, specimens were stained en bloc with 2% aqueous uranyl acetate for 15 min, dehydrated in ethanol and embedded in Poly/Bed 812 for 24 hr. Sections (60 nm) were post-stained with uranyl acetate and lead citrate and viewed with a JEOL 1200 EX transmission microscope.

Electrophysiology

Cultures were incubated in the modified Tyrode solution containing 67 nM folimycin (Calbiochem, La Jolla, CA) dissolved in DMSO (Sigma, St Louis, MO) or vehicle alone, at 37°C for 10 minutes in the presence of 1μM TTX. Following treatment, pyramidal cells were voltage-clamped to -70 mV using whole-cell patch clamp technique. Electrode solution contained (in mM): 115 Cs-$MeSO_3$, 10 CsCl, 5 NaCl, 10 HEPES, 0.6 EGTA, 20 TEACl, 4 Mg-ATP, 0.3 Na_2GTP, 10 QX-314 (Sigma, St Louis, MO, pH 7.35, 300 mOsm). Data was acquired using an Axopatch 200B amplifier and Clampex 8.0 software (Axon Instruments, Union City, CA). Recordings were filtered at 2 kHz and sampled at 5 kHz. Spontaneous events were recorded in the presence of 1μM TTX. For measuring evoked responses, electrical stimulation was delivered through parallel platinum electrodes in modified Tyrode solution without CNQX or AP-5. All statistical comparisons were performed with two-tailed unpaired t test; values are given as mean ± SEM.

Modeling spontaneous synaptic vesicle recycling

The recycling of spontaneous vesicles was fit with a single pool model with four states: s_0 = Dye loaded vesicles, s_1 = Mobilized vesicles, s_2 = Empty vesicles, s_3 = Recycled

and mixed empty vesicles using rate constants: α = rate of mobilization, δ = rate of dye loss, β = rate of recycling. The data in Figure 5.8 could be fit with $\alpha = 0.0008\ s^{-1}$ (~1 vesicle per 120s for a pool of 15 vesicles), $\delta = 1.67\ s^{-1}$, $\beta = 0.5\ s^{-1}$ (Figure5B, bold line; 5C).

$$\frac{ds_0}{dt} = -\alpha \cdot s_0 \cdot \left(\frac{s_0}{s_0 + s_3} \right)$$

$$\frac{ds_1}{dt} = -\delta \cdot s_1 + \alpha \cdot \left(\frac{s_0}{s_0 + s_3} \right) \cdot s_0$$

$$\frac{ds_2}{dt} = -\beta \cdot s_2 + \delta \cdot s_1$$

$$\frac{ds_3}{dt} = \beta \cdot s_2$$

Changes in the rate of exocytosis caused dramatic shifts in the simulated destaining pattern (data not shown). The rate of recycling also altered the kinetics of dye loss due to the mixing parameter although not as dramatically as changes to the exocytosis rate. The pool size used in the simulation shown is 15 vesicles, however since the plot shows kinetics normalized to the total pool size, as is the case with the FM measurements, the absolute pool size (i.e. the number of vesicles used for the simulation) did not affect the normalized kinetics of destaining. Once vesicles in the simulation exocytose and release their dye, the empty vesicles were then equally mixed with the population of vesicles that remained labeled. Without this mixing the kinetics of destaining was more rapid (Figure 5.8B). A two-compartment model for evoked vesicle recycling is described in Appendix A.

Results

Synaptic vesicles recycle at rest and preserve their molecular identity during recycling

To visualize spontaneous vesicle trafficking at presynaptic terminals we incubated mature hippocampal cultures with AM1-44, which is a fixable version of the styryl dye FM1-43, together with a polyclonal antibody generated against the lumenal domain of the synaptic vesicle protein synaptotagmin 1 (syt1). The incubation was carried out for 15 minutes in the presence of tetrodotoxin (TTX) to block action potential firing. AM1-44 indiscriminately labels endocytosing membranes whereas the antibody against the lumenal domain of syt1 can specifically label endocytosing synaptic vesicles under the same condition (Malgaroli et al., 1995; Matteoli et al., 1992). Figure 5.1 shows that the distribution of fluorescent AM1-44 puncta after spontaneous dye uptake was similar to the labeling with syt1 antibody visualized by a fluorescent secondary antibody after permeabilization. AM1-44 and syt1 staining patterns avoided dendrites and cell bodies but marked presynaptic terminals. Fluorescent intensities of the two labels showed significant co-localization suggesting that the AM1-44 signal originates from synaptic vesicles as identified by their syt1 immunoreactivity (Figure 5.1A-E). We also compared spontaneous AM1-44 labeling to the activity-dependent uptake of syt1 antibody in the same synapse. Both signals were again co-localized as measured by the correlation of pixel fluorescence intensities (Figure 5.1F-J). In contrast to the spontaneous uptake of both probes, which resulted in similar fluorescence intensities (Figure 5.1E), activity dependent labeling with syt1 resulted in brighter fluorescence compared to spontaneous AM1-44 uptake (Figure 5.1I-J).

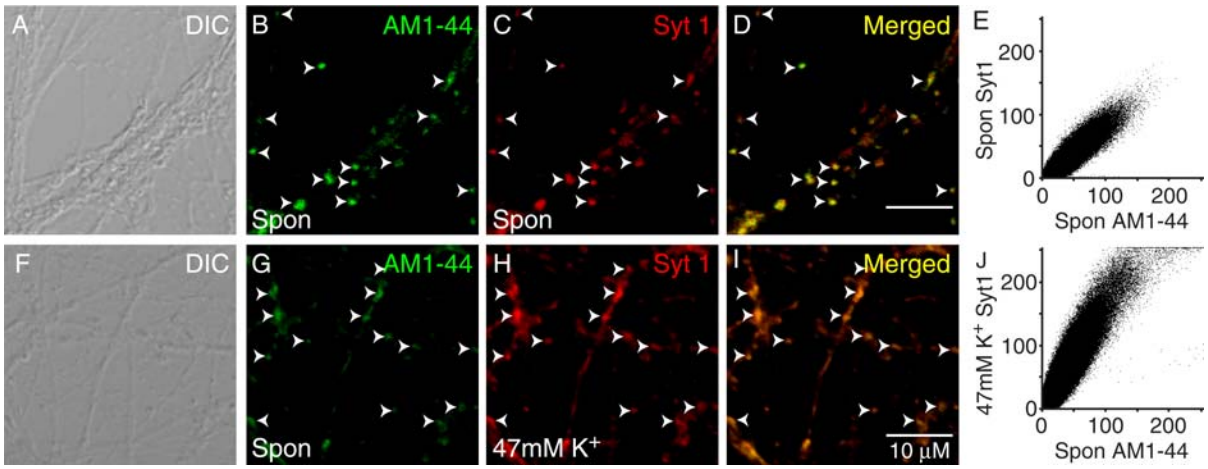

Figure 5.1. Visualization of spontaneous endocytosis in hippocampal cultures. **(A-D)** Fluorescent images of synapses loaded by spontaneous AM1-44 uptake (B) and spontaneous uptake of synaptotagmin 1 (syt1) lumenal domain antibody (C) show co-localization (D) suggesting that the fixable FM1-43 analog (AM1-44) is taken up into synapses by spontaneously recycling synaptic vesicles. **(E)** Cytofluorogram (joint distribution of pixel intensity values from the two fluorescence detection channels) showing co-localization of spontaneous AM1-44 and syt1 antibody uptake. **(F-I)** Fluorescent images of synapses loaded by spontaneous AM1-44 uptake (G) and 47 mM K^+ (activity) induced uptake of synaptotagmin 1 (syt1) lumenal domain antibody (H) show co-localization (I) suggesting that the fixable FM dye (AM1-44) is taken up by the same synapses that show activity dependent vesicle recycling. **(J)** Cytofluorogram showing co-localization of spontaneous AM-144 and activity dependent syt1 antibody uptake. The leftward skew is consistent with a larger pool of activity dependent recycling vesicles than spontaneously recycling vesicles (see Figure 5.4E).

We next tested whether spontaneously endocytosed synaptic vesicles recycle and become re-available for fusion and thus take up a second probe. To test this possibility we exposed cultures to the antibody against the lumenal domain of syt1 for 15 minutes in the presence of TTX. After wash out of the primary antibody (>15 minutes) we incubated cultures with the fluorescently conjugated secondary antibody (in the presence of TTX), which can only recognize the primary antibody once it is exposed to the extracellular medium (Figure 5.2A). This experiment resulted in significant punctate immunolabeling of hippocampal cultures without permeabilization (Figure 5.2B). When we introduced the secondary antibody through permeabilization after the spontaneous uptake of the primary antibody, the amount and the pattern of fluorescence labeling was comparable to the one seen

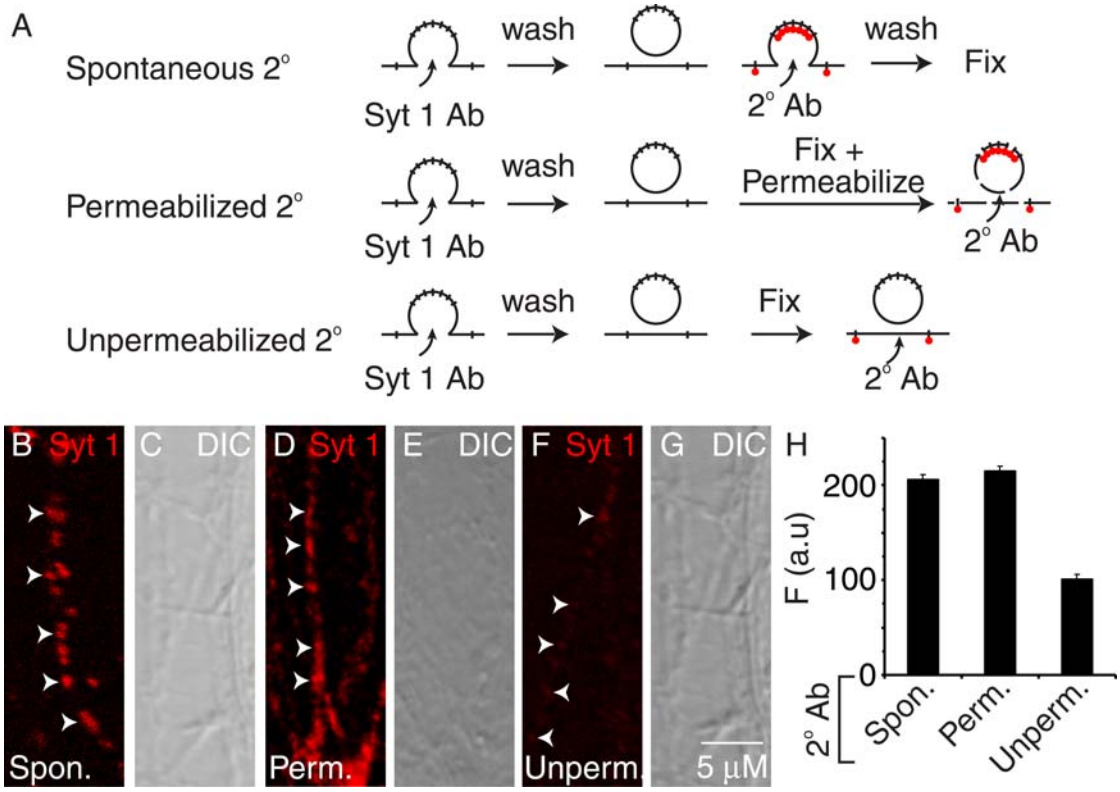

Figure 5.2. Spontaneous recycling of synaptic vesicle protein synaptotagmin 1. **(A)** Experimental protocol. Synapses were loaded spontaneously with synaptotagmin 1 lumenal domain antibody. After wash out of the primary, secondary antibodies were either loaded spontaneously (spontaneous 2º), or delivered after fixation. In the case of "permeabilized 2º" experiments secondary antibody was delivered after permeabilization with saponin. For "unpermeabilized 2º" experiments synapses were fixed and secondary antibodies loaded without permeabilization to check for surface epitopes. **(B-G)** Synapses that were labeled with the secondary antibody spontaneously (B-C) or after fixation and permeabilization (D-E) show strong punctuate fluorescence, while synapses labeled with the secondary after fixation without permeabilization only show weak fluorescence (F-G) suggesting that the fluorescent labeling is primarily due to uptake of secondary antibody into spontaneously recycling vesicles and not entirely due to residual surface antibody or fluorescence background. **(H)** Quantification of fluorescence intensity of puncta in the three loading paradigms (n=150 synapses for each condition, 10 cells, 15 synapses per cell).

before when the secondary antibody was introduced by uptake without permeabilization (Figure 5.2D-E, H). To check the amount of syt1 epitope available on the surface membrane at any given time during spontaneous vesicle recycling we labeled cultures with the

secondary antibody after fixation but without permeabilization (Figure 5.2A, F-G). This maneuver resulted in substantially diminished fluorescence labeling, which can be partly due to non-specific reactivity of the secondary antibody. This finding suggests that most of the fluorescence in earlier experiments originated from internalized syt1 (Figure 5.2H). Taken together, the re-availability of the primary syt1 antibody for interaction with the fluorescent secondary after a 15-minute wash period indicates that synaptic vesicles are spontaneously recycled with minimal loss of their molecular identity.

Spontaneously endocytosed vesicles preferentially populate a reluctant/reserve pool

If some synaptic vesicles recycle at rest, then do these vesicles randomly mix with the activity-dependent recycling vesicles? To address this question, we exposed hippocampal cultures to the styryl dye FM2-10 for 10 minutes in the presence of TTX (Figure 5.3A). This allowed vesicles that exocytose spontaneously and subsequently endocytose to take up FM2-10. After dye washout, spontaneously loaded synapses emerged as fluorescent puncta (similar to AM1-44 puncta seen in Figure 5.1) that could subsequently be destained in response to stimulation. Surprisingly, application of 90 mM K^+/ 2 mM Ca^{2+} depolarizing solution to the spontaneously stained puncta resulted in slow monophasic destaining (Figure 5.3B). In contrast, when we labeled the same set of synapses with elevated potassium (47 mM K^+) stimulation after a 10-minute rest period they were labeled intensely and destained with the typical biphasic pattern generally observed in response to a 90 mM K^+ challenge (Klingauf et al., 1998) (Figure 5.3B). When we challenged spontaneously labeled synapses with 10-Hz field stimulation, this low intensity stimulation also led to slower destaining compared to the destaining induced by 10-Hz stimulation of the same synapses labeled with 47 mM K^+ stimulation (Figure 5.3C). This result suggests that spontaneously endocytosed vesicles selectively populate a reserve pool from which they are only reluctantly available for release.

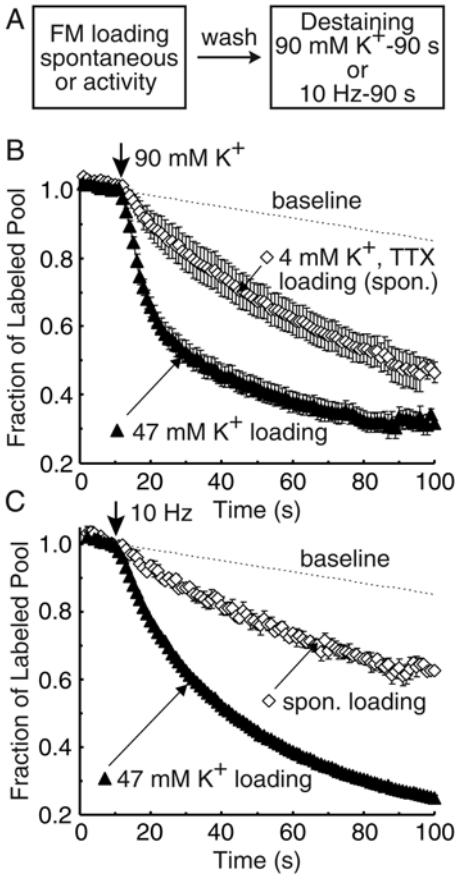

Figure 5.3. Spontaneously endocytosed vesicles preferentially populate a reluctant/reserve pool. **(A)** Experimental protocol. **(B)** Spontaneously loaded synapses (N = 10 [# of experiments], (495) [# of synapses]) show slow monophasic destaining kinetics in response to 90 mM K^+ application. In contrast, the same synapses loaded maximally by high potassium stimulation display rapid biphasic destaining. **(C)** Application of action potentials at 10Hz to hippocampal cultures results in slower destaining of synapses loaded in the presence of TTX (N = 3 (119)) compared to synapses labeled with 47 mM K^+ stimulation.

To examine this premise in depth we investigated three additional parameters. First, we analyzed the rates of 90 mM K^+-induced dye loss from individual synapses labeled through spontaneous fusion or elevated potassium (47 mM K^+) stimulation (Figure 5.4). Interestingly, this analysis revealed that approximately 10% (out of 295) of synapses showed rapid destaining after spontaneous dye labeling albeit still slower than dye release after activity-dependent labeling. This finding is in agreement with previous observations (Prange and Murphy, 1999). However, such rapid destaining patterns had random occurrence within

the synapse population since there was no correlation between the rate of destaining and initial fluorescence levels nor with the amount of fluorescence sequestered within the synapses determined after background subtraction (R^2<0.05) (Figure 5.4). Second, we tested whether the rate of destaining was affected by the duration of dye wash out after staining. When we rapidly washed out FM dye within 2 minutes (instead of the usual 10-minutes) using fast perfusion (10 ml/min) and applied 90 mM K^+ stimulation immediately after dye washout, spontaneously labeled synapses still destained slower than synapses labeled with activity (Figure 5.5) suggesting that the 10-minutes time delay for dye wash did not mask a fast component of release for spontaneously labeled synapses. Finally, we examined whether synapses labeled through spontaneous recycling could release dye in response to hypertonic sucrose stimulation. Brief hypertonic sucrose application releases vesicles from the readily releasable pool (Rosenmund and Stevens, 1996). Therefore, if spontaneously labeled vesicles randomly mixed within the total activity-dependent recycling pool then some of these vesicles should be resident within the readily releasable pool and thus could be released by hypertonic sucrose application. When we perfused hyperosmolar solution (+0.5 M sucrose) onto spontaneously labeled synapses they did not release appreciable dye (Figure 5.6). In contrast, synapses labeled with activity released more than 20% of the dye in response to the same stimulation similar to previous observations (Pyle et al., 2000; Mozhayeva et al., 2002). These three observations reinforce the hypothesis that spontaneously fused vesicles once endocytosed do not mix with the total recycling pool and evade populating the readily releasable pool.

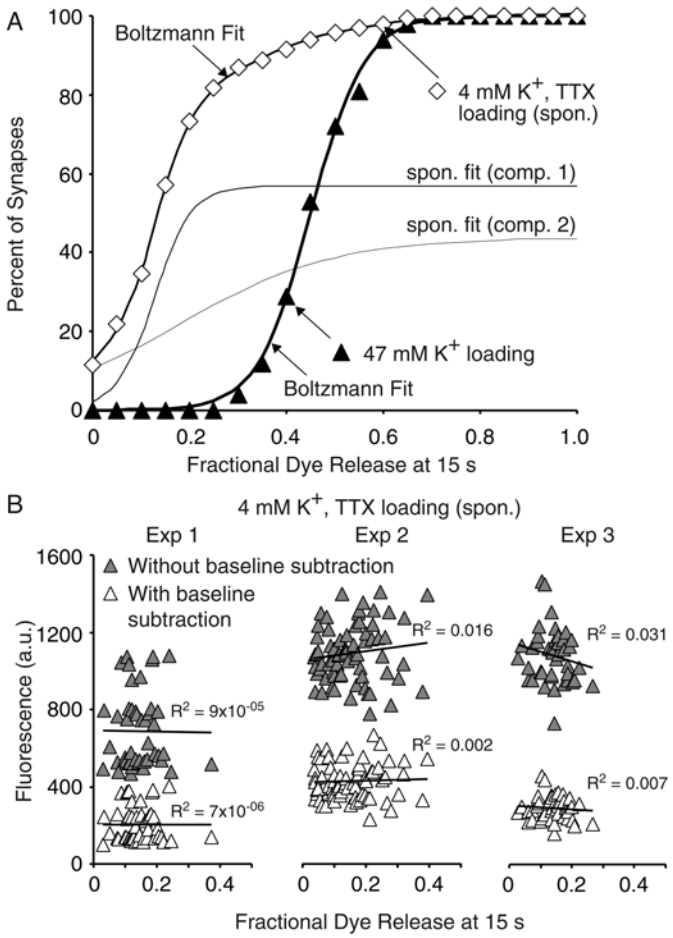

Figure 5.4. Distributions of destaining kinetics **(A)** Cumulative histogram of the fractional dye release after 15s of 90 mM K^+ stimulation from synapses loaded either spontaneously or by 47 mM K^+ (activity) in the data set from Figure 5.3A. While 80% of spontaneously loaded synapses only release up to 25% of trapped dye after 15s of 90 mM K^+ application, 100% of synapses labeled with activity release more than 25% of their dye load. The distribution of fluorescence values for spontaneous dye uptake (diamonds) was skewed towards positive values (skewness factor =1.48). This distribution had two components with median values 0.15 and 0.23 (thin lines). The distribution for activity-dependent dye uptake (filled triangles) was less skewed (skewness factor=0.25), accordingly, it could be described with a single Boltzmann function with a median of 0.45. Note that medians of the two distributions for spontaneous dye uptake were less than the median for activity-dependent dye uptake. **(B)** Sample experiments of spontaneously dye loaded synapses, plotting the distribution of fractional dye release after 15s vs. either the ΔF value (open triangles) or the un-normalized absolute fluorescence (gray triangles) for each individual synapse in the experiment. These plots show that there is no correlation between the fluorescence intensity and the rate of 90 mM K^+-induced dye release for spontaneously loaded synapses.

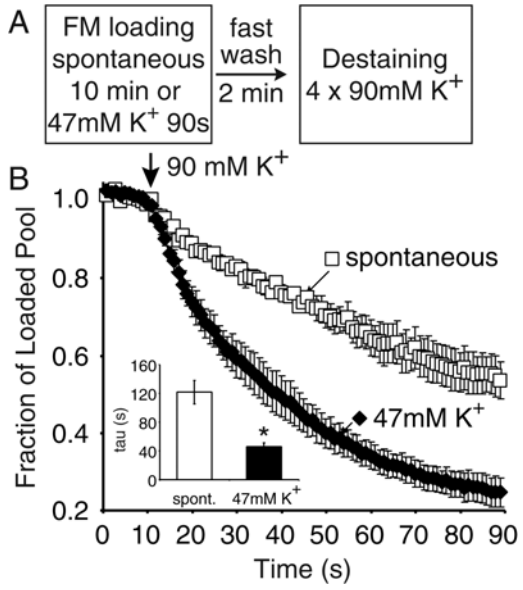

Figure 5.5. Dye washout time does not affect relative rates of dye release. **(A)** Experimental protocol. Synaptic vesicles were loaded with FM dye either spontaneously for 10min or with 47mM K^+ for 90s. Following rapid washout of the dye (10ml/min) for 2 min, synapses were imaged during 4 rounds of 90mM K^+ application. **(B)** Spontaneously loaded synapses release with slower kinetics compared to activity dependent loaded synapses. (B, inset) Single exponential fits of the destaining curves show significantly slower release of spontaneously loaded synapses (N = 3 each, $p<0.05$).

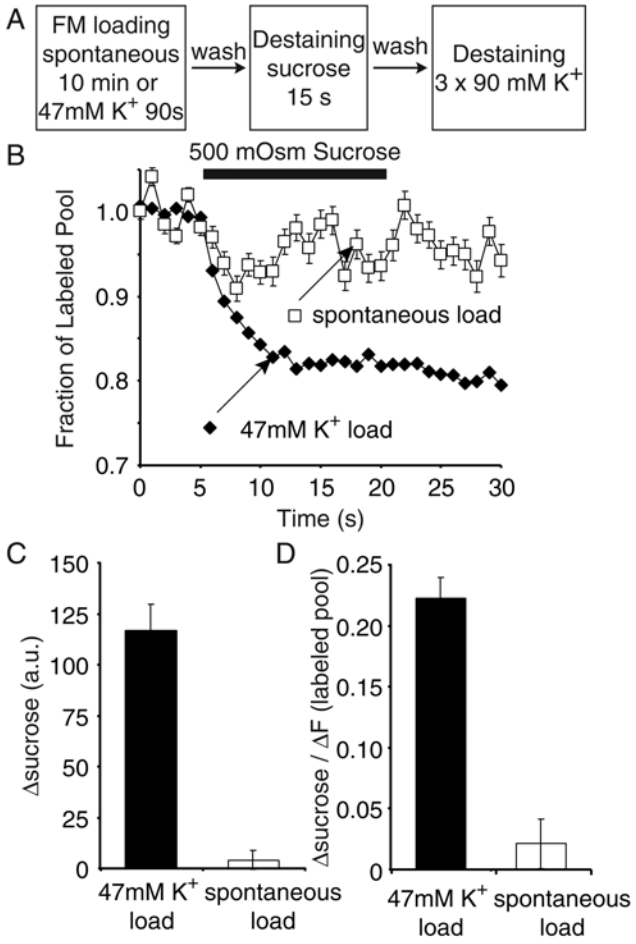

Figure 5.6. Spontaneously loaded vesicles do not populate the sucrose releasable pool **(A)** Experimental Protocol. Synaptic vesicles were loaded either spontaneously for 10min or with 47mM K^+ for 90s. Following washout of the dye, synapses were imaged during a 15s application of sucrose followed by 4 rounds of 90mM K^+ application. **(B)** Spontaneously loaded vesicles show minimal release during sucrose application compared to synapses loaded with activity. **(C-D)** Quantification of dye release as absolute fluorescence (C) and as a fraction of the pool loaded (D) by each stimulus protocol shows minimal sucrose responsiveness of spontaneously loaded synapses. Only 2 ± 2 % (normalized with respect to the amount of dye labeling) of spontaneously loaded dye was released by sucrose application compared to 22 ± 2 % of dye taken up during activity (N = 4 each, $p<0.0001$).

Vesicles labeled with minimal activity randomly mix within the total recycling pool

Comparison of the amount of dye loaded after spontaneous and 47 mM K^+ staining protocols revealed that during 10 min. spontaneous activity we could label only about 25% of the total recycling pool stained using the 47 mM K^+ challenge. To test whether the extent of dye loading or the number of dye loaded vesicles is a determinant of subsequent destaining kinetics; we labeled synapses with 60 action potentials applied within 2 seconds (30Hzx2s) (Figure 5.7A). This stimulation stained approximately 30% of the total vesicle pool and, in contrast to the behavior of spontaneously labeled vesicles; application of 90 mM K^+/ 2 mM Ca^{2+} solution resulted in biphasic destaining. The kinetics of destaining was identical to that seen after labeling of the total recycling pool with 47 mM K^+ stimulation (Figure 5.7B). This result suggests that vesicles labeled with 30Hzx2s stimulation randomly mix within the total recycling pool. In the case of spontaneously exo-endocytosed vesicles, however, equal mixing of endocytosed vesicles within the recycling pool does not occur during the 10 minute long wash out period after dye uptake. The comparable magnitude of dye labeling after 30Hzx2s stimulation and spontaneous labeling indicates that this observation is not simply due to low signal to noise ratio at low fluorescence intensities but is an outcome of the presence or absence of stimulation during dye uptake.

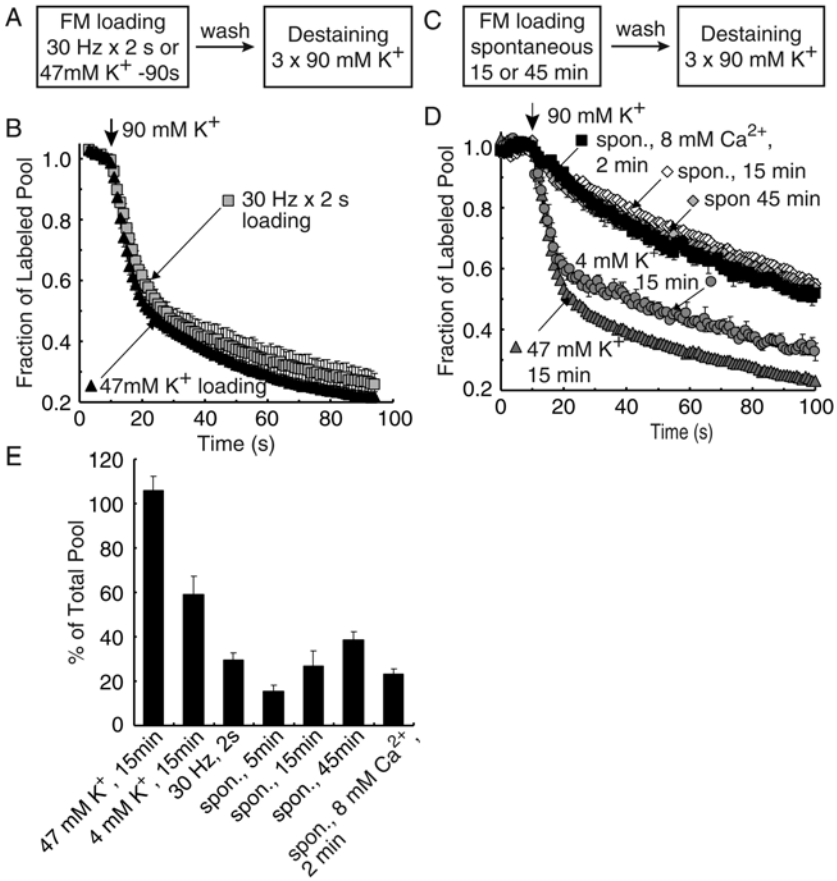

Figure 5.7. The kinetics of destaining is strictly dependent on the presence or absence of stimulation during the loading phase but not to the duration of dye labeling or the number of vesicles labeled. **(A)** Experimental protocol. Synapses were loaded with FM dye using either a 30Hzx2s AP stimulation or 47mM K^+ stimulation. Following a 10 min washout period synapses were imaged during the application of 90 mM K^+ solution. **(B)** The kinetics of vesicle mobilization is similar for synapses loaded by activity irrespective of the size of the fluorescently labeled pool. **(C)** Experimental protocol. **(D)** Synapses loaded by spontaneous exo-endocytosis of vesicles in 4 mM K^+/2 mM Ca^{2+} (in TTX) for 15 (or 45) minutes (N = 7 (691) and 7 (571) respectively) or in 4 mM K^+/8 mM Ca^{2+} (in TTX) solution for 2 minutes (N = 3 (239)) all show slow monophasic release kinetics during 90 mM K^+ induced destaining. In contrast, synapses loaded by activity induced by 47mM K^+ for 15 min (N = 3 (318)) or by the network activity existing in the neuronal circuits in the culture (4 mM K^+ 15 min; N = 3 (305)) show biphasic kinetics similar to synapses loaded with high potassium for 90s. **(E)** Normalized fluorescence values (ΔF) for the different loading paradigms described above. While 30Hzx2s stimulation loads a pool size comparable to the synapses loaded by the various spontaneous loading protocols, the kinetics of vesicle mobilization after 30Hzx2s is faster (D). Changing the duration of spontaneous loading or the concentration of Ca^{2+} does not affect the size of the labeled

pool. Removing of TTX from the solution to allow network activity increases the size of the pool loaded (E), but also changes the distribution of loaded vesicles (D). Prolonged application of 47 mM K^+ for 15 min does not significantly increase the size of labeling over that labeled during 90s. Decreasing the duration of spontaneous dye loading from 15 minutes to 5 minutes, however, significantly decreased the amount of dye labeling (0.15±0.03 for 5 min. vs. 0.27±0.07 for 15 min., $p<0.05$).

The size of the spontaneously endocytosed vesicle pool is limited and independent of the duration of dye labeling or external Ca^{2+} concentration

We next tested whether longer duration incubation with FM dye would increase dye labeling and give more time for vesicle mixing and thus change the destaining kinetics of spontaneously labeled vesicles. Incubating hippocampal cultures with FM2-10 for 45 minutes in the presence of TTX did not significantly increase dye labeling from the level seen after 15 minutes incubation (Figure 5.7E). Furthermore, in response to 90 mM K^+ stimulation the destaining kinetics of these spontaneously labeled synapses was still monophasic and slow compared to the mobilization of vesicles after activity-dependent labeling (Figure 5.7C-D). However, reducing the duration of spontaneous labeling to 5 minutes significantly decreased dye uptake compared to 15-minute labeling ($p<0.05$) indicating that 5-minutes is not sufficient for mobilization of the total pool of spontaneously recycling vesicles (Figure 5.7E).

To further examine the relationship between the conditions for dye uptake and ensuing high potassium induced dye release we elevated extracellular Ca^{2+} from 2 mM to 8 mM to increase spontaneous fusion rate [3.02±0.74-fold increase measured electrophysiologically (n=5)]. In 8 mM Ca^{2+}, a two-minute incubation with FM dye labeled up to 25% of the total recycling pool. Vesicles stained in this manner still destained slowly when exposed to a 90 mM K^+ challenge. In contrast, incubation of synapses in 47 mM K^+ solution for 15 minutes or 4 mM K^+ solution for 15 minutes in the absence of TTX (to allow network activity) resulted in a significantly higher level of labeling with these synapses displaying typical biphasic destaining kinetics during 90 mM K^+ stimulation (Figure 5.7D, E). Taken together, these results show that the kinetics of destaining was strictly dependent on the presence or absence of stimulation during the loading phase but not to the duration of

dye labeling or the number of vesicles labeled. In addition, irrespective of extracellular Ca^{2+} levels or the duration of stimulation, spontaneous dye uptake labeled a limited pool size, less than one third of the total recycling pool, which was only reluctantly releasable during sustained stimulation (Figure 5.7E). Our analysis also showed that the size of the spontaneously labeled vesicle pool was correlated with the size of the total recycling pool labeled with high K^+ stimulation in a given synapse (R^2 = 0.67±0.05, n=8). This result indicates that spontaneous and activity-dependent dye uptake labels the same presynaptic terminal as suggested in an earlier study by Prange and Murphy (1999). However, this correlation was not as tight as the one we normally observe between 30 Hzx2s labeling and the total recycling pool size (R^2 = 0.84±0.03, n=6). This is consistent with the argument that spontaneous dye uptake and 30 Hzx2s labeling originate from distinct pools.

Vesicles in the spontaneously labeled pool are more likely to re-fuse spontaneously

What is the relative tendency of spontaneously endocytosed vesicles to re-fuse spontaneously? To address this question we labeled synaptic terminals either through spontaneous dye uptake or activity-dependent stimulation. Then, after dye wash out we monitored the rate of spontaneous fluorescence decay for twenty minutes (Figure 5.8A). In these experiments to minimize fluorescence loss due to photobleaching we acquired images using brief exposures at 30-second time intervals. Surprisingly, spontaneously stained synapses showed more pronounced spontaneous destaining compared to fluorescence destaining after activity-dependent loading with 30Hzx2s or high K^+ stimulation (Figure 5.8B). Despite the difference of staining levels reached after high K^+ stimulation versus the brief burst of action potentials (Figure 5.8B inset), both staining levels lost less than 25% of their initial amplitudes within twenty minutes (Figure 5.8B). In contrast, synapses labeled with spontaneous dye uptake showed accelerated destaining with the loss of 45% of the initial level within the same time frame. Thus the acceleration in the rate of spontaneous dye loss was not dependent on the number of labeled vesicles but was rather a consequence of the absence of stimulation during dye uptake. This result suggests that spontaneously endocytosed vesicles were more likely to be reused spontaneously.

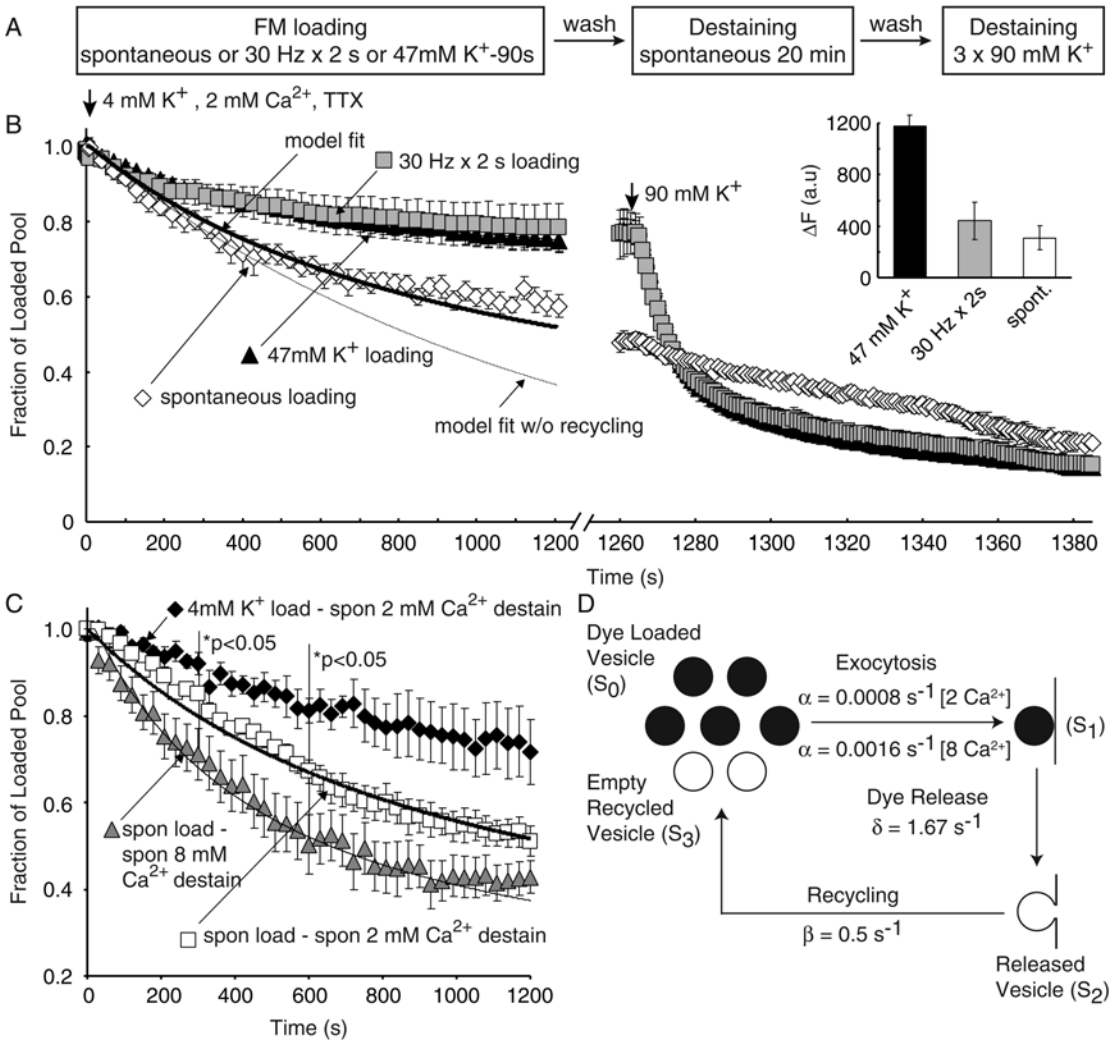

Figure 5.8. Vesicles in the spontaneously labeled pool are more likely to re-fuse spontaneously. **(A)** Experimental Protocol. **(B)** Spontaneously loaded vesicles preferentially re-exocytose spontaneously. Approximately 45% of the spontaneously loaded pool had spontaneously exocytosed after 20 minutes (N = 9 (571), less than 25% of the 47 mM K+ or the 30Hzx2s loaded pool (N = 6 (605) and 10 (983) respectively) had fused spontaneously within the same time frame ($p<0.01$). (B, inset) F values for different loading paradigms. Even though a larger pool of vesicles is loaded by 47 mM K+ stimulation compared to spontaneous or 30Hzx2s loading, the kinetics of spontaneous exocytosis from the activity-dependent pool is slower than the spontaneous pool (B). **(C)** Spontaneous recycling is regulated by extracellular Ca^{2+} concentration. Spontaneously loaded vesicles showed faster exocytosis kinetics in the presence of 8mM Ca^{2+} compared to 2mM Ca^{2+}. While 33% of the spontaneously loaded pool had released in 10 minutes with 2mM extracellular Ca^{2+}, 50% had released with 8mM extracellular Ca^{2+} (N = 5 (557) and 7 (696) respectively, $p<0.05$). Vesicles that were loaded with endogenous network

activity present in the cultures for the same time as in the spontaneous loading paradigms (10 min), showed slower spontaneous release kinetics compared to spontaneously loaded vesicles (19% release by 10 minutes, N = 5 (539), $p<0.05$), similar to activity loaded vesicles in Figure 5.8B. **(D)** Spontaneous dye loss from the spontaneously labeled pool can be described with a simple model in which a fixed set of vesicles are released with a rate of 1 vesicle per 120s (for 2 mM extracellular Ca^{2+}) and recycle with a rate of 1 vesicle per 2s (bold line in B and C). In the presence of 8 mM extracellular Ca^{2+}, the data could be fit with an exocytosis rate of 1 vesicle/60s keeping the recycling rate constant (lower line in C).

We next compared the rate of spontaneous dye loss in the presence of 2 mM or 8 mM Ca^{2+} after spontaneous dye uptake. In 8 mM Ca^{2+}, spontaneous dye loss was significantly faster in accordance with the earlier observation that elevated extracellular Ca^{2+} concentration increases frequency of spontaneous fusion (Figure 5.8C). We also tested whether prolonged loading (10 min.) in the presence of background network activity (0.83 ± 0.15 Hz, n = 3) altered the rate of subsequent spontaneous dye loss. Vesicles labeled in this way were mostly endocytosed in response to network activity since the amount of dye uptake is at least 2-fold larger than spontaneous dye uptake (in TTX) for the same duration. These vesicles endocytosed during network activity were also slow in their ability to fuse spontaneously compared to vesicles that were labeled spontaneously (black diamonds, Figure 5.8C). These findings also confirm the specificity of the spontaneous dye loss paradigm we used here to monitor spontaneous vesicle recycling.

Spontaneous recycling can be fit with a single pool model

Previous studies have estimated the rate of spontaneous vesicle fusion per synapse to be on the order of 1 vesicle per 90s (Geppert et al., 1994; Murthy and Stevens, 1999). This estimate is faster than the rate we observed for dye loss from spontaneously labeled vesicles in the absence of stimulation (Figure 5.8B). A simplified kinetic model allowed us to resolve this discrepancy with the assumption that spontaneously endocytosed vesicles rapidly mix with other vesicles in the same pool within seconds (~2 sec) (Figure 5.8D). This assumption is in line with a recent finding by Sun and colleagues (2002) who demonstrated that spontaneously fused vesicles can be endocytosed quite rapidly within 100 milliseconds as well as findings of Pyle and colleagues (2000) that endocytosed synaptic vesicles rapidly mix

with vesicles from the same pool. Incorporation of these parameters in a simple recycling scheme can accurately describe our data. In the absence of this recycling step, dye release is expected to decline by more than 60% within twenty minutes (Figure 5.8B, D). Furthermore, this kinetic model, by a two-fold increase in the rate of spontaneous exocytosis "α", could also successfully account for the increased rate of dye loss in the presence of 8 mM Ca^{2+} in the extracellular medium (Figure 5.8C,D). However, it is possible that increased extracellular Ca^{2+} may also affect other parameters such as the rate of recycling "β"(Figure 5.8D).

Blocking vesicle refilling at rest selectively depletes neurotransmitter from spontaneously fusing vesicles

Optical experiments we described so far suggest that a discrete pool of spontaneously recycling vesicles give rise to the electrophysiologically detected spontaneous fusion events (miniature synaptic currents or "minis"). To test this prediction we designed the following experiments in which we tagged spontaneously recycling vesicles by blocking neurotransmitter refilling after endocytosis at rest (Zhou et al., 2000) (Figure 5.9A). Recordings obtained after ten minutes incubation of hippocampal cultures with the vacuolar ATPase inhibitor folimycin in the presence of TTX demonstrated a six-fold reduction of mini frequency (Figure 5.9B, C and E). In contrast, this treatment only produced a 20% decrease in the amplitudes of minis (Figure 5.9F). Similarly, the decrease in the size of evoked synaptic current was only 25% after prolonged folimycin treatment (Figure 5.9D and G). These observations are consistent with the results of the earlier optical experiments demonstrating that spontaneously fusing vesicles originate from a distinct pool other than the ones that fuse in response to presynaptic action potentials. Therefore blocking vesicle refilling at rest (in TTX) selectively depletes neurotransmitter from spontaneously recycling vesicles since these vesicles would lose their neurotransmitter upon exo-endocytosis. In contrast, activity-dependent recycling vesicles are only affected by neurotransmitter leakage due to slow intravesicular alkalinization during folimycin treatment (Sankaranarayanan and Ryan, 2001). However, evoked transmission in folimycin treated cultures showed a rapid

use-dependent depression during repetitive stimulation suggesting these vesicles also cannot be refilled with neurotransmitter once they recycle (see Appendix A).

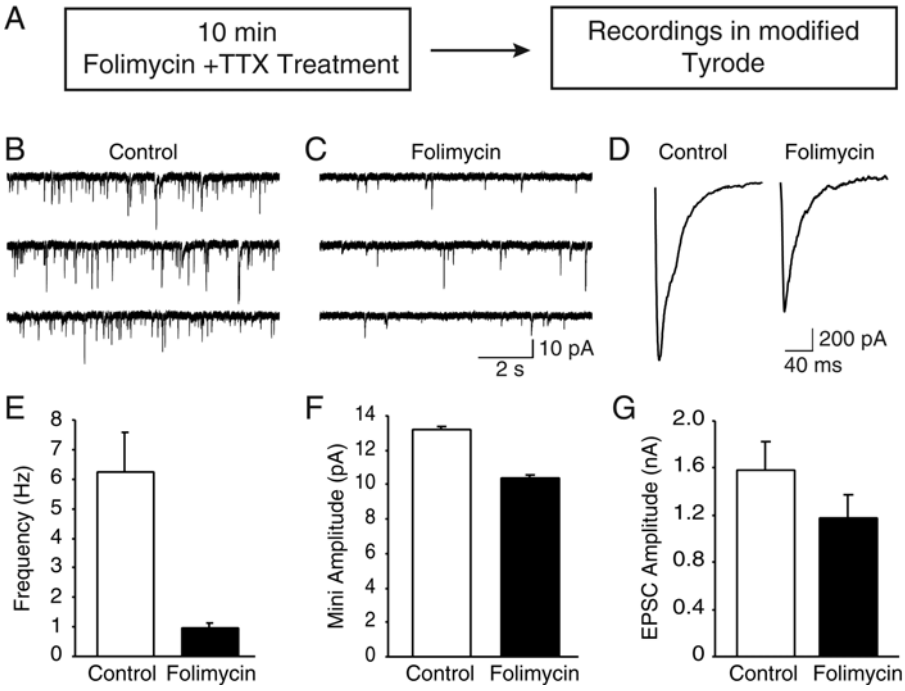

Figure 5.9. Blocking vesicle refilling at rest selectively depletes neurotransmitter from spontaneously fusing vesicles. **(A)** Experimental Protocol. **(B and C)** Sample traces of miniature postsynaptic currents from vehicle (DMSO) treated (B) and folimycin treated cultures (C). **(D)** Sample evoked responses for vehicle treated and folimycin treated cultures. **(E)** Summary graph showing 85% reduction in the frequency of spontaneous events (N = 7 and 8 for vehicle and folimycin treated cells respectively; $p<0.01$) **(F)** Summary graph showing 21% reduction in amplitude of spontaneous events (N = 7 and 8 for vehicle and folimycin treated cells respectively; $p<0.01$). **(G)** Summary graph showing 25% reduction in amplitude of evoked postsynaptic responses (N = 29 and 27 for vehicle and folimycin treated cells respectively; $p=0.19$).

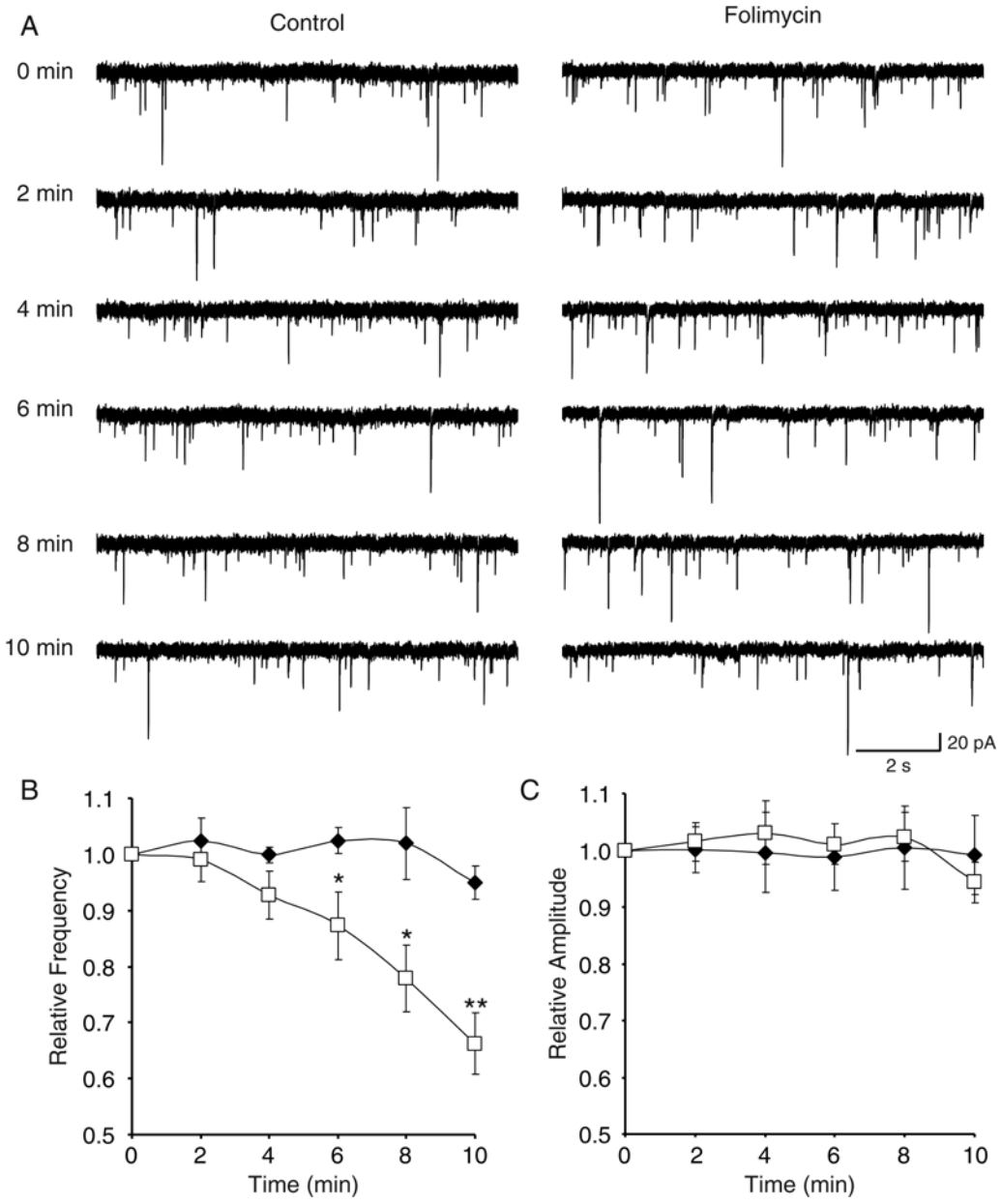

Figure 5.10. Time course of folimycin application on spontaneous event frequency and amplitude. **(A)** Sample traces of miniature spontaneous event recordings performed during 10 minutes of folimycin or vehicle (control) application to cultures. **(B)** Time course of mini frequency after application of folimycin or vehicle control shows a significant decrease in frequency by around 6 minutes of drug treatment ($p<0.05$, N = 7 cells each) which becomes increasingly significant by 10 minutes ($p<0.01$). **(C)** Amplitudes of minis do not significantly change over the 10-minute time course of the experiment.

In order to directly monitor the effect of folimycin, we recorded minis during folimycin application during the 10-minute period. In these experiments, we detected a significant gradual drop in mini frequency, whereas the amplitude of individual events remained relatively constant (Figure 5.10). This finding is consistent with the premise that the decrease in mini frequency is due to "all or nothing" loss of electrical quantal responses resulting from the absence of neurotransmitter refilling during vesicle recycling. The decrease in mini frequency recorded during the 10-minute folimycin perfusion was about 2-fold less than the decline seen in Figure 5.9. We believe this difference is due to the 5 to 10 minutes delay between the incubation with folimycin and the actual recordings shown in Figure 5.9.

Ultrastructural identification of spontaneously recycling synaptic vesicles

To visualize the spontaneously recycling vesicles at the ultrastructural level, we quantified the uptake of horseradish peroxidase (HRP) using electronmicroscopy (Heuser and Reese, 1973). In these experiments hippocampal cultures were treated with 90 mM K^+ for 120 seconds or were incubated with TTX for 15 minutes. HRP was present during the depolarization period or during the TTX treatment. In 90 mM K^+ treated synapses, the number of labeled vesicles per synapse per section was around 10 (9.7±1.2, n=22, Figure 5.11A, B). In contrast, spontaneously labeled vesicles were few in number (4±0.4, n=22, per synapse/section, range=1-8, median=4, Figure 7A, B). Both activity-dependent vesicles and spontaneously labeled vesicles had similar normal morphology (Figure 5.11C) and all labeled vesicles appeared to be evenly distributed within the synaptic vesicle cluster. These observations complement previous experiments using antibodies against synatotagmin-1 and FM dyes and suggest that the activity-dependent and spontaneously recycling vesicles have a molecular rather than an overt physical difference.

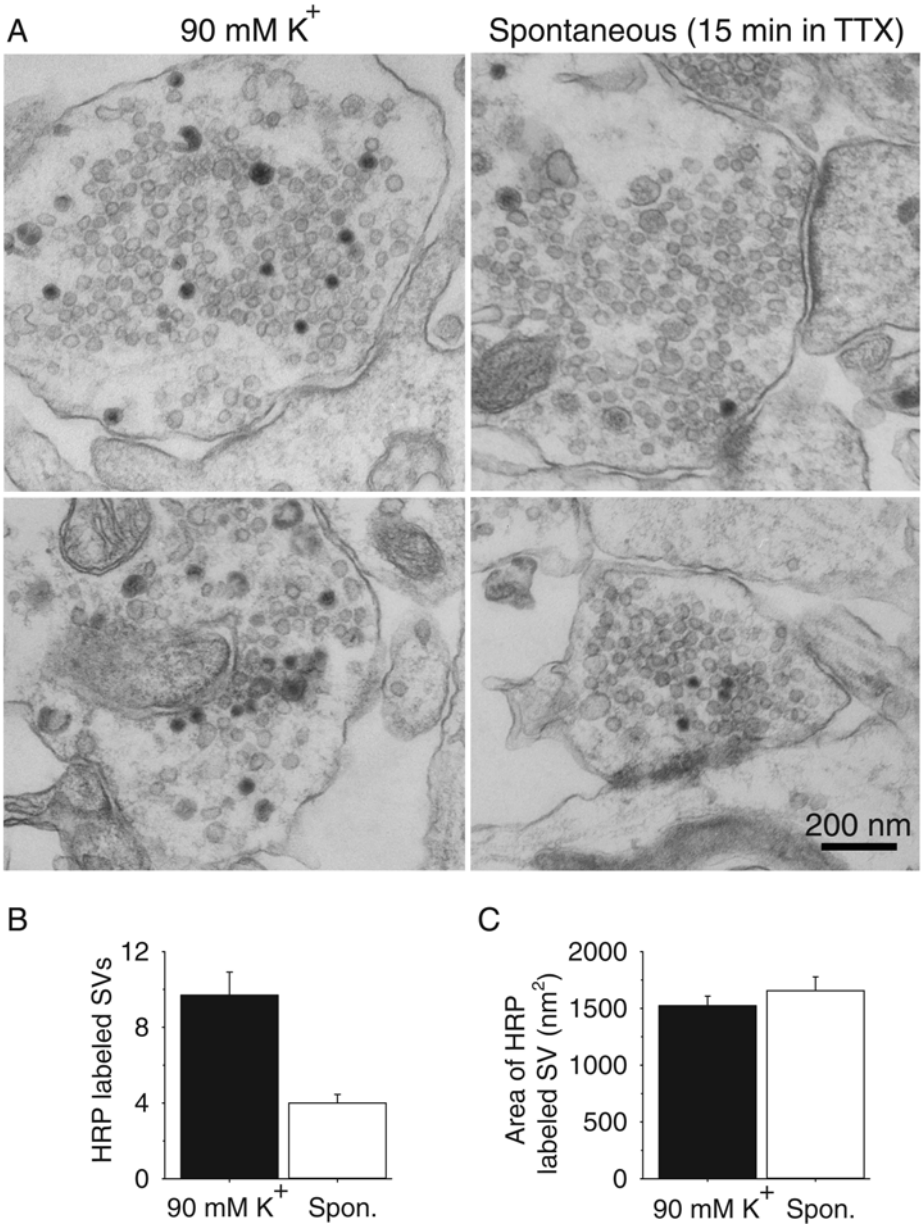

Figure 5.11. Electronmicroscopy of spontaneous uptake of horseradish peroxidase into synaptic vesicles. **(A)** Representative synapses labeled with horseradish peroxidase (HRP) during activity-dependent (left panels) and spontaneous staining (right panels). For activity-dependent HRP labeling hippocampal cultures were treated with 90 mM KCl containing solution for 120 s. HRP was present only during the stimulation. For spontaneous labeling cultures were incubated with HRP in the presence TTX for 15 minutes. **(B)** The number of HRP positive synaptic vesicles (SVs) was higher in the case of activity-dependent loading compare to spontaneous HRP uptake ($n \geq 20$ for all cases). **(C)** We did not detect a clear morphological or size difference, as depicted by labeled vesicle area, between the two vesicle populations.

The role of synaptobrevin/VAMP in spontaneous synaptic vesicle recycling

To gain insight to the molecular mechanisms that underlie spontaneous synaptic vesicle recycling, we monitored spontaneous FM dye uptake and release in embryonic hippocampal cultures derived from synaptobrevin-2 (VAMP-2) deficient mice. Synaptobrevin-2 is the major SNARE protein of synaptic vesicles and is required for fast Ca^{2+}-triggered synaptic vesicle exocytosis. The genetic deletion of synaptobrevin-2 partially abolishes fusion. Synaptobrevin-2-deficient (syb2-/-) synapses showed a six-fold reduction in spontaneous fusion frequency and they still exhibited ~10% of wild type (WT) release when stimulated by an application of hypertonic sucrose (Schoch et al., 2001). In contrast, the mutant synapses displayed <1% of WT release when stimulated by Ca^{2+}-influx during an action potential. However, syb2-/- synapses were capable of vesicle recycling on a slow time scale in response to high potassium stimulation or repetitive action potential stimulation (Deák et al., 2004). We first tested littermate WT cultures for the validity of our earlier observations in postnatal rat cultures (Figure 5.12). Spontaneous dye loss after activity-dependent dye loading (47 mM K^+) was significantly slower than dye loss from vesicles labeled spontaneously (Figure 5.12B). In the syb2-/- synapses, in agreement with previous electrophysiological experiments, the overall rate of spontaneous fusion was 3-fold slower than WT synapses. In addition, the amount of spontaneous dye labeling was 2-fold reduced compared to WT synapses. We attribute this apparent reduction in the difference between WT and syb2-/- synapses (compared to the earlier electrophysiological results) to the inherent bias towards selection of brighter puncta presumably corresponding to more active synapses during analysis of optical experiments. However, in striking contrast to WT synapses, the syb2-/- synapses showed similar rates of spontaneous dye loss after activity-dependent and spontaneous dye uptake (Figure 5.12B). This observation suggested that in the absence of synaptobrevin activity-dependent and spontaneous vesicle pools mix randomly. Next, we tested this premise using 90 mM K^+ induced destaining. Here, as in rat cultures, spontaneously labeled vesicles in littermate WT synapses displayed slow activity-dependent destaining in response to 90 mM K^+. In contrast, vesicles labeled with activity displayed typical robust destaining. In syb2-/- synapses vesicles labeled either with activity (47 mM

K^+) or with spontaneous dye uptake destained slowly with similar rates (Figure 5.12D). Taken together, these findings suggest that in the absence of synaptobrevin-2, activity-dependent and spontaneously recycling vesicle pools mix implicating the involvement of a synaptobrevin-mediated process in segregation of the two pools.

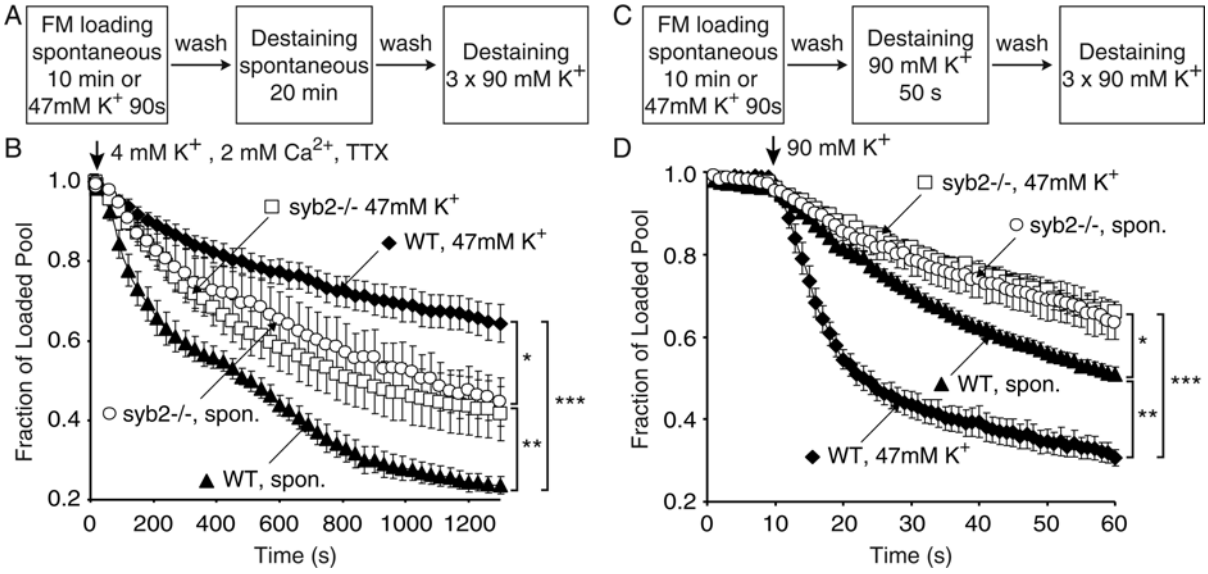

Figure 5.12. The role of synaptobrevin/VAMP in spontaneous synaptic vesicle recycling. **(A)** Experimental Protocol. **(B)** Spontaneously loaded vesicles in cultures lacking synaptobrevin-2 (syb2-/-) show slower spontaneous release kinetics compared to wild-type (WT) synapses (71% release in WT compared to 47% in syb2-/- after 15 minutes, N = 7 each, $p<0.01$). Synaptic vesicles loaded with activity dependent stimulation show slower spontaneous release in WT compared to syb2-/- cultures (30% release in WT compared to 52% in syb2-/-, N= 7 each, $p<0.05$). While spontaneously loaded vesicles in the WT embryonic mouse cultures (similar to rat cultures) preferentially re-released spontaneously compared to activity loaded synapses ($p<0.001$), surprisingly spontaneous exocytosis of vesicles in syb2-/- synapses was independent of the presence of activity during dye uptake ($p>0.6$) **(C)** Experimental protocol. **(D)** In WT cultures, spontaneously loaded vesicles showed slow activity dependent mobilization compared to activity-loaded vesicles (similar to rat cultures). Synapses lacking synaptobrevin-2 showed similar activity dependent dye release patterns irrespective of loading protocol. The kinetics of this release was significantly slower than WT synapses loaded either spontaneously ($p<0.05$) or with activity ($p<0.01$). (* $p<0.05$, ** $p<0.01$, *** $p<0.001$)

PMA redistributes activity dependent vesicles from the RP to the RRP irrespective of activity during treatment

Experiments using DAG analogs, phorbol esters, have shown a positive regulation of synaptic transmission (Malenka et al., 1986; Shapira et al., 1987). Several lines of evidence have shown that this regulation is mediated through increases in the size of the readily releasable pool (RRP). In hippocampal synapses this result has been shown electrophysiologically, using styryl dyes, and by biochemistry (Lonart and Südhof, 2000; Stevens and Sullivan, 1998; Waters and Smith, 2000). Similar effects of phorbol esters on the RRP have also been obtained in multiple different cell types including chromaffin cells (Yang et al., 2002), retinal bipolar cells (Berglund et al., 2002) and frog neuromuscular junction (Angleson and Betz, 2001). Phorbol esters have also been shown to increase the frequency of spontaneous vesicle release (Angleson and Betz, 2001; Rhee et al., 2002; Shapira et al., 1987). This increase in spontaneous release has been suggested to result from activation of L-type calcium channels and independent of phorbol ester action on the RRP (Waters and Smith, 2000).

To further explore the role of phorbol esters on regulation of spontaneous release we utilized the styryl dye FM2-10 to monitor the effect of phorbol 12-myristate 13-acetate (PMA) and its inactive form 4-α- phorbol 12-myristate 13-acetate (4α-PMA) on the evoked and spontaneously recycling vesicle pools. We used two different loading protocols on two populations of synapses. We either treated synapses with PMA or α-PMA during dye loading with 47mM K^+ or after washout of extracellular dye (Figure 5.13A). Synapses that were loaded by activity in the presence of PMA had an increased rate of sucrose dependent dye loss compared to 4α-PMA control synapses (Figure 5.13B). Somewhat surprisingly, yet not completely unexpectedly, synapses treated with PMA after dye loading and washout, also showed an increased rate of sucrose dependent dye release (Figure 5.13B). When we plotted the average median size of the total recycling pool in these four conditions, there was no significant change (Figure 5.13C). However, there was a significant increase in the ratio of dye released by 15 s sucrose application either when PMA was applied during the dye loading stage, or after dye loading and extracellular washout compared to two conditions of

4α-PMA treatment (Figure 5.13D). Given the fact that the PMA application increases the kinetics and amount of sucrose dependent dye loss from vesicles loaded by activity, irrespective of the application during or 5 minutes after loading, this suggests, that PMA dependent cascades are shuttling vesicles from the actively recycling reserve pool into the RRP and stabilizing them in this pool. They do not acquire vesicles from the dormant pool, as the total recycling pool size is not altered.

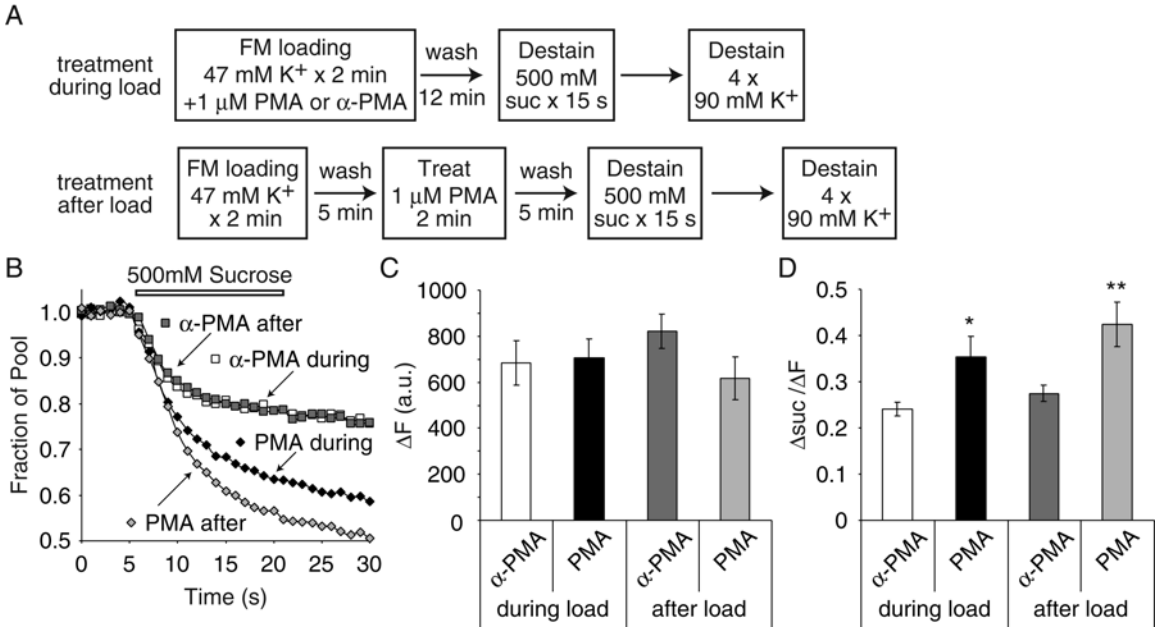

Figure 5.13. Activity is not necessary during PMA treatment for redistribution of evoked vesicle pools. **(A)** Experimental design. Separate sets of synapses were treated with PMA or 4α-PMA either during loading with 47 mM K+ or after 5 minutes of dye washout. Following washout of dye or residual phorbol ester for an additional 5 minutes, synapses were imaged during a 15 s application of 500 mM sucrose, followed by multiple rounds of 90 mM K^+ solution to maximally destain the synapses. **(B)** Sample responses of approximately 100 synapses from a single coverslip during 15s of 500 mM sucrose application. Synapses treated with PMA showed faster kinetics of dye loss compared to synapses treated with 4α-PMA as a control. **(C)** Total vesicle pool size as measured by the dye fluorescence trapped in synapses (ΔF) was not significantly different between the different loading paradigms (N = 6-7 coverslips each), although there was a tendency towards a smaller pool size in cultures treated with PMA after dye loading and washout compared with 4α-PMA (PMA treatment after load = 75 ±11% of 4α-PMA treated synapses, p=0.12). **(D)** The ratio of dye loss during sucrose application to the total pool size labeled (Δsuc/ΔF) showed a significant increase in synapses treated with PMA either during or after dye loading (N = 6-7 coverslips each, *p<0.05, **p<0.02).

PMA does not reorganize the spontaneous vesicle pool

We next tested whether PMA had any affect on the spontaneously recycling pool of vesicles. To this end, we loaded spontaneously recycling vesicles with FM2-10 dye for 10 minutes using a solution of 4 mM K^+ / 2 mM Ca^{2+} in the presence of 1μM tetrodotoxin (TTX) to inhibit the recurrent network activity present in the culture. Once again we either treated the synapses with PMA or 4α-PMA during the dye loading period, or for 10 minutes after the loading protocol when extracellular dye had been removed. We then imaged the synapses during multiple rounds of destaining with 90 mM K^+ (Figure 5.14A).

When we plot the total dye uptake during the different loading conditions, we observed that there was a selective increase in the amount of dye uptake when PMA was present during the FM dye loading (Figure 5.14B). This was coupled with an increased rate of dye release and the development of bi-exponential release kinetics in response to 90 mM K^+ (Figure 5.14C). Treatment with PMA after dye loading and washout did not show any change in pool size and the release kinetics showed normal slow mono-exponential activity dependent release similar to 4α-PMA control treatments. Fitting the release curves under these various loading conditions with two exponential curves we find that there was a selective decrease in the time constant of the fast component of release in synapse treated with PMA during the loading (Figure 5.14D) without any change in the slow time constant (Figure 5.14E). Additionally, the ratio of the proportion of the fast component to the slow component is significantly increased in synapses treated with PMA during loading (Figure 5.14F). This increase in fast release kinetics would suggest that vesicles are present in the activity dependent ready releasable pool.

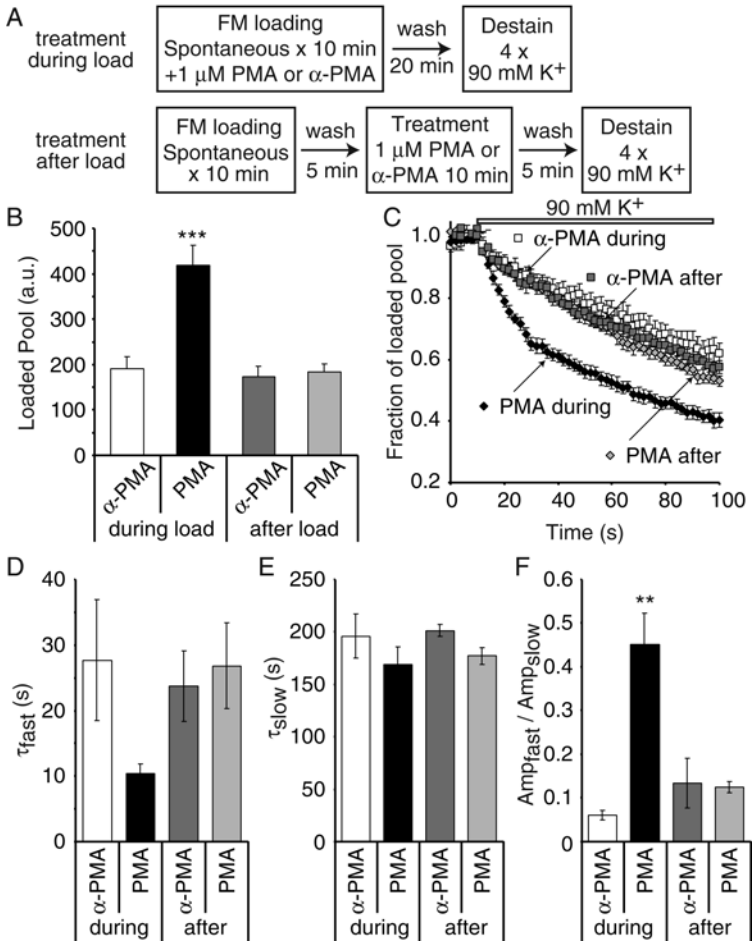

Figure 5.14. Spontaneous dye uptake in the presence of PMA labels a larger vesicle pool and shows biphasic kinetics of destaining with 90 mM K^+. **(A)** Experimental Design. Synapses were treated with 1 μM PMA or 4α-PMA either during spontaneous FM2-10 dye loading (in 4 mM K^+ / 2 mM Ca^{2+} and 1μM TTX) or after 5 minutes of dye washout for 10 minutes. Following an additional 5 minutes of dye washout, synapses were imaged during multiple rounds of 90 mM K^+ application. **(B)** Plot showing that the average median size of the dye labeled pool increases when PMA is present during dye loading (***$p<0.001$ for PMA during dye load compared to all other loading conditions, N = 5-9 coverslips for each condition). **(C)** Plot showing the average kinetics of dye destaining in response to high K^+ application different loading conditions. Dye destaining in synapses where PMA was present during the loading protocol show bi-phasic release typical of dye release from the evoked pool. Dye release in all other conditions shows mono-exponential slow dye loss typical of high K^+ destaining of the spontaneous vesicle pool. **(D)** The fast time constant of release in a double exponential fit of dye release under 90 mM K+ application is faster in synapses loaded in the presence of PMA compared to other loading paradigms. However this was not significant ($p = 0.12$) due to the large scatter in the fast time constants where effectively there is mono-exponential release.

(E) The slow time constant in a double exponential fit of the release kinetics was not altered by PMA. **(F)** The ratio of the amplitude of the fast to slow component of dye release was significantly larger in synapses that were loaded in the presence of PMA (**p<0.005 between PMA during load and all other loading conditions.

PMA dependent increase in pool size in the absence of activity is partly due to the loading of vesicles that normally populate the RRP

When synapses were loaded using activity (Figure 5.13), PMA treatment during or after loading had a similar affect on the RRP size. However PMA treatment during and after spontaneous loading does not lead to parallel effects. The increase in the pool size loaded in addition to the bi-exponential release kinetics suggest that when PMA is present during loading, it is able to load vesicles that populate the RRP. It has been previously shown that spontaneously loaded vesicles are excluded from this primarily activity dependent releasable pool (Figure 5.6).

To test this possibility, we loaded FM2-10 into vesicles again in the presence of TTX, with either PMA or 4α-PMA present during the 10 minutes of dye application. After dye washout, synapses were first imaged during a 15 s pulse of sucrose to release the readily releasable pool of vesicles, followed by maximal destaining using multiple rounds of 90 mM K^+ (Figure 5.15A). We found that when PMA was present during loading, there was a component of loaded dye that was releasable by sucrose, in contrast to the minimal dye loss on sucrose application of 4α-PMA treated synapses (Figure 5.15B). The absolute amount of dye released by sucrose (Figure 5.15C) as well as the fraction of the dye loaded pool (Figure 5.15D), was significantly larger in synapses treated with PMA during loading compared to 4α-PMA controls. This would suggest that the additional loading observed during PMA treatment, is due to a PMA dependent release of vesicles that would normally release under activity, and these vesicles then populate the normal activity dependent pool and show bi-phasic release kinetics. Alternatively PMA could shuttle spontaneously endocytosing vesicles into the RRP when present during loading. Our data cannot preclude either of these options. However the absence of a change in release kinetics when PMA treatment was

performed after loading strongly suggests that PMA does not act on spontaneously recycling vesicles after they have endocytosed.

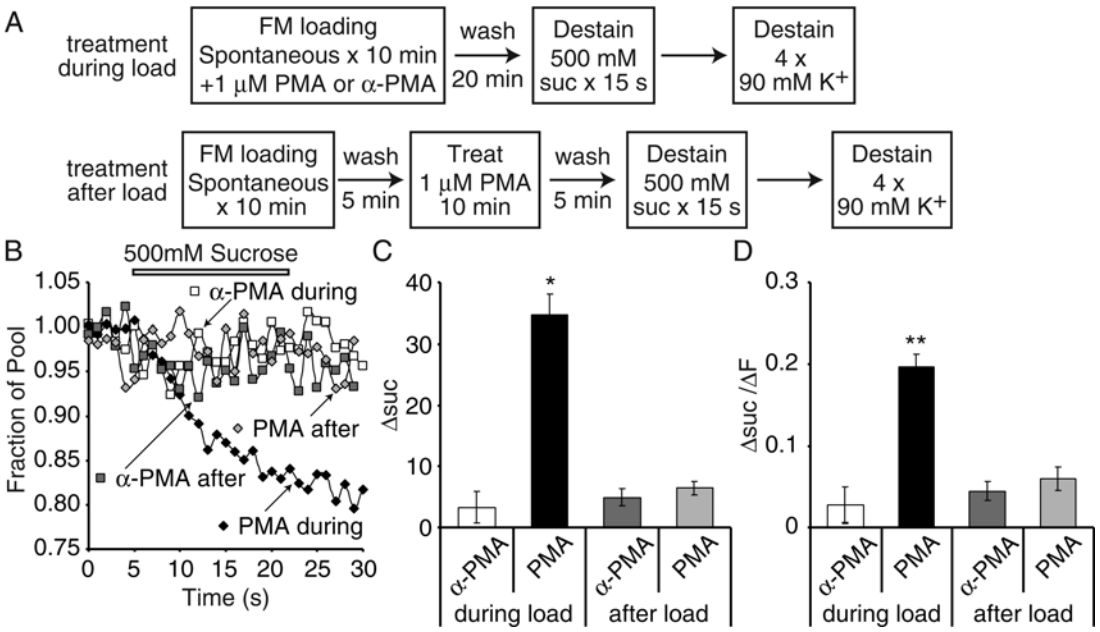

Figure 5.15. Vesicles labeled with dye during PMA application in the presence of TTX populate the RRP. **(A)** Experimental design. Synapses were treated with 1 μM PMA or α-PMA either during spontaneous FM2-10 dye loading (in mM K^+ / 2 mM Ca^{2+} and 1μM TTX) or after 5 minutes of dye washout for 10 minutes. Following an additional 5 minutes of dye washout, synapses were imaged during 15 s of sucrose application followed by multiple rounds of 90 mM K^+ application. **(B)** Sample traces of dye release during 15 s of sucrose application. Synapses loaded in the presence of PMA show faster dye release than α-PMA treated synapses that show minimal sucrose release. **(C)** Plotting the absolute dye loss during sucrose we see a significant increase in synapses treated with PMA during loading (**p< 0.002, N = 3 coverslips each). **(D)** Plotting the ratio of sucrose loss to total labeled pool we again observe a significant increase in RRP loaded when PMA is present during due loading (*p<0.01).

Discussion

The results of this study suggest that synaptic vesicles recycle at rest, which can be detected by uptake and re-availability of an antibody against the lumenal domain of synaptic vesicle protein synatotagmin-1 as well as internalization and release of styryl dyes. From these findings we can reach three major conclusions on the nature of spontaneous vesicle recycling in hippocampal synapses. First, spontaneously endocytosed vesicles preferentially populate a reluctant/reserve pool, which has limited cross talk with vesicles in the activity-dependent recycling pool. Second, the size of this spontaneously recycling vesicle pool is limited. Lastly, vesicles in the spontaneously recycling pool are more likely to re-fuse spontaneously. The evidence that supports these results can be summarized as follows: using uptake and release of fluorescent styryl dye FM2-10 we could show that the kinetics of dye release strictly depends on the manner in which the dye was taken up into vesicles. Whenever we allowed activity (action potentials or high K^+) during dye uptake the vesicles were equally mixed within the total recycling pool and showed similar rapid mobilization kinetics in response to sustained stimulation. In contrast, these activity-dependent recycling vesicles were not as readily available for release in the absence of stimulation. This situation was the opposite of what we observed with spontaneous dye uptake. Vesicles that took up dye during spontaneous exo-endocytosis were only reluctantly available for release during sustained stimulation whereas they were swiftly mobilized in the absence of activity compared to activity-dependent recycling vesicles. Here, it is interesting to note that vesicles labeled in response to hypertonic sucrose stimulation can be mobilized with similar kinetics as activity-dependent recycling vesicles suggesting that they equally mix within this pool (Mozhayeva et al., 2002; Pyle et al., 2000). This result is not surprising since vesicles released by hypertonic sucrose stimulation originate from the readily releasable pool and therefore are more likely to mix with other activity-dependent recycling vesicles. Accordingly, we were unable to release a significant fraction of spontaneously labeled synaptic vesicles by hypertonic sucrose stimulation (Figure 5.6). These two observations are consistent with this study demonstrating

that most of the spontaneously fusing vesicles originate from a vesicle pool other than the readily releasable pool.

We could also verify the predictions of the optical experiments with an approach where we electrophysiologically tagged spontaneously recycling synaptic vesicles using a blocker of vacuolar ATPase. This maneuver selectively depleted neurotransmitter from spontaneously recycling vesicles and thus resulted in a six-fold decrease in miniature postsynaptic current frequency. In contrast, the amplitudes of evoked events were minimally affected by this treatment suggesting that the vesicles that give rise to evoked events were not recycled spontaneously.

Additionally, using the phorbol ester PMA as a tool we could show that PMA specifically acts on the evoked vesicle pool. PMA is able to redistribute vesicles from the reserve pool into the readily releasable pool of vesicles (Figure 5.13). When we loaded vesicles spontaneously in the presence of PMA there was an increased dye labeling and a shift in kinetics from mono-exponential release to bi-phasic release (Figure 5.14C). This suggests that in the presence of PMA, labeled vesicles that endocytose populate the evoked pool even when TTX was present during loading. We also showed that this pool of vesicles was releasable by sucrose (Figure 5.14G-I), unlike normal spontaneously recycling vesicles. These findings agree with recent evidence that munc13 is the likely downstream effector of PMA (Rhee et al., 2002) contrary to previous studies that suggest PKC is the primary effector (Shapira et al., 1987; Stevens and Sullivan, 1998; Waters and Smith, 2000).

These findings raise the question whether spontaneously recycling vesicles fuse at the active zone or at an ectopic site as suggested by some earlier studies in the neuromuscular junction (Colmeus et al., 1982; Van der Kloot, 1996). The evidence presented in this study does not exclude either possibility. However we should note that a recent study in the frog neuromuscular junction showed that the docked vesicle pool might not directly correspond to the readily releasable pool (Rizzoli and Betz, 2004). This finding increases the plausibility of the argument that both spontaneous and activity dependent vesicles can fuse at the active zone despite their distinct origins.

The results presented here address a major question raised by earlier work on whether there are distinct vesicle trafficking pathways for spontaneous and evoked release in synapses. The only insight to this question so far has come from genetic studies which showed that spontaneous fusion rate was unchanged in the knockout of synaptotagmin 1 or complexins, proteins critical for evoked synchronous neurotransmitter release suggesting lack of a Ca^{2+} triggering step for spontaneous fusion (Geppert et al., 1994; Reim et al., 2001). Loss of the active zone scaffolding protein RIM1α impairs vesicle priming, thus hypertonic sucrose-induced and Ca^{2+}-evoked transmission, but does not significantly alter spontaneous fusion rate (Calakos, et al., 2004). In contrast, spontaneous fusion rate is significantly reduced after deletion of synaptobrevin2/VAMP2 or completely abolished after genetic deletion of munc-18 or munc-13 isoforms (Schoch et al., 2001; Varoqueaux et al., 2002; Verhage et al., 2000). The selective role of proteins such as synaptotagmin 1, complexin and RIM1α in evoked neurotransmitter release in contrast to the substantial role of synaptobrevin, munc-18 or munc-13 in both forms of vesicle trafficking is consistent with the premise that the two forms of release may originate from distinct recycling pathways. Interestingly, *Drosophila* neuromuscular junctions mutant in rab5, a small GTPase critical for vesicle trafficking through early endosomes, showed no differences in the frequency and amplitude of miniature excitatory junction potentials compared to wild type junctions (Wucherpfennig et al., 2003). In contrast, evoked neurotransmitter release probability was significantly altered in these mutants supporting the argument that both forms of release operate through distinct vesicle trafficking pathways. This premise is further supported by experiments performed by Koenig and Ikeda in the *Drosophila* neuromuscular junction where they monitored the recovery of evoked and spontaneous synaptic responses after *shibire*-induced vesicle depletion (Koenig and Ikeda, 1999). In this study they observed that the active zone population of vesicles and evoked neurotransmitter release recovered in parallel within 30s, in contrast, full recovery of spontaneous release took 10 to 15 minutes and required the recovery of the non-active zone population of vesicles.

In summary, these earlier results are consistent with our finding that spontaneous and activity-dependent vesicle recycling operates independently with limited cross talk. This

view may seem to contradict the notion that spontaneous release occurs through low probability random fusion of primed vesicles in the absence of an external trigger (Murthy and Stevens, 1999; Prange and Murphy, 1999). However, it is important to note that in the current study we cannot fully exclude this possibility; we only postulate that the spontaneous fusion probability of activity-dependent vesicles is low, at the limit of our technical resolution. Therefore, some spontaneous fusion events may still arise from primed vesicles albeit with a lower probability. The major caveat of our approach is that we only have an indirect way of assessing if the two vesicle populations are different. High-resolution ultrastructural analysis of vesicles after spontaneous and activity-dependent uptake of distinguishable probes would be the most direct way of testing whether the two sets of vesicles are indeed distinct. The limited electron microscopic analysis in this study did not reveal an obvious physical (or spatial) difference between the vesicle populations labeled with spontaneous versus activity-dependent uptake of HRP. Therefore, we propose that the functional segregation of the two sets of vesicles may be mediated by differences in the protein and/or lipid composition of the synaptic vesicles that make up the two pools. This premise is difficult to ascertain in the absence of direct biochemical evidence for synaptic vesicle heterogeneity. The finding that the antibodies to synaptotagmin-1 can readily label spontaneously recycling vesicles as well as the activity-dependent vesicles (Figure 5.1 and 6.2) argue against the absence or presence of synaptotagmin-1 as the underlying reason for this phenomenon. In contrast, our experiments in synaptobrevin-2-deficient synapses suggest a role for molecular interactions of synaptobrevin-2 or a synaptobrevin-2-dependent process (e.g. priming) in the segregation of the activity-dependent and spontaneous pools. The exact nature of the molecular diversity between the two vesicle pools and the mechanistic role of synaptobrevin-2 in this process remains to be identified. A divergence in the molecular composition of vesicles, as suggested by our findings, may also make differential regulation of these two recycling pathways a possibility. Such selective regulation may provide neural networks a means to distinguish between evoked and spontaneous synaptic activity.

CHAPTER 6: Synaptic Deficits in Neuronal Ceroid Lipofuscinosis-1 Knockout Mice

Background

Can presynaptic function be a substrate for certain disease states of the central nervous system? This is an important question because given our current ability to analyze synaptic vesicle dynamics in exquisite detail we are now in a position to start unraveling whether dysfunction of the presynaptic apparatus is the cause of certain diseases of the CNS. We can also begin to elaborate on which parameters, if any, are the most susceptible? To start to address this rather broad question we collaborated with Sandra Hofmann and colleagues to study a mouse model for one of the neuronal ceroid lipofuscinoses, infantile Batten disease.

The neuronal ceroid lipofuscinoses are a newly-recognized class of lysosomal storage disorders caused by single gene defects in lysosomal hydrolases or lysosomal or ER membrane proteins (Hofmann and Peltonen, 2001). These defects lead to the accumulation of autophagolysosomes (residual bodies) that produce a characteristic autofluorescence under fluorescent microscopy. In contrast to the classical lysosomal storage disorders, the storage material is relatively scant and the clinical picture (brain atrophy) more closely resembles purely neurodegenerative disorders. The most severe form of NCL is caused by autosomal recessive mutations in a lysosomal hydrolase, palmitoyl protein thioesterase (PPT1), that functions to cleave fatty acids from modified cysteine residues in proteins (Vesa et al., 1995). Loss-of-function mutations in the enzyme in humans results in normal early development in the first year followed by cognitive and motor difficulties, blindness, myoclonic jerks and seizures, and progression to a chronic vegetative state by the age of three (Haltia et al., 1973). Especially notable is a diffuse cerebral cortical and subcortical atrophy, with relative sparing of the brainstem and spinal cord. Similar changes were observed in a recently available mouse model of infantile NCL (Bible et al., 2004; Gupta et al., 2001). Why this single enzyme deficiency should be relatively selective for these neuronal populations (or neurons in general) is unknown and the mechanisms leading to cell death are unclear.

While PPT1 can be regarded as a classical lysosomal enzyme in non-neuronal tissues (Hellsten et al., 1996; Sleat et al., 1995; Verkruyse and Hofmann, 1996), the subcellular localization of PPT1 in neurons is somewhat unclear. Localization to synaptic vesicles has been suggested by several studies (Ahtiainen et al., 2003; Heinonen et al., 2000; Lehtovirta et al., 2001). PPT1 is found in synaptic vesicles in neuronal cultures when overexpression is driven through viral transfection (Ahtiainen et al., 2003; Lehtovirta et al., 2001) but localization under conditions of endogenous expression remains to be determined.

In the current study, we have studied cultured cortical neurons derived from *Ppt1* knockout mice in order to gain insights into how PPT1 deficiency may eventually lead to neuronal cell death. While we did not find evidence for a synaptic vesicle localization for endogenous PPT1 in cultured neurons, we find that neurons deficient in PPT1 demonstrate a reduction in total synaptic vesicle pool size (with a proportional decrease in the rapidly releasable pool) and corresponding decrease in the frequency of spontaneous miniature synaptic currents. These changes increase with time in culture. The neurons were shown to be otherwise robust by a number of stringent criteria and storage material was scant. Endogenous PPT1 was clearly demonstrated in a lysosomal compartment associated with the cell soma, and the pH of this compartment was shifted toward a more neutral pH. These results suggest that metabolites arising from PPT1 deficiency may have an effect on synaptic vesicle formation or recycling and may account for some of the clinical manifestations of INCL.

Materials and Methods

Cell culture

Dissociated cortical cultures were prepared from 1-2 day-old homozygous *Ppt1*$^{tm1Hof-/-}$ knockout or littermate control mice as described (Kavalali et al., 1999a) as determined by PPT1 enzymatic assay on tail clips and later confirmed by genotyping. The knockout was originally produced on a 129S6/SvEvTac background (Gupta et al., 2001) and then bred for 17 generations with C57BL/6J mice to produce the mutation on the C57BL/6J background used for this study. The knockout was produced through targeted deletion of exon 9 of *Ppt1*, which contains a portion of the enzyme active site, and results in no detectable enzyme activity or immunoreactivity (Gupta et al., 2001). Control cultures were derived from wild-type or heterozygous animals; no significant differences between *Ppt1*$^{tmHof+/+}$ and *Ppt1*$^{tmHof+/-}$ were observed (data not shown) and pooled data is presented unless otherwise indicated. Experiments were performed at 13-15 days in vitro (div) or 23-25 div as indicated in the Figure Legends. By 13 div, synapses have reached full maturity in culture (Mozhayeva et al., 2002).

Immunofluorescence microscopy

Primary cortical cultures from wild type and *Ppt1* knockout pups were fixed in freshly prepared 4% phosphate buffered paraformaldehyde (pH 7.4) for 30 min. After washing, cells were permeabilized in phosphate-buffered saline containing 0.4% saponin and 2% normal goat serum for 1 hour at ambient temperature. Immunostaining was performed by overnight incubation with rabbit anti-rat PPT1 polyclonal antibodies (raised in rabbits using full-length recombinant rat PPT1 exactly as described for the preparation of anti-bovine PPT1 antibodies (Verkruyse and Hofmann, 1996), mouse anti-synaptophysin monoclonal antibodies, rabbit anti-synaptophysin polyclonal antibodies, or monoclonal map2 antibodies (each a gift of Dr. Thomas Südhof, University of Texas Southwestern Medical Center) as indicated in the Figure Legends. Goat anti-human cathepsin D antibodies were from Santa Cruz (sc-6486). Alexa 488 conjugated goat anti rabbit and Alexa 568 conjugated goat anti

mouse (Molecular Probes) were used as secondary antibodies. Imaging was performed using a Leica TCS-SP2 Laser Scanning Spectral confocal microscope.

Tunel staining

Tunel staining was performed according to directions supplied by Promega (cat# G3250). Cells were counterstained with propidium iodide (1 μg/ml) in PBS for 15 min prior to visualization under the fluorescence microscope.

Fluorescence imaging

Synaptic boutons were loaded with FM1-43 (16 mM) (Molecular Probes, Eugene, OR) using either electric field stimulation in the presence of 4 mM K^+ and 2 mM Ca^{2+}, or 90 s incubation in hyperkalemic solution (47 mM K^+/2 mM Ca^{2+}). Modified Tyrode solution containing 150 mM NaCl, 4 mM KCl, 2 mM $MgCl_2$, 10 mM glucose, 10 mM HEPES, and 2 mM $CaCl_2$ (pH 7.4, ~310 mOsm) was used in all experiments. Solutions containing 90 mM K^+ were adjusted to provide an equimolar substitution of KCl for NaCl. Field stimulation was applied through parallel platinum electrodes immersed into the perfusion chamber delivering 25 mA - 1 ms pulses. All staining protocols were performed with 10 mM CNQX (6-cyano-7-nitroquinoxaline-2,3-dione) and 50 mM AP-5 (2-amino-5-phosphonopentanoic acid) to prevent recurrent activity. Images were taken after 10-min washes in dye-free solution in nominal Ca^{2+} to minimize spontaneous dye loss. Destaining of hippocampal terminals with high-potassium challenge was achieved by direct perfusion of solutions onto the field of interest by gravity (2 ml/min). Images were obtained by a cooled-intensified digital CCD camera (Roper Scientific, Trenton, NJ) during illumination (1 Hz-60 ms) at 480 ± 20 nm (505 DCLP, 535 ± 25 BP) via an optical switch (Sutter Instruments, Novato, CA). Images were acquired and analyzed using Axon Imaging Workbench Software (Axon Instruments, Union City, CA).

For pH indicator dye fluorescence experiments, LysoSensor Yellow/Blue DND-160 (Molecular Probes L-7545) was used to label the acidic organelles of 25 div primary cortical neurons in culture. Briefly, neurons grown on coverslips were incubated in prewarmed (37ºC) probe (1 μM) containing medium for 4 min. Cells were then imaged immediately

under a fluorescent microscope equipped with a DAPI filter according to directions supplied by Molecular Probes for dual (yellow or blue) emission.

Electrophysiology

Whole-cell recordings from pyramidal cells were acquired with an Axopatch 200B amplifier and Clampex 8.0 software (Axon Instruments, Union City, CA). Recordings were filtered at 2 kHz and sampled at 200 ms. Pipette internal solution included 115 mM Cs-$MeSO_3$, 10 mM CsCl, 5 mM NaCl, 10 mM HEPES, 0.6 mM EGTA, 20 mM TEACl, 4 mM Mg^{2+}-ATP, 0.3 mM Na_2GTP, 10 mM QX-314 (pH 7.35, 300 mOsm). Hypertonic sucrose solution was prepared by the addition of 500 mM sucrose to the modified Tyrode solution. Recordings were performed during brief 15 s bath applications of sucrose. Spontaneous event recordings were performed in the presence of 1 μM tetrodotoxin (TTX). For measuring evoked responses, electrical stimulation was delivered through parallel platinum electrodes in modified Tyrode solution without CNQX or AP-5.

Electron microscopy

Cells were fixed for 30 min in 2% glutaraldehyde buffered with 0.1 M sodium phosphate, pH 7.2, at 4°C. They were rinsed twice in buffer and then incubated in 1% osmium tetroxide for 30 min at room temperature. After being rinsed with distilled water, the specimens were stained en bloc with 2% aqueous uranyl acetate for 15 min, dehydrated in ethanol, and embedded in poly/bed812 for 24 hr. The 50 nm sections were post-stained with uranyl acetate and lead citrate and were viewed with a JEOL 1200 EX transmission electron microscope. Sample sections were taken and synaptic vesicles were counted in synapses containing both pre- and post-synaptic densities in the section. Active zone vesicles were defined as those within 1 vesicle radius of the active zone density.

Miscellaneous

All error bars denote standard error of the mean (SEM), all n values correspond to individual coverslips unless mentioned otherwise, and all statistical assessments were performed with the two-tailed Student's t-test.

Results

Localization of PPT1 in cultured cortical neurons

An antibody raised against recombinant rat PPT1 was used to assess colocalization of PPT1 with synaptophysin, a well-established synaptic vesicle marker (Figure 6.1). Cultured neurons derived from *Ppt1* knockout mice served as a control for the specificity of the anti-PPT1 antibody. In these experiments, PPT1 immunofluorescence (red) appeared as discrete puncta in the cell body and dendrites of wild type cells (Figure 6.1A and 6.1G, arrowheads). This immunofluorescence pattern was absent in *Ppt1* knockout cells (Figure 6.1D). In wild type neurons, PPT1 did not appear to co-localize with the presynaptic protein synaptophysin (Figure 6.1B-C). Excellent co-localization was seen with cathepsin D, a soluble lysosomal enzyme (Figure 6.1, G-I).

Enhanced lysosomal acidification in the absence of PPT1

The pH of the acidic compartment of PPT1-deficient fibroblasts had previously been shown to be shifted toward neutrality (Holopainen et al., 2001). To assess the pH of the acidic compartment in PPT1-deficient neurons, we used a dye with a pH-sensitive emission spectrum (LysoSensor Yellow/Blue DND-160). Living control neurons (Figure 6.1J) showed the characteristic yellow-green fluorescence associated with normal acidic pH of lysosomes in nearly every cell examined. In contrast, *Ppt1* knockout neurons showed a clear qualitative shift toward blue fluorescence, indicating a more alkaline pH (Figure 6.1K).

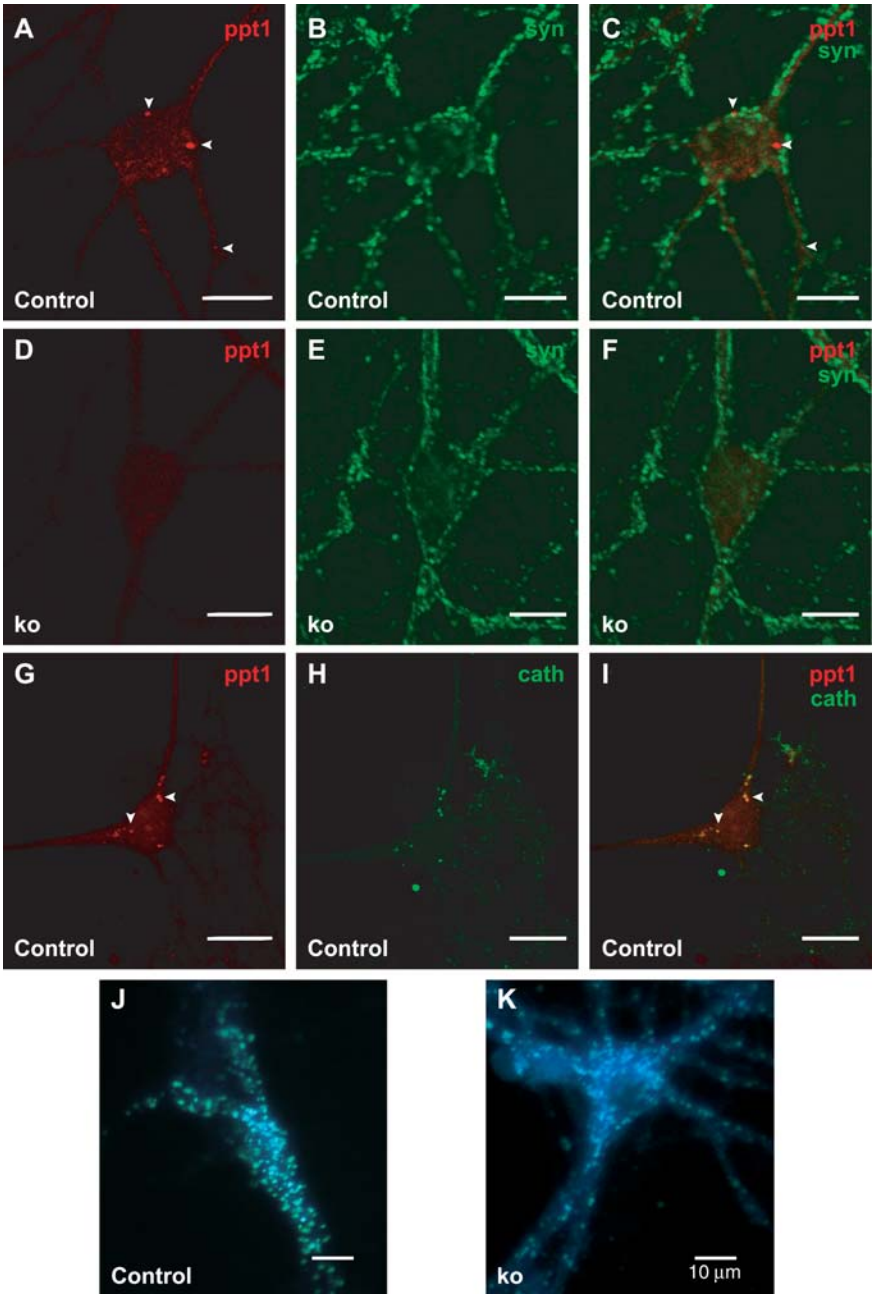

Figure. 6.1. Fluorescent microscopy of dissociated cortical cultures derived from control and *Ppt1* knockout mice. **(A-I)** Staining of primary cortical cultures using antibodies against PPT1 shows punctate staining in the cell body and dendrites of control cells (A, G, arrowheads) in addition to lower levels of diffuse background staining, both of which are absent in *Ppt1* knockout (ko) cells (D). In wild type neurons, PPT1 does not appear to be colocalized with the presynaptic protein synaptophysin (A-C). However, colocalization of PPT1 with the lysosomal marker cathepsin D was seen in wild-type neurons (G-I).

(J-K) Loading of LysoSensor dye into living neurons shows normal acidic pH (yellow-green fluorescence) of lysosomes in control neurons (J), but a more alkaline pH (blue fluorescence) in *Ppt1* knockout neurons (K). Data shown in (J) and (K) are representative of 18 different panels for each condition taken in two different experiments. Although occasional wild-type cells showed blue rather than yellow-green fluorescence, correlation of blue color with *Ppt1* knockout and yellow-green with control by a blinded observer was highly reproducible over a panel of 36 randomly chosen photographs from two experiments ($p<0.0001$, Fisher's exact test).

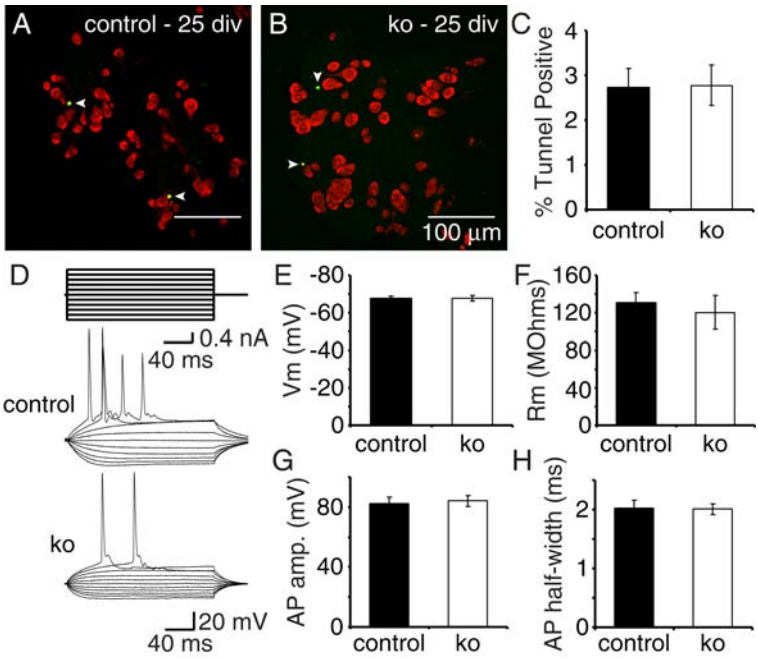

Figure. 6.2. Assessments of neuronal cell death and passive and active electrical properties of *Ppt1* knockout and control neurons show no abnormalities up to 25 div. **(A-B)** Sample regions of tunel staining of neuronal cultures after 25 div show minimal cell death in control (A) or *Ppt1* knockout (B) cultures (arrowheads show very few tunel positive cells, which appear yellow; nuclei are counterstained with propidium iodide, red). **(C)** The level of cell death is similar in cultures made from *Ppt1* knockout mice and littermate controls suggesting that neuronal degeneration is not a prominent phenotype up to 25 days in culture ($p = 0.98$, $N = 22$ regions each). **(D)** Sample traces of whole cell current clamp recordings from control and knockout neuronal cultures during the injection of a current ladder show normal action potential firing in wild type and *Ppt1* knockout neurons. **(E-H)** Quantification of passive and active membrane properties of knockout and control littermate cells shows no change in resting membrane potential (Vm) (E, $p = 0.98$), membrane resistance (Rm) (F, $p = 0.61$), action potential amplitude (G, $p = 0.77$) or action potential half-width (H, $p = 0.91$, $N = 10$-11 cells each).

Viability and excitability of neurons in culture are unaffected by the loss of PPT1

No macroscopic abnormalities were seen in *Ppt1* knockout cortical neurons up to 25 div. Neuronal apoptosis as assessed by tunel staining showed similar low levels of tunel positive cells in *Ppt1* knockout and control cells (Figure 6.2, A-C). In addition, a number of passive and active membrane properties of knockout and control cells were normal. Sample traces of whole cell current clamp recordings from control and knockout neuronal cultures during the injection of a current ladder show normal action potential firing in wild type and *Ppt1* knockout neurons (Figure 6.2D). In addition, there was no change in resting membrane potential, membrane resistance, action potential amplitude or half-width (Figure 6.2, E-H).

Assessment of abnormalities in synaptic transmission

An important finding was a decreased frequency of spontaneous miniature events ("minis") in cells lacking *Ppt1* that became more pronounced with time. Figure 6.3A shows sample trace recordings from control and knockout cells at 13-15 div and at 23-25 div. As expected (Mozhayeva et al., 2002), mini frequency increased with time in culture in control cells (Figure 6.3A, B); however, this increase was severely attenuated in *Ppt1* knockout cells, such that a 45% reduction in mini frequency was seen in *Ppt1* knockout cells of older cultures at 23-25 div as compared to control cells. The amplitudes of spontaneous miniature currents were normal (Figure 6.3C).

Next, we tested whether the decrease in the frequency of spontaneous events was paralleled by a decrease in the number of readily releasable vesicles. The size of the readily releasable vesicle pool (RRP) at the synapse can be estimated by measuring the synaptic response to an application of hypertonic sucrose (Rosenmund and Stevens, 1996). The responses to hypertonic sucrose application in young and old cultures of cortical neurons from control and *Ppt1* knockout mice revealed a decreasing trend that did not reach significance. (Figure 6.3D and E). Synaptic density was normal in *Ppt1* knockout cultures when measured at 25 div (Figure 6.4).

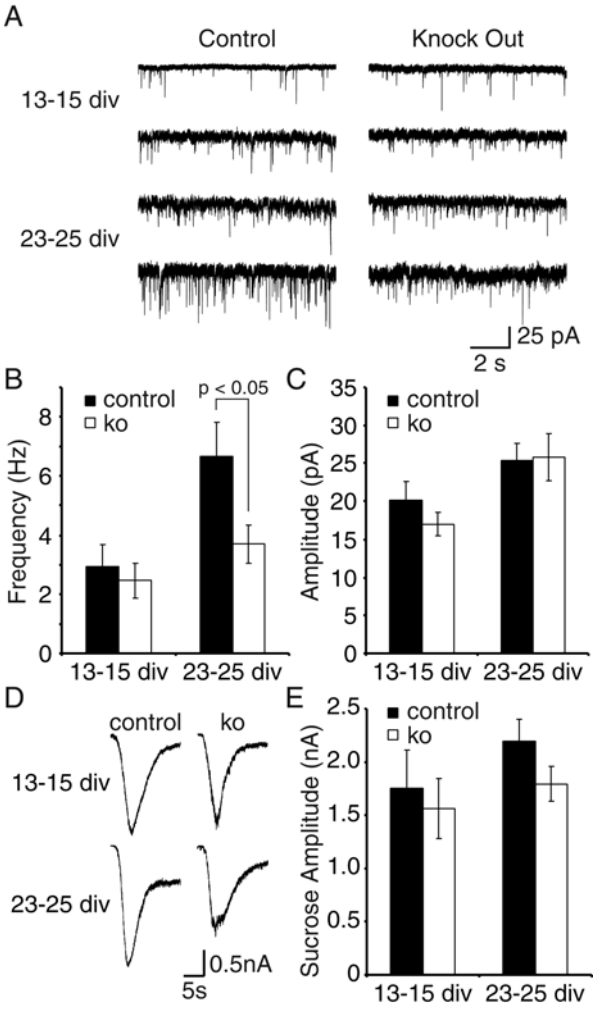

Figure. 6.3. Decreased spontaneous miniature event frequency in cells lacking PPT1. **(A)** Sample traces showing recordings from control and knockout cells at 13-15 div and 23-25 div. **(B)** Bar graph of the quantification of mini frequency shows no change in young cultures ($p = 0.63$, $N = 10$ cells each) but a 45% reduction of mini frequency in *Ppt1* knockout cells in older cultures ($p<0.05$, $N = 12$-15 cells each). **(C)** Bar graph depicting mini amplitude quantification shows no significant change at either time point ($p = 0.32$ and 0.91 for 13-15 div and 23-25 div, respectively). **(D)** Sample traces of responses to hypertonic sucrose application. **(E)** Quantification of the peak amplitudes of sucrose-evoked currents shows a small decrease in the mean amplitude at 23-25 div, but this was not statistically significant ($p = 0.15$, $N = 10$ cells each).

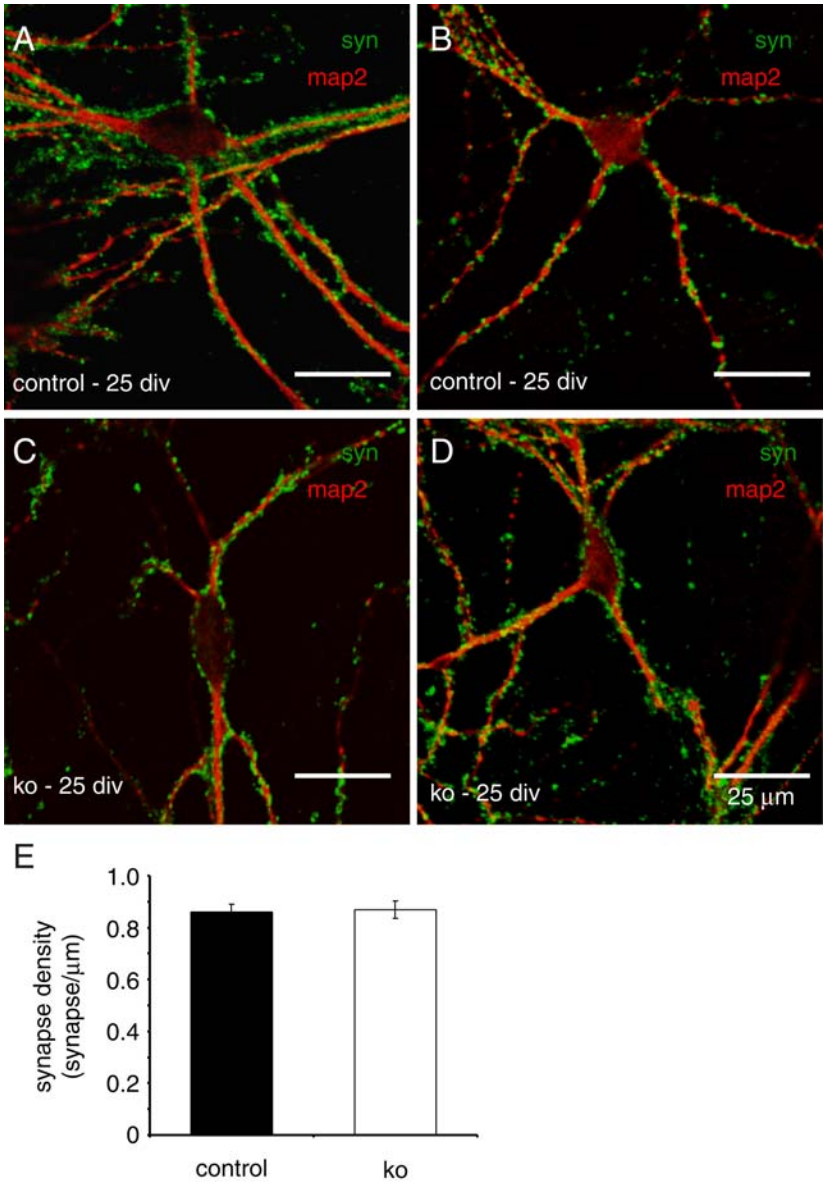

Figure. 6.4. Normal synaptic density in *Ppt1* knockout cultures. **(A-D)** Sample regions showing similar synapse density in control (A-B) and knockout (C-D) cortical cultures at 25 div. **(E)** Quantification of synaptic density as measured as synapses per micron length of dendrite show no significant difference between knockout and littermate control cells (28-29 cells each). Quantitation was performed by an observer blinded as to the genotype of the culture.

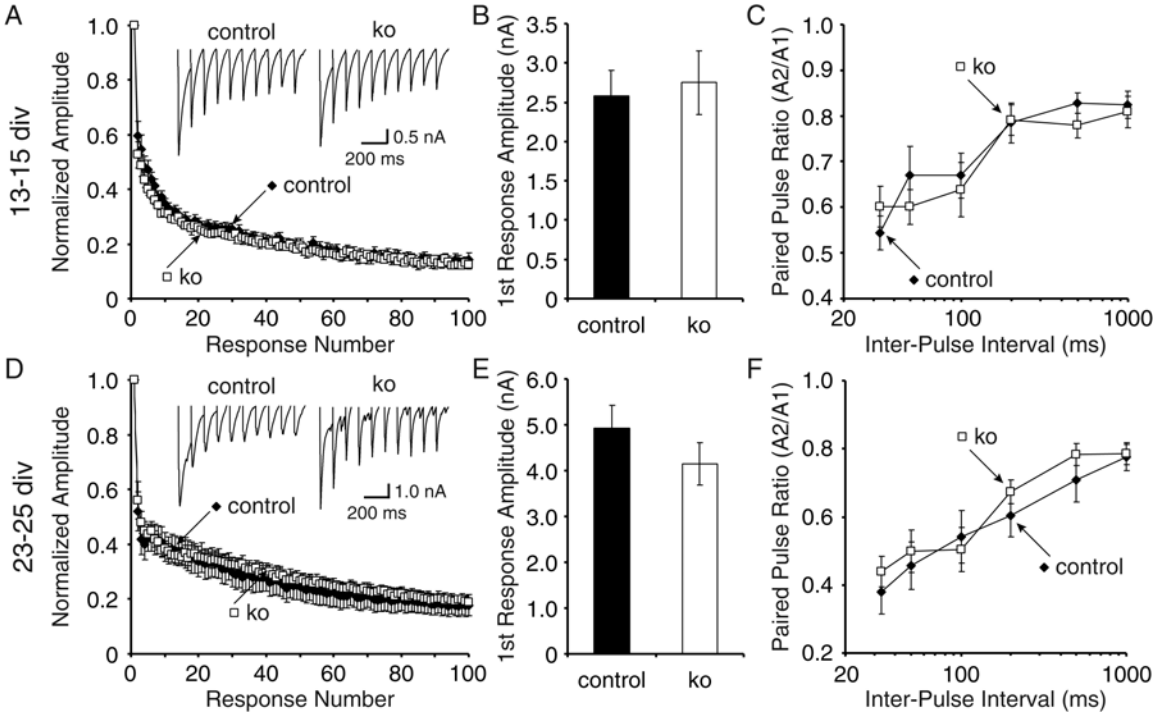

Figure. 6.5. Properties of evoked neurotransmitter release show no significant change in *Ppt1* knockout neurons. **(A, D)** Field stimulation of 13-15 div (A) or 23-25 div (D) cultures at 10 Hz showed no significant difference between the rate of synaptic depression of control and knockout cells. Normalized response amplitudes are shown with sample response traces shown in inset (N = 12-15 cells each). **(B, E)** The amplitude of the EPSC in response to a single AP was not different in control and knockout cultures either at 13-15 div (B, p = 0.75) or 23-25 div (E, p = 0.26). **(C, F)** Paired pulse ratios depicting the proportion of the second response to the first response of a paired stimulus protocol at various inter-pulse intervals showed no difference between control or knockout cultures (N = 8-15 cells each).

Properties of neurotransmitter release evoked by electrical stimulation did not show a significant change in neurons derived from *Ppt1* knockout mice. Field stimulation of cultures at 13-15 div (Figure 6.5A) or 23-25 div (Figure 6.5D) at 10 Hz showed no significant differences in the rate of synaptic depression between control and knockout cells at either age. In addition, the amplitude of the excitatory postsynaptic currents (EPSC) in response to a single action potential was not different (Figure 6.5, B and E), and paired pulse ratios depicting the proportion of the second response to the first response of paired stimuli at

various inter-pulse intervals showed no difference between control or knockout cultures at either time tested (Figure 6.5, C and F).

Visualization of synaptic vesicle recycling with FM1-43 reveals a reduction in recycling pool size

What is the origin of the decrease in spontaneous miniature event frequency in aged *Ppt1* knockout cultures? Decrease in the frequency of miniature synaptic currents without significant changes in the size of the readily releasable pool (measured with hypertonic sucrose application) and the properties of evoked neurotransmission on the number of synapses detected by immunocytochemistry prompted us to examine synaptic vesicle pools in *Ppt1* knockout synapses using a more sensitive method. Activity-dependent uptake and release of the fluorescent dye FM1-43 can be used to quantify total and rapidly releasable synaptic vesicle pool size in cultured neurons (Betz et al., 1996). To measure these parameters in *Ppt1* knockout and control neurons, the total pool size was first determined according to the scheme depicted in Figure 6.6A. Presynaptic terminals were loaded with the fluorescent dye FM1-43 using one of two protocols: a 90 s application of 47 mM K^+ or a 10 Hz electrical stimulation for 2 minutes (10 Hz x 2 min). Both of these are strong stimuli that label the total pool of recycling vesicles (Harata et al., 2001). After a 10-minute washout period with dye-free medium, synapses were imaged after 4 applications of 90 mM K^+ to release the entire pool, and the total releasable fluorescence was quantified. There was no significant change in total pool size between control and knockout synapses at 13-15 div using either loading protocol, but there was an approximately 30% reduction in pool size in synapses lacking PPT1 enzyme compared to littermate controls at 23-25 div using the 47 K^+ release (Figure 6.6B) and a 25% reduction in pool size in synapses lacking PPT1 enzyme using the 10 Hz x 2 min loading protocol (Figure 6.6C). To determine whether the rapidly releasable pool size is affected in the knockout mice, a second labeling protocol was undertaken as depicted in the scheme in Figure 6.6D. Only older (23-25 div) cultures were examined. Cultures were loaded with FM1-43 using 10 Hz x 2 min stimulation. After a washout period, synapses were imaged during a brief 2 s pulse of 30 Hz stimulation (30Hz x 2s) to examine the rapidly releasable pool followed by 4 rounds of 90 mM K^+ to release all

the dye trapped in the synapses. As shown in Figure 6.6D, there was a significant decrease in the amount of dye released by the brief 30 Hz pulse in knockout cultures as compared to littermate controls, suggesting a decrease in the number of vesicles in the readily releasable pool. However, calculation of the ratio of the dye released during the 30 Hz x 2 s pulse to the total 10 Hz x 2 min pool size for each synapse showed no change (Figure 6.6E), suggesting that the fraction of recycling vesicles that populate the readily releasable pool is unaffected in *Ppt1* knockout neurons.

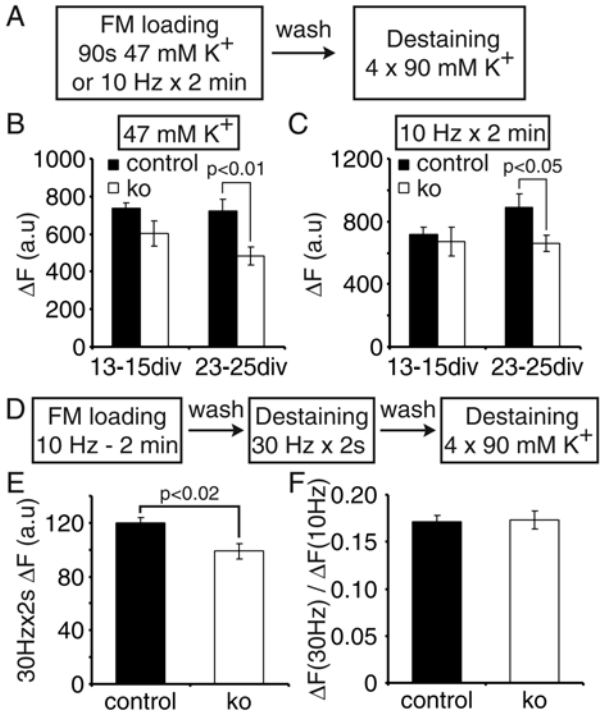

Figure. 6.6. Progressive decrease in synaptic vesicle pool size without a change in the ratio of the readily releasable pool to total pool. **(A)** Experimental protocol. Presynaptic terminals were loaded with FM1-43 either using a 90 s application of 47 mM K^+ or 10 Hz stimulation for 2 minutes (10 Hz x 2 min). After a 10-minute washout period with dye-free medium, synapses were imaged during four applications of 90 mM K^+ and the total dye trapped quantified. **(B)** Quantification of FM1-43 labeling in response to 47 mM K^+ stimulation. There was no significant change in pool size between control and knockout synapses at 13-15 div ($p = 0.11$, N = 8-9 coverslips each), but there was an approximately 30% reduction in pool size in synapses lacking PPT1 enzyme compared to littermate controls at 23-25 div ($p<0.01$, N = 9-10 coverslips each). **(C)** Quantification of 10 Hz x 2 min loading. There was no significant change in pool size between control and knockout synapses at 13-15 div ($p = 0.68$, N = 8 coverslips each), but there was approximate 25%

reduction in pool size in synapses lacking PPT1 enzyme compared to littermate controls at 23-25 div ($p<0.05$, N = 9 coverslips each). **(D)** Experimental protocol. Synapses in old age cultures were loaded with FM1-43 using 10 Hz x 2 min stimulation. After a washout period, synapses were imaged during a brief 2s pulse of 30 Hz stimulation (30Hz x 2s) followed by 4 rounds of 90 mM K+ to release all the dye trapped in the synapses. **(E)** There was a significant decrease in the amount of dye released by the brief 30 Hz pulse in knockout cultures compared to littermate controls ($p<0.02$, N = 5 coverslips each) suggesting a decrease in the number of vesicles present in the readily releasable pool (RRP). **(F)** Bar graph of quantification of the ratio of the dye released during the 30 Hz x 2 s pulse to the total 10 Hz x 2 min pool size for each synapse shows no change in this ratio suggesting that the RRP to total pool ratio is unaffected in neurons lacking PPT1.

Ultrastructural analysis of synapses in cortical culture derived from *Ppt1* knockout mice

To obtain morphological confirmation of the synaptic vesicle pool size measurements, we analyzed electron micrographs of *Ppt1* knockout and control cultures at 13-15 div and 23-25 div (Figure 6.7, A-F). The number of synaptic vesicles present at each synapse and the number of morphologically docked vesicles in the active zone were quantified (Figure 6.7, I-K). Consistent with the fluorescent dye studies above, no differences were seen in the younger cultures, but at 23-25 div, there was an approximately 30% decrease in the pool size of docked and total vesicles, with no change in the ratio of docked vesicles to total. Of note, no granular osmiophilic deposits were seen in synaptic boutons, though rare deposits similar to those seen in infantile NCL brain were identified in neuronal cell bodies and in glial cells (data not shown).

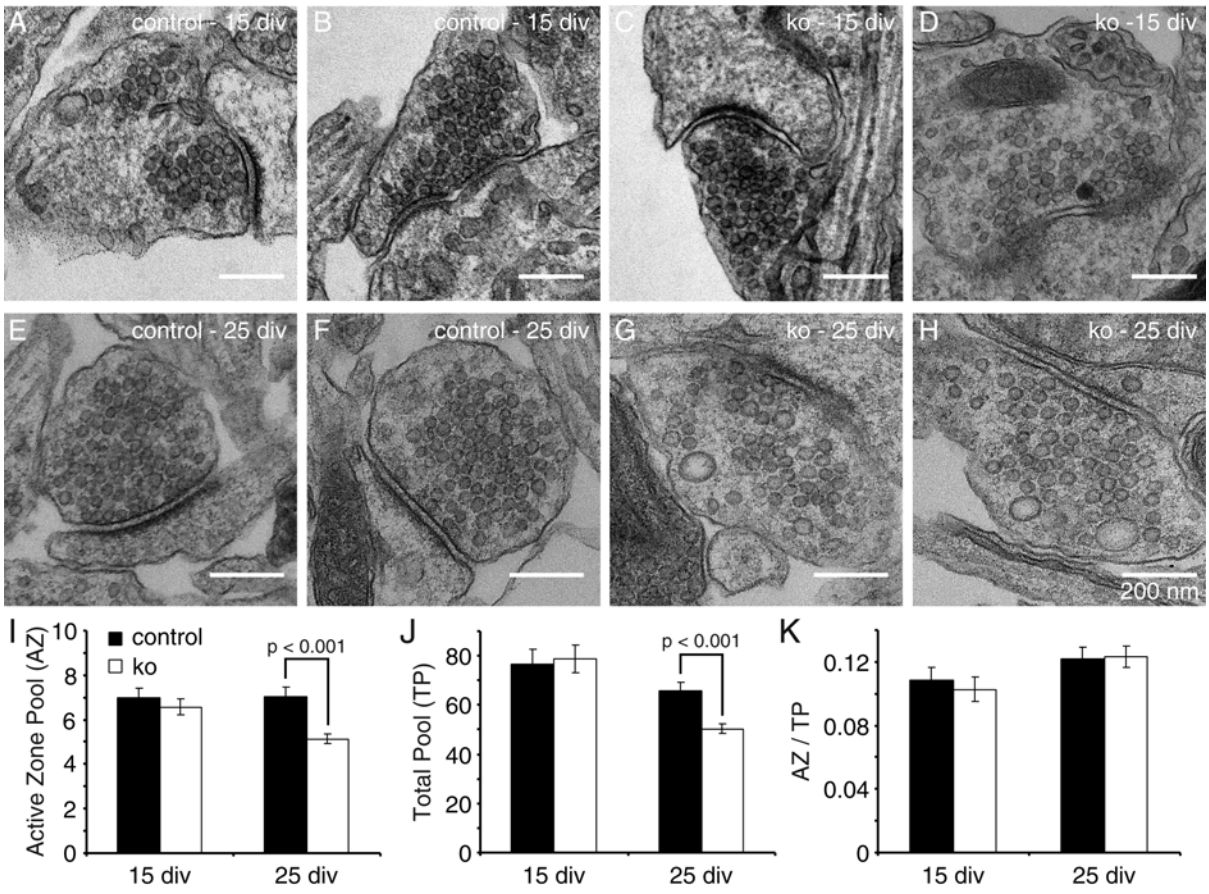

Figure. 6.7. Analysis of electron micrographs of *Ppt1* knockout cultures show decreased number of synaptic vesicles. **(A-D)** Sample EMs of control (A, B) and knockout (C, D) synapses from 15 div cultures. **(E-H)** Sample EMs of control (E, F) and knockout (G, H) synapses from 25 div cultures. **(I)** Bar graph showing a decreased number of vesicles at the active zone (AZ) in *Ppt1* knockout synapses of mature cultures ($p<0.001$). **(J)** Bar graph showing a decrease in the total number of vesicles present per synapse per section in *Ppt1* knockout synapses in older cultures ($p<0.001$). **(K)** Bar graph showing that the ratio of the morphologically docked vesicle pool (AZ) to the total vesicle pool (TP) does not differ between control and knockout synapses (N = 69 and 86 synapses from control and knockout cultures at 15 div respectively, and N = 149 and 158 from control and knockout cultures at 25 div respectively).

Discussion

In the current study, we examined a number of properties of cultured cortical neurons derived from a mouse model of infantile Batten disease. Although several previous studies had suggested that PPT1 is present within synaptic vesicles, these studies were largely based upon overexpression in cultured neurons (Ahtiainen et al., 2003; Heinonen et al., 2000; Lehtovirta et al., 2001) and on electron microscopy of brain tissue to detect endogenous PPT1 (Ahtiainen et al., 2003; Heinonen et al., 2000; Lehtovirta et al., 2001). We were unable to confirm the presence of endogenous PPT1 in synaptic vesicles by immunofluorescence despite robust staining of a cathepsin D-positive compartment in cell soma consistent with lysosomes. This may be an issue of antibody sensitivity but more likely due to difficulties encountered in determining antibody specificity in earlier studies before the availability of knockout mice.

The most striking and specific finding in the current paper was a decline in the synaptic vesicle pool size with time in culture as compared to control cells. The decrease in pool size affected both the rapidly releasable and total pools and was seen using fluorescent dye loading and electron microscopy. These changes were reflected functionally as a decrease in the frequency of spontaneous miniature currents. A number of passive and active membrane properties of the cells were normal, demonstrating that the neurons were otherwise healthy and intact over the period examined. These observations suggest a relatively early and specific effect on synaptic vesicle pools.

Factors that determine vesicle pool size are not well understood (Zhen and Jin, 2004). Loss-of-function mutations in a number of genes have been reported to cause a decrease in synaptic vesicle pool size. Hippocampal neurons cultured from mice lacking β-catenin show a 40% decrease in synaptic vesicle pool size with a corresponding decrease in the number of docked vesicles, which is similar in magnitude to the effect that we have observed here (Bamji et al., 2003). β-catenin appears to play a role in localizing the reserve pool of vesicles at presynaptic sites with a corresponding dispersion of vesicles along axons. Mutants that are defective in genes involved in endocytosis such as dynamin (Hinshaw, 2000), endophilin and

synaptojanin show both reduction and an abnormal arrangement of synaptic vesicles at synapses. Endophilin mutants (unc57 in C. elegans) show a 65% decrease in synaptic vesicles pool size and an even greater decrease in docked vesicles (88%) (Schuske et al., 2003). Loss of synapsin function also results in a reduction in the size of the reserve pool of vesicles (Pieribone et al., 1995; Rosahl et al., 1993). It is interesting that several of these proteins are enzymes (endophilin and synaptojanin) that have lipidic substrates that reside in the lipid bilayers of the synaptic terminal.

A mutation in the spinster (spin) gene in Drosophila has been associated with a 50% decline in quantal content but without a change in quantal size. In this model, bouton number was also increased by two-fold, which we had not observed in *Ppt1* knockouts (Sweeney and Davis, 2002). Interestingly, mutations in spin are associated with widespread neurodegeneration, multilamellar and granular osmiophilic bodies in both neurons and glial cells, and dramatic expansion of a low pH compartment in presynapses at the Drosophila neuromuscular junction (Nakano et al., 2001). Furthermore, an endosomal/lysosomal localization for Spin has been suggested, but in contrast to PPT1, its function in this compartment is unknown.

An important question is whether the decrease in synaptic vesicle pool size we observed plays a causative role in the severe neurodegenerative phenotype in PPT1 deficiency. Humans deficient in synapsin I, also associated with reduced synaptic vesicle number, have epilepsy and learning difficulties, but not a neurodegenerative phenotype (Garcia et al., 2004). However, these data are difficult to interpret in light of the fact that hypomorphic mutant alleles of PPT1 in humans are associated with a prolonged course in which neurodegeneration is not apparent until very late in the course of the disease (van Diggelen et al., 2001). Perhaps the influence of PPT1 deficiency on synaptic vesicle pool size plays a role in some of the manifestations of NCL (such as seizures) but not on the ultimate neurodegenerative phenotype.

Although reduced vesicle numbers (such as those seen in the synapsin and synaptojanin knockouts) do not necessarily lead to synapse elimination and degeneration, the progressive and gradual decline in vesicle numbers and decrease in miniature event

frequency we observed here may well be an early indicator of synapse degeneration. Our findings are reminiscent of observations during competitive synapse elimination in the neuromuscular junction (Colman et al., 1997; Gillingwater and Ribchester, 2003; Kopp et al., 2000; Wyatt and Balice-Gordon, 2003) or age-related synapse elimination in parasympathetic ganglia (Coggan et al., 2004) in which alterations in synaptic strength occur prior to axonal withdrawal.

The increasing loss of synaptic vesicle pool size with time suggests that metabolites accumulating as a result of PPT1 deficiency may play a role. Known substrates of PPT1 include palmitoylated proteins and peptides and palmitoyl CoA (Calero et al., 2003; Camp and Hofmann, 1993; Camp et al., 1994; Lu et al., 1996). Palmitoylated peptides have been shown to accumulate in cells derived from PPT1-deficient patients (Lu et al., 1996; Lu et al., 2002). Given the well-understood role of the palmitate modification for protein-protein interactions at the plasma membrane (Smotrys and Linder, 2004), it is entirely plausible that palmitoylated peptides or their metabolites interfere with the function of one or more palmitoylated proteins in a way that influences synaptic vesicle pool size. This would be particularly likely if the metabolites remained membrane-bound. A number of proteins important in presynaptic function are palmitoylated, such as synaptotagmin 1, synaptobrevin 2, SNAP-25, GAD 65, cysteine string protein, and GAP-43 (reviewed in (el-Husseini Ael and Bredt, 2002; Patterson, 2002)). Palmitoylation of at least one synaptic vesicle protein (GAD65) is required for its targeting to presynaptic vesicle clusters (Kanaani et al., 2004). Cysteine string protein-deficient mice develop a fatal neurodegenerative disorder at neuromuscular junctions and the Calyx of Held synapse that includes severe impairment of neuromuscular transmission (Fernandez-Chacon et al., 2004).

Increased levels of palmitoyl CoA, palmitoyl-cysteine or palmitoylated peptides at cellular membranes may possibly directly inhibit fatty acylation of proteins, perhaps by interference with fatty acyl transferases known as DHHC proteins (reviewed in (Smotrys and Linder, 2004)). GODZ is one such protein that is found at high levels only in the central nervous system (Keller et al., 2004).

Another way in which PPT1 metabolites may interfere with presynaptic function is through inhibition of autophagosome-lysosome fusion via SNARE proteins. Eukaryotic membrane fusion is controlled by amino-terminal longin domains of SNARE proteins, and these domains are also found in fatty acid binding proteins (reviewed in (Dietrich et al., 2003)). For example, Ykt6 is a SNARE/VAMP/synaptobrevin homolog of the longin family that presents palmitoyl CoA via its N-terminal longin domain to the yeast fusion factor Vac8 (Dietrich et al., 2004). Abnormal elevations of palmitoyl CoA at the neuronal cell membrane may inhibit fusion, cause accumulation of autophagosomes, and perhaps lead to expansion of the lysosomal compartment.

It is also interesting that overexpression of select dually acylated minimal protein motifs such as those present in GAP-43 and paralemmin will induce filopodia in neurons (even in heterologous cells) (Gauthier-Campbell et al., 2004). These effects are reversed by 2-bromopalmitate, an inhibitor of palmitoylation. An interpretation of this data is that on-going palmitoylation may be needed to maintain existing filopodia and for transformation to dendritic spines. Loss of spines and altered dendritic morphology has been observed in PPT1 deficient mice (Bible et al., 2004).

Which metabolites of PPT1 may play a role in reducing synaptic vesicle pool size in PPT1 deficient neurons? PPT2 is a second lysosomal thioesterase with a distinct but overlapping specificity as compared to PPT1 (Gupta et al., 2001; Soyombo and Hofmann, 1997), and PPT2 deficiency in mice causes a mild form of neuronal lipofuscinoses with extraneuronal manifestations (Gupta et al., 2003). Comparison of cultures derived from PPT1 and PPT2 deficient mice could be used in future experiments to further define the role of palmitoylated compounds to changes in properties of cultured neurons associated with lipofuscinoses and neurodegeneration.

CHAPTER 7: Conclusions And Future Directions

As the experiments described in the preceding chapters clearly demonstrate we have made some significant progress in the understanding of several fundamental processes involved in synaptic vesicle trafficking. In this chapter I will briefly highlight some of these advances and at the same time discuss some of the important questions raised as a result of this work.

Clathrin-independent modes of synaptic vesicle endocytosis exist in central nervous system synapses

The role of clathrin and its adaptor proteins in the endocytosis of vesicles is a highly studied topic (for detailed review see (Cremona and De Camilli, 1997; De Camilli et al., 2001; Galli and Haucke, 2004)). This form of endocytosis occurs not only in neurons, but numerous other cell types, as well as in cells of less complex organisms such as yeast and bacteria. However, the complexity of clathrin coat formation and its subsequent reorganization results in significant kinetic limitations on the ability of vesicles to become re-available for reuse once they exocytose. It has been postulated that this slow time course would not allow central synapses, with their limited vesicle pool sizes, to maintain efficient neurotransmission (Sara et al., 2002). Recent evidence has suggested that these synapses may actually utilize other faster modes of endocytosis (Aravanis et al., 2003; Gandhi and Stevens, 2003). However, until now, evidence for such a pathway has been limited.

We utilized the special characteristics of the synaptic plasma membrane protein synaptotagmin 7 to explore whether such fast modes of vesicle recycling could exist (chapter 2). Syt7 undergoes a high degree of splicing resulting in numerous splice variants of multiple lengths. Most importantly, a short splice form that exists endogenously essentially demonstrates dominant negative inhibition of clathrin-mediated endocytosis in a number of non-neuronal cell lines (Sugita et al., 2001; von Poser et al., 2000). Using the overexpression of this splice form in hippocampal primary cell culture, we found that synapses with dominant negative inhibition of clathrin-dependent endocytosis still exhibited exo-endocytosis of synaptic vesicles. More surprising though was our observation that the

synapses overexpressing the short form of syt7 actually had a much faster rate of synaptic vesicle endocytosis than either untransfected control synapses or synapses expressing a full-length splice form of syt7.

These results suggest that synaptic vesicles can undergo exocytosis and endocytosis in the absence of clathrin-dependent endocytosis in central synapses. This is contrary to the results from the *shibire* dynamin mutation in *drosophila* neuromuscular junction synapses where at the restrictive temperature there is a complete loss of synaptic vesicle endocytosis and recycling (Delgado et al., 2000; Kawasaki et al., 2000). Our discovery that in central synapses, the clathrin-independent vesicle endocytosis is actually kinetically faster than in the presence of clathrin is also quite critical, as it would allow central synapses to more efficiently utilize their limited vesicle pools. Since the short splice variants have been shown to exist endogenously, these findings also provide a potential mechanism for regulation of vesicle endocytosis rate. By regulating the levels of this splice variant a synapse could theoretically regulate the kinetics of vesicle endocytosis dependent upon the demands that were placed on it.

Our analysis of synaptotagmin 7 function in endocytosis was not limited to overexpression studies. We further explored the function of this molecule using genetic approaches (chapter 3). In cortical synapses of mice lacking synaptotagmin 7 there was a selective decrease in synaptic vesicle endocytosis. This effect was small but statistically quite significant. Additionally, in cortical synapses of mice with mutations of the calcium binding sites of syt7, there was an increased rate of synaptic vesicle endocytosis. This is analogous to the condition were we expressed the dominant negative short form of the protein, which could be the dominant form remaining in these mutant mice (chapter 2). These results provide further evidence for the role of synaptotagmin 7 in regulating the kinetic pathway by which a vesicle undergoes endocytosis.

This regulation of synaptic vesicle endocytosis may not be limited to synaptotagmin 7, but may be a more general function of the entire family of synaptotagmins. It has recently been shown that in synapses deficient in synaptotagmin 1 the rate of endocytosis is also decreased, independent of the decreased synchronous release (Nicholson-Tomishima and

Ryan, 2004; Poskanzer et al., 2003). Since synaptotagmin 1 is the major calcium sensor for vesicle exocytosis (Geppert et al., 1994) this could also explain the tight coupling that exists between exo- and endocytosis. Synaptotagmin 12, another member of this family has been shown to heterodimerize with synaptotagmin 1 and inhibits its normal functioning (Maximov and Südhof, 2005b). To test whether this might be the mechanism by which endocytosis function is altered in synaptotagmin 1 null mice we expressed this protein in hippocampal cultures and found that there was a selective decrease in slow vesicle endocytosis in these synapses (chapter 4).

Taken together, these results suggest that through its different family members synaptotagmin may regulate kinetically distinct modes of vesicle recycling. Our evidence suggests that while synaptotagmin 7 regulates the targeting of vesicles to fast modes of endocytosis through its short splice variant, synaptotagmin 1 and synaptotagmin 12 may function together to direct vesicles to slower endocytosis modes. It is worth mentioning at this point that whether the fast endocytosis pathways described in these studies relates to the so-called "kiss and run" pathway remains to be determined. However the kinetics of vesicle endocytosis and retrieval with syt7 short form overexpression would fit with the extremely tight coupling between exocytosis and endocytosis and the maintenance of molecular identity of synaptic vesicles proposed by the "kiss and run" hypothesis.

Synaptic vesicle trafficking can be regulated

Monitoring the rate of vesicle reuse in synapses expressing the short and long synaptotagmin 7 splice variants also yielded very interesting results (chapter 2). We found that in synapses expressing the short splice form, vesicles that were fast endocytosed were also preferentially fast recycled. In contrast, in synapses expressing the full-length form we saw slower vesicle recycling, without a shift in endocytosis kinetics. This would suggest that in addition to a regulatory step at the endocytosis stage, a control point exists at the recycling stage as well. This would allow endocytosing vesicles to either recycle slowly through the reserve pool, or locally recycle rapidly back into the readily releasable pool. The endogenous levels of synaptotagmin 7 splice variants may form a molecular switch, allowing the synapse

to regulate the targeting of vesicles to these kinetically distinct recycling pathways. Higher levels of the shorter variant can shuttle vesicles through faster endocytosis and recycling pathways, while longer variants direct vesicles towards slower recycling pathways.

How such a process is coordinated requires additional experimental evidence, but one could imagine that dependent upon the baseline levels of activity to which a synapse is exposed, it could establish a steady state level of these splice variants. To test if synaptic vesicle recycling is influenced by the demand imposed by network activity, we compared the physiological properties of hippocampal and neocortical neurons, which have clear intrinsic differences in network activity. We found that hippocampal synapses, have higher levels of network activity, faster vesicle mobilization rates and slower recycling kinetics than neocortical synapses. These two synapse types also alter different properties in response to changes in activity levels. While hippocampal synapses regulate the rate of synaptic vesicle mobilization from the reserve vesicle pool, neocortical synapses modulate their rate of vesicle recycling. Taken together, these results strongly suggest that synaptic vesicle trafficking and the resulting synaptic dynamics can adapt to demand, and different synapses can use alternate strategies to adjust to changes in activity (Virmani et al., 2005). Preliminary evidence from a host of other brain regions also shows broad differences in pool size and vesicle mobilization rates between brain regions (data not shown).

We also began to address this important question by studying the levels of the different splice variants in different brain regions. Preliminary analysis of western blots using antibodies against the alternatively spliced domain of syt7 show that different brain regions may have different endogenous levels of these proteins (chapter 2). This result needs to be repeated using different antibodies and appropriate controls for it to be conclusive. However, these results provide indirect support for the levels of syt7 splice variants in establishing the steady state synaptic recycling properties in these regions.

Another possible role for these splice variants would be an activity dependent modulation of the splice variants. Up regulation of short C2 domain-lacking forms during periods of intense activity would increase the availability of vesicles for reuse thereby allowing the presynaptic terminal to maintain efficient levels of neurotransmission.

Alternatively, during phases of relative silence, down-regulation of full-length forms, could shuttle vesicles to slower recycling pathways possibly involving endosomal intermediates and allow for the turnover of synaptic vesicle proteins. Such a process is not completely hypothetical as there is recent evidence that levels of synaptotagmin 7 could be modulated by activity (Piedras-Renteria et al., 2004). Further exploration of this idea could prove quite fruitful.

More molecular information on vesicle trafficking pathways in the synapse may also give clues on the regulation and heterogeneity of vesicle recycling amongst different synapses. Activity-dependent and synapse type specific variations in the levels and alternative splicing patterns of the key proteins involved in these pathways may underlie plasticity of vesicle recycling.

Recycling in hippocampal synapses excludes recycling through endosomes

Expression of the full-length synaptotagmin splice variant also resulted in the formation of large vesicular structures in electron micrographs of synapses fixed immediately after intense synaptic stimulation using 90 mM K^+ (chapter 2). These structures are quite likely to be endosomal intermediates as they were able to repopulate the synaptic vesicle pool. However, these large membranous structures were not observed upon stimulation of control synapses or synapses expressing the short syt7 variant, suggesting that the formation of these intermediates was a result of the high levels of the syt7 full-length form. There was also no evidence for the formation of these structures during less intense stimulation with action potentials delivered at a frequency of 10 Hz.

The recycling of vesicles through endosomes has been described in neuromuscular junction synapses and it has been found that rab5 plays an important role in the fusion of endocytosing vesicles to endosomes (Wucherpfennig et al., 2003). Therefore, to further investigate the extent to which central synapses utilize slow trafficking through early endosomes, we also expressed wild-type rab5 protein or dominant negative (S34N) and constitutively active (Q79L) mutant forms of rab5 in hippocampal neurons. The wild type and dominant negative forms had minimal effects on synaptic vesicle pool size and vesicle

mobilization. Only expression of the constitutively active mutant substantially decreased synaptic vesicle pool size and slowed vesicle mobilization. This effect was similar to that observed when synapses were treated with the PI3-kinase inhibitor wortmannin, which has been shown to inhibit vesicle budding from endosomes (Richards et al., 2004). These results suggest that in hippocampal synapses under physiological levels of activity, vesicles do not actively recycle through endosomal intermediates. However, our data does not rule out the existence of these pathways for other functions such as synaptic vesicle protein turnover. These findings add to our growing evidence that central synapses are tuned towards faster recycling pathways to maximally utilize their limited vesicle pool size.

Spontaneous vesicle release occurs independent of evoked vesicle fusion

The current model of synaptic vesicle fusion assumes that the same vesicles that can release neurotransmitter in response to a single action potential also have a very low probability of spontaneous fusion. The calcium influx into the terminal during an action potential increases this probability of release several fold. Spontaneous neurotransmitter release has been assigned multiple functions including the proper wiring of neurons in the brain during early development as well as the maintenance of these synaptic connections well into adulthood. However, despite the importance of this mode of neurotransmitter release, the precise origin of these vesicles has never been directly tested. Modeling the synaptic response of neurons to trains of action potentials we predicted that the release of spontaneous vesicles is excluded from the evoked vesicle pool (Appendix A). We then tested this hypothesis using fluorescent imaging, electrophysiology and electronmicroscopy, and were able to show that vesicles in the activity dependent pool release preferentially in response to stimulation, while spontaneously recycling vesicles have the propensity to re-release spontaneously, with minimal mixing between the two pools (chapter 5). We also showed that the spontaneously releasing vesicles are excluded from the readily releasable pool, from which evoked release occurs. These findings suggest that there are indeed two sets of vesicle pools, one for evoked release, and one for spontaneous release that function independent of one another.

These findings help reconcile decades of literature where a single vesicle performing these two diverse functions could not adequately explain the experimental results. However, they also raise a number of interesting questions that need to be addressed. One question relates to the molecular markers that label a vesicle to be part of the evoked or spontaneous pool. We know from some genetic studies that the knock out of molecules such as synaptotagmin 1 and complexin do not alter spontaneous event frequency (Geppert et al., 1994; Reim et al., 2001), while synaptobrevin significantly decreases it (Schoch et al., 2001). However, both sets of vesicles appear to have all these markers. Determining the exact molecular composition therefore will not be easy. Screening through the host of molecules known using knockout strategies would be a formidable task. Alternatively, labeling these vesicles with distinct markers, and then performing immuno-electron microscopy on different known vesicle proteins could produce results. However, the current resolution of this technology is limited and the tissue manipulations necessary also decrease ultrastructural resolution. Hopefully with the continuing advancement of our technological tools, and a combination of multiple methods, this matter can be addressed in the future.

Our results also do not provide any direct evidence as to the location of spontaneous vesicle exocytosis and endocytosis. However, the similar kinetics of the postsynaptic response to evoked release and a scaled spontaneous release event suggests that spontaneous fusion must occur at the active zone. It has been shown that there are numerous empty docking sites at the active zone (Schikorski and Stevens, 2001), and these could potentially be the sites at which release occurs. We can only speculate however on whether or not the endocytosis of spontaneous vesicles occurs in a clathrin-dependent or independent manner, and the location of such a process. The fast kinetics of mixing of spontaneously endocytosed vesicles with the remaining pool required to fit the rate of spontaneous dye release, suggests however that this process occurs in a clathrin independent manner.

It has been proposed that in adults, post-synaptic local protein synthesis is regulated by the level of spontaneous vesicle release (Sutton et al., 2004). If this is the case, and the post-synapse performs differential functions dependent upon whether neurotransmission is spontaneous or evoked, it would be very important to understand the mechanism for such an

effect. The similar size and shape of the vesicles from these distinct pools would suggest that the neurotransmitter content could not be a factor. We have already discussed that the similar kinetics of the responses suggest that release of both occurs at the active zone. Are their secondary molecules on the vesicle membrane that not only provide the vesicle its pool identity, but also signal to the post-synaptic terminal? Is there a secondary signaling molecule packaged with the neurotransmitter in the vesicle that allows the post-synaptic terminal to differentiate between the different signals? Or is it simply that evoked release usually occurs in bursts whereas spontaneous release is more random, and the post synapse can differentiate between these based on the post-synaptic calcium concentration establishing some sort of release history? These are all extremely interesting questions and can hopefully be addressed in the future to allow us to determine the exact role of these different vesicle pools.

Proposed model for synaptic vesicle recycling in central synapses

Based upon our findings we would suggest the model of vesicle recycling shown in figure 7.1. In this model separate pools for spontaneous and evoked vesicle release exist. In addition there is a pool of vesicles that does not actively partake in synaptic vesicle recycling labeled the resting pool. The function of the resting pool is yet to be determined. Vesicles in the evoked pool are docked and held in a very stable state, ready to release in response to increased calcium concentration at the active zone. After release, evoked vesicles can either endocytose and recycle rapidly in the RRP, or recycle slowly through a clathrin-dependent mode of endocytosis in the peri-active zone area. The synaptotagmin 7 splice forms, and possibly the interaction between synaptotagmin 1 and 12, facilitate this decision. The slowly recycling vesicles re-populate the reserve pool without recycling through endosomal intermediates. The reserve pool vesicles are then mobilized to empty docking sites at the active zone. On the other hand, spontaneous vesicles are relatively excluded from the readily releasable pool. However, the spontaneously releasing vesicles dock and fuse at the empty docking sites on the active zone and rapidly mix back with the remaining pool of spontaneous vesicles. These vesicles are morphologically mixed in with the reserve and resting vesicle pools, but functionally distinct from them.

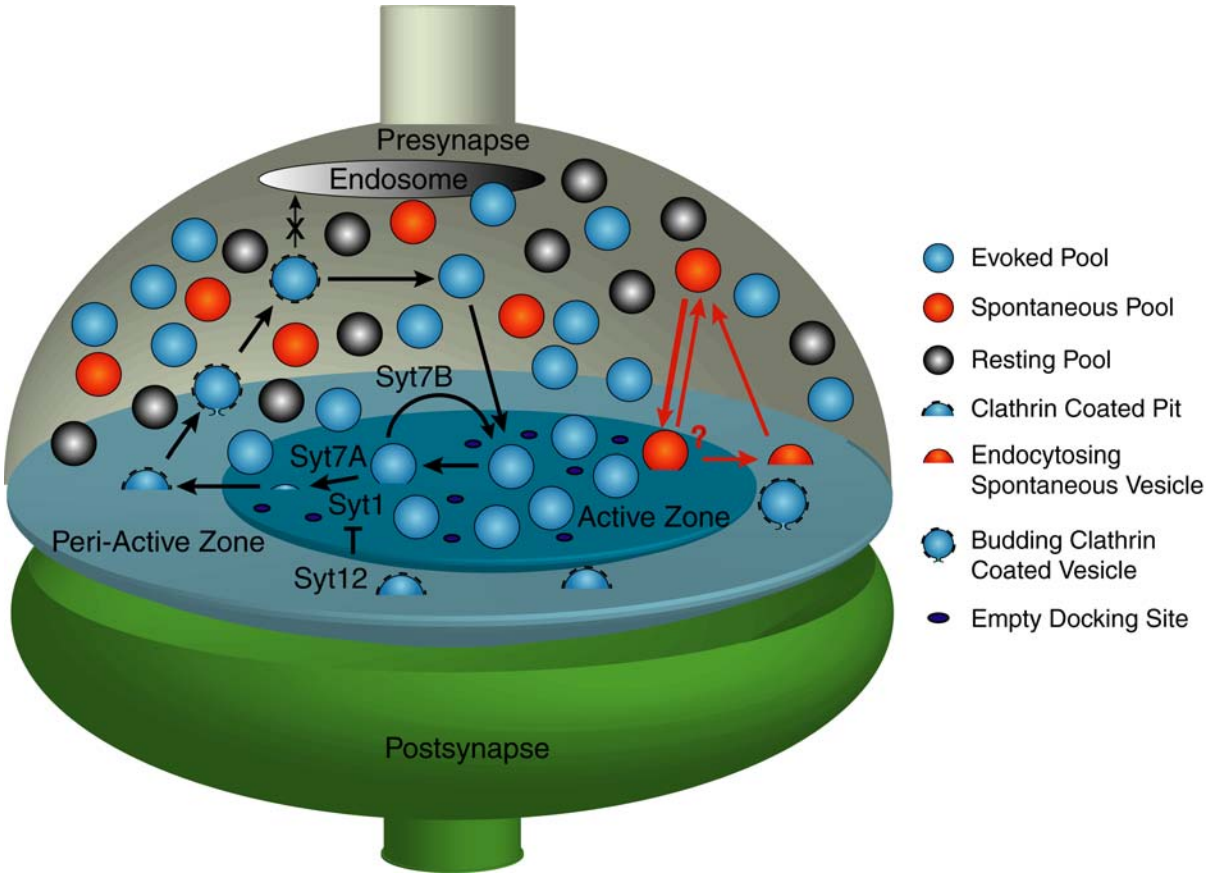

Figure 7.1. Model of Synaptic Vesicle Recycling In Central Synapses. Vesicles are divided into 3 major functional pools, an evoked pool, a spontaneous pool, and a resting pool. The evoked pool populates docking sites at the active zone and these vesicles are highly stabilized and ready to release in response to an incoming action potential. After fusion, vesicles can either rapidly endocytose and recycle locally at the active zone, or endocytose and recycle through a slower clathrin-dependent process in the peri-active zone areas. The slowly recycling vesicles repopulate the reserve pool without trafficking through endosomal intermediates. These vesicles in turn are mobilized back into the readily releasable pool. The spontaneous vesicle pool is excluded from the functional readily releasable pool but these vesicles fuse and release their neurotransmitter at empty docking sites at the active zone. They then rapidly endocytose and recycle to mix back with the remaining spontaneous vesicle pool. The function of the resting pool of vesicles is yet to be determined.

Presynaptic dysfunction can account for some neurological diseases

Can presynaptic function be a substrate for certain disease states of the central nervous system? Given our current ability to analyze synaptic vesicle dynamics in exquisite detail, we are now in a position to start unraveling whether dysfunction of the presynaptic apparatus is the cause of certain diseases of the CNS. Can we also find out which parameters, if any, are the most susceptible? Our recent work constitutes an initial attempt to address this rather broad question. The current view on neurodegenerative diseases is that cell death leads to the manifestation of clinical symptoms building up to the ultimate demise of the patient. In collaboration with the Hofmann laboratory, we studied a mouse model for infantile Batten disease, a condition that causes psychomotor retardation, visual failure, and seizures in patients at a very early age (Gupta et al., 2001; Hofmann and Peltonen, 2001). We found a selective deficit in synaptic vesicle pool size in cortical synapses of these mice (chapter 6). This onset and progression of this phenotype was age dependent, with older cultures showing more severe phenotypes. The physiological outcome of this decreased pool size was a decreased frequency of spontaneous miniature events, without a change in the evoked or sucrose responsiveness. Cells from these mice were otherwise healthy, with normal resting membrane potentials and input resistance, as well as normal levels of cell death compared to wild-type littermate control synapses up to 25 days in culture.

These findings suggest that synaptic dysfunction may be the basis for the neurological symptoms observed in this disease. Whether or not this applies as a general rule for other neurodegenerative disease states remains to be determined. However, in the case of infantile Batten disease, the simple phenotype observed provides an ideal model in which to study drug targets and possible therapeutic interventions. There are many diseases in which overt symptomatology is similar but the underlying mechanisms may not be. Some of these have neurodegeneration associated with them. This raises the interesting question as to what synaptic disruptions lead to neuronal cell death. Better knowledge of the synaptic vesicle cycle could also provide us with strategies to target and treat these CNS disease states before the cells reach the stage where they signal death.

Concluding thoughts

In summary, this body of work has helped show that synaptic vesicle recycling is indeed a very plastic entity. We found that this plasticity allows different synapse types to establish optimal steady state conditions. Synapses also have the intrinsic ability to modulate their vesicle trafficking pathways under the varying demands placed on them. A single recycling pathway could not adequately explain this diversity, which lead to our discovery that spontaneous vesicle release occurs from a recycling pathway independent of evoked vesicle fusion. Disruption of normal vesicle turnover can also explain certain CNS disease phenotypes. However, these findings are merely a stepping-stone for further elaboration of the molecular diversity that allows for the regulation of these complex synaptic functions.

APPENDIX A: Computational Model of Synaptic Vesicle Recycling

At some stage in the vesicle recycling pathway between synaptic vesicle endocytosis and vesicle docking for reuse, synaptic vesicles are refilled with neurotransmitter. This is accomplished by a v-type ATPase establishing a proton gradient across the synaptic vesicle membrane, thereby lowering the pH inside the vesicle and allowing neurotransmitter to be pumped into the vesicle. Therefore, the family of v-type ATPase inhibitors can be used as tools to block neurotransmitter refilling and monitor synaptic depression. Yildirim Sara performed these experiments in the lab using the v-type ATPase inhibitor folimycin. We treated synapses for 10 minutes with 67 nM folimycin in the presence of TTX and found that there was a faster rate of use dependent synaptic depression than in cells treated with vehicle (DMSO). In order to explore the different parameters that may be involved in synaptic depression, we developed a computational model to fit the experimental observations and tested how perturbations in the steady state parameters affected the resultant depression kinetics.

We used the simple model for vesicle recycling shown in figure A.1A, where at steady state, vesicles populate the readily releasable pool (s_0) and the reserve pool (r) with a ratio of 1:2. Under the influence of an incoming action potential, the rate constant for release (a) is altered from ~0 to 0.1s resulting in the release of a vesicle into state s_1. The parameters a and b define the probability of release for a vesicle. The vesicles then undergo endocytosis with a rate constant c followed by neurotransmitter refilling with a rate constant d. The filled synaptic vesicle in state s_3 is then shuttled either through a slow recycling pathway with an intermediate step through the reserve pool, or is directly recycled back to the readily releasable pool. All rates are constant over time except for the rate constant a, which only activates with an incoming action potential.

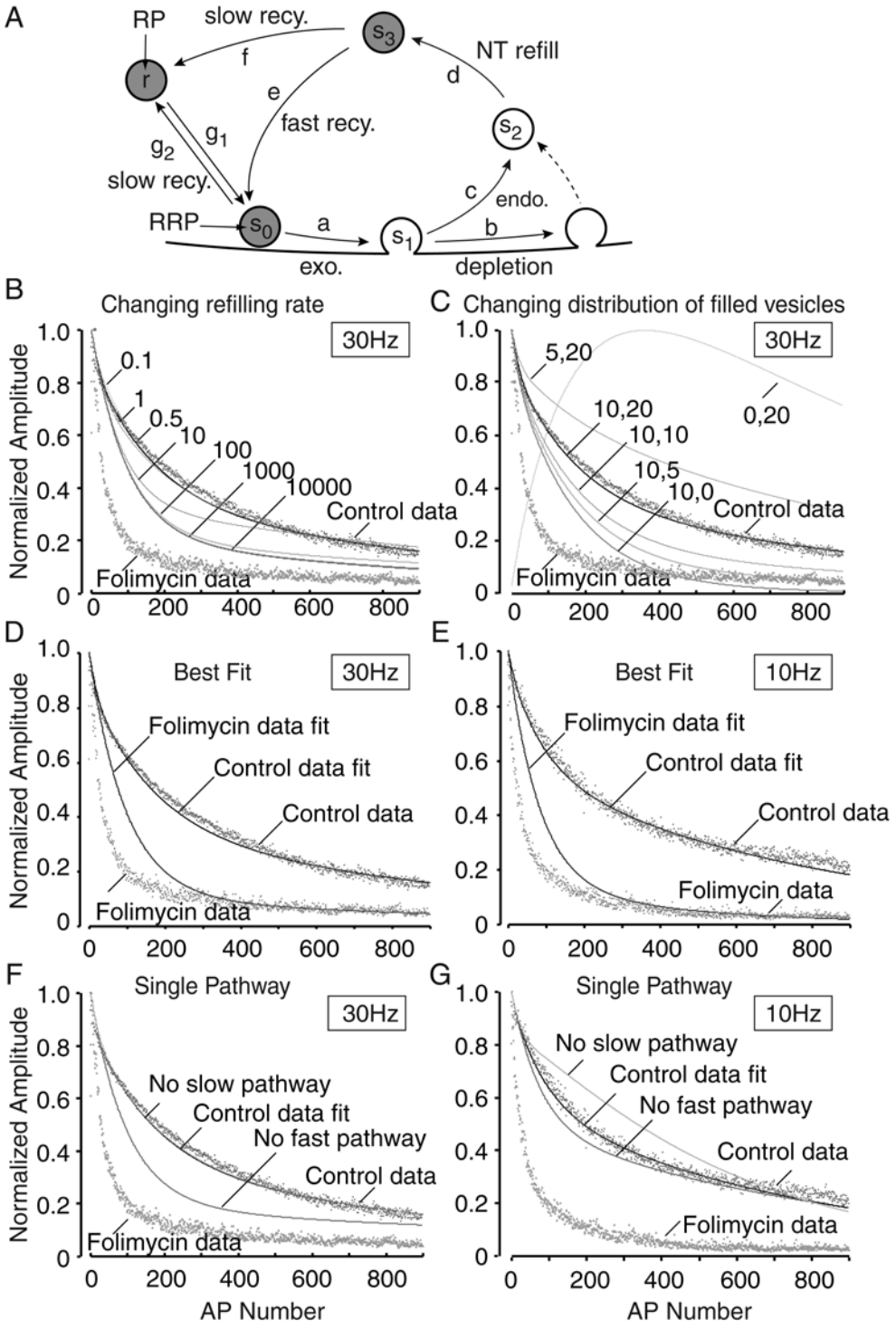

Figure A.1. Kinetic model to simulate synaptic vesicle recycling. **(A)** Model synapse. Three compartmental model showing RP, RRP, endocytosis pathway and interactions

between the pools. **(B)** The control data for synaptic depression at 30Hz was fit with a neurotransmitter refilling time constant (d) of up to 1s. Increasing the time constant to values larger than 1 s resulted in faster synaptic depression and a lower steady state plateau **(C)** The rates of vesicle recycling were kept constant and the distribution of vesicles in the RRP and RP were changed. The control 30 Hz data was best fit with a ratio of 1:3 between RRP:Total Pool. Decreasing this ratio resulted in a shift towards slower synaptic depression and higher steady state plateaus. Without a RRP, the model synapses become highly facilitating. Increasing the ratio resulted in faster depression and a lower steady state plateau. **(D-E)** The best fits for folimycin data at 30Hz (D) and 10 Hz (E) were obtained by a combination of a decreased vesicle refilling rate and a shift in vesicle distribution towards a larger ratio of RRP:Total Pool. **(F-G)** The contribution of fast and slow vesicle recycling at 30 Hz (F) and 10 Hz (G) was studied. During 30 Hz stimulation there is a significant contribution of fast vesicle recycling to the maintenance of efficient neurotransmission (F). During 10 Hz stimulation the rate of vesicle recycling does not appear to limit the synaptic efficacy (G).

Using the simple differential equations shown below we generated a computer simulation in MATLAB to model synaptic vesicle recycling. We were able to fit the control data for both 10 Hz and 30 Hz action potential train with time constants well within the limits of experimental values proposed by a number of different investigators (Figure A.1). If the sole action of folimycin were to prevent synaptic vesicle refilling then by slowing down the refilling rate of vesicles in the model (Figure A.1A, time constant d) we should be able to fit the data. Modeling the 30 Hz depression data, we found that while increasing the time constant for refilling shifts the curve in the correct direction (Figure A.1B), simply shutting down neurotransmitter refilling was not sufficient to account for the extremely rapid phase of depression in our experimental data.

$$\frac{ds_0}{dt} = -(a + g_2)s_0 + g_1 r + e s_3$$

$$\Rightarrow \left(\frac{1}{a + g_2}\right)\frac{ds_0}{dt} = \frac{g_1 r + e s_3}{a + g_2} - s_0$$

$$\frac{ds_1}{dt} = -(b + c)s_1 + a s_0$$

$$\Rightarrow \left(\frac{1}{b + c}\right)\frac{ds_1}{dt} = \frac{a s_0}{b + c} - s_1$$

$$\frac{ds_2}{dt} = -d s_2 + c s_1$$

$$\Rightarrow \left(\frac{1}{d}\right)\frac{ds_2}{dt} = \frac{c s_1}{d} - s_2$$

$$\frac{ds_3}{dt} = -(e + f)s_3 + d s_2$$

$$\Rightarrow \left(\frac{1}{e + f}\right)\frac{ds_3}{dt} = \frac{d s_2}{e + f} - s_3$$

$$\frac{dr}{dt} = -g_1 r + g_2 s_0 + f s_3$$

$$\Rightarrow \left(\frac{1}{g_1}\right)\frac{dr}{dt} = \frac{g_2 s_0 + f s_3}{g_1} - r$$

Since we treated our cells for ten minutes with folimycin in the present of tetrodotoxin (TTX) to block action potentials, we wanted to test whether there was any redistribution of vesicle pools during this time period. Since spontaneously releasing vesicles, which were thought to release from the readily releasable pool (RRP), could release and endocytose without neurotransmitter refilling, it was possible that these blank vesicles could effect the depression kinetics. Therefore we next tested the effect of altering the initial steady state distribution of vesicles on the kinetics of depression in response to a 30 Hz train of action potentials. What we found was that if blank vesicles existed in the RRP before stimulation, then we saw either facilitation of response amplitudes (in the extreme case where no vesicles were present in the RRP), to slower rates of synaptic depression with each additional blank vesicle insertion into the RRP (Figure A.1C). This would suggest that the

vesicles that release and endocytose during TTX application most likely do not populate the RRP. However, decreasing the size of the reserve pool of vesicles (RP) we found that the response amplitude depressed faster the lesser the number of vesicles present in the RP. This would suggest that the blank vesicles that endocytose preferentially populate this back pool and do not mix with the RRP. This is contrary to classical models that predict that spontaneous vesicle release is merely a very low probability release event from the RRP that would normally release on the influx of an action potential. This idea was explored in detail in chapter 6 (or also see (Sara et al., 2005)).

Using this shift in pool distribution as a parameter, in addition to a greatly decreased rate of neurotransmitter refilling, we were able to fit two major differences between control and folimycin treated cells, that is, the induction of a fast phase of depression, and a lower steady state amplitude of the post synaptic response (Figure A.1D-E). However, the experimental data appears to have a much faster rate of depression, which we were unable to achieve using this simple model for vesicle recycling.

In this model of synaptic vesicle recycling (Figure A.1A), we have both a slow and fast component of vesicle recycling. In order to test the extent to which these different pathways play a role in vesicle recycling at different frequencies, we first fit the control data with the best fits as described above and then perturbed the system by turning off (setting at an extremely high time constant) either the fast or the slow pathways (Figure A.1F-G). As we would expect, at high frequency stimulation, we found that shutting down the fast pathway in the model resulted in a much faster rate of synaptic depression (Figure A.1F), while shutting down the slow pathway had minimal effect. Surprisingly, when we performed the same manipulations with the data for 10Hz depression we found that at this frequency, the fast vesicle recycling pathway resulted in only a slight increase in synaptic depression. The loss of slow vesicle recycling had a much larger, yet still minor effect on this pathway. This suggests that the limited synaptic vesicle pool size in central synapses is adequate to maintain neurotransmission at relatively lower stimulation frequencies around 10 Hz without requiring faster recycling modes. However, in order to keep up under more intense stimulation (30Hz) faster modes of vesicle recycling are essential.

From these simulations we were able to gain two fundamental insights into the properties of synaptic vesicle recycling. Firstly, the model suggests that spontaneously recycling vesicles are excluded from the readily releasable pool of vesicles. This idea has been tested and the results are described in chapter 5. Secondly, the model predicts that there is a frequency dependent modulation of synaptic vesicle recycling rate. This idea is currently under investigation, but preliminary evidence using stryl dyes to directly monitor synaptic vesicle recycling suggest that there is a frequency dependence to vesicle recycling, with faster rates of recycling at faster stimulation frequencies (Kale and Kavalali, 2005). However a possible molecular mechanism by which this regulation might occur has been studied in chapter 2.

REFERENCES

Achiriloaie, M., Barylko, B., and Albanesi, J. P. (1999). Essential role of the dynamin pleckstrin homology domain in receptor-mediated endocytosis. Mol Cell Biol *19*, 1410-1415.

Ahtiainen, L., Van Diggelen, O. P., Jalanko, A., and Kopra, O. (2003). Palmitoyl protein thioesterase 1 is targeted to the axons in neurons. J Comp Neurol *455*, 368-377.

Angleson, J. K., and Betz, W. J. (2001). Intraterminal Ca(2+) and spontaneous transmitter release at the frog neuromuscular junction. J Neurophysiol *85*, 287-294.

Aravanis, A. M., Pyle, J. L., and Tsien, R. W. (2003). Single synaptic vesicles fusing transiently and successively without loss of identity. Nature *423*, 643-647.

Bamji, S. X., Shimazu, K., Kimes, N., Huelsken, J., Birchmeier, W., Lu, B., and Reichardt, L. F. (2003). Role of beta-catenin in synaptic vesicle localization and presynaptic assembly. Neuron *40*, 719-731.

Barbieri, M. A., Hoffenberg, S., Roberts, R., Mukhopadhyay, A., Pomrehn, A., Dickey, B. F., and Stahl, P. D. (1998). Evidence for a symmetrical requirement for Rab5-GTP in in vitro endosome-endosome fusion. J Biol Chem *273*, 25850-25855.

Barylko, B., Binns, D. D., and Albanesi, J. P. (2001). Activation of dynamin GTPase activity by phosphoinositides and SH3 domain-containing proteins. Methods Enzymol *329*, 486-496.

Berglund, K., Midorikawa, M., and Tachibana, M. (2002). Increase in the pool size of releasable synaptic vesicles by the activation of protein kinase C in goldfish retinal bipolar cells. J Neurosci *22*, 4776-4785.

Betz, W. J., and Bewick, G. S. (1993). Optical monitoring of transmitter release and synaptic vesicle recycling at the frog neuromuscular junction. J Physiol *460*, 287-309.

Betz, W. J., Mao, F., and Smith, C. B. (1996). Imaging exocytosis and endocytosis. Curr Opin Neurobiol *6*, 365-371.

Bible, E., Gupta, P., Hofmann, S. L., and Cooper, J. D. (2004). Regional and cellular neuropathology in the palmitoyl protein thioesterase-1 null mutant mouse model of infantile neuronal ceroid lipofuscinosis. Neurobiol Dis *16*, 346-359.

Brumberg, J. C., Nowak, L. G., and McCormick, D. A. (2000). Ionic mechanisms underlying repetitive high-frequency burst firing in supragranular cortical neurons. J Neurosci *20*, 4829-4843.

Bucci, C., Parton, R. G., Mather, I. H., Stunnenberg, H., Simons, K., Hoflack, B., and Zerial, M. (1992). The small GTPase rab5 functions as a regulatory factor in the early endocytic pathway. Cell *70*, 715-728.

Butz, S., Fernandez-Chacon, R., Schmitz, F., Jahn, R., and Südhof, T. C. (1999). The subcellular localizations of atypical synaptotagmins III and VI. Synaptotagmin III is enriched

in synapses and synaptic plasma membranes but not in synaptic vesicles. J Biol Chem *274*, 18290-18296.

Calakos, N., Schoch, S., Südhof, T. C., and Malenka, R. C. (2004). Multiple roles for the active zone protein RIM1alpha in late stages of neurotransmitter release. Neuron *42*, 889-896.

Calero, G., Gupta, P., Nonato, M. C., Tandel, S., Biehl, E. R., Hofmann, S. L., and Clardy, J. (2003). The crystal structure of palmitoyl protein thioesterase-2 (PPT2) reveals the basis for divergent substrate specificities of the two lysosomal thioesterases, PPT1 and PPT2. J Biol Chem *278*, 37957-37964.

Camp, L. A., and Hofmann, S. L. (1993). Purification and properties of a palmitoyl-protein thioesterase that cleaves palmitate from H-Ras. J Biol Chem *268*, 22566-22574.

Camp, L. A., Verkruyse, L. A., Afendis, S. J., Slaughter, C. A., and Hofmann, S. L. (1994). Molecular cloning and expression of palmitoyl-protein thioesterase. J Biol Chem *269*, 23212-23219.

Carter, A. G., and Regehr, W. G. (2002). Quantal events shape cerebellar interneuron firing. Nat Neurosci *5*, 1309-1318.

Ceccarelli, B., Hurlbut, W. P., and Mauro, A. (1973). Turnover of transmitter and synaptic vesicles at the frog neuromuscular junction. J Cell Biol *57*, 499-524.

Chen, M. S., Obar, R. A., Schroeder, C. C., Austin, T. W., Poodry, C. A., Wadsworth, S. C., and Vallee, R. B. (1991). Multiple forms of dynamin are encoded by shibire, a Drosophila gene involved in endocytosis. Nature *351*, 583-586.

Christoforidis, S., Miaczynska, M., Ashman, K., Wilm, M., Zhao, L., Yip, S. C., Waterfield, M. D., Backer, J. M., and Zerial, M. (1999). Phosphatidylinositol-3-OH kinases are Rab5 effectors. Nat Cell Biol *1*, 249-252.

Coggan, J. S., Grutzendler, J., Bishop, D. L., Cook, M. R., Gan, W., Heym, J., and Lichtman, J. W. (2004). Age-associated synapse elimination in mouse parasympathetic ganglia. J Neurobiol *60*, 214-226.

Colman, H., Nabekura, J., and Lichtman, J. W. (1997). Alterations in synaptic strength preceding axon withdrawal. Science *275*, 356-361.

Colmeus, C., Gomez, S., Molgo, J., and Thesleff, S. (1982). Discrepancies between spontaneous and evoked synaptic potentials at normal, regenerating and botulinum toxin poisoned mammalian neuromuscular junctions. Proc R Soc Lond B Biol Sci *215*, 63-74.

Connors, B. W., and Amitai, Y. (1997). Making waves in the neocortex. Neuron *18*, 347-349.

Cremona, O., and De Camilli, P. (1997). Synaptic vesicle endocytosis. Curr Opin Neurobiol *7*, 323-330.

Cremona, O., Di Paolo, G., Wenk, M. R., Luthi, A., Kim, W. T., Takei, K., Daniell, L., Nemoto, Y., Shears, S. B., Flavell, R. A., *et al.* (1999). Essential role of phosphoinositide metabolism in synaptic vesicle recycling. Cell *99*, 179-188.

David, C., McPherson, P. S., Mundigl, O., and de Camilli, P. (1996). A role of amphiphysin in synaptic vesicle endocytosis suggested by its binding to dynamin in nerve terminals. Proc Natl Acad Sci U S A *93*, 331-335.

De Camilli, P., Slepnev, V. I., Shupliakov, O., and Brodin, L. (2001). Synaptic Vesicle Endocytosis. In Synapses, W. M. Cowen, T. C. Südhof, and C. F. Stevens, eds. (Baltimore, The Johns Hopkins University Press), pp. 217-274.

de Heuvel, E., Bell, A. W., Ramjaun, A. R., Wong, K., Sossin, W. S., and McPherson, P. S. (1997). Identification of the major synaptojanin-binding proteins in brain. J Biol Chem *272*, 8710-8716.

de Hoop, M. J., Huber, L. A., Stenmark, H., Williamson, E., Zerial, M., Parton, R. G., and Dotti, C. G. (1994). The involvement of the small GTP-binding protein Rab5a in neuronal endocytosis. Neuron *13*, 11-22.

Deák, F., Schoch, S., Liu, X., Südhof, T. C., and Kavalali, E. T. (2004). Synaptobrevin is essential for fast synaptic-vesicle endocytosis. Nat Cell Biol *6*, 1102-1108.

Deitcher, D. L., Ueda, A., Stewart, B. A., Burgess, R. W., Kidokoro, Y., and Schwarz, T. L. (1998). Distinct requirements for evoked and spontaneous release of neurotransmitter are revealed by mutations in the Drosophila gene neuronal-synaptobrevin. J Neurosci *18*, 2028-2039.

Del Castillo, J., and Katz, B. (1954). Quantal components of the end-plate potential. J Physiol *124*, 560-573.

Delgado, R., Maureira, C., Oliva, C., Kidokoro, Y., and Labarca, P. (2000). Size of vesicle pools, rates of mobilization, and recycling at neuromuscular synapses of a Drosophila mutant, shibire. Neuron *28*, 941-953.

Di Paolo, G., Sankaranarayanan, S., Wenk, M. R., Daniell, L., Perucco, E., Caldarone, B. J., Flavell, R., Picciotto, M. R., Ryan, T. A., Cremona, O., and De Camilli, P. (2002). Decreased synaptic vesicle recycling efficiency and cognitive deficits in amphiphysin 1 knockout mice. Neuron *33*, 789-804.

Dietrich, L. E., Boeddinghaus, C., LaGrassa, T. J., and Ungermann, C. (2003). Control of eukaryotic membrane fusion by N-terminal domains of SNARE proteins. Biochim Biophys Acta *1641*, 111-119.

Dietrich, L. E., Gurezka, R., Veit, M., and Ungermann, C. (2004). The SNARE Ykt6 mediates protein palmitoylation during an early stage of homotypic vacuole fusion. Embo J *23*, 45-53.

Dittman, J. S., and Regehr, W. G. (1996). Contributions of calcium-dependent and calcium-independent mechanisms to presynaptic inhibition at a cerebellar synapse. J Neurosci *16*, 1623-1633.

Dittman, J. S., and Regehr, W. G. (1998). Calcium dependence and recovery kinetics of presynaptic depression at the climbing fiber to Purkinje cell synapse. J Neurosci *18*, 6147-6162.

Duncan, R. R., Greaves, J., Wiegand, U. K., Matskevich, I., Bodammer, G., Apps, D. K., Shipston, M. J., and Chow, R. H. (2003). Functional and spatial segregation of secretory vesicle pools according to vesicle age. Nature *422*, 176-180.

el-Husseini Ael, D., and Bredt, D. S. (2002). Protein palmitoylation: a regulator of neuronal development and function. Nat Rev Neurosci *3*, 791-802.

Fernandez-Chacon, R., Konigstorfer, A., Gerber, S. H., Garcia, J., Matos, M. F., Stevens, C. F., Brose, N., Rizo, J., Rosenmund, C., and Südhof, T. C. (2001). Synaptotagmin I functions as a calcium regulator of release probability. Nature *410*, 41-49.

Fernandez-Chacon, R., Wolfel, M., Nishimune, H., Tabares, L., Schmitz, F., Castellano-Munoz, M., Rosenmund, C., Montesinos, M. L., Sanes, J. R., Schneggenburger, R., and Südhof, T. C. (2004). The synaptic vesicle protein CSP alpha prevents presynaptic degeneration. Neuron *42*, 237-251.

Ford, M. G., Pearse, B. M., Higgins, M. K., Vallis, Y., Owen, D. J., Gibson, A., Hopkins, C. R., Evans, P. R., and McMahon, H. T. (2001). Simultaneous binding of PtdIns(4,5)P2 and clathrin by AP180 in the nucleation of clathrin lattices on membranes. Science *291*, 1051-1055.

Frerking, M., Borges, S., and Wilson, M. (1997). Are some minis multiquantal? J Neurophysiol *78*, 1293-1304.

Fukuda, M., Kanno, E., Satoh, M., Saegusa, C., and Yamamoto, A. (2004). Synaptotagmin VII is targeted to dense-core vesicles and regulates their Ca2+ -dependent exocytosis in PC12 cells. J Biol Chem *279*, 52677-52684.

Gaidarov, I., and Keen, J. H. (1999). Phosphoinositide-AP-2 interactions required for targeting to plasma membrane clathrin-coated pits. J Cell Biol *146*, 755-764.

Galli, T., and Haucke, V. (2004). Cycling of synaptic vesicles: how far? How fast! Sci STKE *2004*, re19.

Gandhi, S. P., and Stevens, C. F. (2003). Three modes of synaptic vesicular recycling revealed by single-vesicle imaging. Nature *423*, 607-613.

Garcia, C. C., Blair, H. J., Seager, M., Coulthard, A., Tennant, S., Buddles, M., Curtis, A., and Goodship, J. A. (2004). Identification of a mutation in synapsin I, a synaptic vesicle protein, in a family with epilepsy. J Med Genet *41*, 183-186.

Gauthier-Campbell, C., Bredt, D. S., Murphy, T. H., and El-Husseini Ael, D. (2004). Regulation of dendritic branching and filopodia formation in hippocampal neurons by specific acylated protein motifs. Mol Biol Cell *15*, 2205-2217.

Geppert, M., Goda, Y., Hammer, R. E., Li, C., Rosahl, T. W., Stevens, C. F., and Südhof, T. C. (1994). Synaptotagmin I: a major Ca2+ sensor for transmitter release at a central synapse. Cell *79*, 717-727.

Gillingwater, T. H., and Ribchester, R. R. (2003). The relationship of neuromuscular synapse elimination to synaptic degeneration and pathology: insights from WldS and other mutant mice. J Neurocytol *32*, 863-881.

Grabs, D., Slepnev, V. I., Songyang, Z., David, C., Lynch, M., Cantley, L. C., and De Camilli, P. (1997). The SH3 domain of amphiphysin binds the proline-rich domain of dynamin at a single site that defines a new SH3 binding consensus sequence. J Biol Chem *272*, 13419-13425.

Grigliatti, T. A., Hall, L., Rosenbluth, R., and Suzuki, D. T. (1973). Temperature-sensitive mutations in Drosophila melanogaster. XIV. A selection of immobile adults. Mol Gen Genet *120*, 107-114.

Gupta, P., Soyombo, A. A., Atashband, A., Wisniewski, K. E., Shelton, J. M., Richardson, J. A., Hammer, R. E., and Hofmann, S. L. (2001). Disruption of PPT1 or PPT2 causes neuronal ceroid lipofuscinosis in knockout mice. Proc Natl Acad Sci U S A *98*, 13566-13571.

Gupta, P., Soyombo, A. A., Shelton, J. M., Wilkofsky, I. G., Wisniewski, K. E., Richardson, J. A., and Hofmann, S. L. (2003). Disruption of PPT2 in mice causes an unusual lysosomal storage disorder with neurovisceral features. Proc Natl Acad Sci U S A *100*, 12325-12330.

Haltia, M., Rapola, J., Santavuori, P., and Keranen, A. (1973). Infantile type of so-called neuronal ceroid-lipofuscinosis. 2. Morphological and biochemical studies. J Neurol Sci *18*, 269-285.

Han, W., Rhee, J. S., Maximov, A., Lao, Y., Mashimo, T., Rosenmund, C., and Südhof, T. C. (2004). N-glycosylation is essential for vesicular targeting of synaptotagmin 1. Neuron *41*, 85-99.

Han, W., Rhee, J. S., Maximov, A., Lin, W., Hammer, R. E., Rosenmund, C., and Sudhof, T. C. (2005). C-terminal ECFP fusion impairs synaptotagmin 1 function: crowding out synaptotagmin 1. J Biol Chem *280*, 5089-5100.

Harata, N., Pyle, J. L., Aravanis, A. M., Mozhayeva, M., Kavalali, E. T., and Tsien, R. W. (2001). Limited numbers of recycling vesicles in small CNS nerve terminals: implications for neural signaling and vesicular cycling. Trends Neurosci *24*, 637-643.

Haucke, V., and De Camilli, P. (1999). AP-2 recruitment to synaptotagmin stimulated by tyrosine-based endocytic motifs. Science *285*, 1268-1271.

Haucke, V., Wenk, M. R., Chapman, E. R., Farsad, K., and De Camilli, P. (2000). Dual interaction of synaptotagmin with mu2- and alpha-adaptin facilitates clathrin-coated pit nucleation. Embo J *19*, 6011-6019.

Heilker, R., Spiess, M., and Crottet, P. (1999). Recognition of sorting signals by clathrin adaptors. Bioessays *21*, 558-567.

Heinonen, O., Kyttala, A., Lehmus, E., Paunio, T., Peltonen, L., and Jalanko, A. (2000). Expression of palmitoyl protein thioesterase in neurons. Mol Genet Metab *69*, 123-129.

Hellsten, E., Vesa, J., Olkkonen, V. M., Jalanko, A., and Peltonen, L. (1996). Human palmitoyl protein thioesterase: evidence for lysosomal targeting of the enzyme and disturbed cellular routing in infantile neuronal ceroid lipofuscinosis. Embo J *15*, 5240-5245.

Henkel, A. W., and Almers, W. (1996). Fast steps in exocytosis and endocytosis studied by capacitance measurements in endocrine cells. Curr Opin Neurobiol *6*, 350-357.

Heuser, J. (1980). Three-dimensional visualization of coated vesicle formation in fibroblasts. J Cell Biol *84*, 560-583.

Heuser, J. E., and Reese, T. S. (1973). Evidence for recycling of synaptic vesicle membrane during transmitter release at the frog neuromuscular junction. J Cell Biol *57*, 315-344.

Hinshaw, J. E. (2000). Dynamin and its role in membrane fission. Annu Rev Cell Dev Biol *16*, 483-519.

Hofmann, S. L., and Peltonen, L. (2001). The Neuronal Ceroid Lipofuscinoses. In The Metabolic and Molecular Bases of Inherited Disease, C. R. Scriver, A. L. Beaudet, W. S. Sly, B. Childs, and B. Vogelstein, eds. (New York, McGraw-Hill), pp. 3877-3894.

Holopainen, J. M., Saarikoski, J., Kinnunen, P. K., and Jarvela, I. (2001). Elevated lysosomal pH in neuronal ceroid lipofuscinoses (NCLs). Eur J Biochem *268*, 5851-5856.

Iezzi, M., Kouri, G., Fukuda, M., and Wollheim, C. B. (2004). Synaptotagmin V and IX isoforms control Ca2+ -dependent insulin exocytosis. J Cell Sci *117*, 3119-3127.

Jahn, R., Lang, T., and Südhof, T. C. (2003). Membrane fusion. Cell *112*, 519-533.

Jaiswal, J. K., Chakrabarti, S., Andrews, N. W., and Simon, S. M. (2004). Synaptotagmin VII restricts fusion pore expansion during lysosomal exocytosis. PLoS Biol *2*, E233.

Jarousse, N., and Kelly, R. B. (2001). The AP2 binding site of synaptotagmin 1 is not an internalization signal but a regulator of endocytosis. J Cell Biol *154*, 857-866.

Jorgensen, E. M., Hartwieg, E., Schuske, K., Nonet, M. L., Jin, Y., and Horvitz, H. R. (1995). Defective recycling of synaptic vesicles in synaptotagmin mutants of Caenorhabditis elegans. Nature *378*, 196-199.

Kale, S., and Kavalali, E. T. (2005). Personal communication.

Kanaani, J., Diacovo, M. J., El-Husseini Ael, D., Bredt, D. S., and Baekkeskov, S. (2004). Palmitoylation controls trafficking of GAD65 from Golgi membranes to axon-specific endosomes and a Rab5a-dependent pathway to presynaptic clusters. J Cell Sci *117*, 2001-2013.

Kang, R., Swayze, R., Lise, M. F., Gerrow, K., Mullard, A., Honer, W. G., and El-Husseini, A. (2004). Presynaptic trafficking of synaptotagmin I is regulated by protein palmitoylation. J Biol Chem *279*, 50524-50536.

Katz, B. (1969). The Release of Neural Transmitter Substances (Liverpool, Liverpool University Press).

Kavalali, E. T., Klingauf, J., and Tsien, R. W. (1999a). Activity-dependent regulation of synaptic clustering in a hippocampal culture system. Proc Natl Acad Sci U S A *96*, 12893-12900.

Kavalali, E. T., Klingauf, J., and Tsien, R. W. (1999b). Properties of fast endocytosis at hippocampal synapses. Philos Trans R Soc Lond B Biol Sci *354*, 337-346.

Kawasaki, F., Hazen, M., and Ordway, R. W. (2000). Fast synaptic fatigue in shibire mutants reveals a rapid requirement for dynamin in synaptic vesicle membrane trafficking. Nat Neurosci *3*, 859-860.
taf/DynaPage.taf?file=/neuro/journal/v853/n859/full/nn0900_0859.html
taf/DynaPage.taf?file=/neuro/journal/v0903/n0909/abs/nn0900_0859.html.

Keller, C. A., Yuan, X., Panzanelli, P., Martin, M. L., Alldred, M., Sassoe-Pognetto, M., and Luscher, B. (2004). The gamma2 subunit of GABA(A) receptors is a substrate for palmitoylation by GODZ. J Neurosci *24*, 5881-5891.

Klingauf, J., Kavalali, E. T., and Tsien, R. W. (1998). Kinetics and regulation of fast endocytosis at hippocampal synapses. Nature *394*, 581-585.

Koenig, J. H., and Ikeda, K. (1989). Disappearance and reformation of synaptic vesicle membrane upon transmitter release observed under reversible blockage of membrane retrieval. J Neurosci *9*, 3844-3860.

Koenig, J. H., and Ikeda, K. (1996). Synaptic vesicles have two distinct recycling pathways. J Cell Biol *135*, 797-808.

Koenig, J. H., and Ikeda, K. (1999). Contribution of active zone subpopulation of vesicles to evoked and spontaneous release. J Neurophysiol *81*, 1495-1505.

Kopp, D. M., Perkel, D. J., and Balice-Gordon, R. J. (2000). Disparity in neurotransmitter release probability among competing inputs during neuromuscular synapse elimination. J Neurosci *20*, 8771-8779.

Lehtovirta, M., Kyttala, A., Eskelinen, E. L., Hess, M., Heinonen, O., and Jalanko, A. (2001). Palmitoyl protein thioesterase (PPT) localizes into synaptosomes and synaptic vesicles in neurons: implications for infantile neuronal ceroid lipofuscinosis (INCL). Hum Mol Genet *10*, 69-75.

Li, C., Ullrich, B., Zhang, J. Z., Anderson, R. G., Brose, N., and Südhof, T. C. (1995a). Ca(2+)-dependent and -independent activities of neural and non-neural synaptotagmins. Nature *375*, 594-599.

Li, G., D'Souza-Schorey, C., Barbieri, M. A., Roberts, R. L., Klippel, A., Williams, L. T., and Stahl, P. D. (1995b). Evidence for phosphatidylinositol 3-kinase as a regulator of endocytosis via activation of Rab5. Proc Natl Acad Sci U S A *92*, 10207-10211.

Li, Z., and Murthy, V. N. (2001). Visualizing postendocytic traffic of synaptic vesicles at hippocampal synapses. Neuron *31*, 593-605.

Liu, G., and Tsien, R. W. (1995). Properties of synaptic transmission at single hippocampal synaptic boutons. Nature *375*, 404-408.

Llano, I., Gonzalez, J., Caputo, C., Lai, F. A., Blayney, L. M., Tan, Y. P., and Marty, A. (2000). Presynaptic calcium stores underlie large-amplitude miniature IPSCs and spontaneous calcium transients. Nat Neurosci *3*, 1256-1265.

Lonart, G., and Südhof, T. C. (2000). Assembly of SNARE core complexes prior to neurotransmitter release sets the readily releasable pool of synaptic vesicles. J Biol Chem *275*, 27703-27707.

Lu, J. Y., Verkruyse, L. A., and Hofmann, S. L. (1996). Lipid thioesters derived from acylated proteins accumulate in infantile neuronal ceroid lipofuscinosis: correction of the defect in lymphoblasts by recombinant palmitoyl-protein thioesterase. Proc Natl Acad Sci U S A *93*, 10046-10050.

Lu, J. Y., Verkruyse, L. A., and Hofmann, S. L. (2002). The effects of lysosomotropic agents on normal and INCL cells provide further evidence for the lysosomal nature of palmitoyl-protein thioesterase function. Biochim Biophys Acta *1583*, 35-44.

Luthi, A., Di Paolo, G., Cremona, O., Daniell, L., De Camilli, P., and McCormick, D. A. (2001). Synaptojanin 1 contributes to maintaining the stability of GABAergic transmission in primary cultures of cortical neurons. J Neurosci *21*, 9101-9111.

Malenka, R. C., Madison, D. V., and Nicoll, R. A. (1986). Potentiation of synaptic transmission in the hippocampus by phorbol esters. Nature *321*, 175-177.

Malgaroli, A., Ting, A. E., Wendland, B., Bergamaschi, A., Villa, A., Tsien, R. W., and Scheller, R. H. (1995). Presynaptic component of long-term potentiation visualized at individual hippocampal synapses. Science *268*, 1624-1628.

Marqueze, B., Berton, F., and Seagar, M. (2000). Synaptotagmins in membrane traffic: which vesicles do the tagmins tag? Biochimie *82*, 409-420.

Martina, J. A., Bonangelino, C. J., Aguilar, R. C., and Bonifacino, J. S. (2001). Stonin 2: an adaptor-like protein that interacts with components of the endocytic machinery. J Cell Biol *153*, 1111-1120.

Matteoli, M., Takei, K., Perin, M. S., Südhof, T. C., and De Camilli, P. (1992). Exo-endocytotic recycling of synaptic vesicles in developing processes of cultured hippocampal neurons. J Cell Biol *117*, 849-861.

Maximov, A., and Südhof, T. C. (2005a). Personal Communication.

Maximov, A., and Südhof, T. C. (2005b). Unpublished data.

McKinney, R. A., Capogna, M., Durr, R., Gahwiler, B. H., and Thompson, S. M. (1999). Miniature synaptic events maintain dendritic spines via AMPA receptor activation. Nat Neurosci *2*, 44-49.

McMahon, H. T., Wigge, P., and Smith, C. (1997). Clathrin interacts specifically with amphiphysin and is displaced by dynamin. FEBS Lett *413*, 319-322.

Mozhayeva, M. G., Sara, Y., Liu, X., and Kavalali, E. T. (2002). Development of vesicle pools during maturation of hippocampal synapses. J Neurosci *22*, 654-665.

Mukhopadhyay, A., Barbieri, A. M., Funato, K., Roberts, R., and Stahl, P. D. (1997). Sequential actions of Rab5 and Rab7 regulate endocytosis in the Xenopus oocyte. J Cell Biol *136*, 1227-1237.

Murthy, V. N., and Stevens, C. F. (1999). Reversal of synaptic vesicle docking at central synapses. Nat Neurosci *2*, 503-507.

Musacchio, A., Smith, C. J., Roseman, A. M., Harrison, S. C., Kirchhausen, T., and Pearse, B. M. (1999). Functional organization of clathrin in coats: combining electron cryomicroscopy and X-ray crystallography. Mol Cell *3*, 761-770.

Nakano, Y., Fujitani, K., Kurihara, J., Ragan, J., Usui-Aoki, K., Shimoda, L., Lukacsovich, T., Suzuki, K., Sezaki, M., Sano, Y.*, et al.* (2001). Mutations in the novel membrane protein spinster interfere with programmed cell death and cause neural degeneration in Drosophila melanogaster. Mol Cell Biol *21*, 3775-3788.

Neher, E. (1998). Vesicle pools and Ca2+ microdomains: new tools for understanding their roles in neurotransmitter release. Neuron *20*, 389-399.

Nicholson-Tomishima, K., and Ryan, T. A. (2004). Kinetic efficiency of endocytosis at mammalian CNS synapses requires synaptotagmin I. Proc Natl Acad Sci U S A *101*, 16648-16652.

Patterson, S. I. (2002). Posttranslational protein S-palmitoylation and the compartmentalization of signaling molecules in neurons. Biol Res *35*, 139-150.

Piedras-Renteria, E. S., Pyle, J. L., Diehn, M., Glickfeld, L. L., Harata, N. C., Cao, Y., Kavalali, E. T., Brown, P. O., and Tsien, R. W. (2004). Presynaptic homeostasis at CNS nerve terminals compensates for lack of a key Ca2+ entry pathway. Proc Natl Acad Sci U S A *101*, 3609-3614.

Pieribone, V. A., Shupliakov, O., Brodin, L., Hilfiker-Rothenfluh, S., Czernik, A. J., and Greengard, P. (1995). Distinct pools of synaptic vesicles in neurotransmitter release. Nature *375*, 493-497.

Poodry, C. A., Hall, L., and Suzuki, D. T. (1973). Developmental properties of Shibire: a pleiotropic mutation affecting larval and adult locomotion and development. Dev Biol *32*, 373-386.

Poskanzer, K. E., Marek, K. W., Sweeney, S. T., and Davis, G. W. (2003). Synaptotagmin I is necessary for compensatory synaptic vesicle endocytosis in vivo. Nature *426*, 559-563.

Pyle, J. L., Kavalali, E. T., Piedras-Renteria, E. S., and Tsien, R. W. (2000). Rapid reuse of readily releasable pool vesicles at hippocampal synapses. Neuron *28*, 221-231.

Reim, K., Mansour, M., Varoqueaux, F., McMahon, H. T., Südhof, T. C., Brose, N., and Rosenmund, C. (2001). Complexins regulate a late step in Ca2+-dependent neurotransmitter release. Cell *104*, 71-81.

Rhee, J. S., Betz, A., Pyott, S., Reim, K., Varoqueaux, F., Augustin, I., Hesse, D., Südhof, T. C., Takahashi, M., Rosenmund, C., and Brose, N. (2002). Beta phorbol ester- and diacylglycerol-induced augmentation of transmitter release is mediated by Munc13s and not by PKCs. Cell *108*, 121-133.

Richards, D. A., Guatimosim, C., and Betz, W. J. (2000). Two endocytic recycling routes selectively fill two vesicle pools in frog motor nerve terminals. Neuron *27*, 551-559.

Richards, D. A., Rizzoli, S. O., and Betz, W. J. (2004). Effects of wortmannin and latrunculin A on slow endocytosis at the frog neuromuscular junction. J Physiol *557*, 77-91.

Ringstad, N., Gad, H., Low, P., Di Paolo, G., Brodin, L., Shupliakov, O., and De Camilli, P. (1999). Endophilin/SH3p4 is required for the transition from early to late stages in clathrin-mediated synaptic vesicle endocytosis. Neuron *24*, 143-154.

Ringstad, N., Nemoto, Y., and De Camilli, P. (1997). The SH3p4/Sh3p8/SH3p13 protein family: binding partners for synaptojanin and dynamin via a Grb2-like Src homology 3 domain. Proc Natl Acad Sci U S A *94*, 8569-8574.

Rizzoli, S. O., and Betz, W. J. (2004). The structural organization of the readily releasable pool of synaptic vesicles. Science *303*, 2037-2039.

Roberts, R. L., Barbieri, M. A., Pryse, K. M., Chua, M., Morisaki, J. H., and Stahl, P. D. (1999). Endosome fusion in living cells overexpressing GFP-rab5. J Cell Sci *112 (Pt 21)*, 3667-3675.

Roberts, R. L., Barbieri, M. A., Ullrich, J., and Stahl, P. D. (2000). Dynamics of rab5 activation in endocytosis and phagocytosis. J Leukoc Biol *68*, 627-632.

Rosahl, T. W., Geppert, M., Spillane, D., Herz, J., Hammer, R. E., Malenka, R. C., and Südhof, T. C. (1993). Short-term synaptic plasticity is altered in mice lacking synapsin I. Cell *75*, 661-670.

Rosenmund, C., and Stevens, C. F. (1996). Definition of the readily releasable pool of vesicles at hippocampal synapses. Neuron *16*, 1197-1207.

Ryan, T. A., Reuter, H., and Smith, S. J. (1997). Optical detection of a quantal presynaptic membrane turnover. Nature *388*, 478-482.

Ryan, T. A., Reuter, H., Wendland, B., Schweizer, F. E., Tsien, R. W., and Smith, S. J. (1993). The kinetics of synaptic vesicle recycling measured at single presynaptic boutons. Neuron *11*, 713-724.

Ryan, T. A., and Smith, S. J. (1995). Vesicle pool mobilization during action potential firing at hippocampal synapses. Neuron *14*, 983-989.

Ryan, T. A., Smith, S. J., and Reuter, H. (1996). The timing of synaptic vesicle endocytosis. Proc Natl Acad Sci U S A *93*, 5567-5571.

Sankaranarayanan, S., and Ryan, T. A. (2000). Real-time measurements of vesicle-SNARE recycling in synapses of the central nervous system. Nat Cell Biol *2*, 197-204.

Sankaranarayanan, S., and Ryan, T. A. (2001). Calcium accelerates endocytosis of vSNAREs at hippocampal synapses. Nat Neurosci *4*, 129-136.

Sara, Y., Mozhayeva, M. G., Liu, X., and Kavalali, E. T. (2002). Fast vesicle recycling supports neurotransmission during sustained stimulation at hippocampal synapses. J Neurosci *22*, 1608-1617.

Sara, Y., Virmani, T., Deák, F., Liu, X., and Kavalali, E. T. (2005). An isolated pool of vesicles recycles at rest and drives spontaneous neurotransmission. Neuron *45*, 563-573.

Schikorski, T., and Stevens, C. F. (2001). Morphological correlates of functionally defined synaptic vesicle populations. Nat Neurosci *4*, 391-395.

Schmid, S. L., Braell, W. A., Schlossman, D. M., and Rothman, J. E. (1984). A role for clathrin light chains in the recognition of clathrin cages by 'uncoating ATPase'. Nature *311*, 228-231.

Schmidt, A., Wolde, M., Thiele, C., Fest, W., Kratzin, H., Podtelejnikov, A. V., Witke, W., Huttner, W. B., and Soling, H. D. (1999). Endophilin I mediates synaptic vesicle formation by transfer of arachidonate to lysophosphatidic acid. Nature *401*, 133-141.

Schneggenburger, R., Meyer, A. C., and Neher, E. (1999). Released fraction and total size of a pool of immediately available transmitter quanta at a calyx synapse. Neuron *23*, 399-409.

Schoch, S., Deák, F., Konigstorfer, A., Mozhayeva, M., Sara, Y., Südhof, T. C., and Kavalali, E. T. (2001). SNARE function analyzed in synaptobrevin/VAMP knockout mice. Science *294*, 1117-1122.

Schuske, K. R., Richmond, J. E., Matthies, D. S., Davis, W. S., Runz, S., Rube, D. A., van der Bliek, A. M., and Jorgensen, E. M. (2003). Endophilin is required for synaptic vesicle endocytosis by localizing synaptojanin. Neuron *40*, 749-762.

Sever, S., Muhlberg, A. B., and Schmid, S. L. (1999). Impairment of dynamin's GAP domain stimulates receptor-mediated endocytosis. Nature *398*, 481-486.

Shapira, R., Silberberg, S. D., Ginsburg, S., and Rahamimoff, R. (1987). Activation of protein kinase C augments evoked transmitter release. Nature *325*, 58-60.

Shin, O. H., Rizo, J., and Südhof, T. C. (2002). Synaptotagmin function in dense core vesicle exocytosis studied in cracked PC12 cells. Nat Neurosci *5*, 649-656.

Sleat, D. E., Chen, T. L., Raska, K., Jr., and Lobel, P. (1995). Increased levels of glycoproteins containing mannose 6-phosphate in human breast carcinomas. Cancer Res *55*, 3424-3430.

Slepnev, V. I., Ochoa, G. C., Butler, M. H., Grabs, D., and De Camilli, P. (1998). Role of phosphorylation in regulation of the assembly of endocytic coat complexes. Science *281*, 821-824.

Smotrys, J. E., and Linder, M. E. (2004). Palmitoylation of intracellular signaling proteins: regulation and function. Annu Rev Biochem *73*, 559-587.

Song, B. D., Yarar, D., and Schmid, S. L. (2004). An assembly-incompetent mutant establishes a requirement for dynamin self-assembly in clathrin-mediated endocytosis in vivo. Mol Biol Cell *15*, 2243-2252.

Soyombo, A. A., and Hofmann, S. L. (1997). Molecular cloning and expression of palmitoyl-protein thioesterase 2 (PPT2), a homolog of lysosomal palmitoyl-protein thioesterase with a distinct substrate specificity. J Biol Chem *272*, 27456-27463.

Stevens, C. F., and Sullivan, J. M. (1998). Regulation of the readily releasable vesicle pool by protein kinase C. Neuron *21*, 885-893.

Stevens, C. F., and Tsujimoto, T. (1995). Estimates for the pool size of releasable quanta at a single central synapse and for the time required to refill the pool. Proc Natl Acad Sci U S A *92*, 846-849.

Stevens, C. F., and Wesseling, J. F. (1998). Activity-dependent modulation of the rate at which synaptic vesicles become available to undergo exocytosis. Neuron *21*, 415-424.

Stevens, C. F., and Williams, J. H. (2000). "Kiss and run" exocytosis at hippocampal synapses. Proc Natl Acad Sci U S A *97*, 12828-12833.

Stowell, M. H., Marks, B., Wigge, P., and McMahon, H. T. (1999). Nucleotide-dependent conformational changes in dynamin: evidence for a mechanochemical molecular spring. Nat Cell Biol *1*, 27-32.

Südhof, T. C. (1995). The synaptic vesicle cycle: a cascade of protein-protein interactions. Nature *375*, 645-653.

Südhof, T. C. (2000). The synaptic vesicle cycle revisited. Neuron *28*, 317-320.

Südhof, T. C. (2002). Synaptotagmins: why so many? J Biol Chem *277*, 7629-7632.

Südhof, T. C. (2004). The synaptic vesicle cycle. Annu Rev Neurosci *27*, 509-547.

Sugita, S., Han, W., Butz, S., Liu, X., Fernandez-Chacon, R., Lao, Y., and Südhof, T. C. (2001). Synaptotagmin VII as a plasma membrane Ca(2+) sensor in exocytosis. Neuron *30*, 459-473.

Sugita, S., Shin, O. H., Han, W., Lao, Y., and Südhof, T. C. (2002). Synaptotagmins form a hierarchy of exocytotic Ca(2+) sensors with distinct Ca(2+) affinities. Embo J *21*, 270-280.

Sugita, S., and Südhof, T. C. (2000). Specificity of Ca2+-dependent protein interactions mediated by the C2A domains of synaptotagmins. Biochemistry *39*, 2940-2949.

Sun, J. Y., Wu, X. S., and Wu, L. G. (2002). Single and multiple vesicle fusion induce different rates of endocytosis at a central synapse. Nature *417*, 555-559.

Sutton, M. A., Wall, N. R., Aakalu, G. N., and Schuman, E. M. (2004). Regulation of dendritic protein synthesis by miniature synaptic events. Science *304*, 1979-1983.

Sweeney, S. T., and Davis, G. W. (2002). Unrestricted synaptic growth in spinster-a late endosomal protein implicated in TGF-beta-mediated synaptic growth regulation. Neuron *36*, 403-416.

Takei, K., Mundigl, O., Daniell, L., and De Camilli, P. (1996). The synaptic vesicle cycle: a single vesicle budding step involving clathrin and dynamin. J Cell Biol *133*, 1237-1250.

Takei, K., Slepnev, V. I., Haucke, V., and De Camilli, P. (1999). Functional partnership between amphiphysin and dynamin in clathrin-mediated endocytosis. Nat Cell Biol *1*, 33-39.

Valtorta, F., Meldolesi, J., and Fesce, R. (2001). Synaptic vesicles: is kissing a matter of competence? Trends Cell Biol *11*, 324-328.

van der Bliek, A. M., and Meyerowitz, E. M. (1991). Dynamin-like protein encoded by the Drosophila shibire gene associated with vesicular traffic. Nature *351*, 411-414.

Van der Kloot, W. (1996). Spontaneous and uniquantal-evoked endplate currents in normal frogs are indistinguishable. J Physiol *492 (Pt 1)*, 155-162.

van Diggelen, O. P., Thobois, S., Tilikete, C., Zabot, M. T., Keulemans, J. L., van Bunderen, P. A., Taschner, P. E., Losekoot, M., and Voznyi, Y. V. (2001). Adult neuronal ceroid lipofuscinosis with palmitoyl-protein thioesterase deficiency: first adult-onset patients of a childhood disease. Ann Neurol *50*, 269-272.

Varoqueaux, F., Sigler, A., Rhee, J. S., Brose, N., Enk, C., Reim, K., and Rosenmund, C. (2002). Total arrest of spontaneous and evoked synaptic transmission but normal synaptogenesis in the absence of Munc13-mediated vesicle priming. Proc Natl Acad Sci U S A *99*, 9037-9042.

Verhage, M., Maia, A. S., Plomp, J. J., Brussaard, A. B., Heeroma, J. H., Vermeer, H., Toonen, R. F., Hammer, R. E., van den Berg, T. K., Missler, M., *et al.* (2000). Synaptic assembly of the brain in the absence of neurotransmitter secretion. Science *287*, 864-869.

Verkruyse, L. A., and Hofmann, S. L. (1996). Lysosomal targeting of palmitoyl-protein thioesterase. J Biol Chem *271*, 15831-15836.

Verstreken, P., Kjaerulff, O., Lloyd, T. E., Atkinson, R., Zhou, Y., Meinertzhagen, I. A., and Bellen, H. J. (2002). Endophilin mutations block clathrin-mediated endocytosis but not neurotransmitter release. Cell *109*, 101-112.

Vesa, J., Hellsten, E., Verkruyse, L. A., Camp, L. A., Rapola, J., Santavuori, P., Hofmann, S. L., and Peltonen, L. (1995). Mutations in the palmitoyl protein thioesterase gene causing infantile neuronal ceroid lipofuscinosis. Nature *376*, 584-587.

Virmani, T., Atasoy, D., and Kavalali, E. T. (2005). unpublished results.

Virmani, T., Han, W., Liu, X., Südhof, T. C., and Kavalali, E. T. (2003). Synaptotagmin 7 splice variants differentially regulate synaptic vesicle recycling. Embo J *22*, 5347-5357.

von Poser, C., Zhang, J. Z., Mineo, C., Ding, W., Ying, Y., Südhof, T. C., and Anderson, R. G. (2000). Synaptotagmin regulation of coated pit assembly. J Biol Chem *275*, 30916-30924.

Walther, K., Krauss, M., Diril, M. K., Lemke, S., Ricotta, D., Honing, S., Kaiser, S., and Haucke, V. (2001). Human stoned B interacts with AP-2 and synaptotagmin and facilitates clathrin-coated vesicle uncoating. EMBO Rep *2*, 634-640.

Wang, L. Y., and Kaczmarek, L. K. (1998). High-frequency firing helps replenish the readily releasable pool of synaptic vesicles. Nature *394*, 384-388.

Waters, J., and Smith, S. J. (2000). Phorbol esters potentiate evoked and spontaneous release by different presynaptic mechanisms. J Neurosci *20*, 7863-7870.

Wu, L. G., and Borst, J. G. (1999). The reduced release probability of releasable vesicles during recovery from short-term synaptic depression. Neuron *23*, 821-832.

Wucherpfennig, T., Wilsch-Brauninger, M., and Gonzalez-Gaitan, M. (2003). Role of Drosophila Rab5 during endosomal trafficking at the synapse and evoked neurotransmitter release. J Cell Biol *161*, 609-624.

Wyatt, R. M., and Balice-Gordon, R. J. (2003). Activity-dependent elimination of neuromuscular synapses. J Neurocytol *32*, 777-794.

Yang, Y., Udayasankar, S., Dunning, J., Chen, P., and Gillis, K. D. (2002). A highly Ca2+-sensitive pool of vesicles is regulated by protein kinase C in adrenal chromaffin cells. Proc Natl Acad Sci U S A *99*, 17060-17065.

Ye, W., and Lafer, E. M. (1995). Bacterially expressed F1-20/AP-3 assembles clathrin into cages with a narrow size distribution: implications for the regulation of quantal size during neurotransmission. J Neurosci Res *41*, 15-26.

Zenisek, D., Steyer, J. A., and Almers, W. (2000). Transport, capture and exocytosis of single synaptic vesicles at active zones. Nature *406*, 849-854.

Zhang, J. Z., Davletov, B. A., Südhof, T. C., and Anderson, R. G. (1994). Synaptotagmin I is a high affinity receptor for clathrin AP-2: implications for membrane recycling. Cell *78*, 751-760.

Zhang, Q., Fukuda, M., Van Bockstaele, E., Pascual, O., and Haydon, P. G. (2004). Synaptotagmin IV regulates glial glutamate release. Proc Natl Acad Sci U S A *101*, 9441-9446.

Zhen, M., and Jin, Y. (2004). Presynaptic terminal differentiation: transport and assembly. Curr Opin Neurobiol *14*, 280-287.

Zhou, Q., Petersen, C. C., and Nicoll, R. A. (2000). Effects of reduced vesicular filling on synaptic transmission in rat hippocampal neurones. J Physiol *525 Pt 1*, 195-206.

VITAE

Tuhin Virmani was born May 18, 1977 in New Delhi, India, the son of Drs. Arvind and Manju Virmani. After graduating from the Doon School, Dehra Dun, India in 1995, he received a Justice Brandeis Scholarship to attend Brandeis University in Waltham Massachusetts. For his research work while an undergraduate he received the "Elihu A. Silver Prize in Scientific Research" as a junior, and the "Stephan Berko Memorial Prize for Outstanding Research" as well as the "Molly W. and Charles Schiff Memorial Award in Science" as a senior. He graduated *summa cum laude*, and *Phi Beta Kappa* with a B.S. degree in Physics and Biology in May 1999. Since July 1999, he has been enrolled in the Medical Scientist Training Program at the University of Texas Southwestern Medical Center in Dallas, TX.